Abstract of
The 62nd Fullerenes-Nanotubes-Graphene General Symposium

Sponsored by: The Fullerenes, Nanotubes and Graphene Research Society

Co-Sponsored by: The Chemical Society of Japan
Center for Integrated Research of Future Electronics, Nagoya University

Supported by: The Physical Society of Japan
The Japan Society of Applied Physics
The Society of Polymer Science, Japan
The Electrochemical Society of Japan

Date: March 2nd (Wed.) - 4th (Fri.), 2022

Place: Online Virtual Symposium

Presentation Time: Special Lecture (25 min presentation + 5 min discussion)
Invited Lecture (10 min presentation + 5 min discussion)
General Lecture (10 min presentation + 5 min discussion)
Poster Preview (1 min presentation without discussion)

第62回フラーレン・ナノチューブ・グラフェン総合シンポジウム講演要旨集

主催： フラーレン・ナノチューブ・グラフェン学会

共催・後援： 日本化学会
名古屋大学 未来材料・システム研究所
未来エレクトロニクス集積研究センター

協賛： 日本物理学会、応用物理学会、高分子学会、電気化学会

日時： 2022年3月2日(水) 〜 3月4日(金)

場所： オンラインバーチャルシンポジウム

発表時間： 特別講演（発表　25 分 + 質疑応答　5 分）
招待講演（発表　10 分 + 質疑応答　5 分）
一般講演（発表　10 分 + 質疑応答　5 分）
ポスタープレビュー （発表　1 分・質疑応答　なし）

展示団体御芳名

（五十音順　敬称略）

テレダイン・ジャパン(株)

(株)日本レーザー

広告掲載団体御芳名

（五十音順　敬称略）

アイクストロン(株)

エクセルソフト(株)

(株)コロナ社

セントラル科学貿易(株)

(株)東京インスツルメンツ

テレダイン・ジャパン(株)

日本電子(株)

(株)日本レーザー

フィルジェン(株)

Contents

目次

Timetable

Mar. 2 (Wed)

08:50 **Opening**

09:00 **Special lecture**
Masafumi Nakayama

09:30 **Invited lecture**
Shinya Hayami

09:50 **Oral session**
Carbon nanotubes:
- Applications
- Others
Others:

10:35 **Coffee break**

10:50 **Special lecture**
Hiroki Ago

11:20 **Invited lecture**
Daisuke Kiriya

11:40 **Oral session**
Graphene and 2D materials:
- Electronic structure

12:10 **Lunch**

13:00 **Tutorial**
Kohei Arakawa

14:30 **Coffee break**

15:30 **Poster preview**

13:15 **Poster session**

(18:45)

Mar. 3 (Thu)

08:45 **Poster preview**

09:30 **Poster session**

12:00 **Lunch**

13:00 **Award ceremony**

13:30 **Special lecture**
Yoji Ishikawa

14:00 **Invited lecture**
Esko I. Kauppinen

14:20 **Oral session**
Carbon nanotubes:
- Synthesis and growth

15:05 **Coffee break**

15:20 **Special lecture**
Yasuhiko Igarashi

15:50 **Oral session**
Carbon nanotubes:
- Applications
Fullerenes:

13:35 **Coffee break**

13:50 **Oral session**
Others:
- Others
Fullerenes:
- Chemistry
- Applications
Others:
- Others
Carbon nanotubes:
- Applications

19:00 **Banquet**

(21:00)

Mar. 4 (Fri)

09:00 **Special lecture**
Der-Hsien Lien

09:30 **Oral session**
Graphene and 2D materials:
- Optical property
- Applications

10:30 **Coffee break**

10:45 **Oral session**
Carbon nanotubes:
- Optical property
- Electronic structure
- Chemistry
- Applications
Others:

12:00 **Lunch**

13:00 **Special lecture**
Yuanbo Zhang

13:30 **Invited lecture**
Katsuaki Sugawara

13:50 **Oral session**
Graphene and 2D materials:
- Others

14:35 **Coffee break**

14:50 **Invited lecture**
Keita Funayama

15:10 **Oral session**
Carbon nanotubes:
- Applications
Graphene and 2D materials:
- Others

13:10 **Closing**

(13:15)

Special Lecture
Presentation 25 min
Discussion 5 min
Invited Lecture
Presentation 15 min
Discussion 5 min
General Lecture
Presentation 10 min
Discussion 5 min
Poster preview
Presentation 1 min

座長一覧(Chiarpersons)

3月2日(水)

（敬称略）

セッション	時 間	座 長
特別講演（中山 勝文）	9:00 ~ 9:30	湯田坂 雅子
招待講演（速水 真也）	9:30 ~ 9:50	湯田坂 雅子
一般講演	9:50 ~ 10:35	稲葉 優文
特別講演（吾郷 浩樹）	10:50 ~ 11:20	岡田 晋
招待講演（桐谷 乃輔）	11:20 ~ 11:40	長汐 晃輔
一般講演	11:40 ~ 12:10	大町 遼
チュートリアル（荒川 公平）	13:00 ~ 14:30	山本 貴博
ポスタープレビュー	15:30 ~ 16:15	福島 知宏 鈴木 弘朗

3月3日(木)

セッション	時 間	座 長
ポスタープレビュー	8:45 ~ 9:30	大塚 慶吾 岡田 光博
特別講演（石川 洋二）	13:30 ~ 14:00	小久保 研
招待講演（Esko Kauppinen）	14:00 ~ 14:20	大野 雄高
一般講演	14:20 ~ 15:05	宮田 耕充
特別講演（五十嵐 康彦）	15:20 ~ 15:50	大淵 真理
一般講演	15:50 ~ 16:35	Esko Kauppinen
一般講演	16:50 ~ 18:20	若林 知成

3月4日(金)

セッション	時 間	座 長
特別講演（Der-Hsien Lien）	9:00 ~ 9:30	北浦 良
一般講演	9:30 ~ 10:30	吾郷 浩樹
一般講演	10:45 ~ 12:00	柳 和宏
特別講演（Yuanbo Zhang）	13:00 ~ 13:30	齋藤 理一郎
招待講演（菅原 克明）	13:30 ~ 13:50	齋藤 理一郎
一般講演	13:50 ~ 14:35	蒲 江
招待講演（舟山 啓太）	14:50 ~ 15:10	平原 佳織
一般講演	15:10 ~ 16:25	白木 智丈

Mar. 2 (Wed)

08:50~09:00 Opening

Carbon nanotubes: Others

09:00~09:30 Special lecture

Graphene and 2D materials: Chemistry

09:30~09:50 Invited lecture

Carbon nanotubes: Applications

09:50~10:05

Carbon nanotubes: Others

10:05~10:20

Others: Others

10:20~10:35

10:35~10:50 Coffee break

Graphene and 2D materials: Synthesis and growth

10:50~11:20 Special lecture

1S-2 From two-dimensional materials to 2.5-dimensional materials science 2
**Hiroki Ago*

Graphene and 2D materials: Electronic structure

11:20~11:40 Invited lecture

1I-2 Electronic state modulation of two-dimensional layered materials by interface engineering with molecules 8
**Daisuke Kiriya*

11:40~11:55

1-4 Electronic structure of bilayer MoS_2/WS_2 with checkerboard interlayer metal arrangement 15
**Mina Maruyama, Nanami Ichinose, Ryo Kitaura, Yanlin Gao, Susumu Okada*

11:55~12:10

1-5 Electronic structure modulation of MoS_2 by nanoscale wrinkles and external electric field 16
**Susumu Okada, Yanlin Gao, Mina Maruyama, Haruna Nakajima, Ryo Kitaura*

12:10~13:00 Lunch

13:00~14:30 Tutorial

1T-1 イノベーション人材
**荒川 公平 (Kohei Arakawa)*

14:30~15:30 Coffee break

15:30~16:15 Poster preview

16:15~18:45 Poster session

Mar. 3 (Thu)

08:45~09:30 Poster preview

09:30~12:00 Poster session

☆: Candidates for the Young Scientist Poster Award

Carbon nanotubes: Synthesis and growth

Carbon nanotubes: Applications

Carbon nanotubes: Applications

17:50~18:05

18:05~18:20

19:00~21:00 Banquet

Mar. 4 (Fri)

Graphene and 2D materials: Optical property

Graphene and 2D materials: Applications

10:30~10:45 Coffee break

Carbon nanotubes: Optical property

Graphene and 2D materials: Transport property

13:50~14:05

3-10 Direct synthesis of graphene nanoribbon ballistic Josephson junction 38
**Sato Naofumi, Toshiro Kaneko, Tomohiro Otsuka, Toshiaki Kato*

14:05~14:20

3-11 Fabrication and electronic transport properties of multilayer $Nb_xMo_{1-x}S_2/MoS_2$ in-plane heterostructures 39
**Hiroto Ogura, Seiya Kawasaki, Zheng Liu, Takahiko Endo, Yusuke Nakanishi, Hong En Lim, Kazuhiro Yanagi, Toshifumi Irisawa, Keiji Ueno, Kosuke Nagashio, Yasumitsu Miyata*

Graphene and 2D materials: Others

14:20~14:35

3-12 Edges of Layered MoS_2 Observed by Field Electron Emission and Field Ion Microscopy 40
**Yahachi Saito*

14:35~14:50 Coffee break

Carbon nanotubes: Applications

14:50~15:10 Invited lecture

3I-2 Carbon nanotube-based nanomechanical receiver for digital data transfer 11
**Keita Funayama, Hiroya Tanaka, Jun Hirotani, Keiichi Shimaoka, Yutaka Ohno, Yukihiro Tadokoro*

15:10~15:25

3-13 Synaptic function in ultra-dense CNT/HfO_2/CNT memristors for reservoir computing applications 41
**Adha Sukma Aji, Yutaka Ohno*

15:25~15:40

3-14 Multi-element photo-thermo-electric devices by a micro-scale CNT film array 42
**Daichi Suzuki, Yuma Takida, Yukio Kawano, Hiroaki Minamide, Nao Terasaki*

特別講演
Special Lecture

1S-1 ~ 1S-2

2S-1 ~ 2S-2

3S-1 ~ 3S-2

Macrophage Inflammatory Responses to Multi-Walled Carbon Nanotubes

○Masafumi Nakayama[1,2]

[1] *Laboratory of Immunology and Microbiology, College of Pharmaceutical Sciences, Ritsumeikan University 525-8577, Japan*
[2] *CREST, JST, Kawaguchi 332-0012, Japan*

Carbon nanotubes (CNTs), the highly representative products of nanotechnology, have been recently added to the so-called SIN ('Substitute It Now') list of chemicals by the international Chemical Secretariat (ChemSec), although the general toxicity of CNTs is still under debate. At least, a certain type of long needle-like multi-walled CNTs (MWCNTs) has been shown in numerous studies to have asbestos-like pathogenicity in lungs and mesothelium of rodent models. Epidemiologic studies of U.S. workers have shown several associations between CNT exposure and biomarkers of fibrosis and inflammation. In both rodents and humans, MWCNTs and asbestos fibers are efficiently recognized by professional phagocytes such as macrophages. However, after being tethered to the macrophage surfaces, these fibers are not easily phagocytosed and instead cause damages to the plasma membrane and/or phagolysosomal membrane. This process, called *frustrated phagocytosis*, induces macrophage cell death and NLRP3 inflammasome activation leading to secretion of IL-1β, a pro-inflammatory cytokine [1,2]. Frustrated phagocytosis initiates inflammatory cascades involving various immune cells and fibroblasts, leading to granuloma and mesothelioma development. Therefore, it is important to understand the molecular mechanism of initial interactions between MWCNTs and macrophages that trigger biological responses to MWCNTs.

We have recently identified T-cell immunoglobulin mucin receptor 4 (Tim4) and Tim1 as MWCNT receptors [3]. These Tim molecules are unique in that they have a cluster of aromatic residues at their apex positions to facilitate direct recognition of MWCNTs and the frustrated phagocytosis (Fig. 1). I here focus on the molecular mechanism of macrophage phagocytosis and discuss therapeutic approaches to combat the toxicity of MWCNTs.

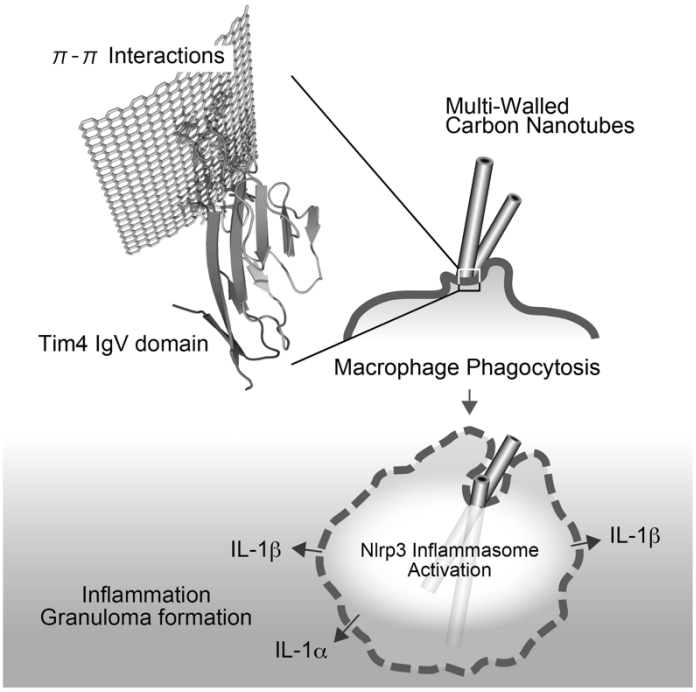

Fig. 1. Tim4 recognizes MWCNTs and mediates phagocytosis leading to granuloma formation.

[1] M. Nakayama. *Front. Immunol.*, **9**, 103 (2018).
[2] M. Tsugita *et al*. *Cell Rep.*, **18**, 1298 (2017).
[3] S. Omori *et al*. *Cell Rep.*, **34**, 108734 (2021).

Corresponding Author: M. Nakayama
Tel: +81-77-599-3264
E-mail: mnakayam@fc.ritsumei.ac.jp
www.ritsumei.ac.jp/~mnakayam/index.html

From two-dimensional materials to 2.5-dimensional materials science

Hiroki Ago

Global Innovation Center (GIC), Kyushu University, Fukuoka, 816-8680, Japan
Interdisciplinary Graduate School of Engineering Sciences, Kyushu University, Fukuoka, 816-8680, Japan
E-mail: h-ago@gic.kyushu-u.ac.jp

Since the discovery of graphene, two-dimensional (2D) materials have been intensively studied because of their unique physical properties and various applications. Their potential increases by vertically stacking 2D layers owing to the flexibility provided by weak van der Waals interaction. The integration of 2D materials and other low-dimensional materials has shown unexpected phenomena, such as unconventional superconductivity in twisted bilayer graphene (BLG) and the formation of moiré excitons in twisted stacks of transition metal dichalcogenides (TMDCs). We expect that such new research can be further developed based on the new concept of "Science of 2.5-dimensional (2.5 D) materials", as shown in the figure below.

Our recent research based on the 2.5 D concept will be reviewed, first showing the controlled CVD growth of BLG and machine learning-based twist angle determination [1-3]. The 2D nanospace in BLG was used to intercalate metal chloride molecules, revealing new 2D superstructures and significantly reducing the sheet resistance of the BLG sheet [4-6]. We have been also developing the CVD growth of high-quality, multilayer hBN to be used as a building block of various 2.5 D materials [7,8]. We observed the enhanced carrier mobility of monolayer graphene [9] and the increased PL emission from WS_2 monolayers when coupled with the CVD-grown hBN [7]. The generation of 2.5 D materials will open a new research field enriched with fascinating properties and promising applications.

I will also introduce our new project, "Science of 2.5 Dimensional Materials: Paradigm Shift of Materials Science Toward Future Social Innovation (Grant-in-Aid for Transformative Research Areas (A))" supported by MEXT that just started from September 2021 [10].

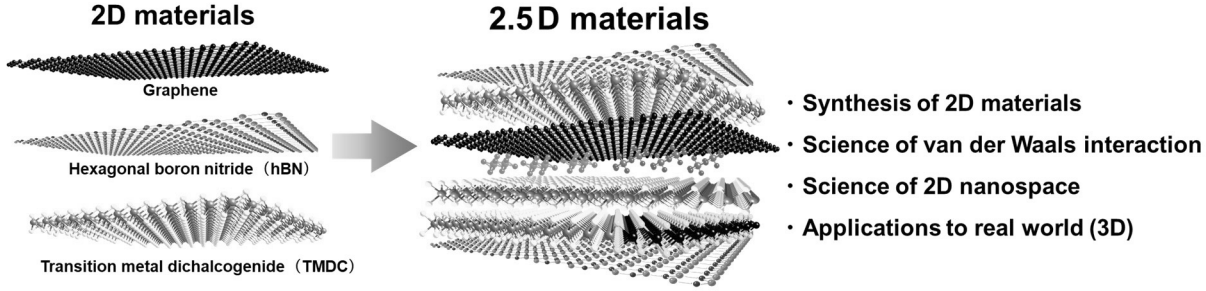

References

[1] *Chem. Mater.*, **28**, 4583 (2016). [2] *ACS Nano*, **14**, 6834 (2020). [3] *ACS Appl. Nano Mater.*, DOI: 10.1021/acsanm.1c03928 (2022). [4] *Adv. Mater.*, **29**, 1702141 (2017). [5] *Adv. Mater.*, **33**, 2105898 (2021). [6] *Nano Lett.*, **21**, 10386 (2021). [7] *ACS Nano*, **12**, 6236 (2018). [8] *ACS Appl. Electron. Mater.*, **2**, 3270 (2020). [9] S. Fukamachi *et al.*, submitted. [10] https://25d-materials.jp

Space elevator and its current development status

Yoji Ishikawa
Obayashi Corporation, Tokyo, Japan

Abstract

The space elevator is a future transportation system that can carry people and goods up into space. It had been a dream until a new material, carbon nanotube (CNT), was found in 1991. This revolutionary material can be used as the cable, a critical component, of the space elevator. The space elevator is a system consisting of 100,000 km-long cables that stand out on the Earth's equator and climbers that travel up and down along them and enables massive shipping of people and goods to space at a much lower cost than conventional transportation methods. While it is expected to become a game-changer in the space business, the space elevator is a challenging project in various aspects. The significant technological challenges include the development of long and durable cable material, the climber's driving mechanism that allows long and fast travel, and remote wireless energy supply system to climbers. CNT survivability in space and cable dynamics are two of the R&D subjects currently carried out and contributed to the development of the space elevator.

Materials Informatics for 2D Materials Combined with Sparse Modeling -Toward Small-Data-Driven Materials Science-

○Yasuhiko Igarashi[1] and Yuya Oaki[2]

[1] *Faculty of Engineering, Information and Systems, Tsukuba University, Ibaraki 305-8573, Japan*
[2]*Department of Applied Chemistry, Faculty of Science and Technology, Keio University, Yokohama, 223-8522, Japan*

Application of data-scientific approach to conventional sciences, such as chemo-informatics, bio-informatics, and materials informatics (MI), has attracted much interest toward data-driven research. The concept enables accelerated discovery of new materials, enhancement of performances, and optimization of processes. However, sufficient bigdata is not always prepared to apply machine learning. For example, experimental scientists have their own small data including success and failure in their laboratory, regardless of academy and industry. If such small data is effectively utilized by data-scientific approach, research activities can be accelerated without energy, resource, and cost consumptions. This account focuses on MI for small data, a recent concept for application of small data, with introduction of model cases, such as control of exfoliation processes to obtain 2D materials. Combination of machine learning and chemical perspective is effective for construction of straightforward and interpretable predictors through the extraction of a limited number of descriptors from small dataset. Although the prediction accuracy is not so precise, the model has enough accuracy to be a guideline reducing the number of next experiments. The present MI for small data opens potentials of small-data-driven chemistry and materials science. [1].

[1] Oaki, Yuya, and Yasuhiko Igarashi. "Materials Informatics for 2D Materials Combined with Sparse Modeling and Chemical Perspective: Toward Small-Data-Driven Chemistry and Materials Science." Bulletin of the Chemical Society of Japan 94.10 (2021): 2410-2422.

Corresponding Author: Y. Igarashi
Tel: +81-29-853-5344,
E-mail: igayasu1219@cs.tsukuba.ac.jp

Exciton recombination dynamics in 2D semiconductors

Der-Hsien Lien

Institute of Electronics, College of Electrical and Computer Engineering, National Yang Ming Chiao Tung University, Hsinchu 30010, Taiwan.

As semiconductors' thickness approaches the monolayer limit, excitonic quasiparticles could be observed at room temperature due to the strong Coulomb interaction between space-confined charge carriers. 2D layered semiconductors in monolayer form (e.g., transition metal dichalcogenide monolayers) provide an ideal platform to investigate the transport properties of excitons and their complexes because surface issues in 2D monolayers are not as severe as in bulk semiconductors. I will show that such thickness-determined excitonic systems are promising for optoelectronic applications due to their near-unity photoluminescence (PL) quantum yields (QYs) [1], a key figure of merit dictating the maximum efficiency achievable in light-emitting diodes, lasers, and solar cells. I will discuss the comprehensive recombination mechanisms of excitons in monolayers and show that the non-radiative recombination pathways can be fully suppressed by electrostatic gating, despite the presence of native defects [2,3]. This research reveals that room-temperature excitons are robust and bright regardless of monolayer quality, indicating the potential of achieving highly efficient excitonic devices. To deal with the injection inefficiency caused by Schottky contacts, I will show an AC carrier injection architecture, a device concept that is capable of efficiently injecting carriers in various excitonic systems [4], including monolayer semiconductors, with demonstrations of bright light-emitting devices from infrared to ultraviolet regimes [5].

[1] D. H. Lien *et al*., *Science* **350**, 1065 (2015).
[2] D. H. Lien *et al*., *Science* **364**, 468 (2019).
[3] H. Kim *et al*., Science, **373**, 448, 2021.
[3] D. H. Lien *et al*., *Nature Communications*, **9**, 1129, 2018
[4] D. H. Lien *et al*., *Nature Electronics*, **3**, 612–621 2020.

Electronic property of low-dimensional black phosphorus

Yuanbo Zhang

Department of Physics, Fudan University, China

We investigate the electric property of black phosphors thin flakes with thickness down to a few atomic layers. Two-dimensional black phosphorus exhibits excellent semiconducting properties. High conductance modulations up to 10^5 and field effect mobility up to 1000 cm^2/Vs at room temperature are achieved in black phosphorus field effect transistors. Further improving the sample quality leads to observation of quantum Hall effect in this material. In this talk, I will discuss the physics in black phosphorus two-dimensional electron system, as well as our recent effort in growing low-dimensional structures of black phosphorus.

招待講演
Invited Lecture

1I-1 ~ 1I-2

2I-1

3I-1 ~ 3I-2

Graphene Oxide as a Super Material

○Shinya Hayami

[1] *Department of Chemistry, Kumamoto University, Kumamoto 860-8555, Japan*

Graphene oxide (GO) is 2D nanosheet, and has many functionalities, for example, proton conductivity.[1] The GO has negative charge because GO has many oxygen functional groups such as epoxide group, carboxyl group, hydroxyl group and so on. Therefore, GO can combine with positive charge cations such as proton, metal ions, complexes and so on. Furthermore, the hybrids can be prepared by not only electrostatic interaction but also π-π stacking or chemical bonding between epoxy and amine groups.[2] After reduction of GO by hydrazine, UV irradiation or annealing, reduced GO (rGO) can be produced, which shows electrical conduction.

Many kinds of possibilities in GO and rGO are demonstrated. Ion conduction through a GO membrane is pH switchable; that is, under acidic conditions GO behaves as a H^+ conductor while under basic conditions it acts as an OH^- conductor. Our findings not only make available a new single-phase GO-based OH^- conductor but also opens a new door for future research on ion conduction switching of H^+ and OH^- ions in a single material. Furthermore, we focused on the effect of different synthesis techniques of metal supported GO for the microwave-assisted catalytic decomposition of carbohydrates to 5-hydroxymethylfurfural (5-HMF), where the effect of reaction conditions, amount of catalyst used, effect of solvent, was also evaluated.

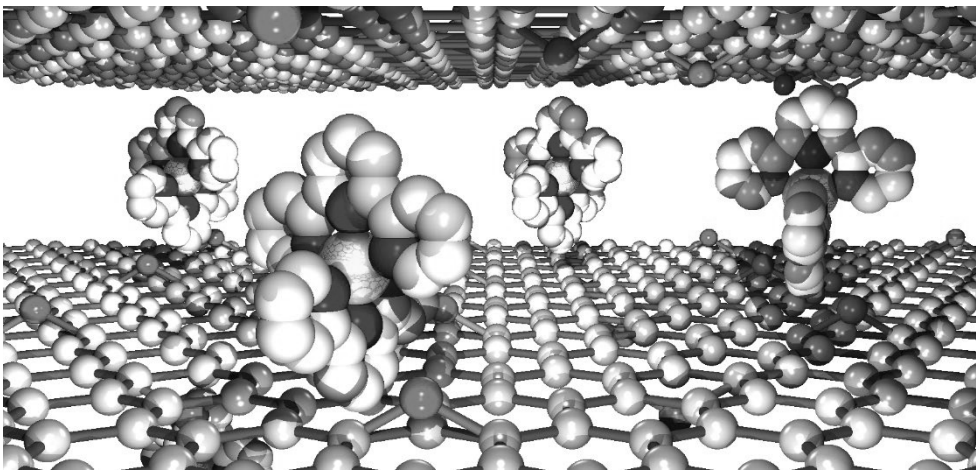

Fig. 1 Structure of GO hybrids with a various of molecules

[1] S. Hayami et al., Chem. Commun., 2014, 50, 14527. Chem. Mater., 2014, 26, 5598. Angew. Chem., Int. Ed., 2014, 53, 6997. J. Am. Chem. Soc., 2013, 135, 8097.
[2] S. Hayami et al., Adv. Funct. Mater., 2013, 23, 323. Dalton Trans., 2015, 44, 5049. Inorg. Chem. Front., 2015, 2, 886.

Corresponding Author: S. Hayami
Tel: +81-96-342-3469, Fax: +81-96-342-3469
E-mail: hayami@kumamoto-u.ac.jp

Electronic state modulation of two-dimensional layered materials by interface engineering with molecules

○Daisuke Kiriya[1]

[1] *Department of Physics and Electronics, Osaka Prefecture University, Osaka 599-8531, Japan*

Transition metal chalcogenides (TMDCs), MX_2 (M = Mo and W; X = S and Se), have gathered attention as thin-layered semiconducting materials. A lot of research has been reported in physics, chemistry, and engineering processing, however, the post-synthetic method to modulate the carrier concentrations in TMDCs has not been well established. In this presentation, I would focus on the modulation of the carrier concentrations of TMDCs by a post-synthetic method using molecules. The important point in the molecular process is the solution process: 1) The process can be carried out under mild conditions near room temperature, 2) the process is scalable (can be applied to large areas), and 3) simple and quick.

We have used redox-active molecules and demonstrated strong carrier modulations to observe metallic states in both n-[1,2] and p-type[3] situations. The doped sample further shows metal-insulator-transition under electrostatic modulation[4]. As the molecules on the TMDC surface were revealed mobile, the molecular assemblies can be further modulated to form patterns. By the modulation, the lateral electronic junctions on TMDCs can be generated. The process of pattern formation happens spontaneously (i.e., spontaneous pattern formation)[5]. Along with the process, we observed a sort of pn junctions at several hundred-nanometer scales, which are formed spontaneously and simultaneously at a macroscopic scale[6].

One of the successful post-synthetic modulation strategies has been surface-charge transfer-doping; the method uses the energy difference between the target molecules and TMDCs. Recently, we are focusing on exploring different strategies using the ability of molecules, "recognition" at atomic scales via such as hydrogen bonding, etc. The molecular recognition systems would be useful, especially for applying to sensing devices. I would also show this type of molecular doping process in this talk.

[1] D. Kiriya *et al*. J. Am. Chem. Soc., **136**, 7853 (2014).
[2] K. Matsuyama *et al*. ChemistryOpen, **8**, 908 (2019).
[3] D. Kiriya *et al*. Adv. Funct. Mater., **25**, 6257 (2015).
[4] K. Matsuyama *et al*. ACS Appl. Mater. Int. accepted (2022).
[5] H. Ichimiya *et al*. ACS NANO, **12**, 10123 (2018).
[6] H. Ichimiya *et al*. ACS Appl. Mater. Int., **11**, 15922 (2019).

Corresponding Author: D. Kiriya
Tel: +81-72-254-9327
E-mail: kiriya@pe.osakafu-u.ac.jp

How many SWNTs can a single catalyst grow in the FCCVD ?

Saeed Ahmad[1,2], Qiang Zhang[1], Er-Xiong Ding[1] and Esko I. Kauppinen[1]

[1]*Department of Applied Physics, Aalto University School of Science, 15100, FI-00076 Aalto, Finland*

[2]*Department of Physics, Government Postgraduate College Mansehra, 21300, Pakistan*

Floating-catalyst CVD (FCCVD) is a highly promising technique for the scalable synthesis of single-walled carbon nanotubes (SWNTs), especially for the direct deposition SWNT thin films for flexible electronics applications. The number concentration (NC) as well as the activity of the catalyst particles are important process parameters influencing the yield and the purity of the as-produced SWNTs. In the conventional FCCVD methods, catalyst particles are usually synthesized by thermal decomposition of gaseous organometallic precursors like e.g. ferrocene inside the FCCVD reactor. Being in-situ catalyst formation in conventional FCCVD, it is an open question that how many SWNTs a single catalyst particle can grow? Herein, we used pre-made catalyst particles by employing our novel spark discharged based FCCVD technique which decouples the formation of catalyst particles and SWNTs synthesis into two subsequent process to investigate effects of catalyst NC on SWNTs synthesis. The NC and number size distributions (NSD) of both catalyst particles and SWNTs in gas-phase were quantitatively determined using an aerosol size spectroscopic method, i.e. the differential mobility analyzer (DMA). The DMA measurements corroborated with atomic force microscopy and X-rays photoelectron spectroscopy revealed that under carefully chosen reaction conditions in FCCVD (where typical residence time is < 10s), a single catalyst particle can grow more than one SWNTs. We propose that after the growth termination of 1st SWNT, the catalyst particle can detach from the SWNT and start nucleating 2nd SWNT and this process can continue as long as the catalyst remains in the growth region of the FCCVD reactor.

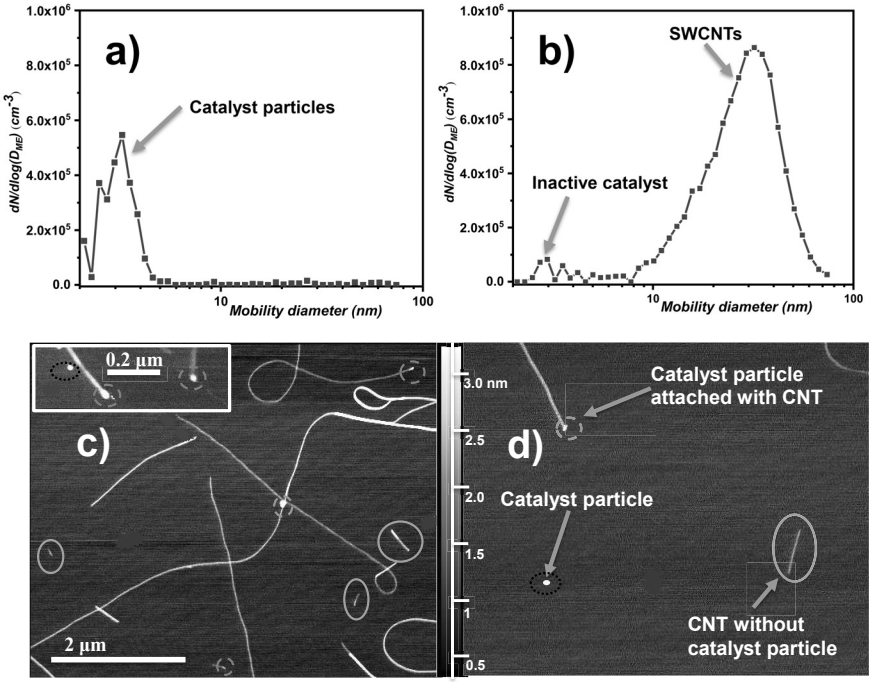

Fig.1 (a) Gas-phase NSDs of **a)** Fe-catalyst particles and **b)** SWCNTs from DMA with higher number concentration than catalyst paraticles, and with small fraction of inactive/detached catalyst roughly 3 nm in size. **c-d)** Typical atomic force microscope (AFM) images of individual/small bundled SWCNTs on mica substrate as collected via thermophoresis method, here catalyst particles attached with CNTs are encircled with red color, inactive/detached catalyst with black circles, and shorter SWCNTs in cyan circles, without catalyst particles attached.

High-resolution ARPES studies of atomic-layer Nb-based TMDs

○Katsuaki Sugawara

[1] *Department of Physics, Tohoku University, Sendai 980-8578, Japan*
[2] *WPI-Advanced Institute for Materials Research, Tohoku University, Sendai 980-8577, Japan*
[3] *Center for Spintronics Research Network, Tohoku University, Sendai 980-8577, Japan*

Two-dimensional (2D) atomic-layer (monolayer) materials have been a target of intensive studies by the discovery of Dirac fermion in the thinnest limit of graphite and its related anomalous physical properties such as integer quantum Hall effect and valley polarization [1]. Recently, monolayer transition-metal dichalcogenides (TMDs) have been intensively studied since it shows the novel quantum physical phenomena related to strongly correlated electron phenomena such as charge-density waves and spin-momentum-locked superconductivity [2]. Amongst bulk TMDs, bulk 2H-$NbSe_2$ has been attracting attention 50 years ago due to competing between superconductivity and charge-density waves[3]. While the physical properties in bulk 1T-$NbSe_2$ are not understood yet, we have recently succeeded in fabricating 1*T*-$NbSe_2$ monolayer as a robust Mott insulator by using a molecular-beam-epitaxy method [4, 5]. Also, in bulk $NbTe_2$ analogous to $NbSe_2$, it has well known that one-dimensional structure with a zigzag chain is the stable structure (called 1T'' phase) which shows the superconductivity below 1K. However, the electronic states in monolayer $NbTe_2$ have not been investigated because of the difficulty to grow high-quality well-ordered atomic-layer materials.

In this talk, we will introduce the recent results that it has been succeeded in obtaining the monolayer $NbTe_2$ films by constructing the combined MBE-ARPES systems and elucidated these electronic structures by ARPES [4-6]. As shown in Fig.1, we find that the metallic band dispersion in monolayer 1T-$NbTe_2$ in stark contrast to the insulating nature with a finite bandgap in monolayer 1T-$NbSe_2$. I will discuss the origin of metallic nature related to strongly correlated electron systems in monolayer $NbTe_2$ films.

[1] A. H. Castro Neto *et al*. Rev. Mod. Phys. **81**, 109 (2009).
[2] Z. Xu *et al*., Nanotech. 32 492001 (2021).
[3] J. A. Wilson, *et al.*, Adv. Phys. **24**, 117 (1975).
[4] Y. Nakata, *et al*., NPG Asia Mater. **8**, e31 (2016).
[5] Y. Nakata, *et al*., Nat. Commun. **12**, 5873 (2021).
[6] *Submitted*

Corresponding Author: K. Sugawara
Tel: +81-22-217-6169, Fax: +81-22-217-6157,
E-mail: k.sugawara@arpes.phys.tohoku.ac.jp

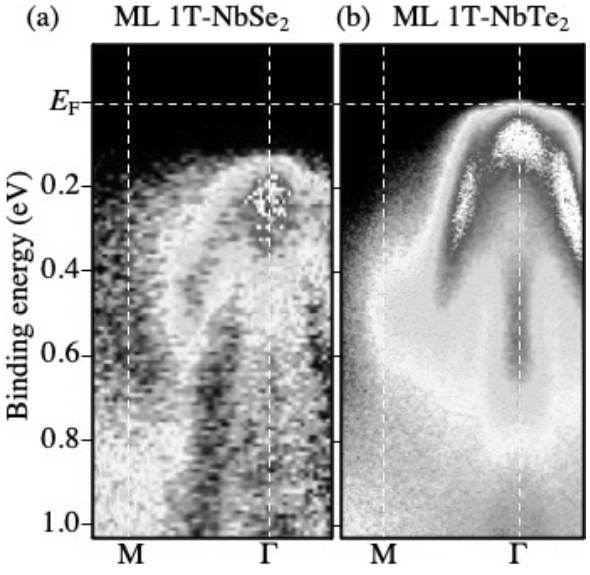

Fig. 1 : ARPES results around Γ point of monolayer (a) 1T-$NbSe_2$ and (b) 1T-$NbTe_2$.

Carbon nanotube-based nanomechanical receiver for digital data transfer

○Keita Funayama[1], Hiroya Tanaka[1], Jun Hirotani[2], Keiichi Shimaoka[1], Yutaka Ohno[2,3], Yukihiro Tadokoro[1]

[1]*Toyota Central Research & Development Laboratory, Inc., Nagakute 480-1192, Japan*
[2] *Department of Electronics, Nagoya University, Nagoya 464-8603, Japan*
[3] *Institute of Materials and Systems for Sustainability, Nagoya University, Nagoya 464-8603, Japan*

Recent developments of nanotechnology enable us to fabricate nanoelectromechanical systems (NEMS). In NEMS, a carbon nanotube (CNT) is one of the future promising materials due to its high elasticity, excellent electric properties, and chemical stability. Accordingly, several research groups have reported the great potential of a CNT-based NEMS for achieving outstanding sensitive sensors for tiny mass, force, and electric fields [1]. In addition, the detection of radio frequency (RF) signal via mechanical vibration has been expected to achieve digital data transfer with nanoscale wireless terminals. Although the theoretical concepts and basic demonstrations have been reported [2], the evaluation of fundamental performance for digital data transfer has not been explained yet.

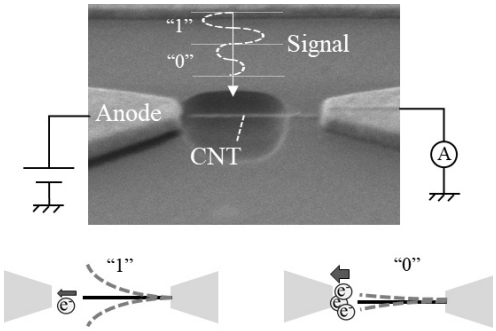

Fig. 1 SEM image of CNT-based nano receiver and schematic images of vibration states during receiving signal "0" and "1".

In our work, we experimentally demonstrate megabit data transfer with a CNT-based signal receiver and evaluate its communication performance for the first time [3]. The fabricated nanomechanical receiver consists of a counter electrode and a CNT cantilever clipped on one side via an electrode as shown in Fig. 1. A color image with 393216 bits is digitally amplitude-modulated and sent toward the receiver. Simply decoded image from the noisy received signal includes errors with 3516 bits which appear as incorrect colors at some pixel in Fig. 2a. On the other hand, employing the error correction method enhances the correct detection rate of the receiver and reduces the errors to 28 bits as shown in Fig. 2b. Combining the nanoscale receiver and digital communication technology, we indicate that the CNT-based receiver has the potential for achieving practical applications and contributing to the development of wireless communication technology, e.g., IoT. In our presentation, we will additionally talk about the results of experimental evaluations of fundamental communication performance with the receiver.

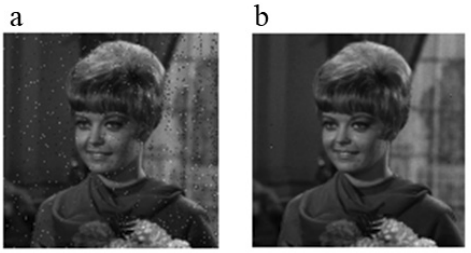

Fig. 2. Estimated digital images obtained by the receiver (a) without and (b) with digitally error correction method.

[1] K. Jensen *et al*. Nano Letters, **7**, 3508 (2007).
[2] V. Gouttenoire *et al.* Small, **6**, 1060 (2010).
[3] K. Funayama *et al.* ACS Applied Nano Materials, **4** 13041 (2021).

Corresponding Author: K. Funayama
Tel: +81-0561-71-7421 E-mail: funayama@mosk.tytlabs.co.jp

一般講演

General Lecture

1-1 ~ 1-5

2-1 ~ 2-12

3-1 ~ 3-16

Superhydrophobic Carbon Nanotubes with Different Orientations as Mask Filters realizing Excellent Anti-viral Effect against SARS-CoV-2

○Sangsu Lee[1], Chae Young Woo[2], Han-Jun Kim[3], Ali Khademhosseini[3], Hyung Woo Lee[2], Il Jeon[1]

[1] Department of Nano Engineering, SKKU Advanced Institute of Nanotechnology (SAINT), Sungkyunkwan University (SKKU), Suwon 16419, Republic of Korea
[2] Department of Nano Fusion Technology, Pusan National University, Busan 46241, Republic of Korea
[3] Terasaki Institute for Biomedical Innovation, Los Angeles, CA, 90024 USA

The COVID-19 outbreak was declared as a pandemic by the World Health Organization (WHO) in December 2019 and is still a highly contagious disease with the number of infections increasing dramatically every day. The difficulty of stabilizing the pandemic lies in the unceasing mutation of SARS-CoV-2, rendering vaccination inadequate via breakthrough infections. Wearing face masks is the ultimate solution for now and will not be optional even until the booster jabs are available to everyone because this disease infection spreads via airborne saliva droplets. Targeting protection against SARS-CoV-2, our investigation and discussion focus on five key aspects: 1) superhydrophobicity, 2) industrial viability, 3) breathability, 4) anti-viral effect and 5) non-toxicity.

In this study, commercially available spunbonded/melt-blown/spunbonded polypropylene (SMS) filter-based face masks are used as the control sample. To find an optimal condition for vertically aligned carbon nanotubes (VACNTs) having the greatest superhydrophobicity, the CNTs were synthesized by changing the amount of catalysts, synthesis time, and substrate types. In order to obtain VACNTs effectively blocking viruses, it is important to synthesize them on SiO_2 substrates for 20 min using a Fe:Al2O3=4:2 catalyst to grow high-density and short-length VACNTs. The average water contact angle of the VACNT filter (175.53°) was approximately 51°, which is greater than that of the SMS filters (124.6°). Even the minimum water contact angle of the VACNT filter was 165.1 °, which is still much larger than the SMS filter. There is a problem of using VACNT as a mask filter, which is that it is nearly impossible to maintain its vertical alignment. VACNT can be transferred onto a mask substrate using the dry-spinning process. However, its vertical alignment is not retained. However, post-transferred VACNTs still possess sufficient hydrophobicity (142.7°) despite the alignment being not perfectly vertical. In addition, since the dry-spinning method can be applied to the roll-to-roll process, the CNT filter could be added on top of the SMS filter or replace one of the existing layers with ease to lower the production cost. It is possible to transfer by adjusting the VACNT thickness. Through this, we can control the breathability. The high thermal conductivity of the CNT filter induced a hyperthermal anti-viral effect as evidenced by the swift temperature rise to 56 °C in less than 5 min when the situation of the mask being worn outside was simulated. Inactivation of the viruses on the heated CNTs was confirmed by TEM imaging of denatured viruses. It transpires hyperthermic antiviral effects which offers stronger protection against the virus as well as reusability. The toxicity test was conducted in vivo test using rats. It was confirmed that CNTs attached on a mask substrate are not toxic. In conclusion, we are positive that VACNTs can be viable on an industrial level within a short time. The VACNT filter warrants its viability, reinforcing the fight against the COVID-19 pandemic.

Corresponding Author: I. Jeon, Hyung Woo Lee, Ali
E-mail: il.jeon@spc.oxon.org (I.J.), LHW2010@pusan.ac.kr (H.L.), parastoo@hms.harvard.edu (A.K.)

Non-enzymatic degradation of carbon nanotubes in the presence of bacterial enzymes

○Katsutoshi Hori[1,2], Seira Takahashi[1], Fumiko Taguchi[1], Junichi Kanie[2], Mitsuo Ueno[3], Mitsugu Uejima[3], Masafumi Ata[3]

[1] *Department of Biomolecular Engineering, Nagoya University, Nagoya 464-8603, Japan*
[2] *Friend Microbe Inc., Nagoya 464-0858, Japan*
CNT Laboratory, Zeon Corporation, Kawasaki 210-9507

The enzymatic degradation of carbon nanotubes (CNTs) by several enzymes has been reported [1-5]. However, because organisms that possess these enzymes have limited habitats and distribution areas, it is unclear whether CNTs can be degraded in the general environment. The investigation of CNTs degradation by enzymes derived from bacteria, which inhabit a wide range of environments and have diverse metabolic systems, is inevitable for predicting the environmental fate of CNTs. In this study, the degradation of oxidized (carboxylated) single-walled CNTs (O-SWCNTs) by mt2DyP, a dye-decolorizing peroxidase of *Pseudomonas putida* mt-2, a common soil bacterium [6], was investigated. Suspensions of O-SWCNTs gradually became transparent and their optical absorbance decreased during 30 d of incubation in the presence of mt2DyP produced by a recombinant *Brevibacillus choshinensis* strain and its substrate, H_2O_2. The degradation was enhanced by higher H_2O_2 concentrations. The measurement of Raman spectra revealed the complete degradation of O-SWCNTs after 30 d of incubation with 100 mM H_2O_2. However, surprisingly, this heme enzyme was inactivated within 60 min of the incubation with O-SWCNTs, which suggested that the degradation of O-SWCNTs was not catalyzed by the enzyme. The inactivation of mt2DyP was accompanied by the release of iron, which suggested that the degradation of the O-SWCNTs was owing to the Fenton reaction caused by the iron released from mt2DyP and the supplied H_2O_2. A chelating agent, diethylenetriaminepentaacetic acid, significantly inhibited the O-SWCNTs degradation, proving the degradation by the Fenton reaction. These phenomena were also observed with another heme enzyme, Cytochrome P450. These results are important for predicting the fate of CNTs in a wide range of environments, as heme enzymes are secreted by many bacteria in the environment.

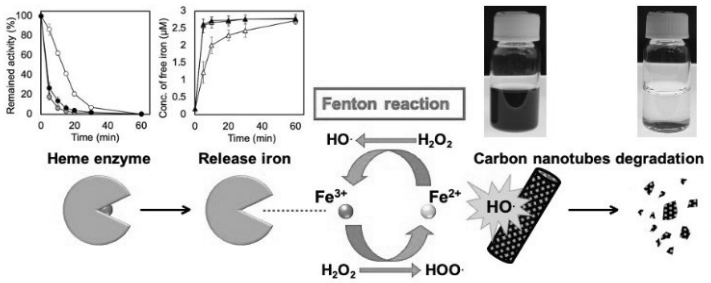

Fig. 1 Degradation of CNT by bacterial heme enzymes

[1] B. L. Allen *et al*. J. Am. Chem. Soc. **131**, 17194 (2009).
[2] V. E. Kagan *et al.* Nat. Nanotechnol. **5**, 354 (2010).
[3] F. T. Andon *et al.* Small **9**, 2721 (2013).
[4] C. Zhang *et al.* Environ. Sci. Technol. **48**, 7918 (2014).
[5] G. Chandrasekaran *et al.* J. Ind. Eng. Chem. **20** 3367 (2014).
[6] T. D. H. Bugg *et al.* Curr. Opin. Biotechnol. **22** 394 (2011).

Corresponding Author: K. Hori
Tel: +81-52-789-3339 E-mail: khori@chembio.nagoya-u.ac.jp

Fabrication of bisphosphonate-loaded carbon nanohorns and their *in vitro* evaluation

○Maki Nakamura[1], Katsuya Ueda[2], Yumiko Yamamoto[1], Kaoru Aoki[2], Minfang Zhang[1], Naoto Saito[2], Masako Yudasaka[1,3]

[1] *National Institute of Advanced Industrial Science and Technology (AIST), Tsukuba 305-8565, Japan*
[2] *Shinshu University, Matsumoto 390-8621, Japan*
[3] *Meijo University, Nagoya 468-8502, Japan*

Carbon nanohorns (CNHs) have great potential for carriers of drug delivery systems. Bisphosphonates (BPs) inhibit osteoclasts to resorb bones, and, in addition, they reduce the osteoclasts proliferation and promote their apoptosis. Therefore, BPs have been used for the treatment of bone metastasis. However, BPs have drawbacks of causing adverse side effects during the systemic circulation. We considered that the BP-loaded CNHs might be applicable to the local treatment of bone metastasis. But ibandronate (IBN), a type of BP, did not adsorb onto CNHs, because the interaction between relatively hydrophilic IBN and hydrophobic CNHs was weak. Therefore, we tried to use calcium phosphates (CaPs), a main mineral component of bones, as mediators between IBN and CNH. An *in vitro* evaluation of the resulting BP-loaded CNHs was also performed.

We prepared a supersaturated CaP solution containing oxidized CNHs (OxCNH) and IBN (final concentrations; Ca: 6.6 mM, P: 3.3 mM, OxCNH: 50 μg/mL, IBN: 0.078 mM). The solution was kept at 25 °C for 30 min to induce coprecipitation. The product was washed with water. The structure and composition of the resulting product were investigated by transmission electron microscopy (TEM), energy dispersive X-ray spectroscopy (EDX), and inductively coupled plasma optical emission spectrometry (ICP). For an *in vitro* evaluation, murine macrophages (RAW264.7 cells) and osteoclasts (differentiated from RAW264.7 cells) were incubated with the product, and cell viability assays and microscopic observations of the cells were performed.

TEM observation and EDX and ICP analyses indicated that the product consisted of many small-sized deposits of IBN-containing CaPs (< 10 nm) on the surface of OxCNHs (ca. 100 nm) (Fig. 1). That is, the IBN-loaded CNHs were successfully fabricated by using CaPs as mediators between IBN and CNHs. The resulting IBN-CaP-CNH composites were engulfed by macrophages and osteoclasts, and strongly suppressed the cell viability. Since IBN-CaP-CNH composites were accumulated in lysosomes, it was presumed that CaPs were dissociated under weakly acidic conditions in lysosomes and IBN was released to suppress the cell viability. These results suggested that the IBN-loaded CNHs have a great potential for the local treatment of bone metastasis [1].

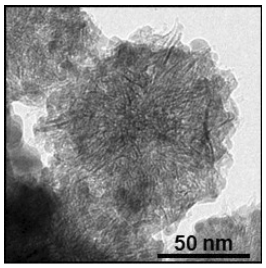

Fig. 1 TEM image of the product.

[1] M. Nakamura *et al.*, ACS Appl. Mater. Interfaces, **13**, 3701–3712 (2021).

Corresponding Author: M. Nakamura
Tel: +81-29-861-4604, Fax: +81-29-861-3005,
E-mail: ma-ki-nakamura@aist.go.jp

Electronic structure of bilayer MoS_2/WS_2 with checkerboard interlayer metal arrangement

○Mina Maruyama[1], Nanami Ichinose[2], Ryo Kitaura[2], Yanlin Gao[1], and Susumu Okada[1]

[1]*Department of Physics, University of Tsukuba, Tsukuba 305-8571, Japan*
[2]*Department of Chemistry, Nagoya University, Nagoya 464-8602, Japan*

Boundaries of condensed matters with vacuum or other materials cause localized electron state at or around the boundaries because of the absence of the translational symmetry across there. Unsaturated covalent bonds at boundaries of semiconductors and insulators usually induce the localized states near the surfaces and in the gap between valence and conduction bands. Two dimensional materials, such as graphene, h-BN, and transition metal dichalcogenides, possesses two different classes of boundaries which also cause unusual electronic structures depending on the constituent elements and their mutual arrangements. Both within and between their atomic planes, the electronic structure is modulated at the borders and interfaces, even though the covalent bonds of constituents are fully saturated.

In this work, using the density functional theory with effective screening medium method, we investigate the electronic structure of the in-plane and out-of-plane heterostructure of MoS_2 and WS_2 where MoS_2 and WS_2 strips are alternately arranged and stacked (Fig. 1). According to the arrangement of the strips, bilayer MoS_2/WS_2 has a checkerboard pattern in terms of interlayer metal arrangement. The band edge alignment of the bilayer MoS_2/WS_2 strongly depends on the interlayer metal arrangement (Fig. 2): The valence band edge of the Mo above Mo is the shallowest among four metal arrangements, while the conduction band edge of W above W is the deepest. Therefore, the dimensionality of accumulated carrier in this system is tunable from 0D to 2D by controlling the carrier concentration.

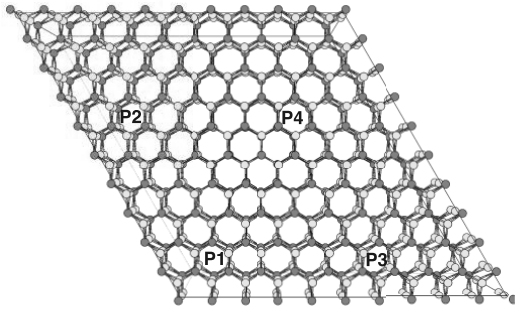

Fig. 1: A geometric structure of bilayer MoS_2/WS_2 with checkerboard structure. Purple, gray, and yellow balls indicate Mo, W, and S atoms, respectively.

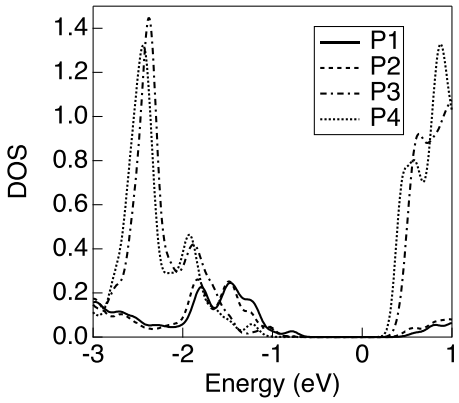

Fig. 2: Projected density of states of bilayer MoS_2/WS_2 with checkerboard structure. P1, P2, P3, and P4 indicate the Mo above Mo, Mo above W, W above Mo, and W above W, respectively.

Corresponding Author: M. Maruyama
TEL: +81-29-853-5921, FAX: +81-29-853-5924
E-mail: mmaruyama@comas-tsukuba.jp

Electronic structure modulation of MoS_2 by nanoscale wrinkles and external electric field

○Susumu Okada[1], Yanlin Gao[1], Mina Maruyama[1], Haruna Nakajima[2], and Ryo Kitaura[2]

[1]*Department of Physics, University of Tsukuba, Tsukuba 305-8571, Japan*
[2]*Department of Chemistry, Nagoya University, Nagoya 464-8602, Japan*

Electronic structure of transition-metal dichalcogenide (TMDC) are sensitive to the constituent elements, mechanical strain, and formation of hybrid structures. In particular, band edge alignment of TMDC strongly depend on the strain and out-of-plane interactions: The most of monolayer TMDC have direct band gap at the K point, while they have indirect band gap under the strain and thin film structures. These facts implies that local electronic structure of monolayer TMDC is tunable by introducing spatially nonuniform structural modulations. For instance, a hybrid system comprising monolayer TMDC and CNT is plausible structure where the electronic structure is locally modulated by CNT [1]. Thus, in this work we aim to investigate the energetics and electronic structures of MoS_2 with nonuniform mechanical strain using the density functional theory combined with the effective screening medium method.

Figure 1 shows an optimized structure of corrugated MoS_2 with a corrugation angle of 20 degree. The energy cost to cause the corrugation is 60 meV per MoS_2 unit. Local electronic structure is estimated by calculating projected density of states on Mo atoms located at peak (Mo_P) and inflection (Mo_I) (Fig. 2). Corrugation causes the upward shift of the valence band edge, which depends on Mo atomic position. The band edge at Mo_P is shallower by 50 meV than that at Mo_I. indicating the formation of one-dimensional potential well on corrugated MoS_2. We further investigate the carrier distribution in corrugated MoS_2 by the external electric field. Carriers are primarily localized in peak area of the corrugated MoS_2.

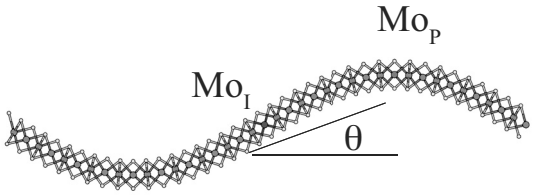

Fig. 1: A geometric structure of MoS_2 with structural corrugation. Mo_P and Mo_I represent Mo atoms situated at the peak and inflection of corrugation. Corrugation is defined as the initial gradient of slope θ.

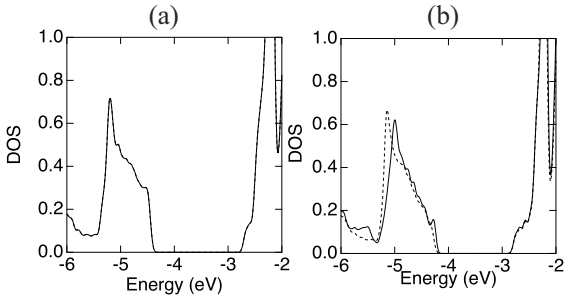

Fig. 2: Projected density of states MoS_2 sheet with corrugation angle (a) 0 and (b) 20 degrees on Mo_P (solid curve) and Mo_I (dotted curve). Energies are measured from the vacuum level energy.

[1] H. Nakajima, et al. Abstracts in the 61st FNTG symposium, p. 46 (2021).

Corresponding Author: Susumu Okada
TEL: +81-29-853-5921, FAX: +81-29-853-5924
E-mail: sokada@comas-tsukuba.jp

Gas-dependent kinetic selectivity in catalytic chemical vapor deposition of single-walled carbon nanotubes

○Keigo Otsuka[1,2], Ryoya Ishimaru[1], Taiki Inoue[3], Rong Xiang[1], Shohei Chiashi[1], Yuichiro K. Kato[2,4], Shigeo Maruyama[1]

[1] *Department of Mechanical Engineering, The University of Tokyo, Tokyo, 113-8656, Japan*
[2] *Nanoscale Quantum Photonics Laboratory, RIKEN Cluster for Pioneering Research, Saitama, 351-0198, Japan*
[3] *Department of Applied Physics, Osaka University, Osaka, 565-0871, Japan*
[4] *Quantum Optoelectronics Research Team, RIKEN Center for Advanced Photonics, Saitama, 351-0198, Japan*

Single-walled carbon nanotubes have been a candidate for outperforming silicon in ultrascaled transistors [1], but the realization of nanotube-based integrated circuits requires dense arrays of purely semiconducting species [2]. In order to directly grow such nanotube arrays on wafers, control over kinetics and thermodynamics in tube-catalyst systems plays a key role, and further progress requires the comprehensive understanding of seemingly contradictory reports on the growth kinetics. Here, we propose a universal kinetic model that decouples the growth rates of nanotubes into the adsorption and removal of carbon atoms on the catalysts, which are caused by carbon source gases (*e.g.*, ethylene) and etching agents (*e.g.*, water), respectively (Fig. 1a) [3]. Labeling experiments involving acetylene and isotopic ethanol are performed to provide the quantitative verification of our model. While the removal of carbon from catalysts dominates the growth kinetics under a low supply of precursors, our kinetic model and experiments demonstrate that chiral angle-dependent growth rates emerge when sufficient amounts of carbon and etching agents are co-supplied. The kinetic maps, as a product of generalizing the model, include several kinetic selectivities that emerge depending on the balance of gases with opposing effects (Fig. 1b). Our findings not only resolve discrepancies existing in literature, but also offer rational strategies to control chirality, length, and density of nanotube arrays for practical applications.

Part of this work was supported by JSPS (KAKENHI JP20K15137, JP20H00220) and JST (CREST JPMJCR20B5). A part of this work was conducted at Takeda Sentanchi Supercleanroom, The University of Tokyo, supported by "Nanotechnology Platform Program" of the Ministry of Education, Culture, Sports, Science and Technology (MEXT), Japan, Grant Number JPMXP09F21UT0047.

[1] C. Qiu *et al*., *Science* **355**, 271 (2017).
[2] A. D. Franklin, *Nature* **498**, 443 (2013).
[3] K. Otsuka *et al*., arXiv:2111.08411 (2021).

Corresponding Author: K. Otsuka
Tel, Fax: +81-3-5841-6408,
E-mail: otsuka@photon.t.u-tokyo.ac.jp

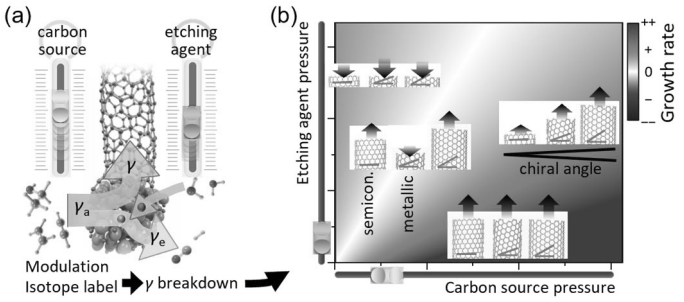

Fig. 1 (a) Schematic of the kinetic model that traces carbon atoms coming in and out of a catalyst. (b) Kinetic map as a function of the pressures of carbon sources and etching agents.

Experimental Synthesis of NbS_2 based 1D van der Waals Heterostructures

○Wanyu Dai[1], Yongjia Zheng[1], Akihito Kumamoto[2], Rong Xiang[1], Yuichi Ikuhara[2], Shigeo Maruyama[1]

[1] *Department of Mechanical Engineering, The University of Tokyo, Tokyo 113-8656, Japan*
[2] *Institute of Engineering Innovation, The University of Tokyo, Tokyo 113-8656, Japan*

We recently presented the experimental synthesis of one-dimensional (1D) van der Waals (vdW) heterostructures which includes single-walled carbon nanotubes (SWCNTs), boron nitride nanotubes (BNNTs) and molybdenum disulfide nanotubes (MoS_2NTs) [1]. Further, the nucleation and crystal growth behaviors over these highly curved nanotube surfaces were investigated [2]. It is believed that all materials in the 2D library could be rolled into their 1D counterparts. [1] Hence, the controlled synthesis of 1D vdW heterostructures based on different transition metal dichalcogenides (TMDCs) are of great research interest. [3]

In this work, we demonstrate the experimental synthesis of 1D vdW heterostructures combine SWCNTs, BNNTs, and niobium disulfide nanotubes (NbS_2NTs) in the radial direction. By chemical vapor deposition (CVD) method, the BNNTs and NbS_2NTs were synthesized over the SWCNTs templates layer by layer. Scanning transmission electron microscopy (STEM) was applied to characterize the structure of as acquired 1D vdW heterostructures. Energy dispersive spectroscopy (EDS) mapping results shown that the as acquired structures are SWCTN-BNNT-NbS_2 1D vdW heterostructures along with several 2D NbS_2 flakes. (Fig. 1) The out layer NbS_2NTs are highly crystalized. (Fig. 2) The experimental synthesis of SWCTN-BNNT-NbS_2 1D vdW heterostructure suggests that it is highly possible to acquire 1D vdW heterostructures based on more TMDCs in the 2D material library.

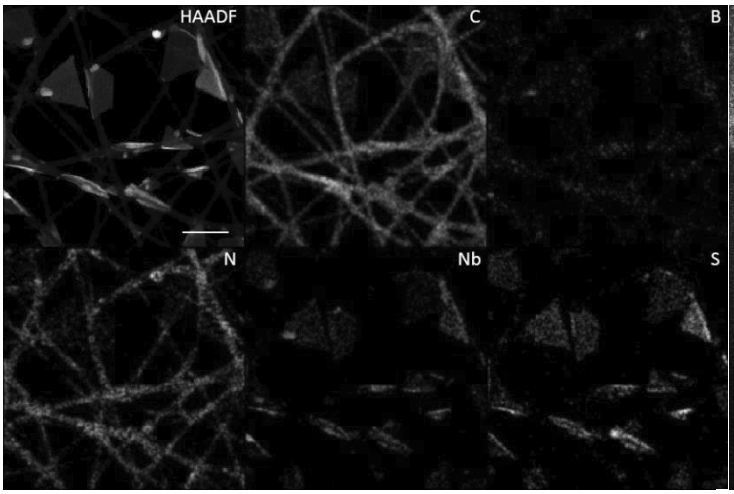

Fig. 1 EDS mapping of as synthesized SWCNT-BNNT- NbS_2 vdW heterostructures. Scale bar, 100 nm.

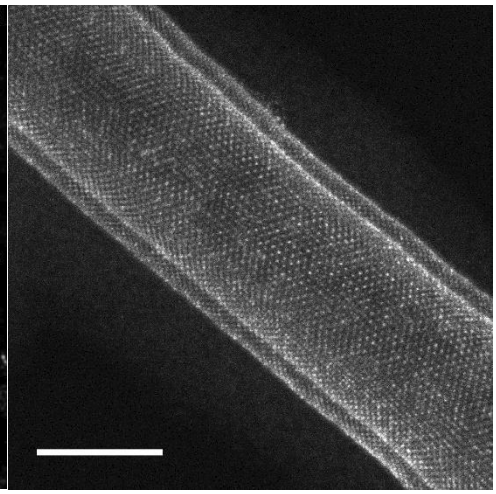

Fig. 2 STEM image of SWCNT-BNNT-NbS_2 1D vdW heterostructure. Scale bar, 5 nm.

[1] R. Xiang, *et al.,* Science, **367**, 537 (2020).
[2] Y. Zheng, *et al.,* PNAS, **118**, e2107295118 (2021).
[3] S. Cambre, *et al.,* Small, **17**, 2102585 (2021)

Corresponding Author: S. Maruyama
Tel: +81-3-5841-6421, Fax: +81-3-5800-6983
E-mail: maruyama@photon.t.u-tokyo.ac.jp

Experimental realization of the WS_2-based 1D vdW heterostructure

○Yongjia Zheng[1], Wanyu Dai[1], Akihito Kumamoto[2], Jenichi Clairvaux Felizco[3], Yuta Sato[4], Kazu Suenaga[3], Keigo Otsuka[1], Qiang Zhang[5], Anton Anisimov[6], Esko I. Kauppinen[5], Rong Xiang[1], Shigeo Maruyama[1]

[1] *Department of Mechanical Engineering, The University of Tokyo, Tokyo 113-8656, Japan*

[2] *Institute of Engineering Innovation, The University of Tokyo, Tokyo 113-8656, Japan*

[3] *The Institute of Scientific and Industrial Research (ISIR), Osaka University, Osaka 567-0047, Japan*

[4] *Nanomaterials Research Institute, AIST, Tsukuba 305-8565, Japan*

[5] *Department of Applied Physics, Aalto University School of Science, Tiilenlyöjänkuja 9A SF-01720 Vantaa, Finland*

[6] *Canatu Ltd., Helsinki FI‐00390, Finland*

We recently presented one-dimensional (1D) van der Waals (vdW) heterostructure that coaxially formed by single-walled carbon nanotubes (SWCNTs), boron nitride nanotubes (BNNTs) and molybdenum disulfide (MoS_2) [1]. Also, the nucleation behaviors of these highly curved outer layers over SWCNT surfaces were investigated [2]. It suggests the family of 2D materials can be possibly rolled into their 1D counterparts, among which 2D transition metal dichalcogenides (TMDC) have been already widely investigated. On the other hand, despite the great variety in 2D TMDC materials, the research on their corresponding 1D structure is still limited and challenging [3].

In this work, we demonstrate the experimental synthesis of another 1D TMDC materials: WS_2-based 1D vdW heterostructure which coaxially includes SWCNTs, BNNTs and WS_2 nanotubes. Not only the 1D WS_2 is highly crystalline, but also its coverage over nanotube networks is very high. In Fig1b, the EELS mapping clearly proves that SWCNT is sequentially wrapped by BNNT and WS_2 nanotube. This can be a big step forward a wider variety of 1D vdW heterostructures, which opens opportunities for further studying their new properties and potential applications.

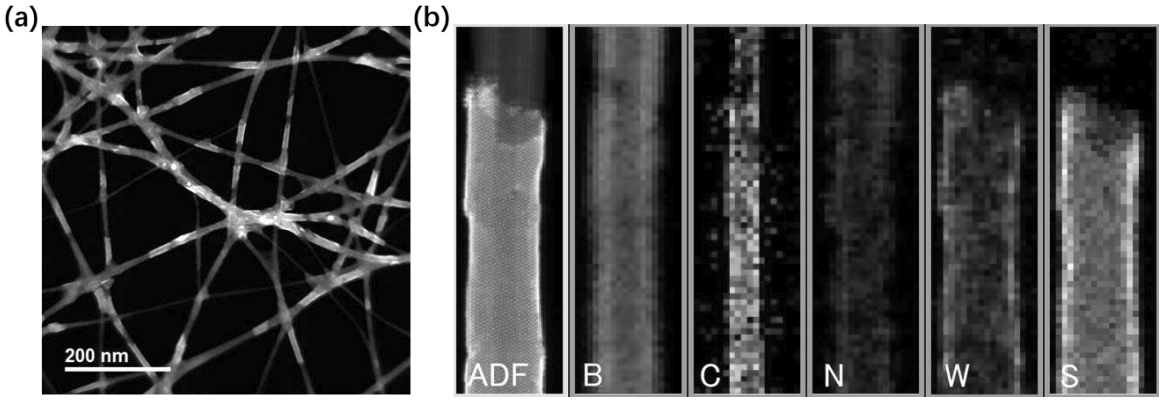

Fig.1 (a) Annular dark-field (ADF) image of 1D SWCNT-BNNT-WS_2 heteronanotubes. (b) ADF image and electron energy-loss spectroscopic (EELS) mapping of a SWCNT partially wrapped with BNNT and WS_2 nanotube.

[1] R. Xiang *et al., Science,* **367**(6477), 537 (2020).

[2] Y. Zheng, *et al., PNAS*, **118**(37), e2107295118 (2021).

[3] R. Xiang and S. Maruyama, *Small Sci.*, **1**(2), 2000039, (2021),

Corresponding Author: S. Maruyama
Tel: +81-3-5841-6421,
Fax: +81-3-5841-6983,
E-mail: maruyama@photon.t.u-tokyo.ac.jp

Poly(triarylamine) wrapped carbon nanotubes as efficient electrodes for high-performance perovskite solar cells

○Bo-wen Zhang[1], Xi-yang Qiu[1], Keigo Otsuka[1], Hao-Sheng Lin[2], Esko I. Kauppinen[3], Yutaka Matsuo[2] and Shigeo Maruyama[1]

[1] *Department of Mechanical Engineering, Graduate School of Engineering, The University of Tokyo*
[2] *Department of Chemical System Engineering, Graduate School of Engineering, Nagoya University*
[3] *Department of Applied Physics, Graduate School of Science, Aalto University*

Perovskite solar cells (PSCs), since the first report in 2009, have outshined other photovoltaic counterparts with a soaring power conversion efficiency (PCE) from 3.8% [1] to 25.2% [2] in 2021, exhibiting a promising future as the photovoltaic devices in next generation.

The layered structure is adopted for perovskite solar cells and gold is employed as top electrode due to its preeminent conductivity and suitable energy level. However, stability issue caused by gold atom migration from top electrode to underlying layers [3] and cost issue of this precious metal is urgent to be solved. One effective method is electrode substitution.

In our group we have published a paper of replacing gold electrode with CNT electrode and achieving a comparable power conversion efficiency (PCE) with gold electrode reference devices [4]. Spiro-OMeTAD is mixed with sponge-like CNT electrode to form the hole transport layer. To enhance the conductivity of hole transport layer and solar cell PCE, Lithium bis(trifluoromethanesulfonyl)imide (Li-TFSI) is heavily added into Spiro-OMeTAD precursor solution while Li-TFSI is hygroscopic, leading to subsequent stability issues of devices. Hence, how to balance PCE and stability, decreasing the usage of Li-TFSI dopant with maintaining high PCE at the same time, becomes an emerging problem.

To solve this problem, we upgrade our hole transport layer from Spiro-OMeTAD to Poly[bis(4-phenyl)(2,4,6-trimethylphenyl)amine(PTAA) and we find that compared with Spiro-OMeTAD, PTAA requires less amount of Li-TFSI doping to reach the best PCE in gold electrode devices (**11.7% wt.** for Spiro-OMeTAD and **8.5% wt.** for PTAA). The doping ratio can be even less when gold electrode replaced by CNT electrode. We optimize the relationship between doping ratio and power conversion efficiency in CNT electrode devices, as shown in figure 1. The optimized doping ratio for PTAA in CNT electrode devices is **1.7% wt.**, which is the lowest required doping ratio for MAPI perovskite solar cell to reach 18% PCE, almost the maximum efficiency for $MAPbI_3$ active layer devices. The requirement of extremely low doping ratio for PTAA as hole transport layer in CNT electrode devices successfully increases the stability of our devices, whereas high PCE can be achieved at the same time. We attribute this ingenious balance to the remarkable combination of CNT and PTAA, where CNTs facilitate carrier transport in the mixed PTAA-CNT layer, thus decreasing the requirement for Li-TFSI doping, while PTAA is distributed in sponge-like CNT mixed structure, breaking the shackles of traditional layered structure, and making thicker hole transport layer to be possible. Our work displays a huge advantage of CNTs to function as electrodes in perovskite solar cells.

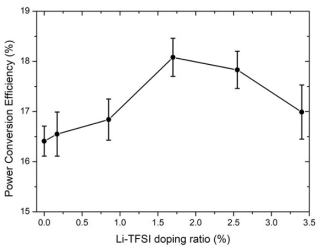

[1] Akihiro Kojima. *et al.* J. Am. Chem. Soc. 2009, 131, 17, 6050–6051

[2] Jeong, J., Kim, M., Seo, J. *et al.* Nature 592, 381–385 (2021)

[3] Konrad Domanski. *et al.* ACS Nano 2016, 10, 6, 6306–6314

[4] Il Jeon.*et al.* J. Mater. Chem. A, 2020, 8, 11141

Figure 1. Optimization of Li-TFSI doping concentration in PTAA layer of CNT electrode

Utilization of Multifunctional Environment-Friendly Organic Dopants Inspired from Nature for Carbon Nanotube-Based Planar Heterojunction Silicon Solar Cells

○Jeong-Seok Nam[1], Jiye Han[1], Seungju Seo[2], Qiang Zhang[3], Esko I. Kauppinen[3], Shigeo Maruyama[2], Il Jeon[1]

[1] *Department of Nano Engineering, SKKU Advanced Institute of Nanotechnology (SAINT), Sungkyunkwan University (SKKU), Suwon, 16419 Republic of Korea*
[2] *Department of Mechanical Engineering, The University of Tokyo, Tokyo, 113-8656 Japan*
[3] *Department of Applied Physics, Aalto University School of Science, Espoo, FI-00076 Finland*

Carbon nanotubes (CNTs) have to be chemically doped for their conductivity to match up with the conventional transparent conductors. Nitric acid and trifluoromethanesulfonic acid (TFMS) have been the common choice of *p*-dopant.[1] However, nitric acid produces toxic NO_2 and explodes when mixed with organic compounds. In addition, TFMS is a superacid with a pKa value of –14.7 and therefore extremely corrosive beyond measure.[2] Natural acids, which consist of hydrocarbons with carboxyl, sulfonic, or phosphoric groups, are biodegradable, easy to synthesize, and easily obtained from nature.[3] It also has the potential to qualify for replacing inorganic acids. In this work, we tested naturally available acids, specifically, acetic acid, formic acid, lactic acid, and citric acid as the *p*-dopant for the CNT transparent electrode. From the result, lactic acid shows the multifunctional effect of *p*-doping with excellent doping stability as well as antireflection. The doping effect and its stability are investigated by diverse methods, such as van der Pauw four-probe measurement as well as Raman, photoelectron yield, and absorption spectroscopy. The sheet resistance decreases by 22.1% when carbon nanotube films are doped by lactic acid and the doped films are stable for more than 20 days. The power conversion efficiency of carbon nanotube-laminated silicon solar cells improves from 8.2% to 10.3% by using nature-inspired lactic acid. Such a great improvement is ascribed to not only the p-doping and antireflection effects but also the passivation effect of lactic acid on the Si surface defect sites as evidenced by both the Fourier-transform infrared and the Quasi-steady-state photoconductance lifetime measurements.

[1] I. Jeon, *et al.* J. Mater. Chem. A, 8, 11141 (2020)
[2] J. W. Lee, *et al.* Nano Lett, 19, 2223 (2019)
[3] J. Han, *et al.* Adv. Energy Mater, 2101221, 1 (2021)

Corresponding Author: I. Jeon
E-mail: il.jeon@spc.oxon.org

Homogeneously Miscible Fullerene inducing Vertical Gradient in Perovskite Thin-Film towards Highly Efficient Solar Cells

○Kyusun Kim[1], Ziang Wu[2], Yue Ma[3,4], Han Young Woo[2], Il Jeon[1,4]

[1] *Department of Nano Engineering, SKKU Advanced Institute of Nanotechnology (SAINT), Sungkyunkwan University (SKKU), Suwon 16419, Republic of Korea*
[2] *Department of Chemistry, KU-KIST Graduate School of Converging Science and Technology, Korea University, Seoul 02841, Republic of Korea*
[3] *Laboratorium für Organische Chemie, ETH Zürich, CH-8093, Zürich, Switzerland*
[4] *Department of Mechanical Engineering, The University of Tokyo, Tokyo 113-8656, Japan*

Fullerene-based n-type charge-collecting materials have emerged as a solution to high-performance perovskite solar cells. However, their application to perovskite solar cells was limited in the device architecture and only a small amount of fullerene additives could be introduced to the device system, because of the immiscibility of the fullerene species with polar solvents. To overcome this, triethylene glycol monomethyl ether chain-attached fullerene derivatives are synthesized and applied to normal-type perovskite solar cells. The newly synthesized fullerenes exhibit excellent solubility in polar solvents. A novel approach to introducing miscible fullerenes into perovskite devices and inducing a favorable vertical gradient is proposed. Forming an overcoat on an electron-transporting layer and waiting for a few minutes, the fullerene derivatives progressively permeate into the fullerene-doped perovskite active film. In this talk, we attached, triethylene glycol monomethyl ether (TEG) chains to $PC_{61}BM$ to greatly enhance its miscibility with the perovskite precursor. The synthesized TEG-attached $PC_{61}BM$, [6,6]-phenyl-C_{61}-butyric acid 2-[2-(2-methoxyethoxy)ethoxy]ethyl ester ($PC_{61}B$-TEG), and a branched substituent with two TEGs-attached $PC_{61}BM$, [6,6]-phenyl-C_{61}-butyric acid 1-methyl 3-[2-(2,5,8,11-tetraoxadodec-1-yl)-4,7,10,13-tetraoxatetradec-1-yl] ester ($PC_{61}B$-BiTEG) were highly polar and miscible with the perovskite precursor. Here, we explored three ways to introduce novel fullerene derivatives into PSCs: direct mixing with the precursor prior to film fabrication, overcoating the electron-transporting layer, and overcoating + waiting between drop-casting and spin-coating of the perovskite precursor solution on the overcoated layer of $PC_{61}B$-TEG to induce gradient dispersion into the perovskite precursor. By fabricating perovskite solar cells combining direct mixing, overcoating and waiting techniques, a remarkably high device efficiency of 23.34% is achieved. The high performance is attributed to the fullerene additives with a vertical gradient passivating the perovskite defect sites effectively and the overcoat enhancing the charge transfer.

The device performance is certified by a national laboratory, which is the highest efficiency among the fullerene additives-used perovskite solar cells.

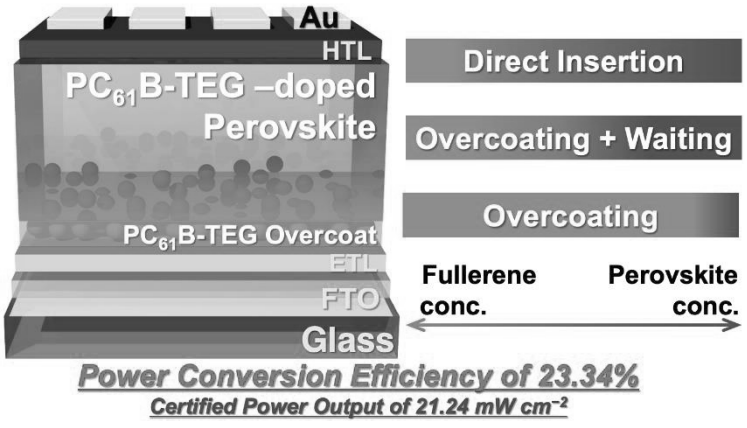

Fig. 1 Configuration of $PC_{61}B$-TEG-added device.

Corresponding Author: I. Jeon
Tel: +82-31-299-4187
E-mail: Il.Jeon@spc.oxon.org

20 years of NanoAmando@ towards Elementary Diamond Nanoparticles: their experimental evidence

○ Toshihiko Tanaka[1], Tetusya Aoyama[2], Yasuhiro F. Miura[3], Eiji Osawa[4]

[1]Department of Chemistry and Biochemistry, National Institute of Technology, Fukushima College, 30 Aza-nagao, Tairakamiarakawa, Iwaki, Fukushima, 970-8034, Japan
[2]Ultrahigh Precision Optics Tech. Team, RIKEN RAP, 2-1 Hirosawa, Wako, Saitama, Japan
[3]Hamamatsu University School of Medicine, 1-20-1 Handayama, Higashi-ku, Hamamatsu City, Shizuoka, Japan
[4]Nano Carbon Research Institute Ltd., Asama Research Extension Center, Shinshu University, 3-15-1 Tokida, Ueda, Nagano, Japan

The last author founded *NanoCarbon Research Institute Ltd.* in 2002 and has kept it over 20 years, thus to all over the world supplying the standard product of the aqueous colloidal solutions of nanodiamonds (NDs), NanoAmando@ (NA). It provided the success of drug delivery system[1] for cancer therapy and most researchers of NDs perhaps know this product through this impact publication. Furthermore, it has often showed unique properties, having both positive ze-ta potentials and a tiny graphitic layer on the surface of NDs. However, the difference between NA and other commercial solutions is an open question. It is to say that the intrinsic properties of NDs have not been clarified enough in spite of huge amount of publications on NDs. One problem should be homogeneity of NDs. I think that he has struggled with this so hard and has reached a certain level. Hence, we will present herein the progress of NA in these years together with recent results on its intrinsic properties: assembly or electric conduction.

We consider that the main NDs component of recent NA are appreciably homogeneous because of the following 3 reasons: 1) DLS measurements often reach a low size value down to 2.6 nm; 2) they also show hierarchic aggregation[2]; and 3) the NA often gives rectangular precipitates such as whiskers or nanosheets. The low value itself indicates a high purity because of its Rayleigh scattering, which is proportional to r^6 (r: diameter of a particle); the contamination of larger particles below 10 nm should shift primary particle‘s peak appreciably larger. In hierarchic aggregation, primary particles first assemble to 1st aggregates (15-25 nm) which aggregates further forms 2nd aggregates (50-70 nm)[**Fig.1**] and there are two blank areas (10-15 nm, 25-50 nm) where aggregates could be unstable. The precipitates perhaps indicate the instant growth of hydrate colloidal crystals through drying. Hence, these three facts strongly suggest that the primary particles are rather elementary diamond nanoparticles (EDIANs) that are similar both in size and shape. Furthermore, recently the high electric conductivity of the soft gel from NA was found and we also presume that it is also due to the progress.

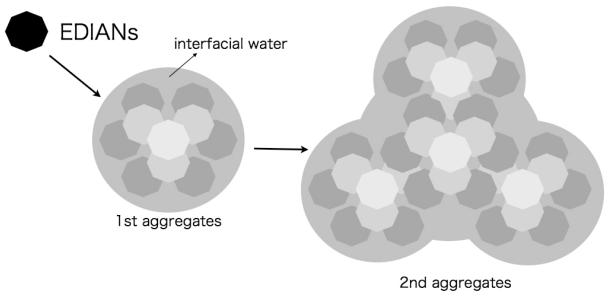

Figure 1. An example of schmatic model of hierarchic aggregation

[1]E.K.Chow, X.-Q. Zhang, M. Chen, R. Lam, E. Robinson, H. Huang, D. Schaffer, E. Osawa, A. Goga, D. Ho, *Sci. Trans. Med*., 3, 73 (2011)
[2] Technical Report No.2, *NanoCarbon Research Institute Ltd.*（2007）
Corresponding Author:Eiji Osawa / Tel: +81-0268-75-8381 / E-mail: osawa@nano-carbon.jp

Isolation of C_{70}-Based Endohedral Fulleride Li@C_{70}

○Daiki Kitabatake,[1] Hiroshi Ueno,[1,2] Fuminori Misaizu[1]

[1] *Department of Chemistry, Tohoku University, Sendai 980-8577, Japan*
[2] *The Frontier Research Institute for Interdisciplinary Sciences, Tohoku University*

Endohedral metallofullerenes (EMFs) are one of the well-studied nanocarbon materials during the past 3 decades. Among EMFs, C_{60} and C_{70}-based EMFs have attracted special interest owing to their predicted electronic properties arising from the superatomic electronic structure. However, these materials are generally known to be difficult to obtain in macroscopic yield, and therefore almost the reported studies have focused on the isolatable higher fullerene-based EMFs. Although Shinohara and co-workers had successfully isolated the La@C_{60} and La@C_{70} as highly extractable trifluoromethylated forms,[1, 2] isolation and unambiguous characterization of C_{60} and C_{70} based-EMFs with no chemical addends have been never accomplished except for Li@C_{60} reported previously.[3]

In this talk, we report the first isolation of neutral Li@C_{70} by selective one-electron reduction of recently isolated cationic Li^+@C_{70}.[4] UV-vis-NIR absorption spectrum of the product in *o*-DCB showed broad absorption at around 700-1000 nm at room temperature (see Fig.), which indicated the formation of singly bonded Li@C_{70}-Li@C_{70} dimer through the coupling of spin centre on Li@C_{70}s.[5] Notably, the absorption of the dimer decreased as temperature increased, and new absorption assignable to Li@C_{70} monomer appeared at 1280 nm.[6] These results revealed the equilibrium behavior between Li@C_{70} and $(Li@C_{70})_2$ in the solvent, which was consistent with the results of theoretical calculation.

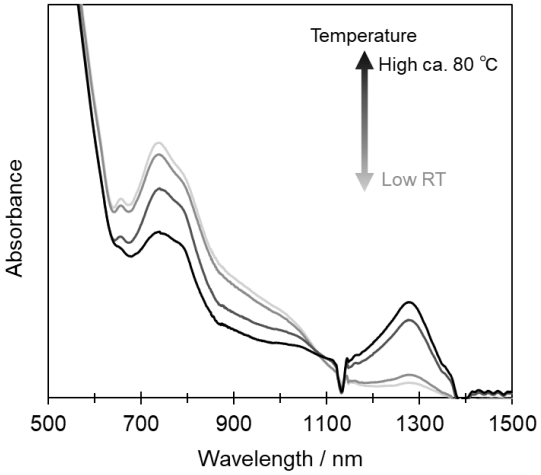

Fig. Temperature dependance of UV-vis-NIR absorption spectra of the product in *o*-DCB.

[1] A. Nakagawa *et al.*, *Nat. Commun.* **2018**, *9*, 3073. [2] Z. Wang *et al.*, *ACIE.* **2016**, *55*, 199.
[3] H. Ueno *et al.*, *Chem. Sci.* **2016**, *7*, 5770. [4] D. Kitabatake *et al.*, The 60th FNTG **2021**, 1P-11.
[5] D. V. Konarev *et al.*, *New J. Chem*. **2019**, *43*, 2726.
[6] D. R. Lawson *et al.*, *J. Phys. Chem*. **1992**, *96*, 7175.
Corresponding Author: H. Ueno, Tel: +81-22-795-7645, E-mail: hiroshi.ueno.d5@tohoku.ac.jp

Kinetic study of photopolymerization and thermal-depolymerization in C_{60} films

○Tatsuma Izumi[1], Masato Nakaya[1], Jun Onoe[1]

[1] *Department of Energy Science and Engineering, Nagoya University, Aichi 464-8603, Japan*

C_{60} film is attracted as a novel thermoelectric material because of its giant Seebeck coefficient ($S = -120$ mV/K). For practical use, it is necessary to increase a very low electrical conductivity ($\sigma = 10^{-6}$ Ω^{-1}cm^{-1}) of the C_{60} film to raise a power factor ($PF = S^2\sigma$). In general, although the σ of solid materials can be controlled by chemical carrier doping, this method reduces the $|S|$ owing to the trade-off relationship between $|S|$ and carrier density. Polymerization is a possible way to realize C_{60}-based high-PF materials, because the C_{60} polymer film exhibits a large σ due to an increase in the carrier mobility [1]. In the present study, we evaluated the proportion distribution of C_{60} monomer, dimer, trimer, and oligomers, which is an important factor for the σ and thermal stability, by examining the kinetics of photopolymerization and depolymerization in C_{60} films.

All experiments were carried out in an ultrahigh vacuum (UHV) chamber (base pressure: 10^{-6} Pa). A C_{60} film (300 nm thick) was formed on a cesium iodide (CsI) substrate by thermal evaporation of C_{60} powder (99.98%) in a quartz crucible. Thereafter, C_{60} polymerization was induced by irradiation of ultraviolet (UV) light (wavelength range: 300–410 nm, fluence: 0.2 W/cm^2). Photopolymerized products in the C_{60} film were evaluated using *in situ* Fourier-transform infrared (FT-IR) spectroscopy (resolution: 2cm^{-1}).

Figure 1 (a) shows the FT-IR spectra before and after 40h photoirradiation of pristine C_{60} film. The intensity of the four intense IR peaks (1429, 1183, 576, 526 cm^{-1}) attributed to C_{60} molecule decreased and new IR peaks appeared in the range of 700–800 cm^{-1} after photoirradiation. These new peaks were assigned to C_{60} dimer, trimer, and oligomers *via* [2 + 2] cycloaddition reaction [2]. We examined the time evolution of the IR peaks corresponding to monomer [$A_M(t)$] and dimer [$A_D(t)$] based on equations (1) and (2). Here, the rate constant k of A_{M0} was assumed to be equal to that of A_{Df} in a short irradiation time region.

$$A_M(t) = A_{M0}\exp(-kt) \quad (1),\ A_D(t) = A_{Df}\{1-\exp(-kt)\} \quad (2)$$

By fitting the time-variation of the experimental absorbance of the monomer (1183 cm^{-1}) and dimer (peak at 796 cm^{-1}) using Eqs. (1) and (2), we evaluated the proportion of C_{60} monomer, dimer, and oligomers in the photo-irradiated C_{60} film [Fig. 1 (b)], and found that the proportion of the oligomers was saturated to be 25% even after 40 h photoirradiation. In other words, C_{60} oligomers are hard to be produced only by varying photoirradiation time. To estimate the activation energy (E_a) of the dissociation of the dimer and oligomers, we examined the kinetics of thermal-depolymerization of the dimer and oligomers, and obtained E_a to be 1.26 eV for the dimer, which is in an excellent agreement with that reported previously [3], whereas 1.78 eV for the oligomers. We will discuss a way to control the proportion distributions of the dimer and oligomers using the difference in E_a between them.

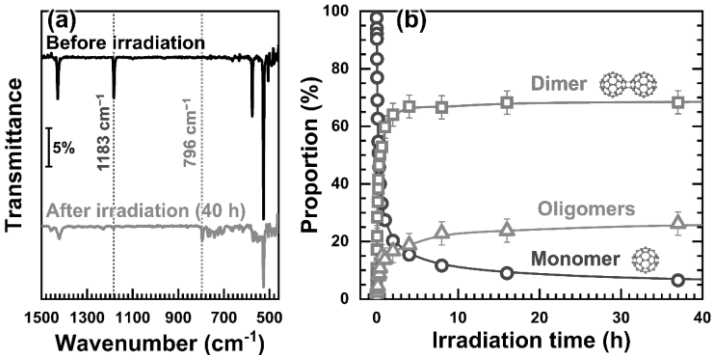

Fig. 1 (a) FT-IR spectra of the C_{60} film before and after 40 h photo-irradiation, and (b) the time evolution of the proportion of C_{60} monomer (circle), dimer (square), and oligomers (triangle) in the photoirradiation C_{60} film.

[1] J. Onoe *et al.*, *J. Appl. Phys.*, **96**, 443 (2004).
[2] J. Onoe *et al.*, *AIP Adv.*, **10**, 085212 (2020).
[3] P. Zhou *et al.*, *Chem. Phys. Lett*. **211**, 337 (1993).

Corresponding Author: Jun Onoe
Tel: +81-52-789-3784
E-mail: j-onoe@energy.nagoya-u.ac.jp

Development of Mobility and Charge Measurement System for Nanomaterials

Tomoya Ono, Kanata Oguri, and ○Toshiki Sugai

Department of Chemistry, Toho University, Miyama 2-2-1 Funabashi, 274-8510, Japan

Ion mobility spectrometry (IMS) combined with mass spectrometry has revealed novel information on nanomaterials such as fullerenes[1]. However, the sizes of nanomaterials have been growing wider and wider to carbon nanotubes or graphene for example. These materials cannot be detected by mass spectrometry so other measurement systems should be combined with IMS to study them. We have been working on nanocarbon materials such as graphene quantum dots with our newly developed IMS combined with ion trap and optical measurement system. Even with the new system it is still difficult to clarify their structures because mobility depends on both of structures and charges of samples. To overcome this difficulty, here we present simultaneous mobility and charge measurement system.

The system consists of an electrospray ion source (ESI) for production of positively charged nanoparticles from polystyrene particles (D=205 nm) dispersed in water, a trap type IMS, and a charge detector. Aggregated polystyrene particles with several tens of charges were produced by ESI and trapped in the IMS system under ambient condition. Then the particles were drifted around several centimeters, and then were detected by the charge detector. Figure 1 shows the correlation between detected charge and diameter calculated from the drift time and the amount of charge with the assumption of spherical structure. The observed distribution is well described by Rayleigh limit model deduced with water surface tension, which is believed as a standard ionization model of ESI[2]. This well fit result shows the whole measurements were performed without contradiction. The left end of the distribution is around 200 nm coming from single particles. This system can be applied any nanomaterials with wide size distribution.

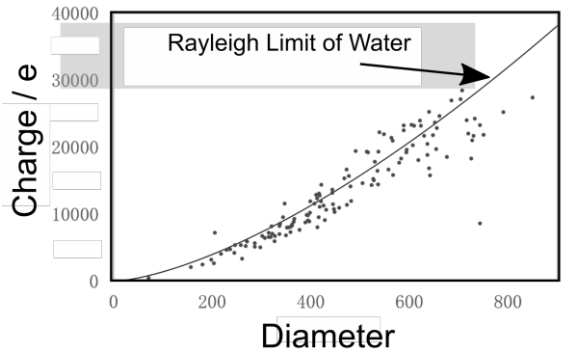

Fig. 1 Charge and size correlation of charged polystyrene particle aggregates.

[1] G. von Helden *et al.*, *J. Chem. Phys.*, **95**, 3835 (1991).

[2] L.Rayleigh, *Philos. Mag.*, **14**, 184 (1882).

TEL: +81-47-472-4406, E-mail: sugai@chem.sci.toho-u.ac.jp

New energy cycle “HI cycle” to repeat solar hydrogen generation and battery power generation

○Shinji Kawasaki, Kenta Kobayashi, Yosuke Ishii

Department of Life Science and Applied Chemistry, Nagoya Institute of Technology, Nagoya 466-8555, Japan

We propose a new energy cycle “HI cycle” to repeat solar hydrogen generation and battery power generation (Fig. 1). Solar hydrogen generation from HI solution enables the use of narrower band gap photocatalyst than that from water does. We demonstrated that the solar hydrogen generation from HI solution with methylammonium lead iodide ($MAPbI_3$) is effectively improved by the addition of single-walled carbon nanotubes (SWCNTs). SEM and TEM observations along with EDS analysis and Raman measurements revealed that SWCNTs improved the hydrogen generation by absorbing the by-product iodine molecules. It was also shown that we can fabricate zinc-iodine battery with the paper form zinc metal and the I@SWCNT sample recovered from the photocatalysis cell. The battery worked very efficiently with initial cell voltage of about 1.2 V. The capacity of the battery, corresponding to the amount of the encapsulated iodine molecules, revealed that SWCNTs had the ability to absorb the by-product iodine molecules very effectively in the photocatalysis cell. We also confirmed that the electrolyte solution after the discharge experiment should include not only iodide ions but also a considerable amount of hydrogen ions. It means that the solution returns to the starting point of the “HI cycle” after the battery discharge. Raman measurements revealed that iodine-filled SWCNTs formed by the solar hydrogen generation experiment were transformed back to empty tubes by the discharge experiment. This confirms that SWCNTs can be used repeatedly for hydrogen generation and energy storage using the proposed “HI cycle”.

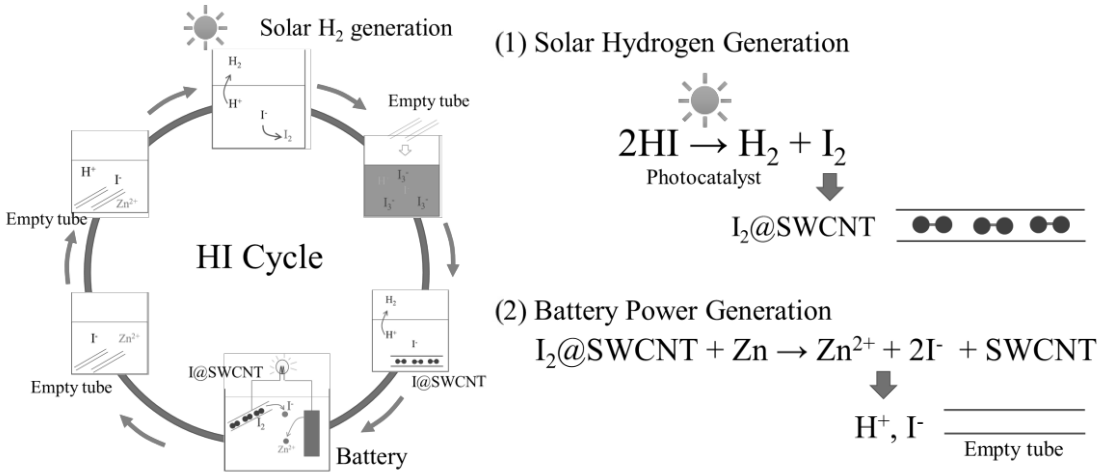

Fig.1 New energy cycle “HI Cycle” for repeated solar hydrogen generation and battery power generation.

Corresponding Author: S. Kawasaki
Tel: +81-52-735-5221, Fax: +81-52-735-5221
E-mail: kawasaki.shinji@nitech.ac.jp.

Synthesis of Pt nanoparticles supported on Single-Walled Carbon Nanotubes and its performance for fuel cell application

○Miftakhul Huda[1], Tomoya Kawahara[1], Satoru Hashimoto[2], Masaya Kawasumi[3], Yutaka Matsuo[1,3]

[1] *Department of Chemical System Engineering, Graduate School of Engineering, Nagoya University, Nagoya 464-8603, Japan*
[2] *Meijo Nano Carbon Co., Ltd., Nagoya 463-0003, Japan*
[3] *Institute of Materials Innovation, Institutes of Innovation for Future Society, Graduate School of Engineering, Nagoya University, Nagoya 464-8603, Japan*

Single-walled carbon nanotubes (SWCNT) is a versatile material for future application in electrochemical fields such as fuel cell electrodes by utilizing its high conductivity, high porosity, and high oxidation resistance. However, it is difficult to utilize SWCNT by synthesizing metallic nanoparticles supported on SWCNT due to its inert surface. Here, we demonstrated a simple solvo-thermal method to synthesize Pt metallic nanoparticles with a uniform size and high metal loading supported on e-DIPS-based SWCNT (diameter of 2 nm) without using any chemical template, harmful acid or oxidant. Similar method has been used to synthesize ultrathin Platinum nanowire without a support [1]. CV/LSV measurements were conducted to measure its performance as a catalyst of oxygen reduction reaction for fuel cell application using rotating disk electrode (RDE) test.

DMF 6 mL, Etylene glycol 4 mL, and $H_2PtCl_6.6H_2O$ 8wt% 100 mg were mixed and stirred before added with SWCNT. Then, the solution was reacted in autoclave at 170℃ to promote the synthesis of Pt nanoparticles. Pt nanoparticles supported on SWCNT with an average size of 3.5 nm and Pt loading of 18.6 wt% were obtained. CV/LSV measurements revealed that the Pt@SWCNT mass activity of 577 A/g-Pt and the specific activity of 800 μ A/cm^2-Pt were two fold higher than those of commercial Pt/C. This result demonstrated that metallic nanocatalysts supported on SWCNT are promising as a cathode electrode for future fuel cell with high current density and high voltage durability. This work is supported by NEDO (20001303-0).

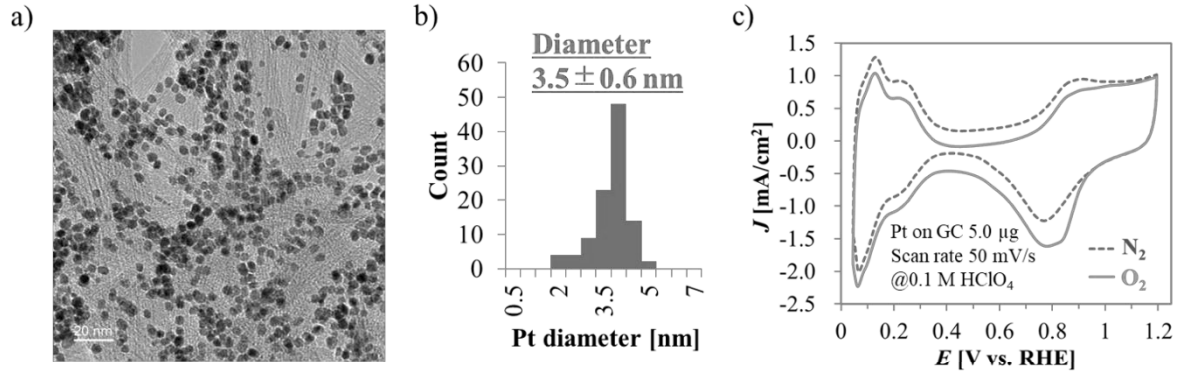

Fig. 1 a) TEM image of Pt@SWCNT. b) The size distribution of Pt nanoparticles. c) CV measurement result of Pt@SWCNT using RDE test.

[1] B.Y. Xia *et al*. J. Am. Chem. Soc., 135, 9480 (2013).

Corresponding Author: M. Huda
Tel: +81-52-789-3231,
E-mail: huda.miftakhul@material.nagoya-u.ac.jp

Optical Properties of Multi-Layer Graphene

○Masahiro Kamada[1], Takamoto Yokosawa[1], Taisuke Ochi[1], Ken-ichi Sasaki[2], and Tomohiro Matsui[1]

[1] *Advanced Research Laboratory, Anritsu Corporation, 5-1-1 Onna, Atsugi, Kanagawa 243-8555, Japan*
[2] *NTT Research Center for Theoretical Quantum Physics, NTT Basic Research Laboratories, NTT Corporation, 3-1 Morinosato Wakamiya, Atsugi, Kanagawa 243-0198, Japan*

Not only monolayer graphene but also multi-layer ones are important to study especially in application point of view. For example, multi-layer graphene has a band gap, and the light absorption is expected to become the maximum at the layer number of 87 [1]. However, an efficient method to identify the number of layers has not been established, although it can estimate rather easily by optical contrast up to 6 layers [2,3]. Here, the contrast of graphene exfoliated on SiO_2/Si substrate is a resultant of the interference of light reflected at interfaces between Si, SiO_2 and graphene. In this context, the contrast is expected to change periodically by increasing the number of graphene layers.

In this paper, optical contrast of multi-layer graphene up to 100 nm thick (300 layers) on SiO_2 with 285 nm thick is studied. The contrast C_i (i = R, G, B) is analyzed from the RGB components of optical images and defined as $C_i = 1 - I_{gr,i} / I_{0,i}$, where I_{gr} and I_0 are the RGB intensity of graphene and SiO_2 surface, respectively. The thickness dependence of C_i is shown in Fig.1. The contrast of G (green) component (C_G) takes its maximum at $t \sim 8$ nm, and then saturates at $t \sim 50$ nm. Such reentrant and saturation behavior is also observed for C_R and C_B but with different maximum values at different thickness. In addition, these are well reproduced by the contrast measured at certain wavelength rather than the RGB values. This reentrant behavior is consistent with the expected periodic behavior and qualitatively reproduced by a detailed calculation, which will be presented elsewhere [4]. On the other hand, the saturation and the difference between C_R, C_G, and C_B was not fully expected. It probably indicates that the thick graphene gradually loses its transparency and gets closer to bulk graphite. By using these RGB contrast, one can estimate the number of layers up to ~120 (40 nm) with ~10 layers of certainty.

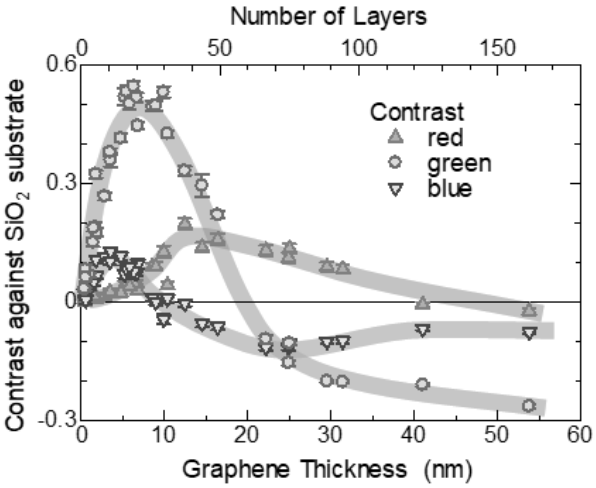

Fig.1 Thickness dependence of RGB contrast between graphene and SiO_2 substrate. The thick lines are guides to the eye.

[1] K. Sasaki and K. Hitachi, Commun. Phys. **3**, 90 (2020).
[2] P. Blake *et al.* Appl. Phys. Lett. **91**, 063124 (2007).
[3] B. Ma *et al.* Carbon **109**, 384 (2016).
[4] K. Sasaki, *et al.*, in this symposium

Corresponding Author: T. Matsui, M. Kamada
Tel: +81-(0)46-296-6594
E-mail: Tomohiro.Matsui@anritsu.com, Masahiro.Kamada@anritsu.com

Complex Raman tensor in Black Phosphorus and 2D materials

○Riichiro Saito[1], Nguyen Tuan Hung[2], Yan Zhao[3], Shiyi Han[3], Lianming Tong[3]

[1] *Department of Physics, Tohoku University, Sendai 980-8578, Japan*
[2]*Frontier Research Institute for Interdisciplinary Sciences, Tohoku University, Japan*
[3]*College of Chemistry and Molecular Engineering, Peking University, Beijing 100871, P. R. China*

Raman tensor, $\boldsymbol{R}$, is a tensor for calculating Raman-scattering amplitude combined with given vectors $\boldsymbol{e_i}$ and $\boldsymbol{e_f}$ of incident and scattered lights. Using the Raman tensor, Raman intensity is given by $\left|\boldsymbol{e_f R e_i}\right|^2$. In the quantum description of Raman tensor, Raman tensor is given by the product of two electron-photon matrix elements and one electron-phonon matrix element. These matrix elements are generally complex values and thus Raman tensor is generally given by a complex tensor. When we represent a complex number Z as $Z = |Z|e^{i\sigma}$, the phase σ does not give any physical meaning since most of physical properties is given by $|Z|^2$. However, when the values of σ for two matrix elements of the complex Raman tensor is different from each other as shown in Fig. 1, the difference of σ's can be seen in Raman spectroscopy.

Here we report that the phase difference of complex Raman tensor is observed for black phosphorus by using circularly polarized light in the polarized Raman spectroscopy after passing the quarter wave plate. In this measurement, the polarized Raman intensity peak is shifted from the crystal orientation as shown in the top of Fig. 1, which can not be explained by real Raman tensor. By comparing with calculated complex Raman tensor for each phonon mode by first principles calculation as a function of laser excitation energy, we explain the origin of the shift in the polarized Raman spectroscopy. Further, we also discuss the calculated Raman tensor of two-dimensional transition metal dichalcogenides and their physical origin

Corresponding Author: R. Saito
Tel: +81-22-795-7754, Fax: +81-22-795-6447,
E-mail: rsaito@flex.phys.tohoku.ac.jp
Web: http://flex.phys.tohoku.ac.jp

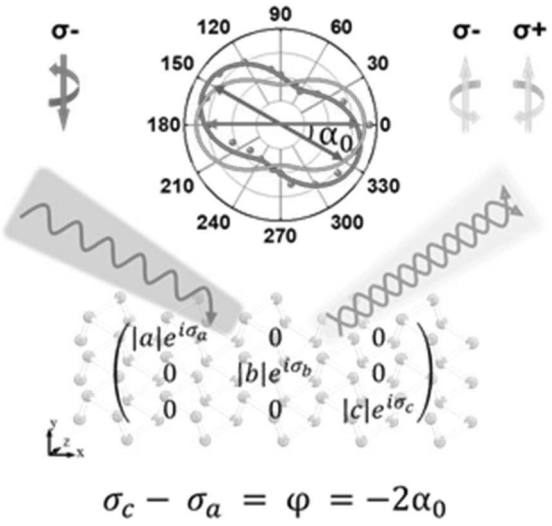

Fig. 1 When the phases, σ_c and σ_a are not the same in the Raman tensor, we can observe the difference of $\sigma_c - \sigma_a$ as a shift of angle α_0 in the polarized Raman measurement in the Raman intensity by using circularly polarized light.

A small number of moiré exciton photoluminescence in nanofabricated $MoSe_2/WSe_2$ heterobilayers

○Yuki Okamura[1], Keisuke Shinokita[1], Kenji Watanabe[2], Takashi Taniguchi[2], and Kazunari Matsuda[1]

[1] *Institute of Advanced Energy, Kyoto University, Uji 611-0011, Japan*
[2] *National Institute for Materials Science, Tsukuba 305-0044, Japan*

Atomically thin transition metal dichalcogenides and their van der Waals heterostructures have attracted tremendous attention because of their new optical properties and functionality [1]. The moiré patterns of van der Waals heterostructures originating from a specific atomic arrangement trap optically excited excitons as a periodic potential, and the confined excitons (moiré excitons) work as a zero-dimensional (0D) and quantum two-level system, which is promising for quantum optics and quantum information process [2-4]. However, in the optical measurements, the broad emission spectra from thousands to millions of inhomogeneously distributed moiré excitons due to the diffraction limit of light would blur the intrinsic 0D optical properties.

Here we studied the optical properties of nanofabricated $MoSe_2/WSe_2$ heterobilayers with a smaller area than the diffraction limit of light. The $MoSe_2/WSe_2$ heterobilayers were fabricated into a pillar shape with a diameter of 200 nm under focused ion beam (FIB) irradiation (the inset of Fig. 1). Figure 1 shows the photoluminescence (PL) spectra of the heterobilayers with and without the FIB process (red and black lines, respectively). The heterobilayers without the FIB process show substantial broad emission with a linewidth of 50 meV and several sharp peaks with a linewidth of 1 meV. The broad emission originates from the inhomogeneously distributed moiré excitions in the optical spot area. On the other hand, the heterobilayers with the FIB process show only a few sharp emission peaks. The sharp emission originates from a small number of moiré excitons from the smaller FIB processed area than the spot diameter (~1 μm), reflecting the intrinsic 0D nature of the moiré excitons. In the presentation, we will discuss further the intrinsic properties of moiré excitons based on the intensity and temperature dependence of PL spectra.

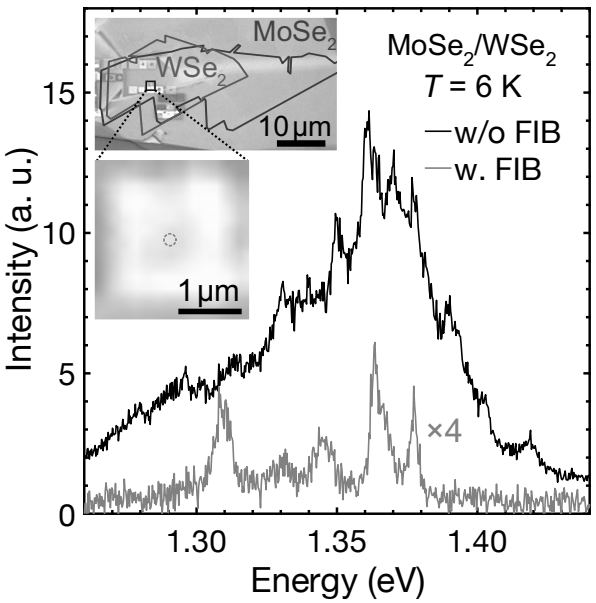

Fig. 1 PL spectra of $MoSe_2/WSe_2$ heterobilayers with and without FIB process. Inset: Optical image of the $MoSe_2/WSe_2$ heterobilayers.

[1] P. Rivera *et al., Nat. Nano*. **13**, 1004 (2018).
[2] K. L. Seyler *et al., Nature* **567**, 66 (2019).
[3] K. Tran *et al., Nature* **567**, 71 (2019).
[4] K. Shinokita *et al., Nano Lett.* **21**, 5938 (2021).

Corresponding Author: Kazunari Matsuda
Tel: +81-774-38-3460,
E-mail: matsuda@iae.kyoto-u.ac.jp

Color-Tunable Light-Emitting Devices Based on Compositionally Graded Monolayer Transition Metal Dichalcogenide Alloys

○Hao Ou[1], Jiang Pu[1,*], Tomoyuki Yamada[1], Naoki Wada[2], Hibiki Naito[2], Zheng Liu[3], Yasumitsu Miyata[2], Taishi Takenobu[1,*]

[1] *Department of Applied Physics, Nagoya University, Nagoya 464-8603, Japan*
[2] *Department of Physics, Tokyo Metropolitan University, Tokyo 192-0397, Japan*
[3] *Inorganic Functional Materials Research Institute, AIST, Nagoya, 463-8560, Japan*

Monolayer transition metal dichalcogenides (TMDCs) show many exotic optical performances, enabling them potential candidates for future optoelectronics [1]. Conventionally, both mechanically exfoliated and chemically grown monolayer TMDCs have binary atomic composition, *i.e.* two types of atoms, and then, their electronic structure are fixed. In contrast, when producing ternary alloy of TMDC, the physical and chemical properties could drastically change as tuning the ratio of hetero-atoms [1]. As a result, the device applicability of the material is also expanded, such as transistors and photodiodes. However, the light-emitting devices using TMDC alloys have not yet been achieved, possibly due to the sample qualities and/or technical issues of device fabrications. Here we report on the realization of color-tunable light-emitting device using $WS_{2x}Se_{2-2x}$ alloy with spatially varying ternary atomic composition.

By the dynamic control of growth parameters during chemical vapor deposition (CVD) process, spatially graded monolayer $WS_{2x}Se_{2-2x}$ alloy was successfully synthesized. From the photoluminescence (PL) spectra, position-dependent PL energy change owing to gradual variation of composition could be confirmed, since the PL peak shifts between typical WS_2 peak and WSe_2 peak. We then utilized the alloy to fabricate light-emitting device, using the two-terminal electrolyte-based light-emitting device structure (Fig. 1) [3].

The alloy device shows clear electroluminescence (EL) at relatively low driving voltage (2 to 4 V), giving the first demonstration of TMDC-based alloy light-emitting device. Furthermore, we found that with tuning the applied voltage for device, the light-emitting position (location of EL) shifts monotonically between two electrodes (Fig. 1, up). Because of the spatially graded composition of alloy, the EL spectrum also changes (Fig. 1, down). As a result, the color of light emission should present voltage (location) dependence. By analyzing both EL images and spectra, it's noticed that the emission color was continuously tuned. Our demonstration on light-emitting device using monolayer TMDC alloy, along with the observed continuous tunability of EL color, provide a new approach to the broadband optoelectronic applications based on monolayer semiconductors.

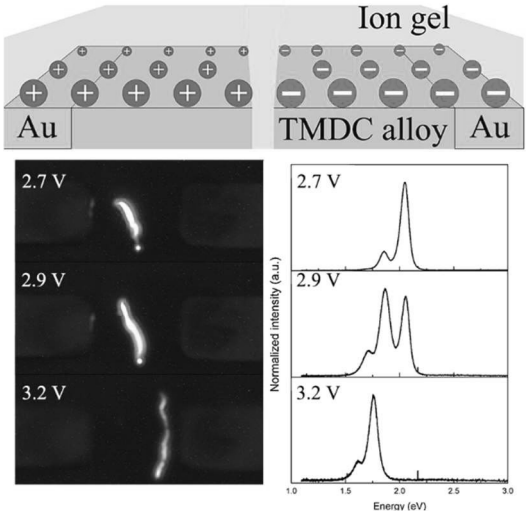

Fig. 1. Light-emitting device structure (up) and EL images with corresponding EL spectra.

[1] J. Mann et al., Adv. Mater. 26, 1304389 (2014).
[2] J. Pu et al., Adv. Mater. 30, 1707627 (2018).
[3] J. Pu et al., Adv. Mater. 29, 1606918 (2017).

Corresponding Author: J. Pu and T. Takenobu
Tel: +81-52-789-5165, Fax: +81-52-789-5165,
E-mail: jiang.pu@nagoya-u.jp, takenobu@nagoya-u.jp

G/D ratio of SWCNT solution

○Hiromichi Kataura[1], Mayumi Tsuzuki[1], Takeshi Tanaka[1]

[1] *Nanomaterials Research Institute, AIST, Tsukuba 305-8565, Japan*

Defect assessment of single-wall carbon nanotubes (SWCNTs) is very important for electronic device applications of SWCNTs, because the electronic mobility is highly depending on their structural defects. Intensity ratio of G-band and D-band (G/D ratio) in Raman spectra is often used for the defect assessment of sp^2 carbon materials including SWCNTs. In case of SWCNTs, however, it is known that we must consider the resonance effects because G-band intensity is highly depending on the optical absorption of the incident laser light. Furthermore, in this work, we found that the G/D ratio depends on the sort of surfactants when we measure the Raman spectra of SWCNT aqueous solutions. Fig.1 shows the G/D ratios of NOPO Hipco solutions for different concentrations of sodium deoxy cholate (DOC) mixed with sodium cholate (SC). Since the used SWCNTs were from same solution without any additional sonication, observed G/D change was simply caused by the difference of wrapping surfactants. We found that both the G-band and D-band intensities were changed by changing DOC concentration. Because the change of G/D value is very large, we must consider this surfactant effects for the defect assessment of SWCNTs.

Since we used mixed chirality sample for this measurement, detailed resonance analysis is very difficult. We are now preparing single chirality sample for the advanced experiments. We will show the latest results in the meeting.

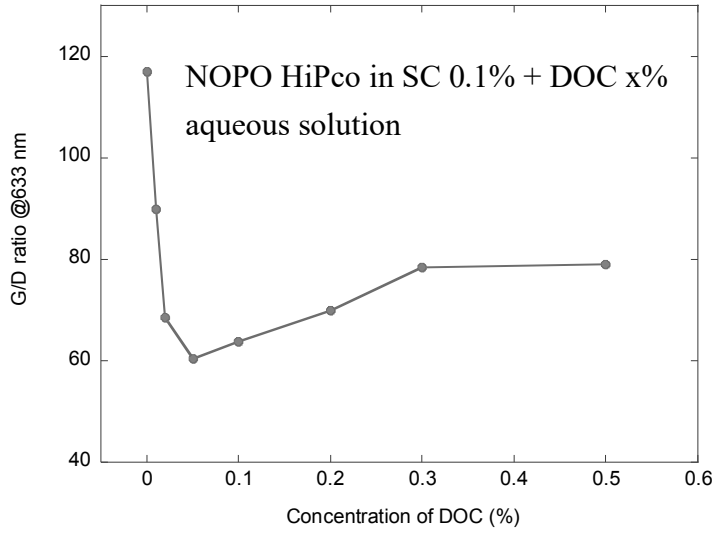

Fig. 1 G/D Raman intensity ratios of NOPO Hipco aqueous solutions. Concentration of DOC was changed from 0.01 to 0.5% keeping both concentrations of SWCNT and SC (0.1%). All measurements were done without any additional sonication.

Corresponding Author: H. Kataura
E-mail: h-kataura@aist.go.jp

Semiconductor nanochannels in metallic carbon nanotubes by thermomechanical chirality alteration

○ Dai-Ming Tang[1], Dmitry G. Kvashnin[2], Ovidiu Cretu[3], Guohai Chen[4], Don N. Futaba[4], Yongjia Zheng[5], Rong Xiang[5], Shigeo Maruyama[5], Hui-Ming Cheng[6], Yoshio Bando[7], Chang Liu[6], Pavel B. Sorokin[8], Dmitri Golberg[1,9]

[1] International Center for Materials Nanoarchitectonics (MANA), National Institute for Materials Science (NIMS), Tsukuba 305-0044, Japan.
[2] Emanuel Institute of Biochemical Physics, Moscow 119334, Russian Federation.
[3] Research Center for Advanced Measurement and Characterization, National Institute for Materials Science (NIMS), Tsukuba 305-0044, Japan.
[4] CNT-Application Research Center, National Institute of Advanced Industrial Science and Technology (AIST), Tsukuba 305-8565, Japan.
[5] Department of Mechanical Engineering, The University of Tokyo, Tokyo 113-8656, Japan.
[6] Shenyang National Laboratory for Materials Science, Institute of Metal Research, Chinese Academy of Sciences, Shenyang 110016, China.
[7] Australian Institute for Innovative Materials, University of Wollongong, North Wollongong NSW 2500, Australia.
[8] National University of Science and Technology MISIS, Moscow 119049, Russian Federation.
[9] Centre for Materials Science and School of Chemistry and Physics, Queensland University of Technology (QUT), Brisbane QLD 4000, Australia.

Carbon nanotubes have a helical structure where the chirality determines them to be metallic or semiconducting. Using in situ transmission electron microscopy,[1] we applied heating and mechanical strain to alter the local chirality and thus to control the electronic properties of individual carbon nanotubes. A transition trend towards larger chiral angle region was observed and explained in terms of orientation-dependent dislocation formation energy. Controlled metal-to-semiconductor transition was realized to create nanotube transistors with a semiconducting nanotube channel covalently bonded between metallic nanotube source and drain. In addition, quantum transport at room temperature was demonstrated for the fabricated nanotube transistors with the channel length down to 2.8 nanometers.[2]

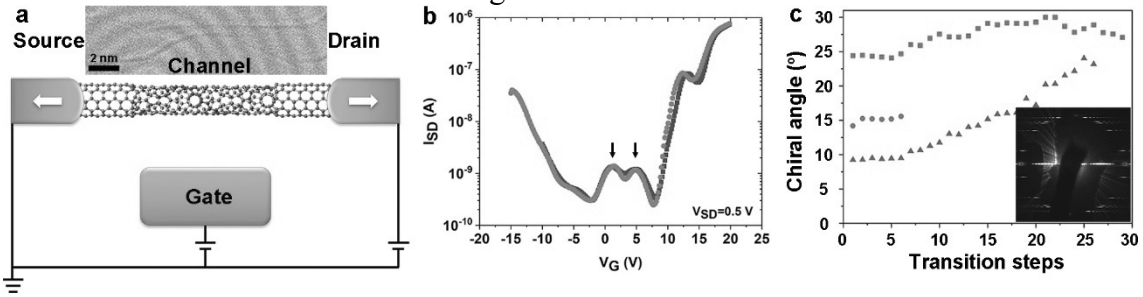

Fig. 1: (a) TEM image and schematic of a CNT intramolecular transistor with local chirality altered. (b) I_{SD}-V_G transport measurements of the ultrashort channel transistor. Resonant conductance peaks in the gap are indicated by arrows. (c) Electron diffraction pattern and changes of the chiral angles revealing a converging trend toward large angles.

[1] D.-M. Tang *et al*. Ultramicroscopy, **194**, 108, (2018).
[2] D.-M. Tang *et al*. Science, **374**, 1616 (2021).

Corresponding Author: D.-M. Tang
Tel: +81-29-860-4949,
E-mail: tang.daiming@nims.go.jp

The influence of pH, temperature and hypochlorite concentration on the removal of carbon nanotubes from aqueous dispersion

○Minfang Zhang[1], Mei Yang[1], Toshiya Okazaki [1]

[1] *National Institute of Advanced Industrial Science and Technology (AIST), CNT Application Research Center1-1-1 Higashi, Tsukuba, Ibaraki, 305-8565, Japann*

The treatment of carbon nanotubes (CNTs) containing wastewater has become to an important issue with the increase of industrial application due to the concerns from potential risk of CNTs to the environment and human health. However, no standard guideline for treatment of the wastewater containing CNTs has been established at this moment. Recently, we have proposed a method to remove CNTs from aqueous dispersions by using sodium hypochlorite (NaClO) [1]. For practical application of this method, in this study, we investigated [2] the influence of various conditions, such as reaction temperature, NaClO concentration, CNT concentration and pH value to the CNT-degradation rates. The results (Table 1) showed that the degradation of CNTs depends strongly on the temperature, and NaClO concentration. The higher temperature and higher NaClO concentration had faster degradation-rates of CNTs. The rational temperature and the concentration of NaClO are suggested to be 50-70°C and 2-3 % (g/g). Lower pH condition accelerated the elimination speed but induced the toxic chlorine and hypochlorite gases during the reaction. Furthermore, the dispersant or other substance in the solution would also consume NaClO, thus affecting the degradation rate. These findings would be of significance to establishing a standard technique for CNT-containing industrial wastewater treatment and then advancing the environmental sustainability of the CNT industry.

Table 1. The times for SG/BSA degradation by NaClO solution at different conditions

Treatment conditions	**NaClO concentration (wt%)** (37°C, pH: 10.20; SG/BSA: 10μg/mL)					**Temperature** (NaClO: 2.26 wt%, pH10.20; SG/BSA: 10μg/mL)					**pH values** (NaClO: 2.26 wt%, 37°C SG/BSA: 10μg/mL)				
	0.22	0.45	1.13	2.26	4.52	25°C	37°C	50°C	70°C	80°C	3.94	6.88	10.20	12.42	13.50
Half-life (h)	6.34	3.31	1.94	0.72	0.43	2.16	0.96	0.50	0.20	0.17	0.44	0.42	0.82	5	15
Complete degradation	>8 days	~144 h	~72 h	~54 h	~41 h	~120 h	~48 h	~24 h	~3 h	~2 h	~48 h	~48 h	~48 h	>7 days	>7 days

[1] M. Zhang *et al*. Scientific Reports, **9**, 1284 (2019).
[2] M. Yang *et al*. Toxics, **9**, 223 (2021)

Corresponding Author: Corresponding author: M. Zhang,
Tel: 029-861-6758
E-mail: m-zhang@aist.go.jp.

Carbon Nanotubes as Materials for Non-precious Metal Electrocatalysts with High ORR and OER Performances and their Applications

Pandian Ganesan[1], Aleksandar Staykov[1],Hiroaki Shu[2], Mitsugu Uejima[2], Naotoshi Nakashima[1]

[1]International Institute for Carbon Neutral-Energy Research (WPI-I2CNER), Kyushu University, Fukuoka, Japan; [2]ZEON Corporation, Chiyoda-ku, Tokyo

In recent years, a sustainable and low-carbon emission energy chain has attracted much attention. Toward the goal, the development of non-precious metal electrocatalysts for fuel cells, water splitting and batteries with high performance, durability, and scalability is a strong social demand for the next-generation eco-friendly energy society[1]. We have already reported that i) nanocarbons/iron phthalocyanine (II) hybrids with well-defined nanostructures show excellent efficiency for oxygen reduction reaction (ORR)[2,3], ii) decorating unoxidized-carbon nanotubes with homogeneous Ni-Co-spinel nanocrystals that show superior performance for oxygen evolution (OER) and ORR[4] and iii) Fe^{III}-doped nickel sulfides/carbon nanotube hybrid catalyst for alkaline electrolyte membrane water electrolyzer and enhanced Zn-air battery performance[5].

Here we report the design and synthesis of a less-expensive metal-coordinated polymer/nanocarbon (Vulcan, porous carbon, 2-differernt multi-walled carbon nanotubes, or single-walled carbon nanotubes) hybrid catalysts. The catalysts were found to show high oxygen electrode performance with ORR: $E_{1/2}$: 0.81V *vs*. RHE, and OER: 1.57 V *vs*. RHE at 10 mA/cm^2. The catalyst also showed an efficient and durable cathode for a rechargeable Zn-air battery (charge-discharge overpotential gap of 0.45 V). Such a study is of importance in the development of advanced energy materials in batteries and molecular catalyst.

References

[1] N. Nakashima (Editor), "Nanocarbons for Energy Conversion-Supramolecular Approach-", Springer, **2018**, pp. 1-564.
[2] J. Yang, J. Tao, T. Isomura, H. Yanagi, I. Moriguchi, N. Nakashima, *Carbon*, **2019**, *145*, 565-571.
[3] J. Yang, F. Toshimitsu, T. Fujigaya, N. Nakashima, *J. Mater. Chem. A*, **2017**, *5*, 1184-1191
[4] J. Yang, T. Fujigaya, N. Nakashima, *Sci. Rep*., **2017**, *7*, art.no.45384.
[5] P. Ganesan, A. Staykov, H. Shu, M. Uejima, N. Nakashima, *ACS Appl. Energy Mater*. **2020**, *3*, 10961-10975.

Corresponding Author: N. Nakashima
Tel: +81-92-802-6745, Fax: Tel: +81-92-802-6745, E-mail:
nakashima.naotoshi.614@m.kyushu-u.ac.jp

Thermoelectric energy conversion of 3D topological insulators

○Nguyen T. Hung[1,2], F. R. Pratama[1], Riichiro Saito[2]

[1] *Frontier Research Institute for Interdisciplinary Sciences, Tohoku University, Japan*
[2] *Department of Physics, Tohoku University, Japan*

Enhancement of thermoelectric energy-conversion has been investigating for low-dimensional materials (1D & 2D) because of the quantum confinement of electrons or holes in the materials [1, 2]. The quantum confinement gives an enhancement of electronic density of state (DOS) at the Fermi energy and kinetic energy of electrons if the typical size of the material is smaller than thermal de Broglie length [3]. However, the thermal de Broglie length (~ 5-100 nm) depends on effective mass of the materials which makes difficult to control the thermal de Broglie length.

On the other hand, the confinement of carriers is possible, too, even for three-dimensional (3D) materials when we apply the magnetic field. Skinner and Fu discussed the enhancement of thermoelectric power (or the Seebeck coefficient) of the 3D Dirac or Weyl materials in the presence of a strong magnetic field [4], in which the forming Landau levels contributes to the enhancement of DOS. In this study, we show two other ways to improve the thermoelectric performance of the 3D topological insulators. One way is that the electrons are confined by 1D nodal line at the Fermi energy for the 3D type-II nodal-line semimetal, as shown in Fig. 1 [5]. Another way is that electrons are confined by not only the high magnetic field but also the electric field applied to the 3D Dirac/Weyl materials. Our results show that the Seebeck coefficient of type II nodal-line semimetal can be larger than the upper limit of the metal (~ 87 μV/K) which was calculated 2D electron gas.

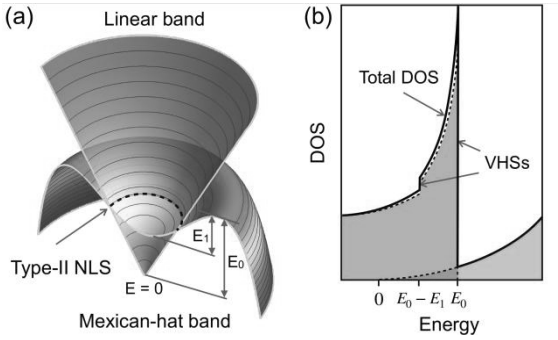

Fig. 1: (a) Two-band model for type II nodal-line (dashed line) semimetal. (b) Total density of states has two van Hove singularities.

[1] L. D. Hicks *et al*. Phys. Rev. B **47**, 16631 (1993).
[2] N. T. Hung *et al.* Phys. Rev. Lett. **117**, 036602 (2016).
[3] N. T. Hung *et al.* Adv. Quantum Technol. **4**, 2000115 (2021).
[4] B. Skinner and L. Fu, Sci. Adv. **4**, eaat2621 (2018).
[5] N. T. Hung *et al.* arXiv:2112.03525

Corresponding Author: Nguyen T. Hung
E-mail: nguyen@flex.phys.tohoku.ac.jp
Home: https://nguyen-group.github.io/

Direct synthesis of graphene nanoribbon ballistic Josephson junction

○Naofumi Sato[1], Toshiro Kaneko[1], Tomohiro Otsuka[2], Toshiaki Kato[1]

[1] *Graduate School of Engineering, Tohoku University, Sendai 980-8579, Japan*
[2] *Research Institute of Electrical Communication, Tohoku University, Sendai 980-8577, Japan*

Graphene nanoribbon (GNR), strips of two-dimensional (2D) graphene into one-dimensional (1D) structure, gather intense attentions because of their superior electrical features. Until now, we developed a novel method based on the advanced plasma CVD with nanoscale metal catalyst (metal nanobar) for position selective synthesis of GNR in wafer scale [1, 2]. In this study, we attempted to grow GNR from MoRe (Molybdenum-rhenium) nanobar, known as a superconductor metal, for the integrated synthesis of GNR-based Josephson junction devices.

Systematic investigation revealed that GNR can be synthesized from the MoRe nanobar (Fig.1). Detailed measurements at cryogenic temperatures revealed that resistance of GNR device rapidly decrease with temperature and clear two-step depletions are observed around 15K and 5K. Furthermore, the zero resistance is realized below 3K (Fig.2). These indicate Josephson junction is successfully formed in our device. The color mapping of the differential resistance dV/dI as a function of gate voltage V_g and source-drain current I_{sd} shows the critical current tends to be modulated by V_g, indicating the Josephson junction may be formed through the MoRe-GNR-MoRe structure. Furthermore, the clear oscillations of critical current were observed in the specific gate voltage region, which can be explained by Fabry–Pérot interferences in the supercurrent through the junction. This means that the carriers in the GNR are ballistically transported in our MoRe-GNR-MoRe Josephson device. These results can contribute to realizing large scale integration of GNR-based high performance Josephson junction devices.

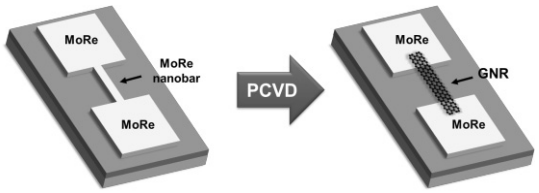

Fig. 1. Schematic illustration of suspended GNR grown from MoRe nanobar by our plasma CVD.

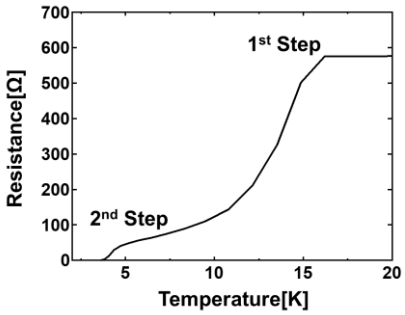

Fig. 2. Temperature dependence of resistance in MoRe-GNR-MoRe junction device.

[1] T. Kato and R. Hatakeyama, *Nature Nanotechnology*, **7**, 651-656 (2012).
[2] H. Suzuki, T. Kaneko, Y. Shibuta, M. Ohno, Y. Maekawa, T. Kato, *Nature Communications*, **7**, 11797-1-10 (2016).

Corresponding Author: T. Kato
Tel: +8122-795-7046, Fax: +8122-263-9225,
E-mail: kato12@tohoku.ac.jp

Fabrication and electronic transport properties of multilayer $Nb_xMo_{1-x}S_2/MoS_2$ in-plane heterostructures

○Hiroto Ogura[1], Seiya Kawasaki[1], Zheng Liu[2], Takahiko Endo[1], Yusuke Nakanishi[1], Hong En Lim[1], Kazuhiro Yanagi[1], Toshifumi Irisawa[3], Keiji Ueno[4], Kosuke Nagashio[5], Yasumitsu Miyata[1]

[1] *Department of Physics, Tokyo Metropolitan University, Hachioji, 192-0397, Japan*
[2] *Innovative Functional Materials Research Institute, AIST, Nagoya, 463-8560, Japan*
[3] *Nanoelectronics Research Institute, AIST, Tsukuba, 305-8562, Japan*
[4] *Department of Chemistry, Saitama University, Saitama 338-8570, Japan*
[5] *Department of Materials Engineering, The University of Tokyo, Tokyo, 113-8656, Japan*

Heterostructures of transition metal dichalcogenides (TMDCs) have attracted much attention for high-performance tunneling field-effect transistors (TFETs) due to their air stability and atomically steep interfaces. So far, band-to-band tunneling at the heterojunction has been often studied for various TMDC-based vertical heterostructures [1, 2]. In contrast, in-plane semiconductor heterojunctions of TMDCs have been also proposed recently to be promising for TFETs [3]. Especially, multilayer TMDCs possess an advantage in terms of the availability of highly doped TMDCs. Therefore, it is important to characterize the in-plane heterostructures based on various multilayer TMDCs. In this study, we have fabricated and investigated the electronic transport properties of multilayer $Nb_xMo_{1-x}S_2/MoS_2$ in-plane heterostructures.

Multilayer $Nb_xMo_{1-x}S_2$ or WSe_2 crystals were prepared on the SiO_2/Si substrates by mechanical exfoliation, and MoS_2 was then grown by chemical vapor deposition [4]. Cross-sectional HAADF-STEM observations reveal the growth of MoS_2 from the edge of the WSe_2 crystal and the formation of an atomically steep interface (Fig. 1a). Multilayer $Nb_xMo_{1-x}S_2/MoS_2$ in-plane heterostructures were also formed in the same manner (Fig. 1b). Interestingly, the $Nb_xMo_{1-x}S_2/MoS_2$ heterostructure shows a negative differential resistance (NDR) trend below 100 K (Fig. 1c). These results provide important insights into the application of multilayer TMDC in-plane heterostructures in future device applications.

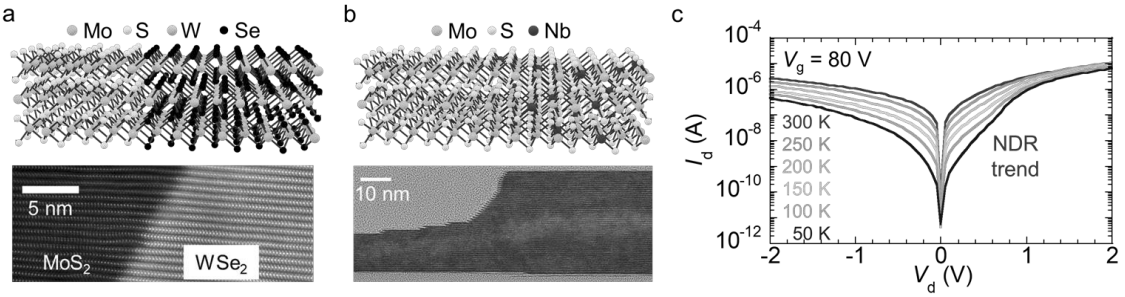

Figure 1 (a) Schematic and cross-sectional HAADF-STEM images of multilayer WSe_2/MoS_2 in-plane heterostructure. (b) Schematic and cross-sectional TEM images of multilayer $Nb_xMo_{1-x}S_2/MoS_2$ in-plane heterostructure. (c) Output curves of the $Nb_xMo_{1-x}S_2/MoS_2$ device at different temperatures at the back-gate voltage of 80 V.

[1] T. Roy *et al*., *ACS Nano*, **9**, 2, 2071–2079 (2015). [2] K. Nakamura *et al*., *ACS Appl. Mater. Interfaces.*, **12**, 51598-51606 (2020). [3] T. Fukui *et al*., The 82nd JSAP Autumn Meeting, 13a-N307-11 (2021). [4] K. Kojima *et al*., *Nanoscale*, **11** 12798 (2019).

Corresponding Author: Y. Miyata, Tel: +81-042-677-2508, E-mail: miyata-yasumitsu@tmu.ac.jp

Edges of Layered MoS_2 Observed by Field Electron Emission and Field Ion Microscopy

○Yahachi Saito

Toyota Physical and Chemical Research Institute, Nagakute 480-1192, Japan

Monolayer MoS2 possesses a variety of polymorphs such as 1H, 1T and 1T'. Among them, the 2-dimentional 1T' structure is predicted to be in a topological insulator (TI) phase [1], and the presence of gapless helical edge states is suggested [2]. Knowledge of atomic and electronic structures of layered MoS_2 would deepen the understanding the fascinating 2-dimentional (2D) TI phase.

Field electron emission and field ion microscopies (FEM and FIM) are powerful techniques to study atomic structures and dynamics of solid surfaces and edges. For graphene, FEM and FIM show characteristic images representing electronic orbitals at its edges [3]. In the present report, experimental results of FEM and FIM study on layered MoS_2 are presented.

MoS_2 field emitters were prepared by mechanical exfoliation of a bulk MoS_2 single crystal. Measurement procedures of FEM/FIM are described in Ref. [4].

A scanning electron microscopy (SEM) image of an edge of the exfoliated MoS_2 single crystal is shown in Fig. 1. Clear-cut edges with polygonal shapes are revealed. The thickness of the MoS_2 flake is estimated to be around 100nm, and thus the emitter is multilayered. Figure 2 (a) is an FEM image of the exfoliated MoS_2, showing an array of elongated broad spots. The elongation of spots is caused by the 2D nature of MoS_2, like graphene emitters [3]. Figure 2 (b) shows the corresponding FIM image, for which Ne gas was used as an imaging gas, exhibiting arrays of streaks and dipole spots (indicated by arrows) running transverse to the layered plane of MoS_2. These FIM patterns, possessing atomic resolutions, originate from atomic positions and empty electronic orbitals at the edges of MoS_2.

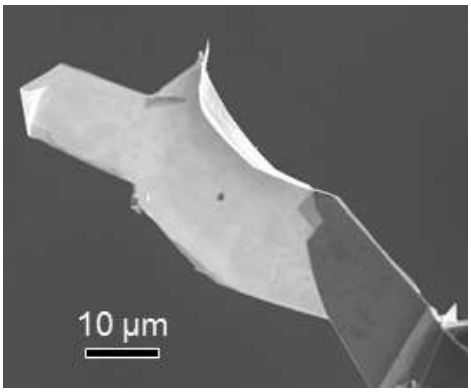

Fig. 1 SEM image of an edge of exfoliated MoS_2. Acceleration voltage of SEM, 5kV.

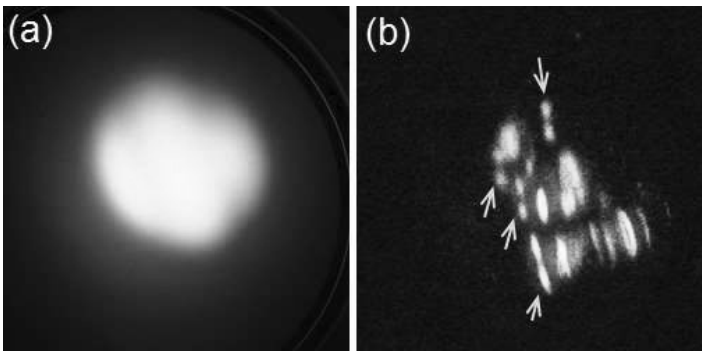

Fig. 2 (a) FEM and (b) FIM images of the exfoliated MoS_2.

[1] X. Qian et al., Science **346**, 1344 (2014). [2] H. Mine et al., Phys. Rev. Lett. **123**, 146803 (2019). [3] Y. Saito, J. Vac. Sci. Technol. B **40**, 012803 (2022). [4] Y. Saito ed., *Nanostructured Carbon Electron Emitters and its Applications* (Jenny Stanford Publishing, Singapore, 2022).

Corresponding Author: Y. Saito
Tel: +81- 561-57-9616, Fax: +81- 561-63-6302, E-mail: ysaito@toyotariken.jp

Synaptic function in ultra-dense CNT/HfO_2/CNT memristors for reservoir computing applications

○Adha Sukma Aji[1] and Yutaka Ohno[2]

[1]*Venture Business Laboratory, Nagoya University, Nagoya 464-8601, Japan*
[2]*Institute of Materials and Systems for Sustainability, Nagoya University, Nagoya 464-8601, Japan*

The increasing information needed to be processed in the artificial intelligence (AI) era requires a breakthrough in a novel computing paradigm. Brain-inspired computing using the hardware-based synaptic device, such as memristor, is gaining attention due to its ability to mimic the biological synapse connections [1]. Moreover, the array of numerous synaptic memristors can be arranged into a reservoir computing machine. Reservoir computing is a novel neural network computing method that has advantages in processing a high amount of data at a short computing time and low training cost while maintaining low power consumption [2]. However, the demonstrated memristors-based reservoir computing is limited in the number of memristors placed in a small area. A higher number of memristors is needed to get a better computing output. Here, we demonstrate the ultra-dense memristors fabricated from interconnected nano-junction of carbon nanotubes (CNT) networks. The system can be trained as a biological brain, promising reservoir computing applications.

The CNT/HfO_2/CNT memristors were fabricated by sandwiching a thin HfO_2 insulator between two CNT network films (Figure 1). Ultra-dense memristors can be obtained by connecting multiple electrodes to the bottom and top CNT films. Each combination of two electrodes can act as a memristor because the current path will be different for each due to the network structure of the CNT films.

To demonstrate the training capability of memristors, we performed Pavlov's dog training regime to the system (Figure 2). The natural response of memristors is "low output current at low input voltage" and "high output current at high input voltage." To achieve the desired response, "high output current at low input voltage," we trained the memristor by alternatingly the low and high input currents. Finally, the desired response of "high output current at low input voltage" can be achieved. Interestingly, each memristors combination can be individually trained even at the same core, confirming the formation of high-density memristors. The demonstration further confirms that our high-density memristors are favorable for physical reservoir computing applications.

[1] D. Silver *et al*. *Nature,* **529**, 484 (2016). [2] C. Du et al. *Nat. Comm.* **8**, 2204 (2017).

Corresponding Author: Y. Ohno; Phone: +81-52-789-5387; E-mail: yohno@nagoya-u.jp

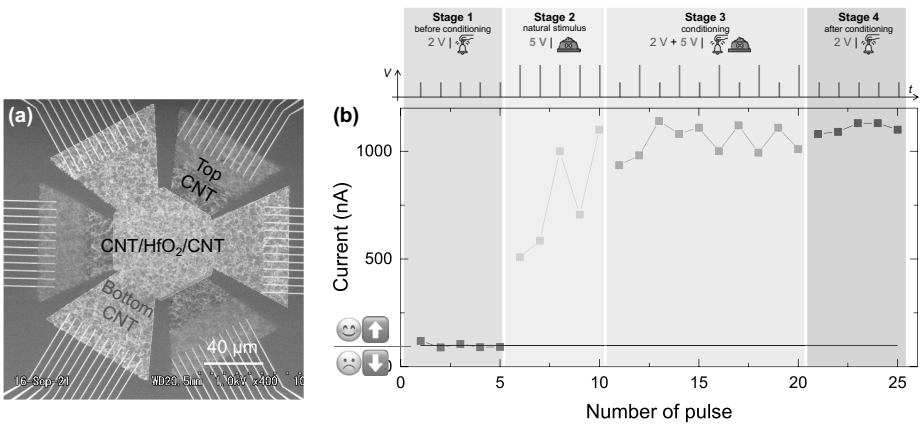

Figure 1. (a) Scanning electron microscope image of the high-density CNT/HfO_2/CNT memristor device.
(b) Memristor's response to the input voltage training at different stages of Pavlov's dog training regime.

Multi-element photo-thermo-electric devices by a micro-scale CNT film array

○Daichi Suzuki[1], Yuma Takida[2], Yukio Kawano[3–5], Hiroaki Minamide[2], Nao Terasaki[1]

[1]*Sensing System Research Center, AIST, Saga 841-0052, Japan*
[2]*RIKEN Center for Advanced Photonics, RIKEN, Miyagi 980-0845, Japan*
[3]*Faculty of Science and Engineering, Chuo University, Tokyo 112-8551, Japan*
[4]*FIRST, Tokyo Institute of Technology, Tokyo 152-8552, Japan*
[5]*National Institute of Informatics, Tokyo 101-8430, Japan*

One of the unique advantages of a carbon nanotube (CNT) film is a high photo-thermo-electric (PTE) efficiency due to the low-dimensional structure of CNTs. The PTE effect, which converts photons and heat to electricity, can be utilized for variety of applications such as broadband sensors and energy harvesters. Meanwhile, we previously have developed a terahertz (THz) soft camera patch sheet through a laser ablation process [1]. In this presentation, we report the high sensitivity THz detector and spectroscopy, achieved by arraying multi-element micro-scale THz detectors in series.

The critical method for enhancing PTE voltage ΔV is to increase the number of detectors in series connection, which is well-known as a structure of thermopile. Especially in photo sensing applications, it is important to reduce the interval spacing between detector elements to increase the aperture ratio of the CNT film (photo absorbing material) to reduce energy loss (Fig. 1a). Figure 1b shows a multi-element THz detector. Each detector element that involves a p-n junction was arrayed in 5 μm intervals by using the laser ablation process and was connected in series on the rear side of the polyimide film via the contact holes on both ends. As a result of the series connection, the THz response increased 4-fold compared to the single-element THz detector (Fig. 1c). We expect that the presented technique of CNT film arrays can be applied not only to sensing applications as shown in Fig. 1d but also to thermoelectric generators.

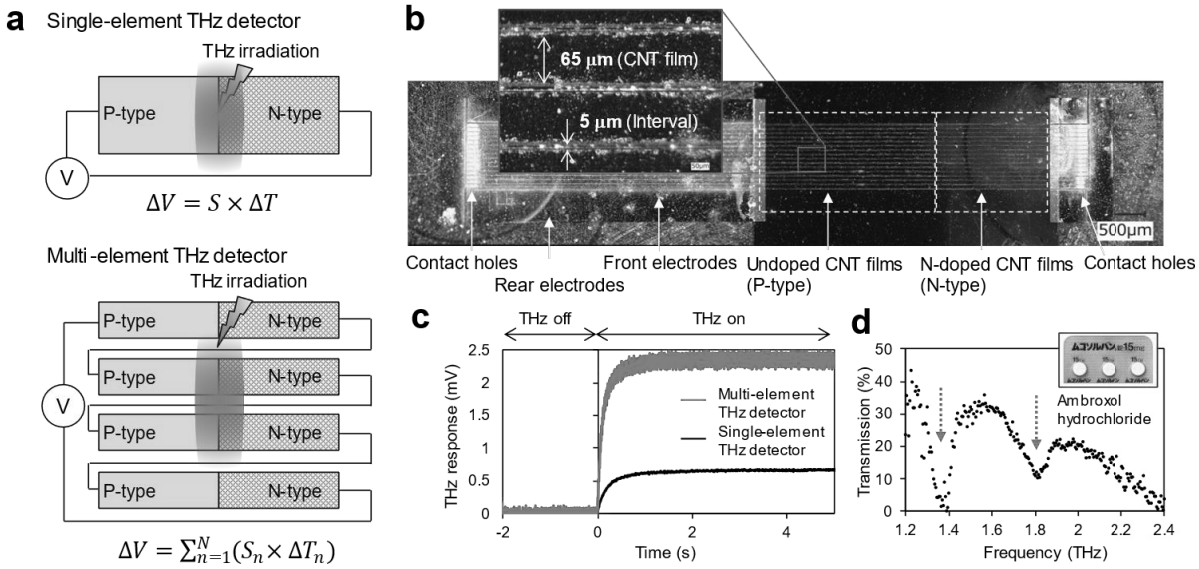

Fig. 1. (a) Schematics of the photo-thermo-electric effect for single/multi-element THz detector. (b) Photographic image of a multi-element THz detector. (c) THz response comparison. (d) THz spectroscopy by the multi-element THz detector. The arrows indicate the resonant peaks (fingerprint spectrum) of the medicine.

[1] D. Suzuki *et al.,* Adv. Funct. Mater., **31**, 2008931 (2021).

Corresponding Author: D. Suzuki, Tel:+81-942-81-3620, Fax:+81-942-81-4018, E-mail: daichi.suzuki@aist.go.jp

Optimization of Fabrication and Post-Treatment Conditions of CNT/Polymer Composite Ribbons for Higher Thermal Conductivity

○Nikita Kumari, Ryo Abe, Naofumi Okamoto, Manish Pandey, Masakazu Nakamura

Nara Institute of Science and Technology, 8916-5 Takayama-cho, Ikoma, Nara 630-0192, Japan

The ongoing development of high-efficiency integrated circuits led to significant heat generation due to increased power density. The undesired heating of the electrical circuits is a major threat to their performance and durability. Therefore, flexible interconnecting materials possessing high thermal conductivity (TC) are highly desirable for the thermal management of equipments. Taking the theoretically calculated TC (> 6000 W/mK) of individual carbon nanotubes (CNT) into consideration, they are getting significant research interest [1]. Moreover, CNTs are also lightweight, corrosion-resistant, and flexible materials. Although the theoretical calculation of isolated CNTs exhibits exceptional TC, the difficulty in handling them as aggregates limits the application of CNTs. In aggregates, CNTs are quite entangled due to the high aspect ratio and strong van der Waals interaction. Therefore, orientation techniques are desirable to utilize the individual-CNT's thermal properties at a macroscopic scale.

We have recently established a new orientation technique to fabricate scalable films of CNT/polymer composite through a programmable robotic dispenser, as schematically shown in Fig. 1(a) [2]. In this work, CNT/polymer composite films were fabricated using this technique. Further, for the quantitative and qualitative analysis of CNT-orientation, the films were subjected to mapping of G-band intensity ratio obtained through polarized Raman spectroscopy ($I_{00°}/I_{90°}$) and scanning electron microscopy (SEM), Fig. 1(b). For the oriented films, improvement in the corresponding thermal diffusivity and TC was also obtained. Moreover, it was found that the post-treatment, i.e., washing the film with a good solvent for organic component, also had a noticeable effect on the TC, which can be attributed to variation in the residual organic components in the film. Further, via optimization of post-treatment of the oriented-CNT films, the state-of-art in-plane TC of more than 200 W/mK was obtained [3].

In this presentation, optimizations of film fabrication and the post-treatment conditions will be discussed in detail.

Acknowledgement: This work was supported by JST CREST (JPMJCR18I3).

[1] B. Kumanek, D. Janas, J. Mater. Sci., **54**, 7397 (2019).

[2] M. Pandey *et al*. Appl. Phys. Express, **13**, 065503 (2020).

[3] H. Ma *et al*. J. Mater. Sci., **56**, 1064 (2021).

Corresponding Author: M. Nakamura
Tel: +81-743-72-6031, Fax: +81-743-72-6047,
E-mail: mnakamura@ms.naist.jp

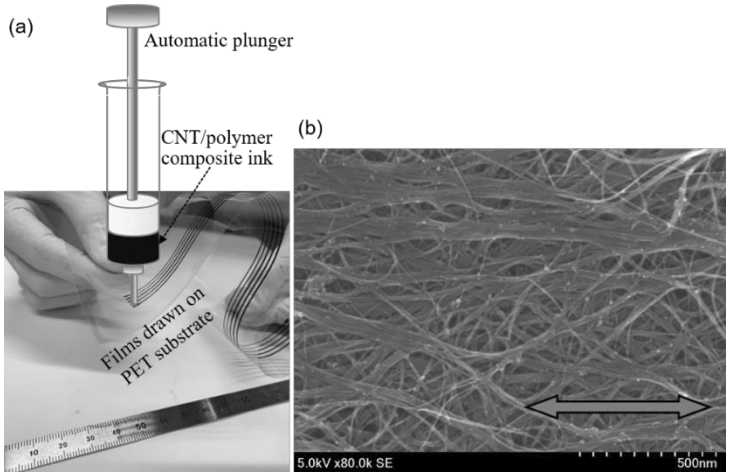

Fig. 1 (a) Schematic representation of film fabrication via robotic dispenser and a digital image of the coated CNT/polymer composite films. (b) The SEM image of a representative film. The two-sided arrow represents the coating direction.

Reduced Graphene Oxide Films with High Structural Quality Fabricated by a Two-Step Reduction of Graphene Oxide

○K. Kanishka H. De Silva, Kazuma Shibata, Pamarti Viswanath, Masamichi Yoshimura

Graduate School of Engineering, Toyota Technological Institute, Nagoya, 468-5811, Japan.

Graphene oxide (GO) has emerged as a precursor to fabricate graphene-like materials due the ability of mass scale production at a low cost. However, the structural quality of graphene obtained by the reduction of GO (known as reduced graphene oxide -RGO) is inferior to pristine graphene. Attempts have been made to obtain RGO with high structural quality by optimizing reduction strategies, such as using catalysts [1], microwave reduction [2], and oxidation of graphite to get less defected graphene oxide [3]. Yet, these methods are energy and time consuming and also result in low yield. Hence, the challenge is still open to fabricate high quality RGO in an easier and productive way. We present a two-step reduction of GO using a mixture of hydroiodic acid and trifluoroacetic acid (HI/TFA) within a few minutes followed by thermal annealing in the presence of ethanol at 800 ºC. Ethanol acts as a lattice defects repairing agent during annealing step [4]. Raman spectrum of the obtained RGO sheets show very sharp peaks with a low intense D-band and a high intense G'-band (Fig. 1(a)). Using the peak widths, I_D/I_G ratio and the following equations, the distance between defects (L_D) in the graphene lattice was determined [5]. According to equation 1, the L_D values for GO, chemically reduced GO, and thermally annealed GO were all less than 2 nm, while according to equation 2, for GO reduced via two-step reduction L_D is about 21 nm (Fig. 1(b)). Following this reduction strategy, we succeeded in fabricating highly conductive and transparent monolayer RGO films, which further confirms the quality of the fabricated RGO films is of high quality.

$$L_D^2\ (nm)^2 = \ 5.4 \times 10^{-2}\ E_L^4(eV^4)\frac{I_D}{I_G} \qquad (1)$$

$$L_D^2\ (nm)^2 = \ \frac{4.3\ \times\ 10^3}{E_L^4\ (eV^4)}\left[\frac{I_D}{I_G}\right]^{-1} \qquad (2)$$

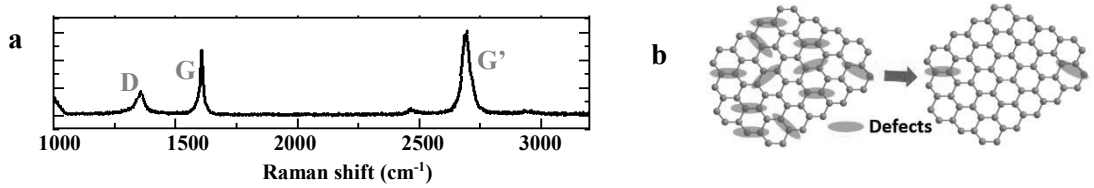

Fig. 1 (a) Raman spectrum of the high quality RGO sheets and (b) Schematic showing the RGO with low defect density after two-step reduction.

[1] J-C. Yoon *et al*. ACS Nano, **15**, 11655 (2021).
[2] D. Voiry *et al*. Science, **353**, 1413 (2016).
[3] Wang *et al*. J. Phys. Chem. Lett., **12**, 10009 (2021).
[4] K.K.H. De Silva *et al*. Jap. J. Appl. Phys. **58**, SIIB07 (2019).
[5] Cançado *et al*., Nano Lett., **11**, 3190 (2011).

Corresponding Author: K. Kanishka H. De Silva
Tel: +81-52-809-1852,
E-mail: sd16501@toyota-ti.ac.jp

ポスター発表

Poster

1P-1 ~ 1P-39

2P-1 ~ 2P-39

Formation of a Large-Area Proton-Conductive Nanofilm by Two-Dimensional Assembly of Fullerene Amphiphiles

○Hikaru Uchida[1], Prince Ravat[1], Ryosuke Sekine[1], Ko Kamei[1], Akihisa Yamamoto[2], Oleg Konovalov[3], Motomu Tanaka[2,4], Teppei Yamada[1], Koji Harano[1], Eiichi Nakamura[1]

[1] *Department of Chemistry, The University of Tokyo, Tokyo 113-0033, Japan*
[2] *Institute for Advanced Study, Kyoto University, Kyoto 606-8501, Japan*
[3] *European Synchrotron Radiation Facility, France*
[4] *Heidelberg University, Germany*

Two-dimensional (2D) nanofilms are of wide interest due to their specific structures and properties. For practical use of 2D materials, large-area synthesis, high uniformity, and precise thickness control are critical issues. However, the ideal synthetic design of nanofilms has been in a difficult situation. In this work, we designed an entangled hydrogen-bonding network to form a 2D reverse bilayer structure from a conical fullerene amphiphile (CFA)[1] with five carboxylic groups, which were capable of intermolecular hydrogen-bonding interaction. Herein, we report the fabrication of a self-assembled fullerene film (FF) with a large area and high uniformity by air/water interface synthesis, precise control of thickness, and 2D proton conduction.[2]

FF was fabricated from CFA solution (toluene/1-butanol = 3/1) by placing it on a water surface and by evaporating, and capable of being transferred onto various substrates. FF was obtained as a 3.0-nm thick nanofilm revealed by atomic force microscopy analysis. X-ray reflectivity analysis of FF on the water surface confirmed reversed bilayer structure, in which carboxylic groups face to the inside of the nanofilm, indicating the formation of bilayer structure via hydrogen-bonding interaction between CFA. Precise and facile control of the thickness of FF was also performed by changing concentration or by transferring one by one. FF was clearly visualized on SiO_2/Si substrate, and the area was evaluated as ca. 30 cm^2. Visible light reflection measurement at some points on FF was also performed to confirm high uniformity in a large area. In addition, relative humidity-dependent conduction measurement indicated high proton conduction via a 2D hydrogen-bonding network.

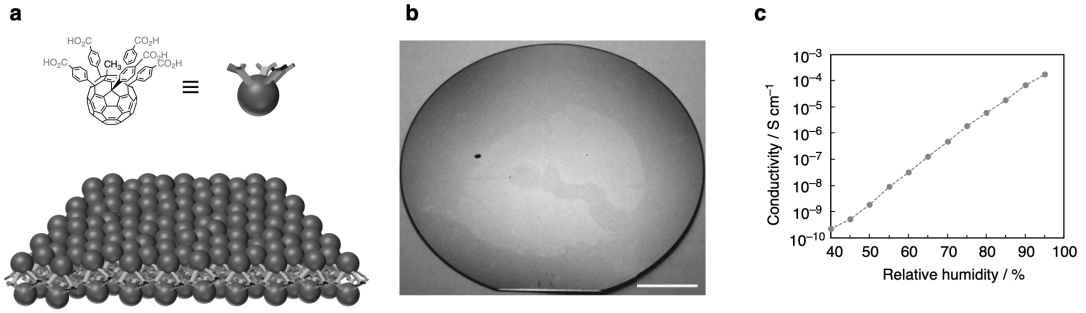

Fig. 1 (a) Structures of the CFA molecule and the bilayer of FF. (b) Optical image of FF on a SiO_2/Si substrate. (c) Humidity dependence of conductivity of FF.

[1] Y.-W. Zhong *et al*. Org. Lett., **8**, 1463 (2006).
[2] P. Ravat, H. Uchida *et al.* Adv. Mater. DOI:10.1002/adma.202106465.

Corresponding Author: E. Nakamura
Tel: +81-3-5841-4356
E-mail: nakamura@chem.s.u-tokyo.ac.jp

Electronic structure of C_{60} thin films under an external electric field

○Susumu Okada, Yanlin Gao, and Mina Maruyama

Department of Physics, University of Tsukuba, Tsukuba 305-8571, Japan

Ever since the prediction and discovery, C_{60} has been keeping a premier position in nanoscale sciences and technologies, because of its beautiful structure and wide variation of its derivatives. In addition to the molecular viewpoint, C_{60} forms condensed phases where C_{60} is bound via weak dispersive interaction and strong covalent bonds. In contrast to condensed structures consisting of other nanoscale carbon materials, these condensed phases sorely consist of C_{60} unit, even though they have morphological variations. Therefore, these C_{60} condensed phases are plausible candidates for structurally well-defined thin films or substrates with remarkable chemical inertness, which are applicable for semiconducting and optoelectronic devices. In this work, we aim to investigate the electronic structure of C_{60} thin films under an external electric field in terms of C_{60} arrangement and morphology. All electronic structures are calculated using the density functional theory (DFT) with generalized gradient approximation. To apply the external electric field and to inject additional carriers, the effective screening medium method is adopted that allows to get self-consistent electronic structure in the framework of DFT.

Figure 1 shows the isosurfaces of accumulated electron in C_{60} thin films where C_{60} forms face-centered cubic lattice and rhombohedral polymer under the top-gate field effect transistor structure. Accumulated electron distribution depends on C_{60} conformation and arrangement: The electron is penetrated into the second molecular layer in the thin film of fcc C_{60}, while it is localized only on the first molecular layer in the thin film of rhombohedral C_{60} polymer. Furthermore, field screening ability is also sensitive to the molecular arrangement and conformations.

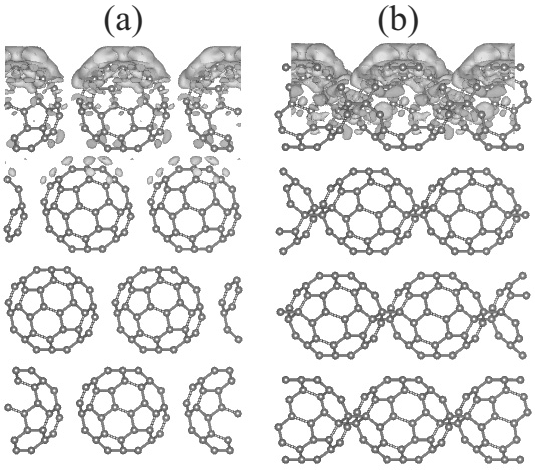

Fig. 1: Isosurfaces of accumulated electron in (a) fcc C_{60} thin film and (b) rhombohedral C_{60} polymer thin film. Yellow and cyan isosurfaces represent the electron accumulation and depression, respectively. Each isosurfaces corresponds with the electron density of $8x10^{-5}$,

Corresponding Author: Susumu Okada
TEL: +81-29-853-5921, FAX: +81-29-853-5924
E-mail: sokada@comas-tsukuba.jp

High area density and small diameter catalyst nanoparticle formation by magnetron sputtering deposition utilizing automated shutter

○Taichi Marui[1], Yuto Sawada[1], Hiroshi Furuta[1,2]

[1] *School of Systems Engineering, Kochi University of Technology, Kochi 782-8502, Japan*
[2] *Center for Nanotechnology, Research Institute, Kochi University of Technology*

High-density and small-diameter carbon nanotube (CNT) forests of the large surface area are expected for high-sensitive sensor electrodes, secondary battery electrodes, etc. Catalyst size and area density control are required to form the high-density and small-diameter CNT forests. In this study, we aim to produce high-density and small-diameter CNTs by a thermal CVD method with catalyst size control. We have been able to fabricate multilayer CNTs with diameters ranging from 10 to several nm by controlling the thickness of the Fe/AlO catalyst and annealing in a vacuum prior to synthesis [1]. In this study, we focused on the cathode shutter control during sputtering deposition and succeeded in reducing the size of fine particles by increasing the Fe film thickness. In addition, we attempted to oxidize the particles by adjusting the vacuum during sputtering.

Fe film thickness of 0.8-1.2 nm, deposited by the intermittent sputtering with the automated-shutter control, were annealed and the surface morphologies were characterized by AFM. In addition, the degree of vacuum is adjusted by the inflow of oxygen or air, and the condition of the fine particles at each degree of vacuum was evaluated. CNTs were synthesized by the thermal CVD method and their shapes were evaluated by SEM.

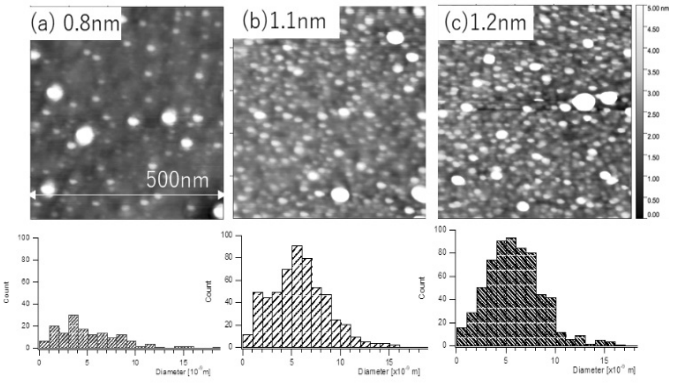

Fig. 1 AFM images and histogram of Fe nanoparticles after annealing process deposited by automated shutter sputtering.

AFM surface morphologies of deposited Fe films after annealing are shown in Fig.1. The diameter of Fe nanoparticles was reduced as the Fe film thickness was increased. High-density, small diameter CNT forests were grown on the relatively thick Fe films of 1.1-1.2nm in thickness. High-density plasma, produced utilizing automated cathode shutter, would increase the adhesion of catalyst resulting in high-area density, small-diameter CNT forests (Fig. 2).

A part of this work was supported by Kakenhi C 20K05093.

[1] A. Pander et al., Appl. Surf. Sci. 371 (2016) 425-435.

Corresponding Author: H. Furuta
Tel: +81-887-57-2211,
E-mail: furuta.hiroshi@kochi-tech.ac.jp

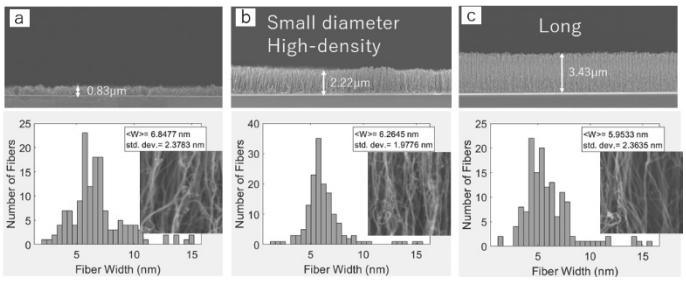

Fig. 2 SEM images and histogram of CNT diameters for CNT forests grown on (a) 0.8, (b) 1.1, and (c) 1.2 nm thick Fe catalyst films deposited by shutter Sputtering.

Growth of single-walled carbon nanotubes with Os catalyst by alcohol catalytic chemical vapor deposition at high temperature

Ibuki Takeichi[1], Shu Kondo[1], Daiki Yamamoto[1], Kamal P Sharma[2]
Takahiro Saida[1,2], Shigeya Naritsuka[3], ○Takahiro Maruyama[1,2],
[1] *Department of Applied Chemistry, Meijo University, Nagoya 468-8502, Japan*
[2] *Meijo Nanomaterial Research Center, Nagoya 468-8502, Japan*
[3] *Department of Materials Science and Engineering, Meijo University, Nagoya 468-8502, Japan*

1.Introduction

Our group reported growth of vertically aligned small-diameter single-walled carbon nanotubes (SWCNTs) on a SiO_2/Si substrate by alcohol catalytic CVD (ACCVD) method using an Ir catalyst [1], where most of SWCNT diameters were less than ~1 nm. Recently, we succeeded in small-diameter SWCNT growth using Os as a catalyst [2]. However, SWCNT yield from an Os catalyst was lower than that from an Ir catalyst. In this study, we performed SWCNT growth with an Os catalyst at 900 °C, which was the higher growth temperature than that in previous report and attained increase of SWCNT yield.

2.Experimental Procedure

Os catalysts were deposited on SiO_2/Si substrates by using an osmium plasma coater (Neoc-STB, Meiwafosis, Tokyo, Japan). After the substrates were set in a cold-wall CVD, the samples were heated to the growth temperature, 900 °C. Then, ethanol vapor was supplied onto the substrate surface to grow SWCNTs. To suppress aggregation of catalyst particles, we investigated the effect of temperature rising time on SWCNT growth. The samples were characterized by Raman, SEM and TEM.

3.Results and discussion

Fig.1 shows the temperature rising time dependence of Raman spectra of SWCNTs grown at 900 °C with Os catalysts on SiO_2/Si substrates. The distribution of wavenumbers of RBM peaks were similar, and the SWCNT diameters were distributed below 1.1 nm. The intensities of both G band and RBM peaks became stronger with the shorter temperature rising time. This indicates that suppression of aggregation of Os catalysts was effective to enhance the SWCNT yield.

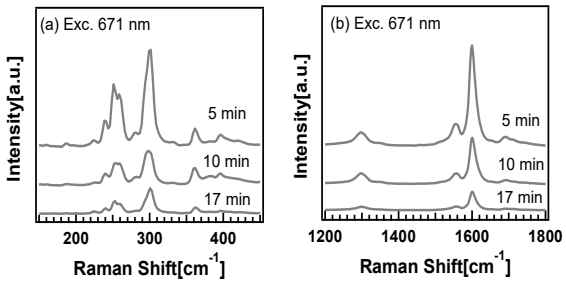

Fig. 1 Temperature rising time dependence of Raman spectra of (a) RBM region and (b) the high frequency region of SWCNTs grown at 900 °C by ACCVD with an Os catalyst.

Acknowledgments

Part of this research was supported by the private university research branding project "Meijo University Brand Building Program by Creating New Nanomaterials".

[1] T. Maruyama et al. Appl. Surf. Sci., **509** (2020) 145340.
[2] T. Maruyama et al. Diamond Relat. Mater., **117** (2021) 108501.

Corresponding Author: T. Maruyama
Phone: +81-52-838-2386, Fax: +81-52-832-1172, E-mail: takamaru@meijo-u.ac.jp

Synthesis of Boron Nitride Nanotubes with the Chirality-Sorted Carbon Nanotubes as the Template

○Ruixi Zhang[1], Ya Feng[1], Yongjia Zheng[1], Ming Liu[1], Shuhui Wang[1], Keigo Otsuka[1], Takeshi Tanaka[2], Hiromichi Kataura[2], Rong Xiang[1], Shigeo Maruyama[1]

[1] Department of Mechanical Engineering, The University of Tokyo, Tokyo 113-8656, Japan

[2] Nanomaterials Research Institute, National Institute of Advanced Industrial Science and Technology (AIST), Tsukuba 305-8565, Japan

Since the one-dimensional van der Waals heterostructures [1] were first synthesized in 2020, many kinds of electronic devices based on this type of heterostructure, such as transistor [1] and diode [2], have been developed and their electrical properties were evaluated. It is well known that the chiral carbon nanotubes are either semi-conducting or metallic. Plenty of research have been conducted to prepare single chirality carbon nanotubes for realizing the controllable electrical properties of carbon nanotubes. Based on this idea, in this research, single chirality carbon nanotubes were used as the template to be wrapped by boron nitride nanotubes(BNNT), which is believed to protect or even improve the intrinsic electrical properties of carbon nanotubes, and to further fabricate electronic devices with better performance.

Currently, the sorted single chirality carbon nanotubes were prepared in water with assistance of surfactants. The wrapping of surfactants on carbon nanotubes prevented the coating of boron nitride outside to form the heterostructure [3]. Therefore, in this research, an annealing method was proposed to remove the surfactant on the surface of single chirality carbon nanotubes. The removal of surfactant from the surface of individual carbon nanotube can be realized in a relatively low temperature (500ºC) and low vacuum (30 Pa) condition. Before annealing, the original solution sample was measured by optical absorption to define the optical density of single-wall carbon nanotubes (SWCNT). The optical density shown in Fig.1. The dispersed SWCNT solution was dropped onto Mo/SiO_2 TEM grid; after drying out, two of such grids were put into the chamber and annealed for 7 hours. After annealing, one of the two grids was put into BN furnace to synthesize BN nanotubes. The BN growth was conducted at 1075ºC for 1 hour. Thereafter, the two grids were examined by TEM to characterize the atomic structures. As shown in Fig. 2, the BNNT well-crystalized structure can be found, which proved that the annealing condition worked well for the removal of the surfactant. In addition, the successful synthesis of SWCNT-BNNT structure indicated that the sorted single chirality carbon nanotubes in water can be processed to synthesize boron nitride nanotubes outside.

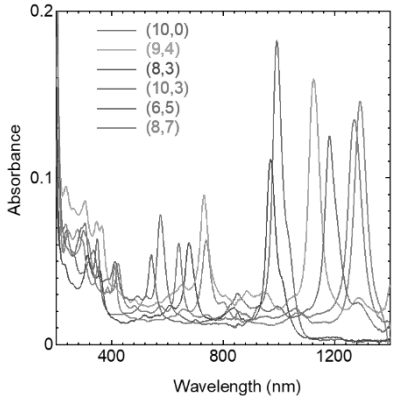

Fig. 1 Absorption spectra of SWCNT samples.

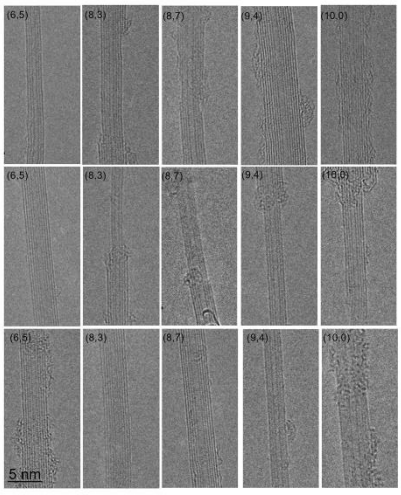

Fig. 2 TEM images of BNNT grown on the chirality-sorted SWCNT

Reference

[1] R. Xiang, et.al, Science, Vol 367, 2020.

[2] Y. Feng, et.al, ACS Nano, Vol 15, 2021.

[3] Y. Zheng, et.al, PNAS, Vol 118, 2021.

Corresponding Author: S. Maruyama
Tel: +81-3-5841-6421,
Fax: +81-3-5841-6408,
E-mail: maruyama@photon.t.u-tokyo.ac.jp

CO_2-driven tuning of growth rate, lifetime, and incubation of horizontal arrays of carbon nanotubes

○Ryoya Ishimaru[1], Keigo Otsuka[1], Taiki Inoue[2], Shohei Chiashi[1], Shigeo Maruyama[1]

[1] *Department of Mechanical Engineering, The University of Tokyo, Tokyo 113-8656, Japan*
[2] *Department of Applied Physics, Osaka University, Osaka 565-0871, Japan*

Single-walled carbon nanotubes (SWCNTs) are an ideal channel material in high-performance transistors provided that their chirality and density are well controlled. Direct growth of long and dense nanotube arrays suitable for the applications requires further understanding of the mechanisms that determine the speed, lifetime, and incubation of SWCNT growth. Thick CNT forests have been synthesized by adding oxidant gases (e.g., CO_2 [1] or H_2O [2]) to carbon source gases, which suggests that oxidants maintain catalyst activity by suppressing catalyst encapsulation with carbon. Here we traced the growth process of individual SWCNTs under the supply of oxidant gases during ethanol chemical vapor deposition (CVD) towards the tuning of the length and density of horizontally aligned SWCNTs.

We employ the isotope decoding technique [3,4], which decouples the growth rate, lifetime, and incubation time of nanotubes. With the total flow rate of ethanol fixed at 5 sccm, three discrete ratios of ^{13}C ethanol were introduced every 1 min, serving as labels embedded in SWCNTs. We conducted two experiments with different flow rates of CO_2, where CO_2 addition started from the middle (6 min) of 24 min CVD process. After the CVD, Raman mapping measurements were performed to locate the isotope labels and thereby obtain the growth rate profiles (Fig. 1) of nanotubes synthesized with additive CO_2 (CO_2/EtOH=3/1). The growth rate decreased for most nanotubes at 6 min upon the introduction of CO_2, and their average change was −17%. Interestingly, the sensitivity to CO_2 significantly differs from tube to tube. We also compare the growth lifetime (Fig. 2) and incubation time (Fig. 3) with/without additive CO_2 (CO_2/EtOH=1/1), indicating that CO_2 has positive influences on lifetime and nucleation in contrast to the suppressed growth rate, likely due to the removal of excessive carbon from catalysts. Our results indicate that long and dense SWCNT arrays could be synthesized through the optimized amount and sequence of additive CO_2.

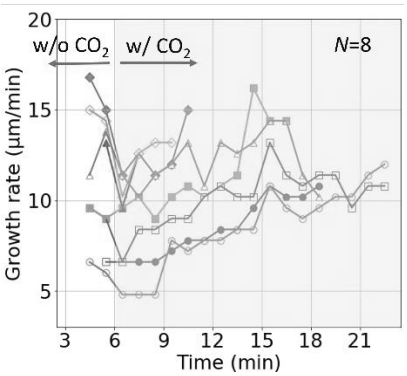

Fig. 1 Growth rate change of individual nanotubes that kept growing after CO_2 addition.

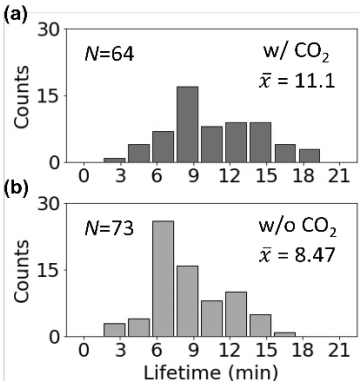

Fig. 2 Lifetime distributions of SWCNTs grown (a) without and (b) with CO_2.

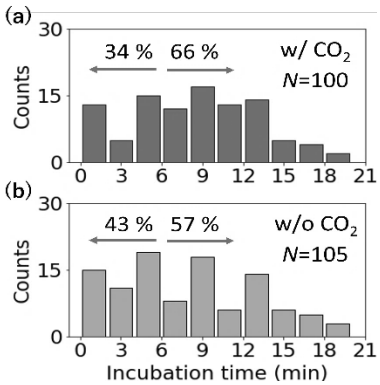

Fig. 3 Incubation time distributions of SWCNTs grown (a) without and (b) with CO_2.

[1] T. Sato *et al*., Carbon, **136**, 143 (2018).
[2] T. Yamada *et al*., Nano Lett., **8**, 4288 (2008).
[3] K. Otsuka *et al*., ACS Nano, **12**, 3994 (2018).
[4] B. Koyano *et al*., Carbon, **155**, 635 (2019).

Corresponding Author: S. Maruyama E-mail: maruyama@photon.t.u-tokyo.ac.jp

Two Sedimentation methods for Nanotube Aggregates: Size and Porosity Ranges where Inner Fluid Buoyancy Occurs

○Yuichi Kato[1], Takahiro Morimoto[2], Kazufumi Kobashi[2], Tetsuji Yamaguchi[3], Tetsuya Mori[3], Takushi Sugino[1], Toshiya Okazaki[2]

1 Nanomaterials Research Institute, National Institute of Advanced Industrial Science and Technology (AIST), Osaka 563-8577, Japan
2 CNT-Application Research Center, AIST, Tsukuba 305-8565, Japan
3 HORIBA, Ltd., Kyoto 601-8510, Japan

Fine tuning of the structure for disentangled carbon nanotube (CNT) agglomerates is important to enhance the CNT composite material's performance. Quantitative analysis of porosity (ϕ) in liquid of the CNT agglomerates (when we disentangle CNTs, ϕ of CNT agglomerates may increase) has been limited despite its importance. Recently, we proposed an analysis of ϕ and sedimentation particle size (D) of the agglomerates by centrifugal sedimentation.[1] We consider "inner fluid buoyancy (IFB)", that is the buoyancy caused by the smaller fluid density inside the agglomerate that sediments in a density gradient than the fluid outside.

Here, we introduce two sedimentation methods to estimate ϕ and D based on the range of ϕ and D where IFB is significant. You will estimate ϕ and D with linear analysis of sedimentations in density gradients (Fig.1b, left) if the particles located in region A (Fig 1a). The other is combination of homogeneous sedimentation and image analysis (Fig.1b, right). This approach can be applicable the particles located in both region A and B because theoretically IFB can be ignored.

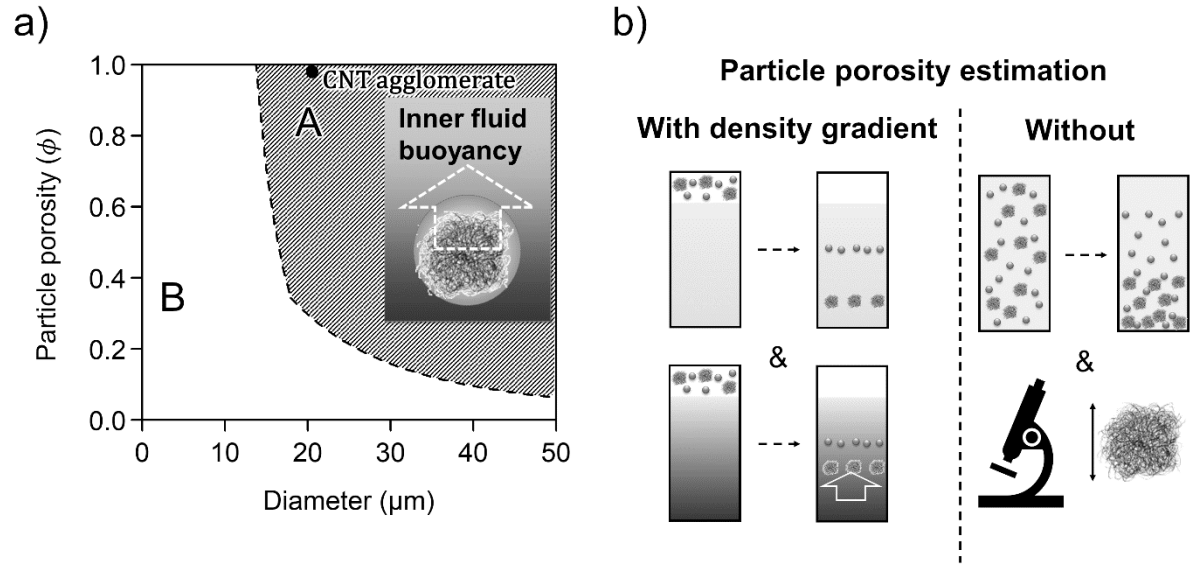

Fig. 1a) Size and porosity ranges where IFB significantly occurs. b) Two sedimentation methods for estimation.

[1] Y. Kato *et al*. The Journal of Physical Chemistry C **123**, 21252-21256 (2019).

Corresponding Author: Y. Kato
Tel: +81-29-861-9275
E-mail: yuichi.katou@aist.go.jp

Bundle structure effects on the electrical conductivity of CNT thin films

○Kazuki Terauchi, Yusaku Shimada, Hiroki Date, Shigeo Maruyama, Shohei Chiashi

Department of Mechanical Engineering, the University of Tokyo, Tokyo 113-8654, Japan

Carbon nanotubes (CNTs) are one-dimensional materials and they are lightweight but have high mechanical strength, and electrical and thermal conductivities. CNT ensembles such as CNT yarns and CNT thin films are expected to be applied on macro-scale. However, the electrical conductivity of CNT ensembles is significantly lower than that of individual CNTs [1]. Both the intrinsic factors such as CNT quality, junction and bundle size, and the external factors such as impurities, the substrate effects and the adsorption effects might affect the electrical conductivity, but there is no unified discussion of these factors, and macroscale CNT materials with high electrical conductivity have not been achieved. In this study, we measured the electrical conductivity of two types of CNT thin films. One was single-walled CNT (SWCNT) films synthesized by a floating catalyst CVD method [2], and the other one was CNT films obtained by dispersing vertically-aligned CNTs (VACNTs) with about 500 μm in height. The VACNTs were synthesized by a CVD method with Co catalyst on Al_2O_3/SiO_2 substrates.

The temperature and gate-voltage (V_g) dependence on the electric resistivity of the SWCNT thin film was shown in Fig. 1(a). The temperature dependence at V_g=-3 V was explained by variable range hopping model of one-dimensionality (d=1). In the SWCNT films, the average number of SWCNTs per bundle was about 10. Due to the small bundle, the SWCNT films exhibited one-dimensional electric conduction [3].The electric resistivity calculated from the real SWCNT volume excluding voids was about 100 μΩ cm in the atmosphere.

On the other hand, the CNT thin films made from VACNT films (Fig. 1(b)) showed high resistivity (10^3 μΩ cm), and the resistivity increased with increasing the dispersion time. As-grown VACNTs were composed of small bundles and they got aggregated during the dispersion process in DMF. SEM image in Fig. 1(c) shows the bundle structure of the CNT thin film after the dispersion in 4 h. The dispersion time dependence suggested that the bundle structure was one of the important factors decreasing the electric resistivity of CNT thin films.

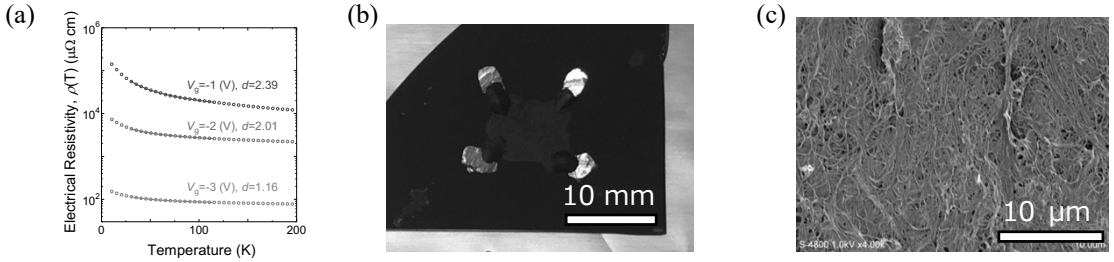

Fig. 1(a) Temperature dependence of the electrical resistivity of the SWCNT thin films with different gate voltages. (b) Optical and (c) SEM images of Dispersed VACNTs on SiO_2 substrate.

[1] N. Behabtu *et al*., Science, **339**, 182 (2013).

[2] A.G. Nasibulin, *et al*., ACS Nano, **5**, 3214 (2011).

[3] H. Date, *et al.*, the 61st Fullerenes-Nanotubes-Graphene General Symposium, 1P-62, (2021).

Corresponding Author: S. Chiashi

Tel: +81-3-5841-6407, Fax: +81-3-5841-6408,

E-mail: chiashi@photon.t.u-tokyo.ac.jp

Unconventional Temperature Dependence of Thermoelectric Properties on Semiconducting SWCNT Films

○Yota Ichinose[1], Manaho Matsubara[2], Akari Yoshida[1], Shigeki Saito[1], Kan Ueji[1], Yohei Yomogida[1], Takahiro Yamamoto[2], and Kazuhiro Yanagi[1]

[1] *Department of Physics, Tokyo Metropolitan University, Tokyo, Japan*
[2] *Department of Physics, Tokyo University of Science, Shinjuku, Tokyo, Japan*

Single-walled carbon nanotubes (SWCNTs) are ideal one-dimensional nanomaterials with the potential to exhibit significant thermoelectric (TE) performance [1]. To understand the TE properties in SWCNT thin films, we need to clarify the relationship between the TE properties and the carrier conduction mechanism. Previously we have experimentally investigated the TE properties of SWCNT thin films by changing the chemical potential (μ) position and measuring the temperature (T) dependence. It is known that the carrier conduction of SWCNT thin-film systems generally follows Mott's variable-range-hopping (VRH) model in the T-dependence [2]. On the other hand, we found that the Seebeck coefficient (S) shows an abnormal increase at low temperatures under certain conditions and reported the phenomenon in the previous FNTG conference. However, the mechanism has not been understood using conventional models. Therefore, we investigated the background of the phenomenon by analyzing the T dependence of S, electrical conductivity (σ), and thermoelectric conductivity (L_{12}).

Here we discuss the T-dependence of the TE properties of semiconducting (6,5) SWCNTs with purity over 99% and with controlled μ position. Figure 1 indicates the T-dependence of S value when μ is located within the conduction (or valence) band or in the bandgap. As shown in figure 1, when μ is located within the conduction (or valence) band, S follows the general Mott-VRH model. However, with μ in the bandgap, S shows an abnormal increase at the low T region. The Mott-VRH model cannot reproduce this unconventional behavior. Therefore, we modified the conventional Mott-VRH model and analyzed the data. As a result, we succeeded in reproducing the experimental results, as shown by the solid line in the figure. Here, the analysis suggested the necessity of the μ shifts with temperature changes and adding an energy-dependent term in the Mott-VRH. In the presentation, we discuss this background in detail.

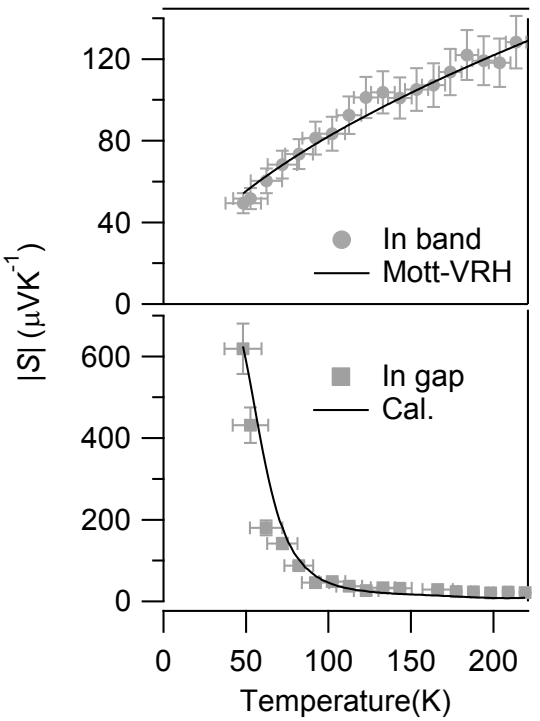

Fig. 1. Temperature dependence of the Seebeck coefficient. The chemical potential in band (top) and in bandgap (bottom). The points indicate the experimental data.

[1] Hicks & Dresselhaus, PRB 47, 16631 (1993). [2] K. Yanagi et al., ACS Nano 4, 4027 (2010).
Corresponding Author: K. Yanagi, +81-42-677-2494, yanagi-kazuhiro@tmu.ac.jp

Photo-induced electron doping of single-walled carbon nanotubes using benzamide derivatives

Taiki Ishii[1], ○Naoki Tanaka[1,2], Tsuyohiko Fujigaya[1,2,3]

[1] *Department of Applied Chemistry, Graduate School of Engineering, Kyushu University, Fukuoka 819-0395, Japan*
[2] *International Institute for Carbon-Neutral Energy Research (WPI-I2CNER), Kyushu University, Fukuoka 819-0395, Japan*
[3] *Center for Molecular Systems (CMS), Kyushu University, Fukuoka 819-0395, Japan*

Single-walled carbon nanotubes (SWCNTs) are expected to be the ideal material for thermoelectric conversion because of their high Seebeck coefficient and electrical conductivity. The development of the wearable thermoelectric device using SWCNTs is now investigated by taking advantage of their film toughness and flexibility. Up to date, the π-shape structure has been proposed for the SWCNT thermoelectric sheet which is composed of p- and n-type legs in series with conductive pastes and metals (Fig. (a)). However, this structure needs to attach to a skin vertically and is not preferable for wearable applications. Therefore, we developed a new planar-type structure using SWCNT sheet without conductive pastes and metals (Fig. (b))[1]. Since sequential repeating of p-type and n-type properties are necessary for the devices, we demonstrated the patterned doping of p-type SWCNT sheet into n-type by thermal deposition of using 2-(2-Methoxyphenyl)-1,3-dimethyl-1H-benzoimidazol-3-ium iodide (DMBI-I). But it takes a long time to make the patterned SWCNT sheet and a large amount of dopant is used for thermal deposition.

In this study, we developed photo-induced electron doping of SWCNTs film using benzamide derivatives. SWCNT films immersed in benzamide solution were partially covered with a mask and irradiated with 360-nm light for 10 min at room temperature (Fig. (c)). While the Seebeck coefficient of the non-masked of SWCNT film was p-type nature, that of the masked area of SWCNT film showed n-type nature.

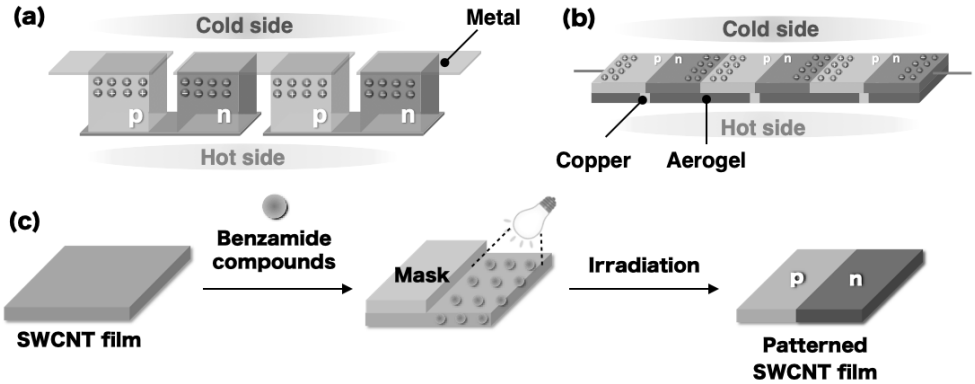

Fig.1 (a) π-shape structure. (b) Planar-type structure. (c) Illustration of photo-induced electron doping of SWCNTs.

[1] R. Yamaguchi, T. Ishii, M. Matsumoto, B. Angana, N. Tanaka, K. Oda, M. Tomita, T. Watanabe, T. Fujigaya, *J. Materials Chem. A.,* **2021**, *9,* 12188.

Corresponding Author: T. Fujigaya
Tel: +81-92-802-2842, Fax: +81-92-802-2842,
Web: https://sites.google.com/view/fujigaya-lab
E-mail: fujigaya.tsuyohiko.948@m.kyushu-u.ac.jp

Empirical modeling of broadband complex refractive index spectra of single-chirality carbon nanotube membranes for optical design

○Taishi Nishihara[1], Akira Takakura[1], Masafumi Shimasaki[1], Kazunari Matsuda[1], Takeshi Tanaka[2], Hiromichi Kataura[2], Yuhei Miyauchi[1]

[1] *Institute of Advanced Energy, Kyoto University, Uji, Kyoto 611-0011, Japan*
[2] *Nanomaterials Research Institute, National Institute of Advanced Industrial Science and Technology (AIST), Tsukuba, Ibaraki 305-8565, Japan.*

Assemblies of carbon nanotubes with single chirality are promising for applications in photonics, because of their strong light–matter interaction arising from sharp optical resonances of quasi-one-dimensional excitons. In semiconducting carbon nanotubes, excitons are thermally robust even at 2000 K [1,2], which offers new platform of photonics at very high temperature. In the design of optical devices using single-chirality carbon nanotubes, their broadband complex refractive index spectra are essential because they include fundamental information of the optical responses of the materials and enable quantitative calculation of optical spectra. However, they have been scarce in the literature, which has prevented researchers and engineers from designing tailor-made devices using single-chirality carbon nanotubes. Here, we report the empirical formulation of the broadband complex refractive index spectra of single-chirality carbon nanotube membranes. We determined the complex refractive index spectra of five kind of single-chirality membranes using transmission and reflection spectroscopy in the mid-infrared to visible wavelength region (Fig. 1). We propose an empirical formula that phenomenologically reproduces these complex refractive index spectra, which will pave the way for the straightforward design of photonic devices using various types of single-chirality nanotube membranes [3].

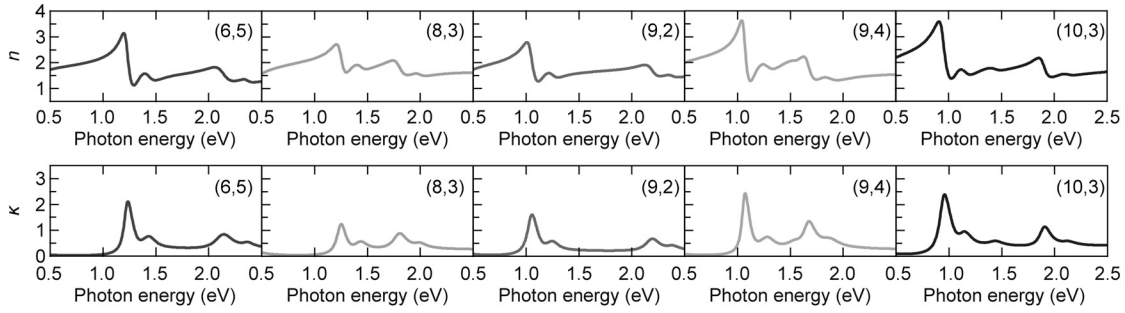

Fig 1. Complex refractive index spectra of five kind of single-chirality carbon nanotube membranes. *n*, real part; *κ*, imaginary part.

[1] T. Nishihara, A. Takakura, Y. Miyauchi, K. Itami, Nat. Commun., **9**, 3144 (2018).
[2] S. Konabe, T. Nishihara, Y. Miyauchi, Opt. Lett., **46**, 3021 (2021).
[3] T. Nishihara, A. Takakura, M. Shimasaki, K. Matsuda, T. Tanaka, H. Kataura, Y. Miyauchi, Nanophotonics (2022). https://doi.org/10.1515/nanoph-2021-0728.

Corresponding Author: T. Nishihara
Tel: +81-74-38-3445
E-mail: nishihara.taishi.8x@kyoto-u.ac.jp

Tailoring optical characteristics of single-chirality carbon nanotube assemblies toward opto-thermal applications

○Hengkai Wu[1], Taishi Nishihara[1], Akira Takakura[1], Kazunari Matsuda[1], Takeshi Tanaka[2], Hiromichi Kataura[2], Yuhei Miyauchi[1*]

[1] *Institute of Advanced Energy, Kyoto University, Uji, Kyoto 611-0011, Japan*
[2] *Nanomaterials Research Institute, AIST, Tsukuba, Ibaraki 305-8565, Japan*

Single-walled carbon nanotubes (SWCNTs) have been considered as promising materials for optical and thermal applications because of the excellent properties experimentally demonstrated in individual SWCNTs, i.e., outstanding thermal stability of lattice structures and excitons that exhibit strong light-matter interactions within narrow spectral window [1,2]. Toward the development of practical opto-thermal devices, how to integrate SWCNTs macroscopically is vital not only for maximizing their distinct functions but also for creating new desirable functions. Solar light-to-heat conversion device is an example of intriguing opto-thermal applications of SWCNTs because even a very thin SWCNT membrane can strongly absorb light at the exciton resonance [3,4]. Since the exciton resonance energies depend on the SWCNTs' chirality [3], use of assemblies composed of various chirality SWCNTs seems proper for broadband light absorption required for solar light-to-heat conversion devices. However, it remains unexplored how the assembly of SWCNTs should be designed to tailor the optical characteristics suitable for the opto-thermal applications.

In this work, we studied the optical properties of two types of SWCNT membranes; the first one was composed of homogeneously distributed (6,5) and (10,3) SWCNTs, and the other one had a stacked double layer structure, each of which composed of either (6,5) or (10,3) single chirality SWCNT membranes. Initially, we simulated the reflectance, transmittance, and absorptance spectra of these two membranes using broadband complex refractive index spectra of single-chirality SWCNT membranes [4], in which the optical spectra of the double layer structure were calculated with the light incident on either the (6,5) or (10,3) SWCNT sides. The thickness of the membranes was set as 100 nm. The signatures of exciton resonances of (6,5) and (10,3) SWCNTs appeared in all simulated spectra of both the membranes, but they appeared in a different manner depending on the form of the assembly and the direction of the light propagation. When the light was incident from the (6,5) SWCNT side of the double layered membrane, the magnitude of the reflectance at the first subband exciton resonance of (10,3) SWCNTs was most suppressed, which resulted in the highest absorptance. In this configuration, the refractive index mismatch between air and SWCNT membranes is small, resulting in suppressing the reflection and enhancing the absorption. This indicates the optical characteristics of SWCNTs assemblies can be significantly tuned through the form they were assembled. In the presentation, these simulations will be compared with experimental results.

[1] T. Nishihara, A. Takakura, Y. Miyauchi, K. Itami, Nat. Commun., **9**, 3144 (2018).
[2] S. Konabe, T. Nishihara, Y. Miyauchi, Opt. Lett., **46**, 3021 (2021).
[3] X. Wei, T. Tanaka, Y. Yomogida, N. Sato, R. Saito, H. Kataura, Nat. Commun., **7**, 12899 (2016).
[4] T. Nishihara, A. Takakura, M. Shimasaki, K. Matsuda, T. Tanaka, H. Kataura, Y. Miyauchi, Nanophotonics (2022). https://doi.org/10.1515/nanoph-2021-0728

Corresponding Author: Y. Miyauchi
Tel: +81-774-38-3463
E-mail: miyauchi@iae.kyoto-u.ac.jp

Rayleigh scattering spectra from SWCNTs with water adsorption and encapsulation

○Koki Kozaki, Ryotaro Kaneda, Shu Sato, Keigo Otsuka, Shigeo Maruyama, Shohei Chiashi

Department of Mechanical Engineering, The University of Tokyo, Tokyo 113-8656, Japan

The synthesis of one-dimensional hetero structures such as single-walled carbon nanotubes wrapped with boron-nitride nanotube (SWCNT@BNNT) was recently reported[1], and their properties have attracted much attention. Technology in encapsulating molecules inside nanotube is also expected to be applicated in fields such as drug delivery system. In this study, Rayleigh scattering spectra from SWCNT@BNNT and SWCNT encapsulating water molecules were measured in various conditions and their optical properties were investigated. Rayleigh spectra measured in water vapor were analyzed based on the temperature dependence, the adsorption of water molecules on the outside, and the water encapsulation.

SWCNTs were synthesized with ACCVD method across a slit substrate. Then boron-nitride layer was synthesized on the outer surface of some SWCNTs using CVD method as shown in Fig. 1(a), and other SWCNTs were opened with a pulse laser irradiation. To control the environment around samples, an environmental chamber suited for measuring Rayleigh scattering light was used. As the chamber was evacuated, heat transfer from SWCNTs is suppressed, and the incident laser irradiation easily heated up SWCNTs. As the result, the peaks in Rayleigh scattering spectra shifted to lower energy. Next, water vapor or air was introduced into the chamber, and Rayleigh spectra were measured with different pressure. With increasing water vapor pressure, the peak shifted to higher energy. In addition, Rayleigh spectra from opened SWCNTs were also measured. The pressure dependance of the peak energy on water vapor and air was shown in Fig. 1(b). In the low pressure range, there was no difference between water and air cases. On the other hand, in the case of water vapor, the optical transition energy was almost the constant above a pressure, indicating that water molecules adsorbed on the most outer surface of SWCNT@BNNT.

(a) (b)

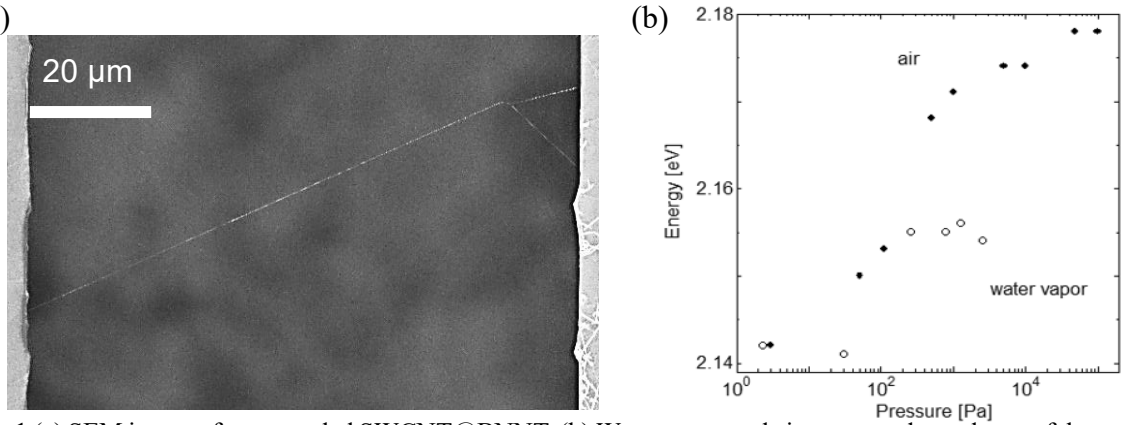

Fig.1 (a) SEM image of a suspended SWCNT@BNNT. (b) Water vapor and air pressure dependance of the optical transition energy of SWCNT@BNNT. The solid circles and the open circles represent air atmosphere and water vapor atmosphere, respectively.

[1] R. Xiang *et al*. Science, **542**, 537 (2020).

Corresponding Author: S. Chiashi
Tel: +81-03-5841-6407, Fax: +81-03-5841-6407,
E-mail: chiashi@photon.t.u-tokyo.ac.jp

Structural dependence of bisaryl-modifiers on photoluminescence wavelength changes of locally functionalized single-walled carbon nanotubes

○Haruka Aoki[1], Boda Yu[1], Tsuyohiko Fujigaya[1,2,3], Tomohiro Shiraki[1,2]

[1] *Graduate School of Engineering, Kyushu University, Fukuoka 819-0395, Japan*
[2] *International Institute for Carbon-Neutral Energy Research (WPI-I2CNER), Kyushu University, Fukuoka 819-0395, Japan*
[3] *Center for Molecular Systems (CMS), Kyushu University, Fukuoka 819-0395, Japan*

Single-walled carbon nanotubes (SWCNTs) show photoluminescence (PL) in the near infrared (NIR) region (900-1600 nm). The NIR PL is applicable to high resolution bioimaging and quantum information technologies. Local chemical functionalization of SWCNTs has been developed to enhance the NIR PL emission properties, in which sp^3 carbon defect doping occurs to the semiconducting sp^2 carbon lattice to produce locally functionalized SWCNTs (lf-SWCNTs) [1, 2]. The lf-SWCNTs emit red-shifted and brighter E_{11}* PL compared to E_{11} PL of non-modified SWCNTs. That is due to the formation of emissive doped sites that have narrow bandgaps and localize diffusive excitons. We have reported proximal modification of SWCNTs using bis-aryldiazonium salts (*b*ADs) [3,4], in which the bis-aryl modified lf-SWCNTs (lf-SWCNT-*b*A) showed largely redshifted PL (E_{11}^{2*}) than E_{11}^{*} PL over 100 nm. Therein, a correlation between the E_{11}^{2*} PL wavelengths and the methylene linker lengths and positions of *b*ADs was found. Therefore, the molecular design of modifiers for proximal modification could be a promising tool to versatilely modulate the NIR PL wavelengths of the lf-SWCNTs.

In this study, we synthesize lf-SWCNTs by the reactions with new *b*ADs that have rigid linker structures to investigate structural effects of the modifier molecules for the NIR PL wavelength modulation. Here, the *b*ADs having aromatic linkers and an alkyne liner were newly synthesized. The synthesized *b*ADs were reacted with the SWCNTs (CoMoCAT, (6,5) rich) solubilized in D_2O containing sodium dodecyl sulfate. In the case of a naphthalene linker structure for *b*ADs, the synthesized lf-SWCNTs (lf-SWCNTs-*b*An) showed a PL peak at 1142 nm, which was assignable to the PL from their defect doped sites. The *b*ADs with an acetylene linker produced PL at different wavelengths, which would be due to molecular structure changes of the doped sites from those of lf-SWCNTs-*b*An. Further discussion based on the structural differences of *b*AD modifiers will be discussed at the presentation.

[1] T. Shiraki et al., *Acc. Chem. Res.*, **53**, 1846 (2020)
[2] S. Tretiak et al., *Acc. Chem. Res*., **53**, 1791 (2020)
[3] T. Shiraki et al., *Sci. Rep*., **6**, 28393 (2016)
[4] T. Shiraki et al., *Chem. Lett.*, **48**, 791 (2019)

Corresponding Author: T. Shiraki
Tel: +81-092-802-2841, Fax: +81-092-802-2840,
Web: http://www.chem.kyushu-u.ac.jp/~fifth/jp/
E-mail: shiraki.tomohiro.992@m.kyushu-u.ac.jp

Potential for improving efficiency and durability of perovskite-silicon tandem solar cells with single-walled CNT electrodes

○Hiroki Nagaya[1], Bowen Zhang[1], Mohamad Almesfer[1], Xiyang Qiu[1], Haosheng Lin[2], Esko I. Kauppinen[3], Shohei Chiashi[1], Yutaka Matsuo[2], Keigo Otsuka[1], Shigeo Maruyama[1]

[1] *Department of Mechanical Engineering, The University of Tokyo, Tokyo 113-8656, Japan*
[2] *Department of Chemical Systems Engineering, Nagoya University, Nagoya 464-8603, Japan*
[3] *Department of Applied Physics, Aalto University, Espoo 02150, Finland*

Tandem solar cell is a photovoltaic device of using the transmitted light of a solar cell (top cell) to generate power in a different type of solar cell (bottom cell), which can overcome the theoretical limit of a solar cell alone. Lee et al. fabricated tandem solar cells using single-walled CNT film as the transparent electrode [1], and further optimization of the transmitted spectrum for the tandem solar cell is required. Figure 1 shows a schematic of a perovskite solar cell as the top cell, with CNT film as a transparent electrode. To improve transmittance, we first calculated the relationship between the thickness of the hole transport layer (spiro-MeOTAD) of the perovskite solar cell and the transmitted spectrum by using the e-ARC software [2]. As shown in Fig. 2, the transmittance of the perovskite solar cell changes with the film thickness by the interference of light, and the power conversion efficiency (PCE) of the bottom cell can be accordingly optimized. However, if the film thickness of spiro-MeOTAD is made thinner than 150 nm, the PCE of the perovskite solar cell itself is expected to decrease, so we ran the calculation for the thicker spiro-MeOTAD. In metal electrodes, the PCE decreases if spiro-MeOTAD is thick [3]. In contrast, since the CNT electrode is in contact with the perovskite layer as shown in Fig. 1, we expect the PCE to remain nearly the same even the spiro-MeOTAD is thicker. In addition to the thickness of the spiro-MeOTAD, the transmitted spectrum can be optimized by depositing the appropriate thickness of PMMA layer on the surface. This will not only improve the PCE of the bottom cell, but also improve the durability [4]. The PCE of the bottom cell [5] was calculated as a function of spiro-MeOTAD and PMMA thickness (Fig. 3). Simulated PCE using the model of the bottom cell was 22.6% under AM 1.5G. The calculation shows that the PCE of the bottom cell can be improved by the appropriate thickness combination of spiro-MeOTAD and PMMA. The calculation indicates the possibility of improving the efficiency and durability of tandem solar cells at the same time.

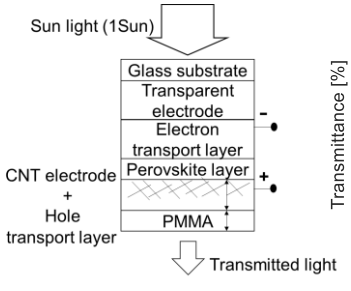

Fig. 1 Schematic of CNT electrode perovskite solar cell (Top cell).

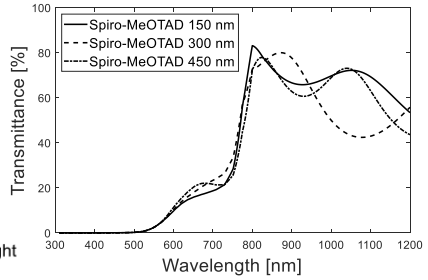

Fig. 2 Simulated perovskite solar cell transmitted spectra.

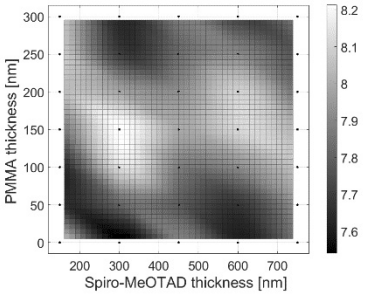

Fig. 3 Simulated PCE of bottom cell as a function of spiro-MeOTAD and PMMA thickness.

[1] C. Lee *et al*. *Solar RRL* 4.12 (2020). [2] A. Nakane *et al*. *Journal of Applied Physics* 120.6 (2016).
[3] I. Grill *et al*. ACS *applied materials & interfaces* 9.43 (2017).
[4] T. Sakaguchi *et al*. *MRS Communications* 8.3 (2018).
[5] H. Sai *et al*. *Progress in Photovoltaics: Research and Applications* 27.12 (2019).

Corresponding Author: S. Maruyama E-mail: maruyama@photon.t.u-tokyo.ac.jp

Fabrication of Single-Walled Carbon Nanotubes Devices by Stacking Nanomaterials

○Shu Sato[1], Satoru Matsushita[1], Ryotaro Kaneda[1], Keigo Otsuka[1], Shigeo Maruyama[1], Shohei Chiashi[1]

[1]*Department of Mechanical Engineering, The University of Tokyo, Tokyo 113-8656, Japan*

Single-walled carbon nanotubes (SWCNTs) are nanomaterials that have high mechanical strength, flexibility, and high electrical conductivity, but their electrical and optical properties are known to vary greatly depending on the surrounding environment. Two-dimensional materials such as hexagonal boron nitride (h-BN) and graphite are atomically thin and tough against bending, so applications to high-performance flexible devices are studied [1]. Heterostructures composed of these nanomaterials are expected to exhibit properties which are not found in individual nanomaterials. For example, SWCNTs on h-BN have a higher current carrying capacity than that on Si/SiO_2 substrates [2]. In this study, we developed methods of transferring and stacking nanomaterials with polymers and investigated the heterostructure devices.

A flake of h-BN was transferred onto a back-gate made of platinum with polypropylene carbonate (PPC) stamps [3], and then horizontally aligned SWCNTs synthesized on quartz substrate were transferred onto the h-BN with polystyrene (PS) stamps. The fabricated device was shown as Fig. 1(a). The G-band Raman mapping in Fig. 1(b) showed that SWCNTs were transferred onto h-BN and their alignment was retained. The G-band intensity above the metal back-gate were weaker than that on h-BN. The output and transfer characteristics of this device were analyzed.

Graphite was transferred with polyvinyl chloride (PVC) film stamps and cut with a pulsed laser to form two back-gates without using photoresist. Then, h-BN and SWCNTs were transferred on the cut graphite with PS (shown as Fig. 1(c)), and the heterostructure of graphite/h-BN/SWCNT was successfully fabricated (Fig. 1(d)). In addition, the similar heterostructures were also fabricated on plastic substrates. The transfer, cutting, and stacking techniques were effective in fabricating heterostructures even on flexible substrates.

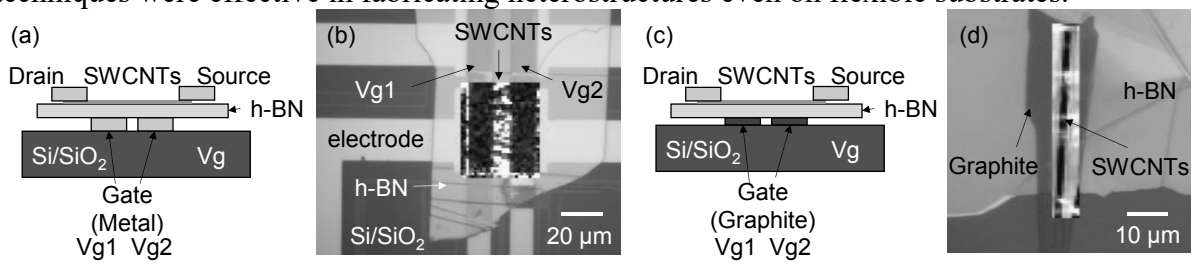

Fig. 1 (a) Schematic image and (b) optical microscope and G-band Raman mapping image of a heterostructure device of h-BN and SWCNTs transferred on a metal back-gate. (c) Schematic image and (b) optical microscope and G-band Raman mapping image of a heterostructure device of h-BN and SWCNTs transferred on graphite cut with a pulsed laser.

[1] Li Xiang, et al., *Carbon*, **161**, 656 (2020).
[2] J. W. Huang, et al., *Nano Lett.*, **15**, 10, 6836 (2015).
[3] K. Kinoshita, et al., *npj 2D Mater Appl*, **3**, 22 (2019).
Corresponding author : S. Chiashi
Tel/Fax: +81-3-5841-6408, E-mail: chiashi@photon.t.u-tokyo.ac.jp

Electrochemical stability of single-walled carbon nanotube electrodes in aqueous electrolyte.

○Namuun Uuganbayar, Shinya Jindo, Yosuke Ishii, Shinji Kawasaki

Department of Life Science and Applied chemistry, Nagoya Institute of Technology, Nagoya 466-8555, Japan

Since single-walled carbon nanotubes (SWCNTs) have excellent electrical conductivity and chemical stability, they are expected as good battery electrode materials. However, their electrochemical stability has not yet been fully understood. It is well known that SWCNTs have various tube diameters and exhibit diverse electronic states depending on their chirality. Therefore, it is necessary to clarify the relationship between these properties and the electrochemical stability of SWCNTs. In this study, we investigate the electrochemical stability of several SWCNTs with different tube diameters (SWCNT1.0, SWCNT1.5, and SWCNT2.5, with average tube diameters of 1.0 nm, 1.5 nm, and 2.5 nm, respectively) under applied potential in an aqueous electrolyte.

We found that I_{G^+}/I_D decreased with the increase in applied potential for all the three SWCNT samples. XPS measurements revealed that the fraction of O 1s increases with increasing applied potential, suggesting that electrochemical oxidation is the cause of the decrease of I_{G^+}/I_D in the Raman spectra with increasing applied voltage.

Fig. 1 (a) shows the change in Radial Breathing Mode (RBM) of SWCNT1.0. As can be seen from Figure 1 (a), the peak on the high wavenumber side decreases. This indicates that SWCNTs with smaller diameters are more reactive. On the other hand, Fig.1 (b) and (c) show the change in G-band peak profile. Judging from Fig.1 (b) and (c), it is plausible that metallic tubes are more reactive than semiconductive tubes.

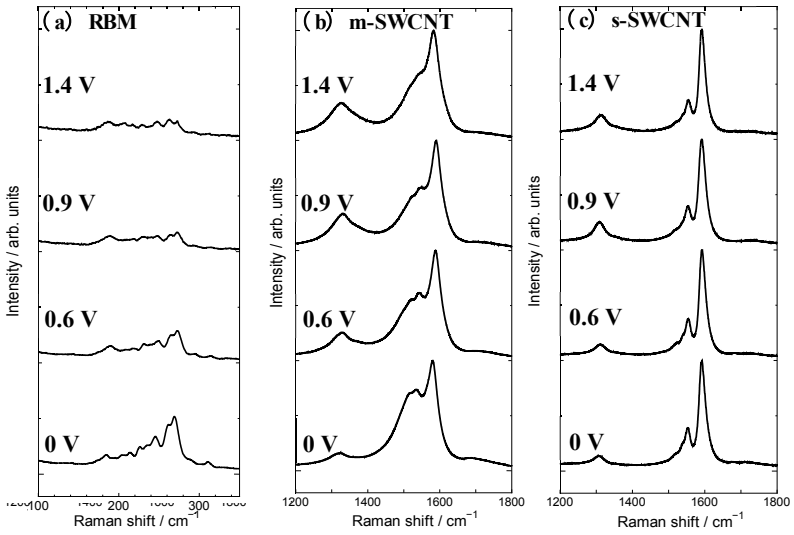

Fig. 1 Raman spectra of SWCNT1.0. Hg/HgO reference electrode was used. (a) and (b) 532 nm laser, (c) 633 nm laser were used as excitation source.

Corresponding Author: S. Kawasaki
E-mail: kawasaki.shinji@nitech.ac.jp

Fabrication and characterization of horizontal arrays of SWCNT-BNNT heteronanotubes

○Satoru Matsushita[1], Taiki Sugihara[1], Guangyao Zhu[1], Keigo Otsuka[1], Taiki Inoue[2], Shohei Chiashi[1], Shigeo Maruyama[1]

[1] *Department of Mechanical Engineering, The University of Tokyo, Tokyo 113-8656, Japan*
[2] *Department of Applied Physics, Osaka University, Osaka 565-0871, Japan*

Carbon nanotube (CNT) arrays have been a promising candidate for transistor channels that could outperform silicon counterparts. In practice, non-ideal CNT-insulator interfaces lead to large subthreshold swing (SS), hysteresis, and threshold voltage variation. In two-dimensional semiconductors, the encapsulation of channel materials between hexagonal boron nitride (BN) layers has reduced SS and hysteresis [1]. We expect CNTs to similarly benefit from the co-axial coating with BN nanotubes (BNNTs) [2]. However, horizontal arrays of such heteronanotubes, which are essential for practical devices, are difficult to prepare because elaborate air-suspended CNTs are required for the co-axial BNNT growth. Here, we develop a procedure to synthesize CNT@BNNT heteronanotube arrays by utilizing two types of transfer techniques towards the transistor applications.

As shown in Fig. 1(a), CNT arrays are grown on single-crystalline quartz substrates and transferred over trenches via anthracene crystals [3]. After synthesizing outer BNNTs by chemical vapor deposition [2], the hetero-nanotube arrays are transferred by a polystyrene-based stamping method onto another substrate for device fabrication. The Raman mapping image in Fig. 1(b) verifies the presence of nanotubes in an array form. The downshift of G-band suggests the coating of BN layers on a CNT (Fig. 1(c)). The hetero-nanotubes are ~30-nm-thick with some in-homogeneity along their axes (Fig. 1(d)). We will also discuss the selective etching of BNNTs [4] for the direct contact of inner CNTs and source/drain metal while the remaining BNNTs serve as gate dielectric layers in transistors.

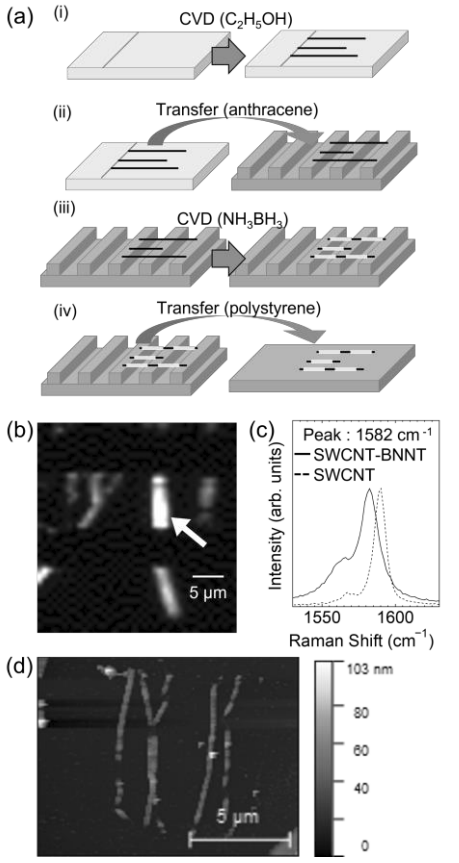

(a) Schematic for fabrication procedure of heteronanotube arrays. (b) G-band mapping image of a nanotube array. (c) Typical Raman spectra of SWCNT-BNNT and SWCNT. (d) AFM image of a nanotube array.

[1] Q. A. Vu *et al*., *2D Mater.* **5**, 031001 (2018). [2] R. Xiang *et al., Science* **367**, 537 (2020). [3] K. Otsuka *et al*., *Nat. Commun.* **12**, 3138 (2020). [4] J. Son *et al*., *Nat. Commun.* **9**, 3988 (2018).

Corresponding Author: S. Maruyama
Tel: +81-3-5841-6421, Fax: 03-5800-6983
E-mail: maruyama@photon.t.u-tokyo.ac.jp

High-frequency characterization of carbon nanotube thin-film transistors based on immersion deposition method

○Shugo Kogure[1], Saya Ishimaru[1], Hiromichi Kataura[2], and Yutaka Ohno[1,3]

[1]Department of Electronics, Nagoya University, Nagoya 464-8603, Japan
[2]Nanomaterials Research Institute, National Institute of Advanced Industrial Science and Technology, Ibaraki 305-8565, Japan
[3]Institute of Material and Systems for Sustainability, Nagoya University, Nagoya 464-8601, Japan

A high-density film of isolated semiconducting carbon nanotubes (CNTs) is the key to realize high-performance device applications. Previously, we have developed a method to obtain a high-density CNT thin film based on the immersion deposition technique to realize CNT TFTs with a high on-current and on/off ratio. [1] In this study, we have investigated the high-frequency characteristics of the CNT TFTs by measuring *S*-parameters.

We fabricated bottom-gate CNT TFTs by the self-align process based on the back-side exposure process on a polyethylene-naphthalate substrate (PEN) as shown in Fig. 1. [2] The semiconducting CNT thin film was deposited by the immersion deposition method. First, the surface of the Al_2O_3 gate insulator was modified by poly-L-lysine, and then a CNT thin film was deposited by immersing the sample in a dispersion of semiconducting CNTs. Here, the semiconducting CNTs separated by gel chromatography were dispersed in a phosphate buffer solution (0.1 mol/l, pH 7.4) containing sodium dodecyl sulfate (0.1 wt%). The high-frequency *S*-parameters were measured by a vector network analyzer (Keysight, E5061B).

Figure 2 shows the current-gain cutoff frequencies (f_T) and maximum oscillation frequencies (f_{max}) evaluated from the *S*-parameters for various channel length (L_{ch}) at V_{DS} of -5 V and V_{GS} of -3 V. f_T and f_{max} of 60.1 and 42.3 MHz were respectively achieved for the device with L_{ch} of 3 μm. Since the channel length can be reached by precision printing techniques, the results imply a possibility of realizing printed radio-frequency devices such as RFIDs.

[1] S. Kogure *et al*., The 61st FNTG General Symposium, 1P-41 (2021).
[2] T. Kashima *et al*., DOI: 10.21203/rs.3.rs-68702/v1.

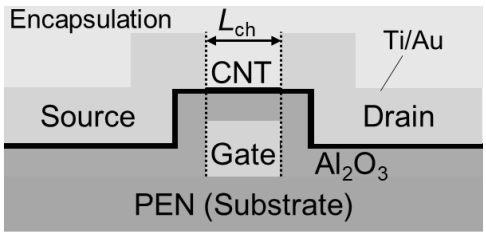

Fig. 1 Schematic device structure.

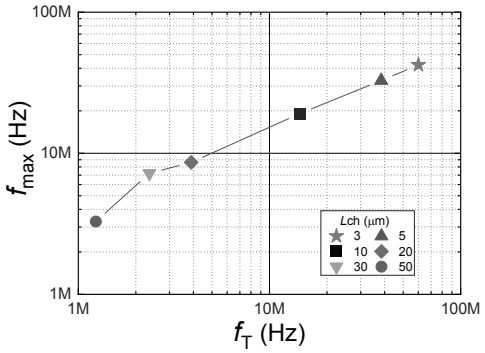

Fig. 2 f_{max} versus f_T.

Corresponding Author: Yutaka Ohno, Phone: +81-52-789-5387, E-mail: yohno@nagoya-u.jp

Design and fabrication of low-power flexible sensing circuits based on carbon nanotube

○Naohiro Mitsuzawa[1], Taiga Kashima[1], Hiromichi Kataura[2], and Yutaka Ohno[1,3]

[1]*Department of Electronics, Nagoya University, Nagoya 464-8603, Japan*
[2]*Nanomaterials Research Institute, National Institute of Advanced Industrial Science and Technology, Tsukuba 305-8565, Japan*
[3]*Institute of Material and Systems for Sustainability, Nagoya University, Nagoya 464-8601, Japan*

Recent developments of CNT-based flexible electron devices [1] and energy harvesters [2] have shown great promise of a realization of self-powered wearable sensors. However, the power generated by energy harvesters is generally small and unstable, and ultra-low power sensing system with a robustness against the instability of power source is needed. In this study, we aim to develop low-power flexible sensing circuits consisting of a small number of CNT TFTs. We propose novel sensing circuits based on ring oscillators that are tolerant to the fluctuation of supply voltage.

Figure 1 shows schematic diagrams of the sensing circuits we proposed in this study. The circuits consist of the ring oscillator in which a resistive sensor is inserted, and the oscillation frequency can vary according to the resistance of the sensor. To compensate the variation in the oscillation frequency due to fluctuations of the supply voltage, the sensing circuits also have a reference ring oscillator. Circuit #1 outputs the logical conjunction of two oscillation signals. Circuit #2 outputs signals of the reference and sensing alternately by switching the signal pass according to the clock signal. In the circuit design, we used the device model based on our fabricated CNT TFTs. [1]

Figure 2 shows the simulation results. In the case of Circuit #1, the reference (V_{ref}) and sensor signals (V_{sen}) oscillated at 150 and 1144 Hz, respectively. The output signal (V_{out}) was V_{sen} modulated by V_{ref}, showing the circuit operation as designed. The power consumption of this circuit was 0.31 μW. Similar operation was obtained for Circuit #2 with a power consumption of 0.68 μW.

The designed circuits were fabricated on a polyethylene naphthalte (PEN) substrate, using semiconducting CNTs as the channel of TFTs. The inverters were configured with a zero-V_{GS} load. The fabricated circuits were able to be operated at a low supply voltage of 3 V, and their fundamental operations were confirmed.

[1] T. Kashima *et al.*, DOI: 10.21203/rs.3.rs-68702/v1
[2] M. Matsunaga *et al.*, Nano Energy **67,** 104297 (2020).

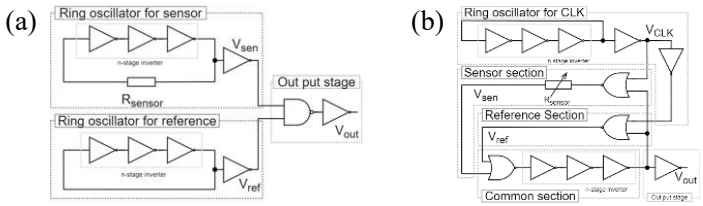

Fig. 1 Schematic circuit diagram of proposed sensor circuits. (a) Circuit #1, (b) circuit #2.

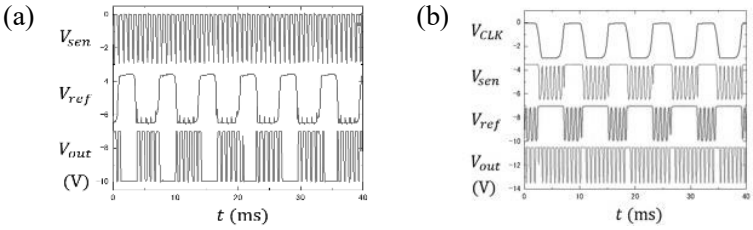

Fig. 2 Simulated voltage waveforms of sensor circuits at V_{DD} = 3 V. (a) Circuit #1, (b) circuit #2.

Corresponding Author: Yutaka Ohno, Phone: +81-52-789-5387, E-mail: yohno@nagoya-u.jp

Suppression of minority current in carbon nanotube thin-film transistors by drain bias stress

○Tomoki Hori[1], Hiromichi Kataura[2], Yutaka Ohno[1,3]

[1]*Department of Electronics, Nagoya University, Nagoya 464-8603, Japan*
[2]*Nanomaterials Research Institute, National Institute of Advanced Industrial Science and Technology, Tsukuba, Tsukuba 305-8565, Japan*
[3]*Institute of Materials and Systems for Sustainability, Nagoya University, Nagoya 464-8601, Japan*

Complementary carbon nanotube thin-film transistors (CNT TFTs) are the key device to realize low-power flexible electronics. However, CNT TFTs often exhibit the minority current at off state and so-called ambipolar characteristics, causing excess power consumption at static state in CMOS circuits. In this study, we report the suppression of the minority current by applying drain bias stress. The fundamental idea is to form the positive trap charges in the gate insulator and passivation layer in the vicinity of drain contact, so that, the electric field causing minority carrier injection from the drain is relaxed.

The schematic structure of the flexible CNT-TFT is shown in Figure 1. The gate insulator and passivation layer of Al_2O_3 were formed by atomic layer deposition. Due to fixed charges in the passivation layer, the carrier type was converted from positive to negative as shown by dotted curve in Fig. 2. [1,2] However, the large minority (hole) current was observed at the negative V_{GS} region. The hole conduction was suppressed by applying a large drain-gate voltage of 6 V for 9 min as shown by solid curve. This can be explained by an accumulation of positive charges jumped in the gate insulator by the high field at the drain end. The positive charges built up at the drain end may increase the potential and prevent the hole injection from the drain at off state. The threshold voltage was also shifted in the negative direction, implying a possibility of tuning the threshold voltage by independently applying gate bias stress.

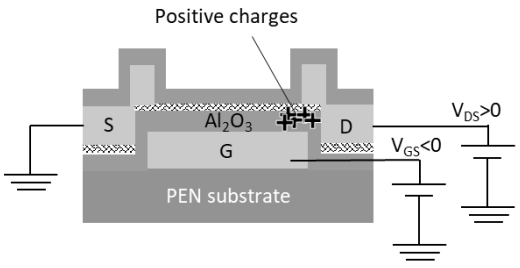

Fig. 1 Schematic structure of CNT-TFT.

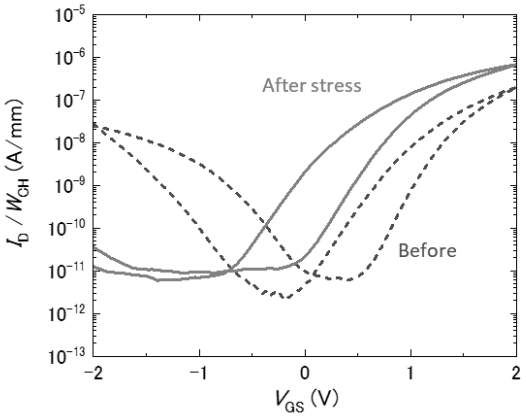

Fig. 2 Transfer characteristics before and after drain bias stress at V_{DS} = 0.2 V.

[1] N. Moriyama *et al*. Nanotechnol. 21, 165201 (2010).
[2] T. Hori *et al*. Int. Conf. on Materials and Systems for Sustainability 2021, 1181 (2021).

Corresponding Author: Y. Ohno, Phone: +81-52-789-5387, E-mail: yohno@nagoya-u.jp

Investigation of Single-walled carbon nanotubes degradation by heme enzymes from soil bacteria

○Seira Takahashi[1], Fumiko Taguchi[1], Junichi Kanie[2], Mitsuo Ueno[3], Mitsugu Uejima[3], Masafumi Ata[3], Katsutoshi Hori[1, 2]

[1] *Department of Biomolecular Engineering, Nagoya University, Nagoya 464-8603, Japan*
[2] *Friendmicrobe Inc., Nagoya 464-0858, Japan*
[3] *CNT Laboratory, Zeon Corporation, Kawasaki 210-9507*

Single-walled carbon nanotubes (SWCNTs) are expected to be used in various applications due to their exceptional properties. On the other hand, the long-term safety of SWCNTs is still unclear, and it is an urgent issue to explore the biodegradability and environmental fate of SWCNTs. The degradation of SWCNTs by peroxidases from several plants, animals, and fungi has been reported [1-5], but the habitats and living conditions of these reported organisms are limited. In this study, the degradation of SWCNTs by bacteria was investigated in order to expect the environmental fate of SWCNTs in a wider range of environments. The recombinant protein of dye-decolorizing peroxidase (DyP) encoded in *Pseudomonas putida*, a common soil bacterium [6], was incubated with SWCNTs in the presence of H_2O_2. After 30 days of incubation, the degradation of SWCNTs was observed and the suspension turned clear (Fig. 1). However, DyP was inactivated within one hour after the start of incubation. The release of iron, the active center, was observed due to the inactivation of DyP, and the degradation of SWCNTs was greatly inhibited in the presence of diethylene triamine pentaacetic acid (DTPA), a chelating agent. These results suggest that the SWCNTs were degraded by the Fenton reaction caused by the iron released from DyP. The recombinant protein of Cytochrome P450, another heme enzyme, gave almost the same results as DyP. This study revealed that CNTs are degraded by the Fenton reaction between iron and H_2O_2 released by the inactivation of heme enzymes. A common soil bacterium, *P. putida*, was found to have the potential to degrade SWCNTs in a wide range of environments because it can provide both iron and H_2O_2, the reactants for the Fenton reaction. These results provide an important insight into the environmental fate of SWCNTs.

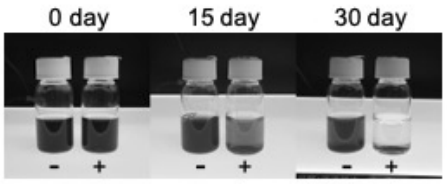

Fig. 1. Photographs of samples at different incubation times

[1] B. L. Allen *et al*. J. Am. Chem. Soc. **131**, 17194 (2009).
[2] V. E. Kagan *et al*. Nat. Nanotechnol. **5**, 354 (2010).
[3] F. T. Andon *et al*. Small **9**, 2721 (2013).
[4] C. Zhang *et al*. Environ. Sci. Technol. **48**, 7918 (2014).
[5] G. Chandrasekaran *et al*. J. Ind. Eng. Chem. **20**, 3367 (2014).
[6] T. D. H. Bugg *et al*. Curr. Opin. Biotechnol. **22**, 394 (2011)

Corresponding Author: K. Hori
Tel: +81-52-789-3339 E-mail: khori@chembio.nagoya-u.ac.jp

Carbon Nanotubes Induce Oxidative Stress in Coenzyme-Dependent Metabolic Reactions

○Atsushi Hirano[1], Tomoshi Kameda[2], Momoyo Wada[1], Takeshi Tanaka[1], Hiromichi Kataura[1]

[1] *Nanomaterials Research Institute, National Institute of Advanced Industrial Science and Technology (AIST), Ibaraki 305-8565, Japan*
[2] *Artificial Intelligence Research Center, 589 National Institute of Advanced Industrial Science and Technology (AIST), Koto, Tokyo 135-0064, Japan*

Carbon nanotubes (CNTs) have the ability to adsorb and oxidize biological molecules [1,2]. The oxidation potentially affects the activity of biological reactions such as metabolism. This study demonstrates that the CNTs suppress coenzyme-dependent metabolic reactions, which is ascribed to oxidation of the coenzymes by the CNTs.

Coenzymes are essential for biological phenomena such as enzymatic reactions involved with metabolism (*i.e.* metabolic reactions). Nicotinamide adenine dinucleotide (NAD) is one of the coenzymes associated with metabolic reactions. A representative NAD-dependent metabolic reaction is as follows:

$$\mathrm{NADH + H^+ + oxaloacetate \rightarrow NAD^+ + malate}$$

where an enzyme—malate dehydrogenase—plays a role as a catalyst. It should be noted that NAD is in a reduced form (NADH) or an oxidized form (NAD^+) in this reaction (Fig. 1).

We examined the effect of CNTs (HiPco CNTs) on the metabolic reaction. The amount of the product (*i.e.* malate) was found to be significantly decreased in the presence of the CNTs (Fig. 2a). This result was attributable to the oxidation of NADH by the CNTs oxidized (hole-doped) in aqueous solutions (Fig. 2b). Molecular dynamics simulations showed that the NAD (both NAD^+ and NADH) molecules have attractive interactions with the CNTs, which suggests that the NAD molecules readily approach the CNT surfaces and hence react with them.

In conclusion, CNTs interfere with the NAD-dependent metabolic reaction through the NADH oxidation, which will be associated with their biological impact in terms of cytotoxicity.

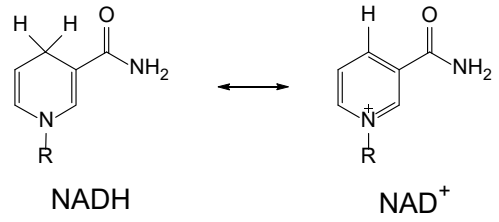

Fig. 1 Chemical structures of NAD molecules. R denotes a moiety composed of ribose and adenosine diphosphate.

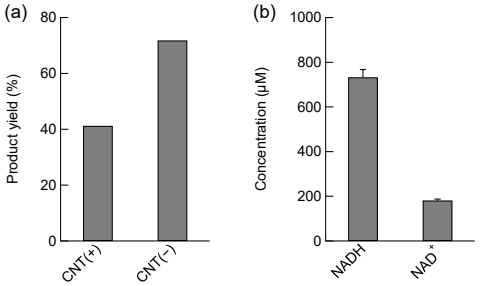

Fig. 2 Redox reaction of the CNTs with NADH. (a) Product (malate) yield from 20 μM oxaloacetate using malate dehydrogenase and 20 μM NADH in the presence and absence of 0.5 mg/ml CNTs. (b) NADH and NAD^+ concentrations after subjecting 1000 μM NADH to mixing with 1 mg/ml CNTs.

[1] A. Hirano and T. Kameda. ACS Appl. Nano Mater., **4**, 2486 (2021).
[2] A. Hirano *et al*. ACS Nano, **13**, 1805 (2019).

Corresponding Author: A. Hirano
Tel: +81-29-849-1064, Fax: +81-29-861-2786,
E-mail: hirano-a@aist.go.jp

Boron-assisted CVD growth of multilayer h-BN and application to heterostructures with MoS_2

Toru Otake[1], Satoru Fukamachi[2], Kenji Kawahara[2], and Hiroki Ago[1,2,*]

[1] Interdisciplinary Graduate School of Engineering Sciences, Kyushu University, Fukuoka, 816-8680, Japan, [2] Global Innovation Center (GIC), Kyushu University, Fukuoka, 816-8680, Japan

Multilayer hexagonal boron nitride (h-BN) is a key material to unveil the intrinsic and unique physical properties of various 2D materials by protecting their surfaces from environmental disturbance. Although monolayer h-BN can be widely synthesized by catalytic CVD, there is no reliable methods to synthesize high-quality multilayer h-BN due to difficulty of growing uniform multilayers. We previously reported the CVD growth of multilayer h-BN using Fe-Ni alloy thin films [1,2], but the h-BN thickness (2-3 nm) was not enough to screen the influences from the environment. Here, we demonstrate that the addition of elemental boron (B) in the catalytic CVD increases the h-BN thickness up to 4-5 nm while keeping the thickness uniformity. Moreover, these h-BN multilayers were stacked with CVD-grown monolayer MoS_2, dramatically increasing the PL intensity of the MoS_2.

Figure 1a shows an optical microscope image of multilayer h-BN grown on a Fe-Ni foil under our standard growth condition. The h-BN was inhomogeneous and contained several very thick flakes with thickness over 100 nm. We have previously reported that decreasing the cooling rate improves the h-BN film uniformity [1]. However, for very slow cooling rates, almost no h-BN was found on the Fe-Ni foil (Figure 1b), probably because both B and N atoms remain inside the foil and the slow segregation induces the etching of growing h-BN. Here, we found that pre-deposition of a B film on the Fe-Ni foil increases the h-BN thickness even after the slow cooling process, as shown in Figure 1c. Such effect was not observed when flowing N_2 gas, so that we speculate that there is a deficiency of B atoms in the Fe-Ni foil during the CVD growth. The TEM (Figure 1d) and AFM measurements indicated that the h-BN has a thickness of 4-5 nm. In the Symposium, we also present the significant enhancement of the PL emission from MoS_2 monolayers integrated with our CVD-grown h-BN multilayers.

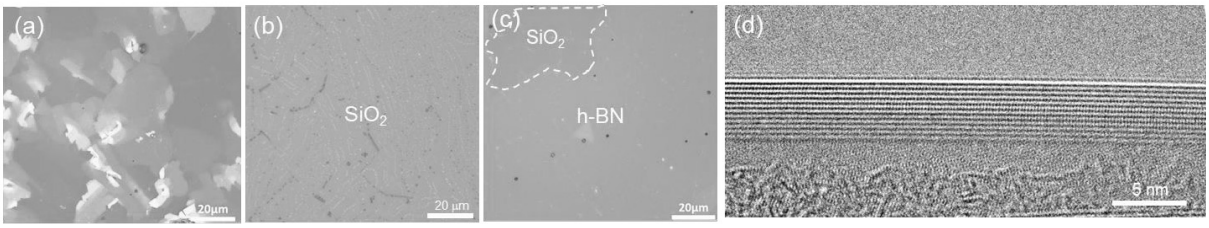

Figure 1. Optical images of transferred h-BN grown under the normal condition (a), the slow cooling condition (b), and the slow cooling condition with a pre-deposited B layer (c). (d) Cross-sectional TEM image of the sample shown in (c).

References: [1] Y. Uchida *et al.*, *ACS Nano*, **12**, 6236 (2018). [2] Y. Uchida *et al.*, *ACS Appl. Electron. Mater.*, **2**, 3270 (2020).

Layer by layer sulfurization of WSe_2 toward formation of Janus WSeS

○X. He, S. Aoki, Y. Iwamoto, T. Kaneko, and T. Kato

Graduate School of Engineering, Tohoku University, Sendai 980-8579, Japan

Since the discovery of graphene, 2D materials with various properties have received increasing attention in the fields of novel electronic, optical, spintronic and valleytronic devices. As important derivatives of 2D materials, Janus 2D materials, such as Janus transition metal dichalcogenides (TMDs), were first discovered in 2017 and have attracted much attention due to their unique structural electrical properties [1]. Janus TMD with mirror asymmetry can obtain carrier confinement and window effects by connecting different TMDs in-plane and out-of-plane, and also Rashba effect and normal piezoelectric polarization, which is expected to be applied in quantum devices, optical devices, sensors, actuators, and other electromechanical devices (Fig. 1(a)) [2]. In spite of the potential abilities of Janus TMD, the number of papers reported about the Janus TMD formation is very limited, denoting synthesis of Janus TMD is still within the early stage. Further understanding of reaction mechanism is important to realize controllable formation of high-quality Janus TMD.

In this study, detailed mechanisms of sulfurization were investigated through the thermal reaction of mechanically exfoliated WSe_2 toward Janus WSeS formation (Fig. 1(b)). It is found that by controlling substrate temperature, reaction time, and sulfur heater temperature, drastic changes of WSe_2 to WS_2 are found, which happened within 15 sec. When the flux of sulfur is reduced by decreasing the sulfur heater temperature, the reactions are slow down and controllable sulfurization are realized. Initially only the outermost layer is replaced by S. After that, sulfur invades the second and subsequent layers, and finally all Se is replaced by S. These are important information for the controllable formation of high-quality Janus TMD.

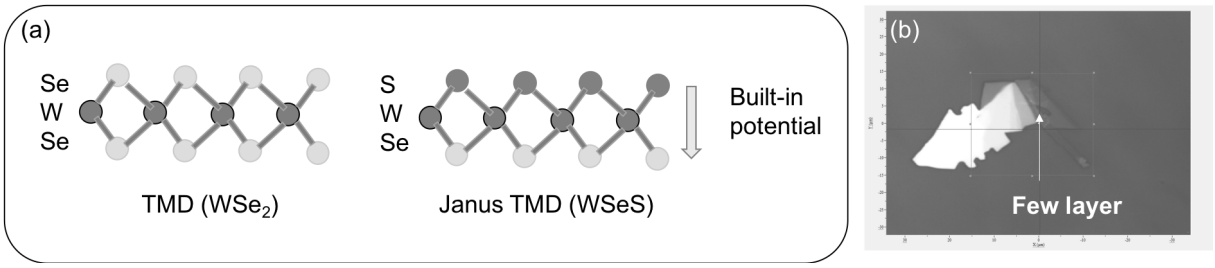

Figure 1: (a) Structure diagram of TMD and Janus TMD. (b) Optical microscope image of few layer WSe_2 used in this study.

[1] A. Y. Lu*et al.*, Nature Nanotechnol., **12,** 744–749 (2017).
[2] R. Li, Y. Cheng, and W. Huang, Small, **14**, 1802091-1–11 (2018).

Corresponding Author: Toshiaki Kato

Tel: +81-22-795-7046, Fax: +81-22-263-9225, E-mail: kato12@ tohoku.ac.jp

Catalyst-free CVD synthesis of graphene on various crystal materials

○Kenta Kusakabe[1], Yuta Fujisaki[1], Taiki Inoue[2], Shigeo Maruyama[1], Shohei Chiashi[1]

[1] *Department of Mechanical Engineering, the University of Tokyo, Tokyo 113-8654, Japan*
[2] *Department of Applied Physics, Osaka University, Osaka 565-0871, Japan*

Graphene is a nanomaterial with excellent thermal and electrical properties, and there are some ways to produce it. Among them, CVD synthesis is one of the methods to produce high-quality and large-area graphene at an acceptable cost [1]. The synthesis of graphene on metal catalysts has been widely studied, but there are few studies on catalyst-free synthesis [2], which is less prone to impurities and have application advantages such as no need for cleaning or other processing. In this study, we report the CVD synthesis of graphene on non-catalytic substrates such as graphite, h-BN, and sapphire.

Mechanically-exfoliated graphite, exfoliated h-BN, and a sapphire substrate (A-face) were placed in an electric furnace and CVD synthesis was conducted with controlling the pressure, temperature, and flow rates of acetylene, argon, and hydrogen (Figs. 1-3). In Fig. 1 and 2, hexagonal-shaped graphene pads were observed, suggesting that graphene on graphite and h-BN was of high quality. Figure 3 shows the SEM image and Fig. 4 shows the Raman spectrum of graphene directly-synthesized on sapphire. The 2D/G intensity ratio is 2.6, suggesting that the material is monolayer graphene [3]. The reticulated patterns in the SEM image were wrinkles of graphene, which may be caused by the difference in thermal expansion between graphene and sapphire during the temperature reduction process after synthesis [4,5].

[1] K.S. Novoselov *et al*. Nature, **490**, 192 (2012).
[2] S. Tang *et al*. Carbon, **50**, 321 (2012)
[3] Y. Hao *et al*. Small, **6**, 195 (2010).
[4] D. Yoom *et al*. Nano Lett., **11**, 3227 (2011).
[5] N. Mishra *et al*. Small, **15**, 1904906 (2019).

Corresponding Author: S. Chiashi
Tel: +81-3-5841-6407, Fax: +81-3-5841-6408,
E-mail: chiashi@photon.t.u-tokyo.ac.jp

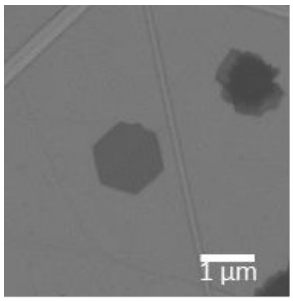

Fig. 1 SEM image of graphene on h-BN.

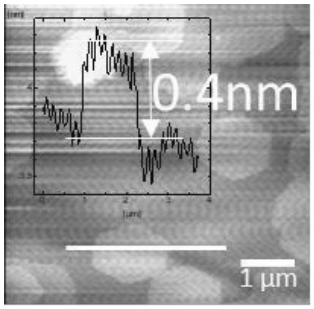

Fig. 2 AFM image of graphene on graphite.

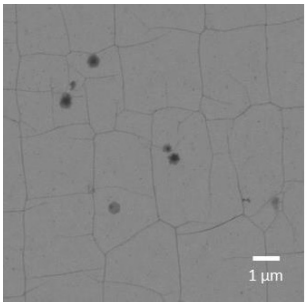

Fig. 3 SEM image of graphene on sapphire.

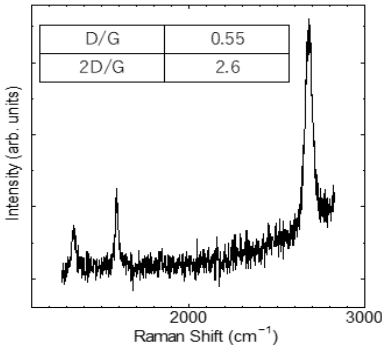

Fig. 4 Raman spectra at one point of graphene on sapphire.

Electronic structure and transport properties of multilayer Nb-doped MoS_2

○ Shota Yamaguchi[1], Ryosuke Mizuno[2], Hiroyuki Mogi[2], Hong En Lim[1], Takahiko Endo[1], Yusuke Nakanishi[1], Kazuhiro Yanagi[1], Kosuke Nagashio[3], Shoji Yoshida[2], Hidemi Shigekawa[2], Yasumitsu Miyata[1]

[1] *Department of Physics, Tokyo Metropolitan University, Hachioji 192-0397, Japan*
[2] *Faculty of Pure and Applied Sciences, University of Tsukuba, Tsukuba 305-8573, Japan*
[3] *Department of Materials Engineering, The University of Tokyo, Tokyo 113-8656, Japan*

In recent years, transition metal dichalcogenides (TMDCs) have drawn significant attention because of their atomically-thin layered structures and superior electronic properties. In some device applications, it is frequently required to use degenerate semiconductors with high carrier density. For such application, previously reported studies have employed multilayer Nb-doped MoS_2, which has a high hole density of approximately 10^{19} cm^{-3} [1,2]. However, their electronic structure has not been investigated in detail. In this study, we have characterized the multilayer Nb-doped MoS_2 by using scanning tunneling spectroscopy (STS) and transport measurements. The results are compared to those of chemical vapor deposition (CVD) grown monolayer MoS_2 for reference.

The multilayer Nb-doped MoS_2 flakes were prepared on SiO_2/Si substrates by mechanical exfoliation, and In/Au electrodes were deposited to fabricate field-effect transistors (FETs). As shown in Fig. 1a, it shows a p-type behavior with weak gate voltage dependence. The CVD-grown monolayer MoS_2, on the other hand, is an n-type semiconductor that exhibits strong gate dependence. Using this combination, a PN junction was fabricated. The vertical heterostructure of these p- and n-type MoS_2 shows a rectification property as expected (Fig. 1b). Meanwhile, the STS measurements reveal that dI/dV curves of the Nb-doped and CVD-grown MoS_2 are almost identical with the Fermi levels located within each respective bandgap (Fig.1c). These results suggest that the carrier density of the surface Nb-doped MoS_2 is much different from that of bulk ones.

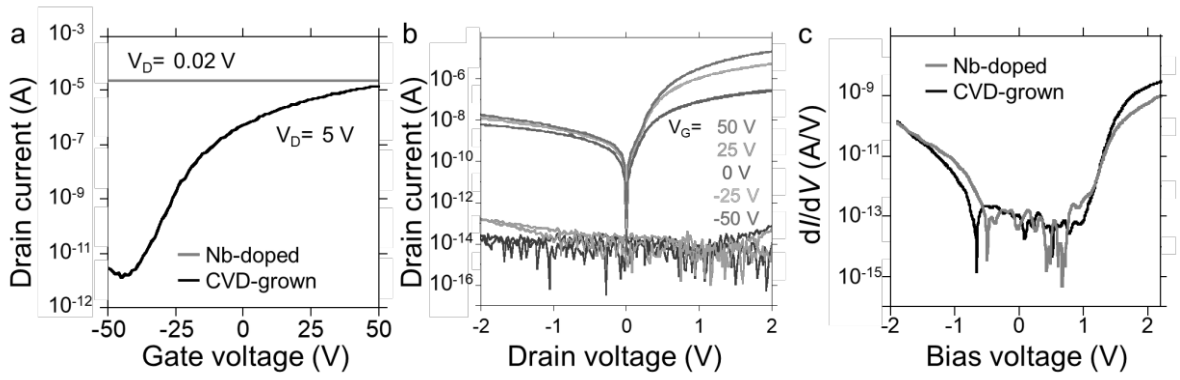

Figure 1 (a) I_D–V_G curves of the FETs fabricated using the Nb-doped multilayer MoS_2 and the CVD-grown monolayer MoS_2. (b) I_D–V_G curves of Nb-doped MoS_2/CVD-MoS_2 vertical heterostructure at different gate voltages. (c) dI/dV curves of the Nb-doped multilayer MoS_2 and the CVD-grown monolayer MoS_2.

[1] J. Suh *et al.* Nano Lett. **14**, 6976-6982 (2014).
[2] K. Nakamura *et al.* ACS Appl. Mater. Interfaces, **12**, 51598–51606 (2020).

Corresponding Author: Y. Miyata, Tel: +81-042-677-2508, E-mail: miyata-yasumitsu@tmu.ac.jp

Highly sensitive temperature sensing for 2D materials using NV centers

○Kazuki Nishibara, Kuniharu Takei, Seiji Akita, Takayuki Arie

Department of Physics and Electronics, Osaka Prefecture University, Osaka 599-8531, Japan

Two dimensional materials are one of the candidates for novel electronic and optoelectronic functional devices. To exploit its performance fully and effectively, understanding the physical characteristics such as heat conduction during device operation is required. Raman thermometry is usually used for measuring the thermal conductivity of 2D materials. Raman peaks, however, change with changing the temperature as well as carrier densities and induced strain in the materials, making it difficult to interpret the measured data. Here we have developed the sensing system using nitrogen-vacancy (NV) centers in diamond, which is expected as a high sensitive magnetometer and thermometer, for visualizing the conducting heat mapping in the devices at the sub-micrometer scale.

We used a single-crystal diamond substrate with the typical nitrogen density of ≈2 ppm for testing the home-made equipment. The optically detected magnetic resonance (ODMR) spectra from NV ensembles were obtained by a 520 nm excitation laser, microwave signal generator, amplifier and antenna. In addition, APD with a lock-in amplifier is used for higher signal-to-noise ratio and rapid data acquisition, which is synchronized with the microwave frequency change of the signal generator automatically.

Figure 1 exhibits the comparison between ODMR spectra with and without a lock-in amplifier. The data at each frequency were obtained by accumulating the photon signal for 2 s and 1 s with a photon counter and a lock-in amplifier, respectively, clearly indicating that the SN ratio is better even though the data acquisition time is shorter. The resonance frequency shifts with changing the local temperature in diamond. Figure 2 shows the temperature dependence of the resonance frequency, in which the slope is −63.0±1.5 kHz/K, comparable with the value previously reported [1]. Since the temperature-dependent frequency shift is independent on the magnetic field, the system we built can be used for temperature mapping during device operation of 2D materials.

[1] V. M. Acosta *et al*. Phys. Rev. Lett., **104**, 070801 (2010).

Corresponding Author: T. Arie
Phone/Fax: +81-72-254-9265
E-mail: arie@pe.osakafu-u.ac.jp

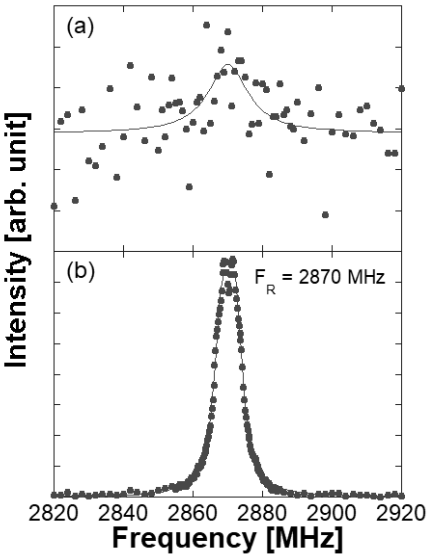

Fig. 1 ODMR spectra of NV ensembles in diamond (a) with a photon counter and (b) with a lock-in amplifier.

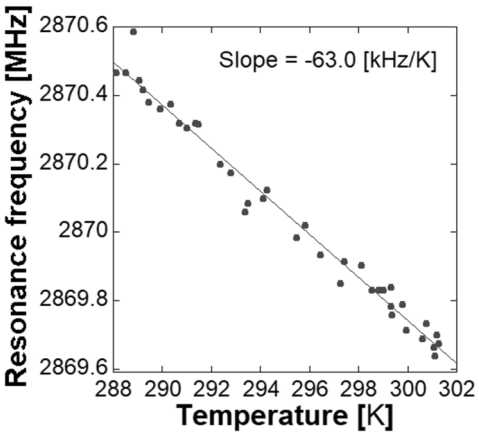

Fig. 2 Temperature dependence of the resonance frequency of NV ensembles.

Introducing lattice vacancies as adsorption sites in monolayer MoS_2

○Yangzhou Zhao[1], Hiroki Yokota[2], Haruna Ichikawa[2], Yasushi Ishiguro[2], Kazuyuki Takai[1,2]

[1] *Graduate School of Science and Engineering, Hosei University, Tokyo 184-8584, Japan*
[2] *Dept. of Chemical Science and Technology, Hosei University, Tokyo 184-8584, Japan*

In view of verifying the influence by lattice vacancies on the structure and electronic properties, the monolayer MoS_2 sample is irradiated with low energy Ar^+ ion beam in order to introduce vacancies under a well-controlled condition, and evaluated by Raman spectroscopy, photoluminescence (PL) and electrical conductivity measurement.

After Ar^+ beam irradiation, both of the line widths of E_{2g} and A_{1g} peaks in the Raman spectra become broad as increasing of irradiation dose which is experimentally controlled by the irradiation time of the beam. The observed increase of the line width is attributed mainly to the increase of the satellite peaks' contribution caused by the introduction of lattice vacancies [1]. Interestingly, the effect of the irradiation is more significant for E_{2g} in spite of less influence of charge transfer by molecular adsorption, where A_{1g} peak is much more sensitive due to its large electron-phonon coupling [2][3].

As for electrical conductivity, the FET measurements indicate that only the Ar gas introduction does not affect the electrical transport properties of MoS_2-FET. However, the threshold voltage for MoS_2-FET shifts to the negative side after Ar^+ beam irradiation, with minor mobility decrease. However, positive shift appears upon the irradiation time, suggesting the hole doping during the Ar^+ ion irradiation. This might be explained by charge transfer from terminating oxygen atoms of introduced defects originating from the residue oxygen gas in the measurement vacuum chamber.

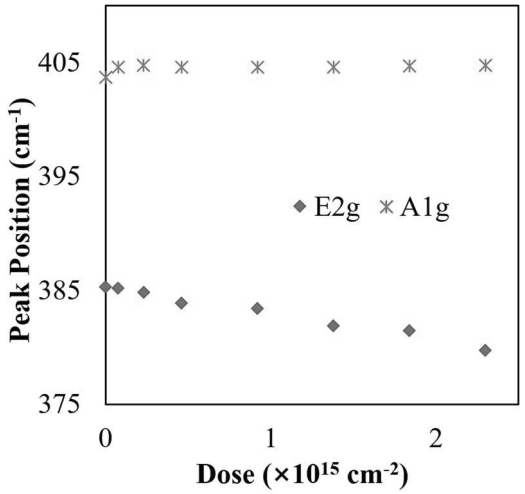

Fig.1 Dosage dependence of Raman peak position for E_{2g} and A_{1g} of monolayer MoS_2 irradiated with Ar^+ ion beam.

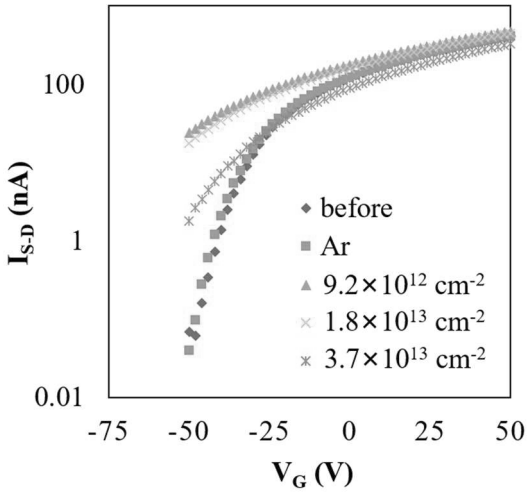

Fig.2 FET-conductivity for monolayer MoS_2 irradiated with Ar^+ ion beam at dosage from 0 to 3.7×10^{13} cm^{-2}.

[1] Soungmin Bae et al., Phys. Rev. App., **7**, 024001(2017).
[2] B. Chakraborty et al., Phys. Rev. B, **85**, 161403(2012).
[3] N. Kodama et al. FNTG(2018).

Corresponding Author: Kazuyuki Takai
E-mail: takai@hosei.ac.jp

Polarized Raman spectroscopy in layered WTe_2

○Hirofumi Nema, Yasuhiro Fujii, Shogo Saito, Eiichi Oishi, Akitoshi Koreeda

Department of Physical Sciences, Ritsumeikan University, Shiga 525-8577, Japan

Layered materials such as graphite and transition metal dichalcogenides (TMDCs) are expected for use in valleytronics and optoelectronics [1,2]. WTe_2 belongs to TMDCs and attracts much attention due to its huge positive magnetic resistance [3] and pressure-induced superconductivity [4,5]. However, the unconventional behavior of a Raman peak in WTe_2 is not fully understood in a previous study [6]. Therefore, additional measurements are necessary to improve our understanding of the behavior.

In this study, we report polarized Raman spectroscopy of bulk WTe_2. Figure 1 (a) shows the obtained spectra for the HH configuration. In the spectra, 7 peaks (P1-P7) were observed, as reported in the previous study [6]. In addition, an unreported peak (P0) was observed at around 9 cm^{-1} (Fig. 1 (b)). Judging from the results of the first-principles calculations [6], the peak corresponds to A_1 mode. We will discuss the detailed results of polarization dependence during the poster presentation.

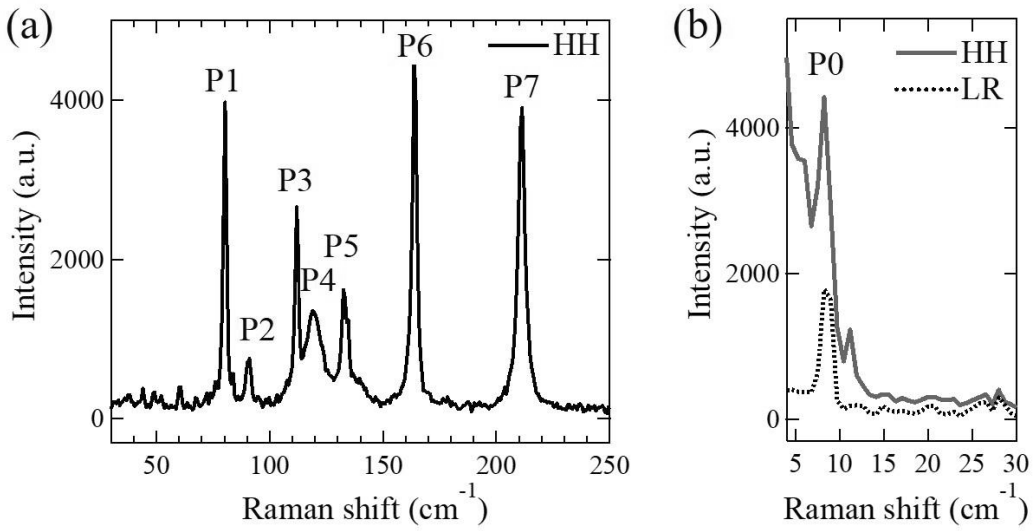

Fig. 1 Raman spectra of WTe_2 at around (a) P1-P7, and (b) P0. R(L) represents the right(left)-handed polarized light.

[1] H. Schomerus, Phys. Rev. B **82**, 165409 (2010).
[2] Q. Wang *et al*., Nat. Nanotechnol. **7**, 699 (2012).
[3] M. N. Ali *et al*., Nature **514**, 205 (2014).
[4] D. Kan *et al*., Nat. Commun. **6**, 7804 (2015).
[5] X. Pan *et al*., Nat. Commun. **6**, 7805 (2015).
[6] W.-D. Kong *et al*., Appl. Phys. Lett. **106**, 081906 (2015).

Corresponding Author: H. Nema
Tel: +81-77-561-5752, Fax: +81-77-561-5752,
E-mail: h-nema@fc.ritsumei.ac.jp

Negative circularly polarization of moiré exciton luminescence in $WSe_2/MoSe_2$ heterobilayers

○Keisuke Shinokita[1], Kunpei Aino[1], Kenji Watanabe[2], Takashi Taniguchi[3], and Kazunari Matsuda[1]

[1] *Institute of Advanced Energy, Kyoto University, Uji 611-0011, Japan*
[2] *Research Center for Functional Materials, NIMS, Tsukuba 305-0044, Japan*
[3] *International Center for Materials Nanoarchitectonics, NIMS, Tsukuba 305-0044, Japan*

Atomically thin transition metal dichalcogenides (TMDs) is an ideal two-dimensional system and possesses intriguing optical properties related to valley degrees of freedom [1]. Van der Waals heterostructures composed of TMDs are a fascinating platform to engineer the optically generated excitonic properties through moiré patterns towards novel quantum phenomena. The moiré pattern as a periodic trap potential can give rise to spatially ordered ensembles of the zero-dimensional exciton (moiré exciton), which offers the possibility for dense coherent quantum emitters and quantum simulation of many-body physics [2,3].

Here we studied the novel moiré exciton properties in a twisted $WSe_2/MoSe_2$ heterobilayer based on circularly polarized photoluminescence (PL) spectroscopy. Figure 1(a) shows the circularly polarized PL spectra under σ^+ excitation with different excitation power conditions. Several peaks observed in the PL spectra reflect the response of the interlayer exciton trapped with the moiré potential (moiré exciton). In addition, because of the optical selection rule of the moiré exciton, the σ^- emission is stronger than the σ^+ emission, showing the negative circular polarization, which is different from those in monolayer TMDs. As increasing excitation power, σ^+ and σ^- emission at lower-emission energy at 1.32 eV have the same intensity, and circular polarization becomes zero. On the other hand, although the emission at 1.36 eV has no circular polarization at low excitation power, it shows stronger σ^+ emission at high excitation power. These results suggest that the energy levels of moiré excitons at lower energy are fully occupied at high excitation power, and the moiré excitons occupy energy levels at another valley, resulting in the cancelation of the σ^+ and σ^- emission from different valleys.

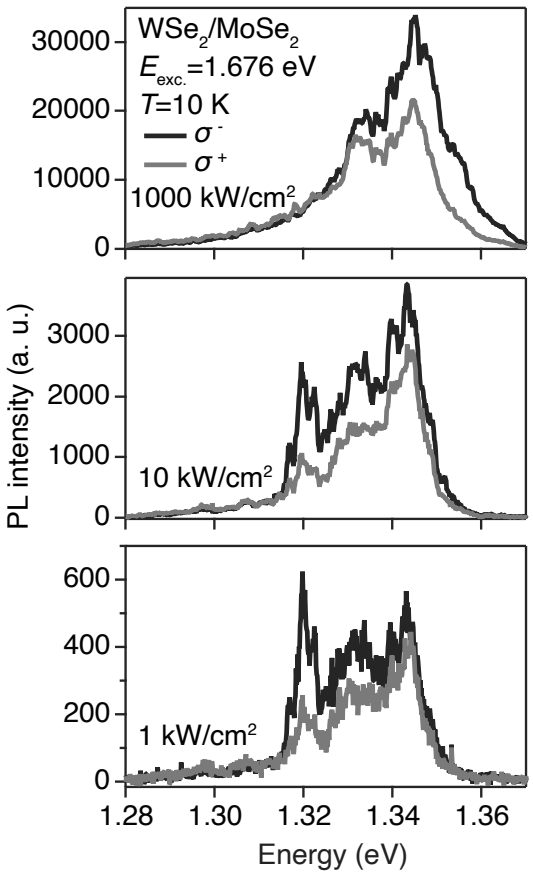

Fig. 1. (a) Circularly-polarized PL spectrum under σ^+ excitation with different excitation power.

[1] K. Shinokita *et al*., Adv. Funct. Mater. **29**, 190260 (2019).
[2] K. Seyler *et al*, Nature **66**, 567 (2019).
[3] K. Shinokita *et al*., Nano Lett. **21**, 5938 (2021).

Corresponding Author: K. Shinokita
Tel: +81-774-38-3465 Fax: +81-774-38-3467,
E-mail: shinokita.keisuke.4r@kyoto-u.ac.jp

Battery electrode properties of HB sheets

○Marina Ukai, Shinya Jindo, Yosuke Ishii, Shinji Kawasaki

Department of Life Science and Applied Chemistry, Nagoya Institute of Technology, Nagoya 466-8555, Japan

Currently, lithium-ion batteries (LIBs) are used in a variety of products such as smartphones and electric vehicles, and the global demand for LIBs is increasing. In LIBs, graphite, whose theoretical capacity is 372 mAh/g, is used as anode electrode materials. Commercially available LIBs charge the graphite anode up to almost the theoretical limit. Therefore, in order to increase the energy density of LIBs, we have to explore new anode materials. Recently, it was predicted by a theoretical study that hydrogen boride (HB) can work as a high capacity (862 mAh/g) anode of LIBs. However, experimental measurements of its electrochemical behavior have not been made yet. Therefore, we conducted an experimental study to verify the theoretically predicted properties by actually synthesizing HB sheets and using them as LIB electrodes.

HB sheets were produced by exfoliation and ion exchange of MgB_2 at room temperature and atmospheric pressure. The successful synthesis of HB sheets was confirmed by X-ray photoelectron spectroscopy (XPS), X-ray diffraction (XRD), and soft X-ray emission spectroscopy (SXES). Mg signal was not detected from the HB sheets by XPS. This result indicates that ion exchange from MgB_2 to HB was carried out completely. We confirmed by transmission electron microscopy (TEM) that the obtained HB sheets were well dispersed and exists as a thin film.

Fig. 1 shows the observed charge-discharge curves of the HB sheet. As shown in Fig. 1, the reversible capacity of the HB sheet is about 75 mAh/g, which is much less than the predicted value 862 mAh/g. We'll discuss Li ion storage property of the HB sheet in more detail in the symposium.

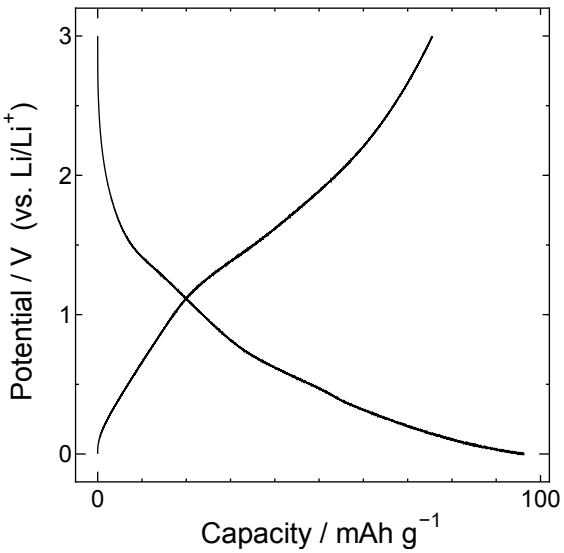

Fig. 1 Charge-discharge curves of HB sheet electrode measured with constant current of 25 mA/g.

Corresponding Author: S. Kawasaki
E-mail: Kawasaki.shinji@nitech.ac.jp

Photovoltaic Effect in MoS_2/hBN Heterostructure

○Shaochun Zhang[1], Mengsong Xue[1], Ryo Kitaura[1]

[1] *Department of Chemistry, Nagoya University, Nagoya 464-8602, Japan*

The photovoltaic effect is an essential process to convert light to electricity. In addition to the pn junction-based photovoltaic effect, which has been utilized in solar cells, another photovoltaic effect (BPVE), the bulk photovoltaic effect [1], has recently attracted attention. BPVE arises not from band bending but from the shift of electron could in real space upon light excitation. Recently, low-dimensional materials, including WS_2 nanotubes [2] and vdW heterostructures [3], have proven to show BPVE.

In this work, we have explored various two-dimensional-based vdW heterostructures, including MoS_2/hBN heterostructures, and observed non-zero photocurrent at zero bias voltage. Figure1 shows the room temperature photo-current mapping image by scanning the laser spot across the device. A typical short circuit current under zero bias was dozens nanoamperes, and the current-voltage (I-V) curves show linear relationship. Laser-power dependence of the photocurrent were also measured, which show the characteristic crossover from linear to square-root dependence. In the presentation, we will discuss more details about the photovoltaic effect in our devices.

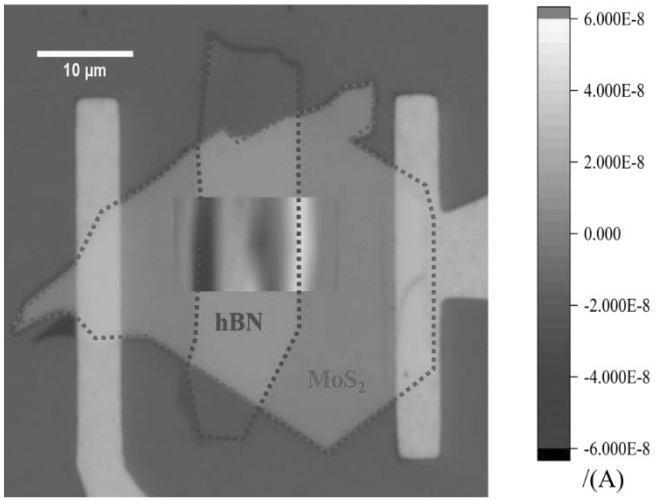

Fig.1 Photo-current mapping for hBN-MoS_2 device

[1] Ashley M. Cook et al. Nat. Commun. **8**, 14176 (2017).
[2] Y.J.Zhang et al. Nature **579**, 349 (2019)
[3] Akamatsu et al. Science **372**, 68 (2021)

Corresponding Author: Ryo Kitaura
Tel: +8152-789-2477, Fax: +81-52-747-6442
E-mail: r.kitaura@nagoya-u.jp

Machine learning determination of the twist angle of bilayer graphene by Raman spectroscopy

○Pablo Solís-Fernández[1], Hiroki Ago[1,2]

[1] *Global Innovation Center (GIC), Kyushu University, Fukuoka 816-8580, Japan*
[2] *Graduate School of Engineering Science, Kyushu University, Fukuoka 816-8580, Japan*

Recent findings on the properties of twisted bilayer graphene (tBLG), specially the discovering of superconductive states at low twist angles [1], have sparked an increased interest in twisted 2D materials. The ability to synthesize BLG by CVD with some control of the twist angle has also improved in recent years [2]. It is thus necessary to find fast, reliable, and non-destructive methods to precisely determine the twist angle of tBLG. Given the large amount of information encoded in the Raman spectrum of tBLG, Raman spectroscopy can provide such method. However, changes in the Raman spectra induced by the twist angle can be very subtle, thus making the angle identification tedious. Here, we propose the use of machine learning (ML) analysis techniques for the automated classification of the Raman spectrum of tBLG into a selected range of twist angles [3]. Distinctive features of the Raman spectrum of a tBLG sample are extracted and provided to a pretrained ML model that can then predict the twist angle of the sample (Figure 1). The proposed ML classification is low computationally demanding, providing fast and accurate results with ~99 % of agreement with the manual labelling of the spectra. Given the ubiquitous nature of the Raman signal in 2D materials, this method can be expanded to determine the twist angle of other 2D heterostructures, or to evaluate different properties, such as the levels of doping and strain. The flexibility and non-invasive nature of the Raman measurements, paired with the predictive accuracy of the ML, is expected to facilitate the exploration of the emerging research field of twisted van der Waals heterostructures.

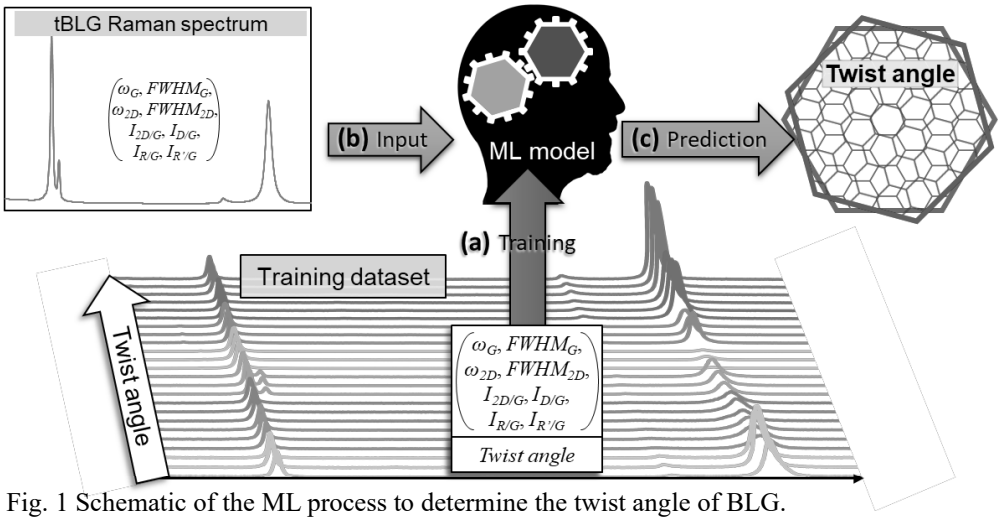

Fig. 1 Schematic of the ML process to determine the twist angle of BLG.

[1] Y. Cao *et al*., Nature, **556**, 43 (2018).
[2] P. Solís-Fernández *et al*., ACS Nano, **14**, 6834 (2020).
[3] P. Solís-Fernández *et al*., ACS Appl. Nano Mat., *accepted,* doi:10.1021/acsanm.1c03928 (2022).

Corresponding Author: P. Solís-Fernández
Tel: +81-92-583-8975, Fax: +81-92-583-8975
E-mail: ps-fernandez@gic.kyushu-u.ac.jp

Hierarchic Aggregation of Elementary Diamond Nanoparticles: Its Tolerance under Various Conditions

○ Tomoya Yoshihara[1], Masaya Nemoto[1], Toshihiko Tanaka[1], Tetsuya Aoyama[2], Yasuhiro F. Miura[3], Eiji Osawa[4]

[1]Department of Chemistry and Biochemistry, National Institute of Technology, Fukushima College, 30 Aza-nagao, Tairakamiarakawa, Iwaki, Fukushima, 970-8034, Japan
[2]Ultrahigh Precision Optics Tech. Team, RIKEN RAP, 2-1 Hirosawa, Wako, Saitama, Japan
[3]Hamamatsu University School of Medicine, 1-20-1 Handayama, Higashi-ku, Hamamatsu City, Shizuoka, Japan
[4]Nano Carbon Research Institute Ltd., Asama Research Extension Center, Shinshu University, 3-15-1 Tokida, Ueda, Nagano, Japan

Elementary diamond nanoparticles (EDIANs) are aggregated by trace ions in their aqueous colloidal solutions and salt out at only ~10^{-3} M of salt.[1] We consider that such sensitivity demonstrates a unique physical insight of them. Protein molecules also have similar sizes in water and never salt out at such a low concentration. We believe that not only their surface functional groups (-NH-, COOH, etc.) but also their intrinsic strong electric polarization[2] should be considered.

We have presented herein their hierarchic aggregation in aqueous solutions. We diluted nanodiamond (ND) solutions （NanoAmando@, *NanoCarbon Research Institute Ltd.*, containing EDIANs）from 2.5% with ultrapure water and measured their size distribution spectra by using the novel analysis method where Rayleigh scattering are concerned in DLS. Usually, commercial DLS spectrometers calculate the spectra according to Mie scattering; and under 100 nm, we have to calculate them rather according to Rayleigh scattering. Diluting aggregation[4] took place and in the mid region from 0.1 to 1 % of ND, EDIANs and their aggregates are mixed as shown in **Fig.1** . Their aggregation is hierarchic: they aggregate discontinuously from EDIANs to 1st aggregates and then further jump to 2nd aggregates except small aggregates such as dimers which sometimes contaminate EDIANs. These aggregates were scarcely observed in two blank zones [(1) 10-15 nm, (2) 30-50 nm, on various conditions (temperature, salt, etc.). Why are the two blanks there? Perhaps their aggregates would not be stable if they should be formed. We will discuss a few models of the hierarchic aggregation with respect to the similarity of EDIANs both in size and shape.

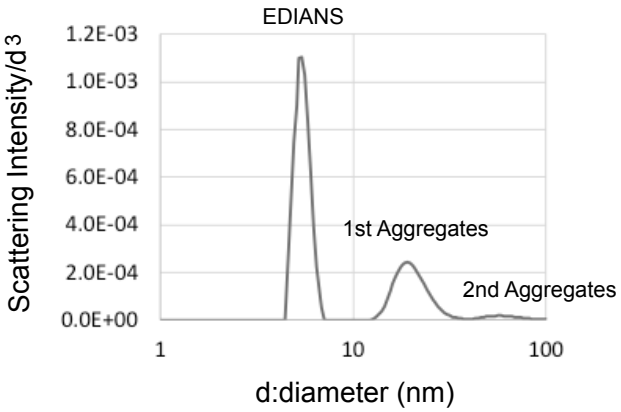

Figure 1. A size distribution spectrum [scattering intensity/(diameter)^3 calculated from a DLS measurement] of a 0.25% NanoAmando aquaous solution.

[1] Nemoto, et al., FNTG 60th Abstract Book (2021); [2] A. S. Barnard, E. Osawa; *Nanoscale* 6, 1188 (2014); [3] Technical Report No.2, *NanoCarbon Research Institute Ltd.*（2007）; [4] N.O. Mchedlov-Petrossyan, N. N. Kamneva, A. I. Marynin, A. P. Kryshtal, E. Osawa, *Phys. Chem. Chem. Phys.*, 17, 16186 (2015).
Corresponding Author:Toshihiko Tanaka / Tel: +81-246-46-0810 / E-mail: ttanaka@fukushima-nct.ac.jp

Synthesis of Hetero Transition Metal Dichalcogenide Nanotubes

○Mai Nagano[1], Yohei Yomogida[1], Md. Ashiqur Rahman[1,2], Yusuke Nakanishi[1], Yasumitu Miyata[1], Kazuhiro Yanagi[1]

[1]*Department of Physics, Tokyo Metropolitan University, Hachioji, Tokyo 192-0372, Japan*

2 Department of Physics, Comilla University, Cumilla-3506, Bangladesh

One-dimensional van der Waals heterostructure, especially coaxially stacked hetero-nanotubes, have attracted much attention because of their unique physical properties [1]. Novel synthesis schemes of hetero structured nanotubes like hexagonal boron nitride (BN)/carbon nanotubes and transition metal dichalcogenide (TMDC) /carbon nanotubes have been developed through the formation of BN or TMDC layers on the surface of carbon or BN nanotubes [1, 2]. These results suggest that the nanotubes can work as templates for formation of another nanotubes. Semiconducting TMDC nanotubes, which are discovered by Tenne et al [3], are one of the inorganic nanotubes. They exhibit semiconducting characteristics regardless how they are rolled. Therefore, for the formation of 1D hetero semiconductor interfaces in hetero-structured nanotubes, hetero structured TMDC nanotubes is the most appropriate. In this study, we tried to synthesize semiconducting hetero-nanotubes consisting only of semiconducting TMDCs nanotubes.

We used WS_2-nanotubes as a template for formation of MoS_2 nanotubes. First, we prepared WS_2 nanotubes through the sulfurization of the tungsten oxide nanowires, which were obtained by solvothermal synthesis [4]. We employed formation of outer-layer nanotubes through the deposition of transition metals and their sulfurization approach, which was reported in the study on two-dimensional TMDCs [5]. In this study, the molybdenum was deposited on the surfaces of the synthesized WS_2 nanotubes and reacted with sulfur for 10 min in Ar flow to synthesize WS_2/MoS_2 hetero-nanotubes.

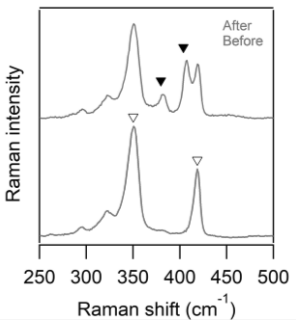

Fig.1 Raman spectra of before and after 2nd sulfurization. ▽ and ▼ show the Raman peaks of WS_2 and MoS_2,

Fig. 1 shows the Raman spectra of samples before and after 2nd sulfurization. After 2nd sulfurization, we observed two Raman peaks of MoS_2 and WS_2. Fig. 2 shows transmission electron microscopy (TEM) image of samples. Comparing the two pictures, we observed the formation of multilayered MoS_2 around WS_2 nanotubes (Fig. 2b). These results indicate the successful synthesis of hetero-nanotubes consisting only of semiconductor TMDCs.

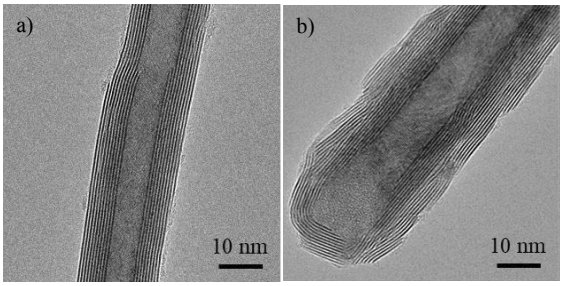

Fig.2 TEM image of samples. (a) Before 2nd sulfurization. (b) After 2nd sulfurization.

References: [1] R. Xiang et al. Science, 367, 537 (2020). [2] M. Liu et al., ACS Nano 15, 8418 (2021), [3] R. Tenne et al., Nature 360 444 (1992), [4] Y. Yomgida et al., Appl. Phys. Exp. 12, 085001 (2019), [5] C-R. Wu et al. Nano Lett., 16, 7093 (2016).

Corresponding to Yohei Yomogida (yomogida@tmu.ac.jp) & Kazuhiro Yanagi (yanagi-kazuhiro@tmu.ac.jp)

Low temperature chemical modification of Nanodiamond and its effects on structure and magnetism

○Takuma Tsuji [1], and Kazuyuki Takai[1,2]

[1]*Graduate School of Science and Engineering, Hosei University, Tokyo 184-8584, Japan*

[2]*Research Center for Micro-Nano Technology, Hosei University, Tokyo 184-0003, Japan*

Surface chemical modification of Nanodiamond (**ND**) covered with graphene layers is an important strategy to tune its electronic / chemical properties owing to its large specific surface area. Especially, oxidation and hydrogenation introduce the large electric polarization on the surface of ND, which could change electric screening of excitons in the photo absorption, carrier density, hydrophilicity and so on. The surface modifications of ND has been generally carried out by chemical reactions at high temperature in the gas phase. However, effects on the core-diamond structure are suggested in the high temperature reactions [1]. In this study, the oxidation and hydrogenation of ND were carried out at low temperature in the liquid phase and their effects are evaluated in terms of structure and magnetism.

NDs repeatedly oxidized three times using the Brodie method [2] and hydrogenated by Lithium Aluminum Hydride (LAH) in anhydrous THF solvent [3], are labeled as **BND3**, **HND-L**, respectively. The core-diamond structure and magnetism of ND were investigated measured by XRD (smartLab, Rigaku), and SQUID magnetometer (MPMS-XL, Quantum Design), respectively.

As shown in Fig. 1, the peak position, intensity, and full width at half maximum do not change from those in pristine **ND** in the oxidized and hydrogenated NDs, confirmed that the crystallinity of the core-diamond structure is maintained in the surface chemical treatments under low temperature liquid phase conditions. In addition, no crystalline impurities were found to be introduced by the synthesis processes. The magnetization curves at 2 K shown in Fig. 2 exhibit increasing in the magnetization with the surface modifications. The observed enhancement in the magnetization upon the oxidation is attributed to the increase in the paramagnetic components due to the modification of the topology in the graphene layer on the surface of ND [4]. Although the contributions of amorphous impurities undetectable by XRD in the synthesized process should be examined, the increase in magnetization during hydrogenation would be also attributed to the same reason as that for the oxidation.

The surface chemical modifications under low temperature liquid phase conditions which did not affect the core-diamond structure of ND are promising methods to control the electronic properties of NDs such as the magnetism.

[1] X. Xu, Z. Yu, *Particuology*, **10**, 339-344, (2012). [2] M. R. Karim, *et. al*, *J.Phys.Chem. C* **120**, 21976, (2016). [3] A. Ambrosi, et al., Chem mater, 24, 2292-2298, (2016). [4] K. Tajima, et al., Polyhedron, 136, 155, (2017).

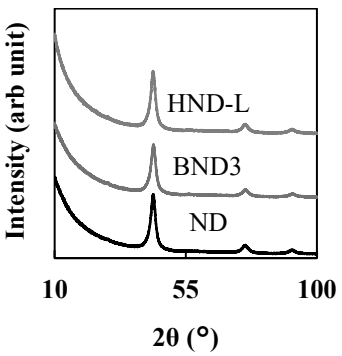

Fig. 1 XRD profiles of NDs

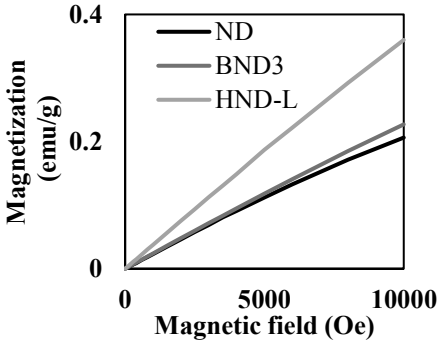

Fig. 2 Magnetization curves to NDs at 2K

Synthesis and Extraction of Carbon-Encapsulated Iron Carbide Nanoparticles for Perovskite Solar Cell Application

Jiye Han[1,2], Kyusun Kim[1], Il Jeon[1,2]

[1] *Department of Nano Engineering, SKKU Advanced Institute of Nanotechnology (SAINT), Sungkyunkwan University (SKKU), Suwon 16419, Republic of Korea*
[2] *Department of Nano Fusion Technology, Pusan National University, Busan 46241, Republic of Korea*

In this study, an effective method for obtaining large amounts of metal nanoparticles encapsulated by carbon layers using aerosol-assisted chemical vapour deposition was introduced [1-3]. By optimizing the conditions, iron carbide nanoparticles with sizes ranging from 5 nm to 100 nm were produced along with carbon nanotubes. Smaller nanoparticles with diameters of less than 20 μm were then extracted from the carbon assortments through sonication, centrifugation, and filtration. The nanoparticles exhibit a tendency to aggregate over time owing to the π–π interaction between the graphitic carbon shells surrounding the iron carbides. The aggregation of the metal ion nanoparticles was controlled to maximise the light absorption by the gap-surface plasmon effect in PSCs. Application of the metal nanoparticles to the devices increased the PCE from 19.71% to 21.15%. The improvement is attributed to the increases in all three major photovoltaic parameters, namely, J_{SC}, V_{OC}, and the fill factor (FF). Both the J_{SC} trend over the nanoparticle aggregation time and the computational study show that the plasmonic effect accounts for the high J_{SC} [4,5]. Meanwhile, high V_{OC} and FF are ascribed to the improved charge transport due to the presence of the nanoparticles, which we postulate the high electron affinity and host–guest interaction within the nanoparticles to have induced favourable effects. The carbon-encapsulated metal nanoparticle-added solar cells exhibited a high device stability analogue to the control devices, confirming that metal ion migration does not occur owing to the protection by the carbon shell.

[1] A.G. Nasibuli *et al*. ACS Nano, **5** (2011).
[2] C.T. Wirth, *et al*. Chem. Mater., **24** (2012).
[3] B. McLean, *et al*. J. Appl. Phys., **129** (2021).
[4] V.L. Dalal, *et al*. J. Appl. Phys., **50** (1979).
[5] T. Liu, *et al*. Energy Environ. Sci., **50** (2020).

Corresponding Author: I. Jeon
Tel: +82-31-299-4187
E-mail: il.jeon@spc.oxon.org

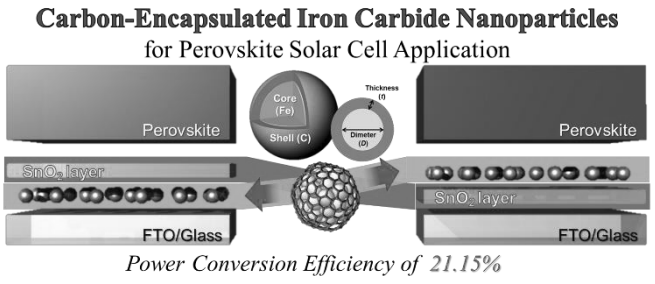

Three-dimensional quantum Hall effect in Weyl semimetal

○F. R. Pratama[1,2], Nguyen T. Hung[1,2], Riichiro Saito[1]

[1] *Department of Physics, Tohoku University, Sendai 980-8578, Japan*
[2] *Frontier Research Institute for Interdisciplinary Sciences, Tohoku University, Sendai 980-8578, Japan*

The quantum Hall effect (QHE) is the quantization of the Hall conductivity in strong magnetic field at low temperature [1]. The QHE provides a useful tool to determine the fine-structure constant and to study the Landau levels in condensed-matter systems. Generally, the QHE is observed in two-dimensional (2D) materials such as 2D electron gas [1] and graphene [2, 3]. Recently, three-dimensional (3D) QHE is discovered in topological materials Cd_3As_2 [4] and $ZrTe_5$ [5], which show some characteristic features distinguishable from that of the 2D QHE, for example, the less-obvious quantization of the Hall conductivity in 3D systems. However, a theoretical study is required to explain the origins of the features of 3D Hall conductivity. In this study, by using a simple model of the Weyl semimetal, we show that the quantization of the Hall conductivity in 3D system arises from a logarithmic singularity of the density of states (DOS), as opposed to that of the delta function singularity in 2D DOS. Further, we discuss temperature and in-plane electric field effects in the quantization of the Hall conductivity.

[1] K. v. Klitzing, Phys. Rev. Lett. **45**, 494 (1980).
[2] Y. Zhang *et al*., Nature **438**, 201 (2005).
[3] K. S. Novoselov *et. al*., Science **315**, 1379 (2007).
[4] C. Zhang *et. al*., Nature **565**, 331 (2019).
[5] F. Tang *et. al*., Nature **569**, 537 (2019).

Corresponding Author: F. R. Pratama
E-mail: pratama@flex.phys.tohoku.ac.jp

Facile synthesis of icosapropyl [60]fullerene

○Kazuhira Miwa[1], Shinobu Aoyagi[1], Takahiro Sasamori[1,2], Shogo Morisako[1,2], Hiroshi Ueno[3], Yutaka Matsuo[4,5], Hideki Yorimitsu[6]

[1] *Graduate School of Science, Nagoya City University, Nagoya 467-8501, Japan*
[2] *Faculty of Pure and Applied Sciences, University of Tsukuba, Tsukuba 305-8571, Japan*
[3] *Frontier Research Institute for Interdisciplinary Sciences and Graduate School of Science, Tohoku University, Sendai 980-8578, Japan*
[4] *Graduate School of Engineering, Nagoya University, Nagoya 464-8603, Japan*
[5] *School of Engineering, The University of Tokyo, Tokyo 113-8656, Japan*
[6] *Graduate School of Science, Kyoto University, Kyoto 606-8502, Japan*

A variety of functionalized C_{60} have been obtained by the introduction of functional groups to the C_{60} surface until now. The reactions of metastable polyanions of C_{60} with electrophiles could be an accessible methodology for the introduction of functional groups. For example, when the corresponding polyanionic C_{60} generated by reduction with Li was trapped by an excess amount of CH_3I, multiply methylated C_{60} was obtained [1]. However, the predominant components were $C_{60}(CH_3)_6$ and $C_{60}(CH_3)_8$, and a variety of methylated C_{60}, i.e., a series of $C_{60}(CH_3)_n$ ($0 \leq n \leq 24$), were formed due to the lability of the polyanionic C_{60}.

We present an efficient multiple alkylation reaction of C_{60} using an in situ reduction/substitution reaction system using sodium dispersion (SD) and dialkyl sulfate (Scheme 1). SD is a well-known and effective reductant, and dialkyl sulfate is an electrophile that is inert to SD. Thus, the coexistence of SD and dialkyl sulfate allows the reactant to undergo repetitive tandem reduction/substitution reactions in situ [2]. The direct analysis in real time mass spectrum (DART-MS) of multiply propylated C_{60} ($C_{60}(nC_3H_7)_n$) obtained by the method (Scheme 1) shows that the distribution of the substitution number (n) was remarkably narrower ($18 \leq n \leq 24$) and the predominant component was icosapropyl C_{60} with n = 20 (Figure 1).

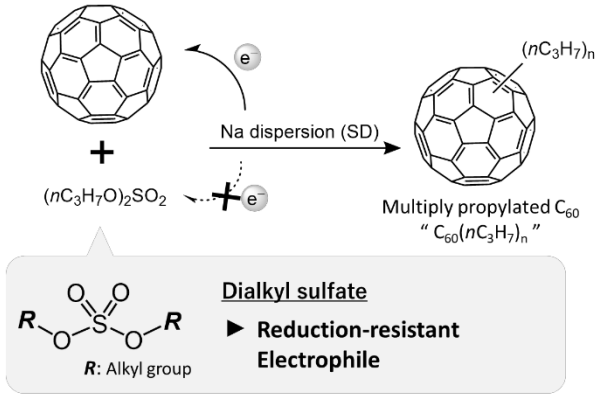

Scheme 1 Strategy for the synthesis of $C_{60}(nC_3H_7)_n$.

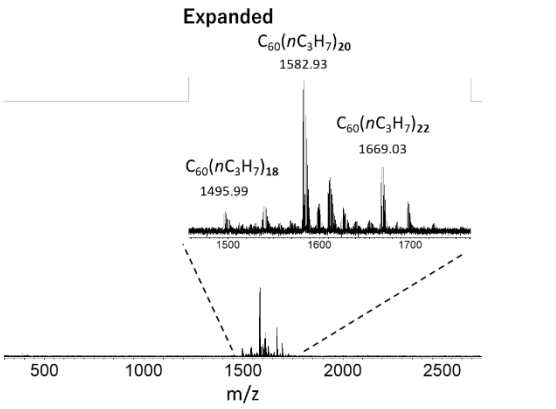

Figure 1 DART-MS spectrum (positive, 500 °C) of $C_{60}(nC_3H_7)_n$.

[1] J. W. Bausch *et al.*, *JACS.* **1991**, *113*, 3205. [2] K. Miwa *et al.*, *Molecules* **2022**, *27*, 450.

Corresponding Author: S. Aoyagi, E-mail: aoyagi@nsc.nagoya-cu.ac.jp

Effect of carrier gas on chemical states of Co catalyst during SWCNT growth: *in situ* XAFS analysis

Meijo Univ.[1], Meijo Nanomaterial Res. Center[2], ○Shusaku Karasawa[1], Daiki Yamamoto[1], Kamal P Sharma[2], Takahiro Saida[1,2], Shigeya Naritsuka[1], Takahiro Maruyama[1,2]

E-mail: takamaru@meijo-u.ac.jp

Introduction

Understanding the growth mechanism of SWCNTs is an important issue to realize structural control of SWCNTs. However, the details of growth process of SWCNTs from catalyst particles is still unclear. Although there have been many studies by *in situ* TEM observations for growth process of SWCNTs, they were mainly performed at relatively low temperature (<700°C) using C_2H_2 or CO as feedstock gases [1]. In this study, we focused on X-ray absorption fine structure (XAFS) measurements to clarify the states of a Co catalyst during SWCNT growth 800°C by alcohol catalytic chemical vapor deposition (ACCVD). Furthermore, we attempted to investigate the effect of carrier gas on the chemical states of Co catalysts during temperature rise and their influence on SWCNT yield.

Experimental procedure

BN powder and cobalt acetate tetrahydrate were mixed in deionized water and calcined. Then, they were grinded into powder and molded to disk-shaped pellets (thickness ~1 mm). Using them, SWCNT growth were performed at 800°C for 10 min by ACCVD (ethanol: 24 sccm) with an Ar carrier gas (1000 sccm) (Ar-CNT). During temperature rise, SWCNT growth, and temperature cooling, *in situ* Co K edge XAFS measurements were performed every two minutes at BL11S2 of Aichi SR. We also performed SWCNT growth under an Ar carrier gas with H_2 gas (Ar/H_2-CNT) and Ar carrier gas with O_2 (Ar/O_2-CNT) during temperature rise, and compared their effects on catalyst composition and SWCNT yield. After *in situ* XAFS analysis, the samples were evaluated using Raman, TEM, and SEM.

Results and discussion

Fig. 1(a) and (b) show Co *K*-edge XAFS spectra of the Ar-CNT and Ar/O_2-CNT during SWCNT growth at 800°C, respectively. From them, time dependences of composition ratios of Ar-CNT and Ar/O_2-CNT were determined by LCF (liner combination fitting) analysis (Fig. 1(c) and (d)). For both samples, most of Co catalysts were carbonized during SWCNT growth, but for Ar/O_2-CNT, the ratio of metallic Co gradually increased. After in situ XAFS analysis, SWCNTs were grown on both samples, but the yield of Ar/O_2-CNT was higher than those of Ar-CNT and Ar/H_2-CNT. We will discuss the effect of concentration of carrier gas on chemical states of Co catalysts and SWCNT yield.

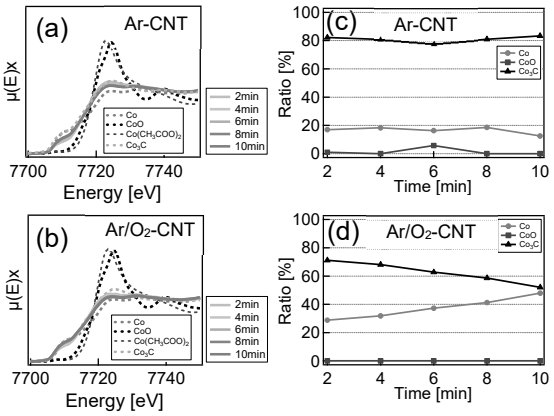

Fig.1 *In situ* XAFS spectra of (a) Ar-CNT and (b) Ar/O_2-CNT. Time dependence of composition change during SWCNT growth for (c) Ar-CNT and (d) Ar/O_2-CNT.

Acknowledgments

This work was partly supported by the Meijo University Research Branding Project for Cultivation and Invention of New Nanomaterials under the MEXT Private University Research Branding Project. Part of this work was supported by JSPS KAKENHI Grant Number JP19H02563 and conducted at the Institute for Molecular Science (IMS) supported by the Nanotechnology Platform of MEXT.

References

[1] H. Yoshida et al. Nano Lett. 8 (2008) 2082.

Corresponding Author: T. Maruyama

Phone: +81-52-838-2386, Fax: +81-52-832-1172, E-mail: takamaru@meijo-u.ac.jp

Efficient and safe purification of carbon nanotubes using $FeCl_3$ vapor

Takuma Goto[1], Hideaki Tanaka[1], Toshio Osawa[1], Mochen Li[2], Hisashi Sugime[2], Suguru Noda[1,2,*]

[1]*Department of Applied Chemistry and* [2]*Waseda Research Institute for Science and Engineering, Waseda University, 3-4-1 Okubo, Shinjuku-ku, Tokyo 169-8555, Japan*

Removal of catalyst metals and purification of carbon nanotubes (CNTs) are highly demanded for various applications of CNTs. Methods including the oxidation and successive acid treatment and the chlorine gas treatment have been developed, however, they suffer from damages to CNTs, poor re-dispersibility of purified CNTs [1], and/or toxic reagents [2].

In this study, an efficient and safe dry purification method was developed that exposes CNTs to $FeCl_3$ vapor at 1000 °C. Fig. 1 shows the transmission electron microscope (TEM) images of three different CNTs before and after purification. Not only Fe (a,c) but also Ni and Y (b) were removed via the reaction of $M(s) + xFeCl_3(g) \rightarrow MCl_x(g) + xFeCl_2(g)$, leaving the hollow graphitic spheres. In this initial trial, a small amount of CNTs (5-10 mg) were treated using an excess amount of $FeCl_3$ (100 mg) using a horizontal reactor.

Then Tuball CNTs were purified at a larger amount (50 mg) using a comparable amount of $FeCl_3$ (100 mg) and a vertical reactor. The purification reaction was proceeded by heating CNTs and $FeCl_3$ simultaneously. The purified CNTs were characterized by scanning electron microscope-energy dispersive X-ray spectroscopy (SEM-EDS) and Raman scattering spectroscopy. The purified CNTs had a significantly reduced Fe content from 20.9 to 5.0 wt% (Fig. 2a) with an increased intensity ratio of G-band to D-band peaks (I_G/I_D) of 106 (Fig. 2b), showing the efficient removal of Fe without damaging CNTs.

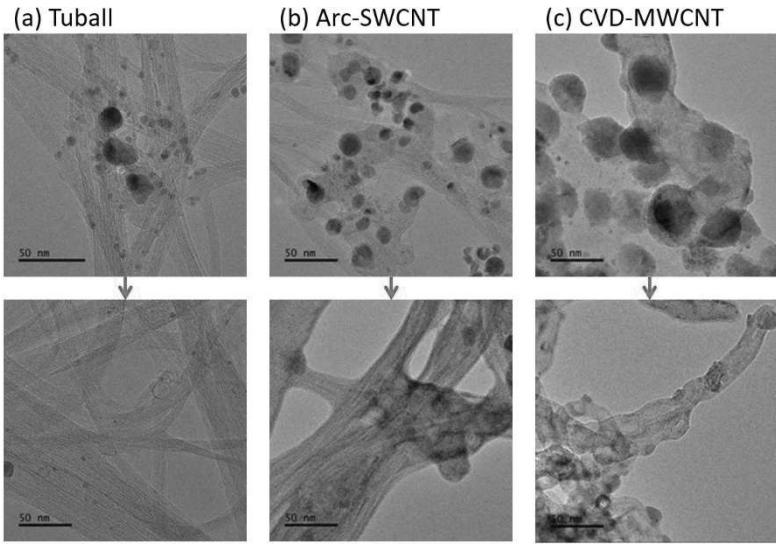

Fig. 1. TEM images of three different CNTs before/after purification.

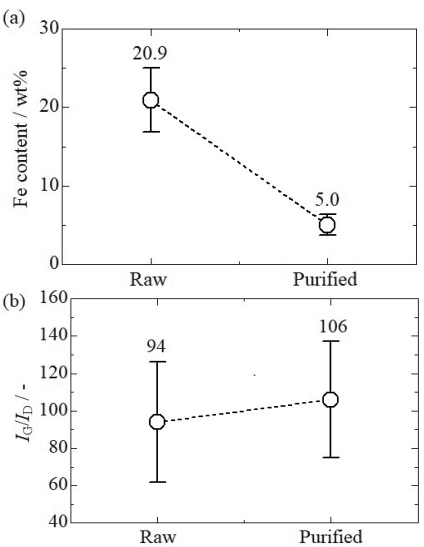

Fig. 2. Fe content (a) and I_G/I_D (b).

[1] P. Hou, et al., Carbon **46**, 2003 (2008). [2] G. Merder, et al., New J. Chem. **37**, 790 (2013).

Corresponding Author: S. Noda, Tel: +81-03-5286-2769, Fax: +81-03-5286-2769, E-mail: noda@waseda.jp

Memristive behavior of hBN-grown CNT assemblies and their repeated *I-V* characteristics

○Misaki Kishibuchi, Kyohei Nasu, Mitsuaki Maetani,Yuichiro Tanaka, Yasuhiko Hayashi, Hiroo Suzuki

Graduate school of Natural Science and Technology, Okayama University, Okayama 700-8530, Japan

Van-der-Waals (VdW) heterostructure is getting a lot of attention because of its potential to develop a new electronic device application. Recently, one-dimensional (1D) VdW heterostructure has been realized by direct growth of two-dimensional (2D) materials such as hexagonal boron nitride (hBN) and transition metal dichalcogenides (TMDCs) on carbon nanotubes (CNTs) [1]. We explored the potential of hBN/CNT heterostructures for device applications by combining our CNT bulk-scaling technology and hBN heterogeneous growth.

Our research group has developed the fabrication technique of bulk-scale CNT assemblies [2]. The CNT sheet and yarn: one of the CNT assemblies, can be fabricated by a dry process with the drawable CNT forest grown by precisely tuned chemical vapor deposition (CVD). In this research, we performed hBN growth directory on the CNT assemblies (sheet and yarn) by conventional powder CVD with a source of NH_3BH_3. The heterogeneous growth of hBN on the CNT sheet was confirmed by optical spectroscope, and transmittance electron microscope (TEM) measurements.

We found the clear hysteresis in *I-V* curves, that is, memristive behavior, with both hBN-grown CNT sheet and yarn [3]. Repeated measurements of the *I-V* characteristics showed abnormal behavior. The disappearance and appearance of hysteresis repeated during repeated measurements (Fig. 1). The numerous measurements presented the stable phase and unstable phase in the repeating characteristics. In the stable phase, the hysteresis continuously appeared. However, in the unstable phase, the unstable *I-V* characteristics with unexpected steep changes in the current appeared. By the systematic experiments, we proposed the possible mechanism of memristive behavior relating to the presence of the amorphous carbon (a-C) and disordered structure of hBN layer. The a-C seemingly formed a conductive filament channel (CFC) in the disordered hBN layer under a high electric field, resulting in the memristive behavior. The abnormal memristive behavior in the repeated measurements can be explained by this model and it might relate to the unstable formation of CFC.

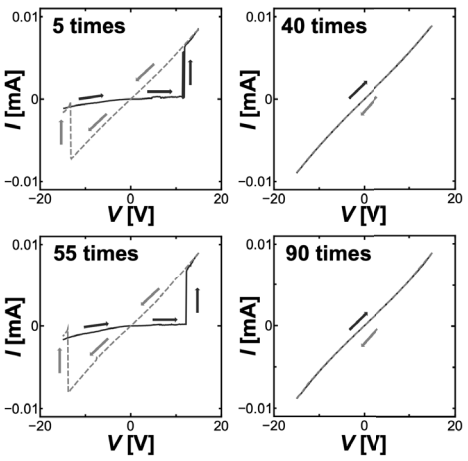

Fig. 1: *I-V* carves of hBN-grown CNT yarns with different measurement times.

[1] R. Xiang, *et al. Science* **367**, 537–542 (2020).
[2] H. Inoue, *et al. Carbon* **158**, 662–671 (2020).
[3] H. Suzuki, M. Kishibuchi *et al.*, *ACS Appl. Electron. Mater.* **3**, 3555-3566 (2021).

Corresponding Author: H. Suzuki
Tel: +81-86-251-8133
E-mail: hiroo.suzuki@okayama-u.ac.jp

Influence of Laser-intensity on the Fermi-level dependence of high-harmonic generation in nanocarbon materials

○Hiroyuki Nishidome[1], Kohei Nagai[2], Kento Uchida[2], Yuta Murakami[3], Kenji Kawahara[4], Takahiko Endo[1], Junko Eda[1], Hitomi Okubo[1], Yohei Yomogida[1], Yasumitsu Miyata[1], Hiroki Ago[4, 5], Koichiro Tanaka[2, 6], Kazuhiro Yanagi[1]

[1] *Department of Physics, Tokyo Metropolitan University, Tokyo 192-0397, Japan*
[2] *Department of Physics, Kyoto University, Kyoto 606-8502, Japan*
[3] *Department of Physics, Tokyo Institute of Technology, Tokyo 152-8551, Japan*
[4] *Global Innovation Center (GIC), Kyushu University, Fukuoka 816-8580, Japan*
[5] *IGSES, Kyushu University, Fukuoka 816-8580, Japan*
[6] *Institute for Integrated Cell-Material Sciences, Kyoto University, Kyoto 606-8501, Japan*

The recent advancement in intense mid-infrared laser sources has enabled us to investigate high-harmonic generation (HHG) in solids [1]. Since this phenomenon demonstrates unconventional behaviors beyond the perturbation regime, a lot of studies have investigated the generation mechanisms. Previously, we have revealed the Fermi-level dependence of HHG in semiconducting single-walled carbon nanotubes (SWCNTs) [2]. We observed significant enhancement and reduction of high harmonics as the sift of Fermi-level [2]. However, recently, we found that HHG in graphene was almost constant as the shift of the Fermi-level. To understand its background, we performed the theoretical calculation by changing various parameters. We found that when the laser power is so strong, such as that the number of laser-driven carriers is larger than the injected carriers, the change in HHG becomes very small. The calculation suggests that the laser intensity significantly influences the Fermi-level dependence of HHG. However, we could not use graphene to confirm this suggestion experimentally, because of the degradation of the graphene at high-intensity laser and the negligibly small signal intensity at the low-intensity laser. Thus, in this study, we investigated the influence of laser-intensity (I_L) on the Fermi-level dependence of HHG in metallic SWCNTs.

We prepared aligned-metallic-SWCNT film and employed a side-gating device with ionic gel to tune Fermi level through the gate voltage V_G. The sample was irradiated by a 0.26 eV mid-infrared pulse laser, and we investigated the relations between HHG and carrier injection. Figure 1 shows HHG intensity under (a) low- and (b) high-power laser and source-drain current as a function of V_G in metallic SWCNTs. Both graphs show the same tendency. However, the HHG with lower laser intensity changes more drastically, indicating that the laser intensity also influences on Fermi-level dependence of HHG.

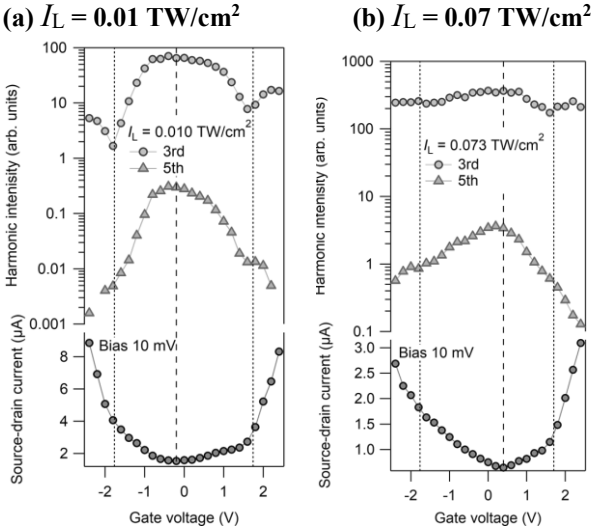

Fig.1 HHG intensity (top) and source-drain current(bottom) in metallic SWCNTs as a function of gate voltage.

[1] S. Ghimire *et al*. Nat. Phys., 15, 10 (2019). [2] Nishidome *et al.*, Nano Lett 20, 6215 (2020)
Corresponding Author: K. Yanagi,
E-mail: yanagi-kazuhiro@tmu.ac.jp

Circular dichroism of metallic and semiconducting doped carbon nanotubes

○Taisei Maeda[1], Riichiro Saito[1]

[1] *Department of Physics, Tohoku University, Sendai 980-8578, Japan*

Chiral carbon nanotubes have a symmetric structure with respect to the mirror symmetry. In the case of circularly polarized light, the left circular polarization and the right circular polarization are mirror-image to each other. Therefore, chiral carbon nanotubes exhibit circular dichroism. The origin of the circular dichroism in undoped carbon nanotubes was shown by Sato et al [1]. When carbon nanotube in doped, a new peak of circular dichroism spectra appears by the new plasma absorption. It has been reported that the plasmon-related peak is much larger than that of undoped nanotubes [2,3].

In this study, we calculated the optical conductivity to obtain of metallic and doped semiconducting nanotubes for a wide range of chiral nanotubes.We calculated the circular dichroism for a variety of chiral nanotubes, including all chiral (*n,m*) metallic and semiconducting nanotubes with *n* less than 20. In Fig. 1,we plot so-called CD Kataura-plot as function of $1/\mathrm{d_t}$ for undoped nanotubes. In Fig2, we show CD Kataura-plot for doped($\mathrm{E_F} = 2.0\mathrm{eV}$) carbon nanotubes.For the plasmon peaks in Fig. 2(shaded area) is expanded in Fig. 3.The results show that undoped nanotubes and doped nanotubes share a strong circular dichroism for light in the UV region. In the case of undoped nanotubes, we can see a family pattern for $\mathrm{E_{ij}}$ transition. Therefore, for nanotubes with larger diameters due to doping, there is a correlation between the diameter and energy of CD peak position. In Fig. 3 the fitting function as shown in Eq. (1) which in concerned with the result by Dairia *et al.*[2].

$$\mathrm{Energy}_{CDpeak}[\mathrm{eV}] = 0.9667/d_t[\mathrm{nm}] + 1.228 \quad (1)$$

[1] N. Sato *et al*. Phys. Rev. B. **9**, 034018 (2018).
[2] S. Daria *et al*. Phys. Rev.B. **99**, 075403 (2019).
[3] R. Saito *et al*. J. Appl. Phys. **128**, 164301 (2020)

Corresponding Author: T. Maeda
E-mail: maeda@flex.phys.tohoku.ac.jp

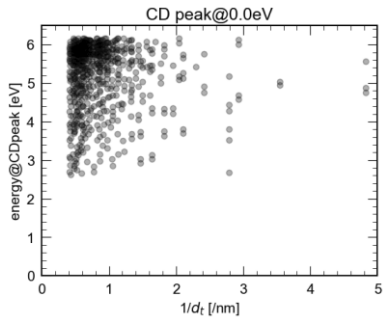

Fig.1 Diameter dependence of the CD peak position of undoped nanotubes appears

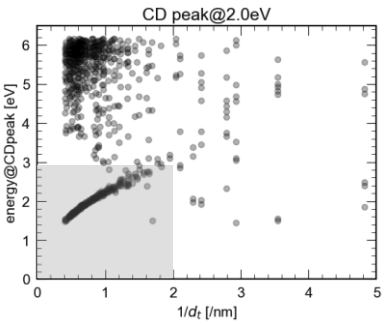

Fig.2 Diameter dependence of the CD peak position of doped($\mathrm{E_F} = 2.0\mathrm{eV}$) nanotubes appears

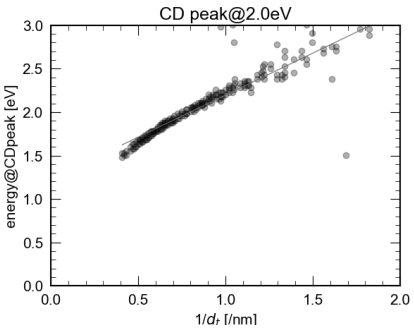

Fig.3 Expanded view of the gray area in Fig. 2 and fitting function

Appropriate properties of carbon nanotube for 3D current collector of lithium-ion battery

○Kentaro Kaneko[1], Suguru Noda[1,2]

[1] *Department of Applied Chemistry, Waseda University, Tokyo, Japan.*
[2] *Waseda Research Institute for Science & Engineering, Waseda University, Tokyo, Japan*

High-energy-density secondary battery is necessary to satisfy the increasing demand for energy storage. Conventional electrodes of lithium-ion battery have heavy foils of metals as current collectors. To achieve high energy density by eliminating non-capacitive components, we developed electrodes based on 1 mass% 3D current collector of submillimeter-long few-wall carbon nanotube (CNT) that held 99 mass% active materials [1]. The metal-foil free CNT-based electrodes were demonstrated, however, only one type of CNT was used. We here report the effects of the structural properties of CNT on the battery performance.

The graphite-CNT negative electrode and the lithium cobalt oxide (LCO)-CNT positive electrodes (97:3 mass ratio) were prepared by ultrasonication in 2-propanol and filtration. 10 types of CNT prepared by fluidized bed CVD method [2] were used. 2032-coin cells were assembled using polypropylene separator and electrolyte (1M $LiPF_6$, EC:DEC=1:1, v:v).

At the first charge, solid electrolyte interphase (SEI) formed on negative electrode, causing irreversible capacity (difference between charge and discharge capacities). The irreversible capacity increased with increasing SSA, causing depletion of active lithium and decreasing reversible capacity (Fig. 1a). Then the rate and cycle performances were evaluated (Fig. 1b). The capacity was higher with CNTs of smaller SSA (187, 240 $m^2\ g^{-1}$) at current densities ≤ 2 mA cm^{-2} while the capacity was higher with CNTs of moderate SSA (287, 501 $m^2\ g^{-1}$) at a high current density of 10 mA cm^{-2}. CNTs of lower SSA is beneficial to suppress the side reaction while those of moderate SSA is beneficial to achieve high rate-performance.

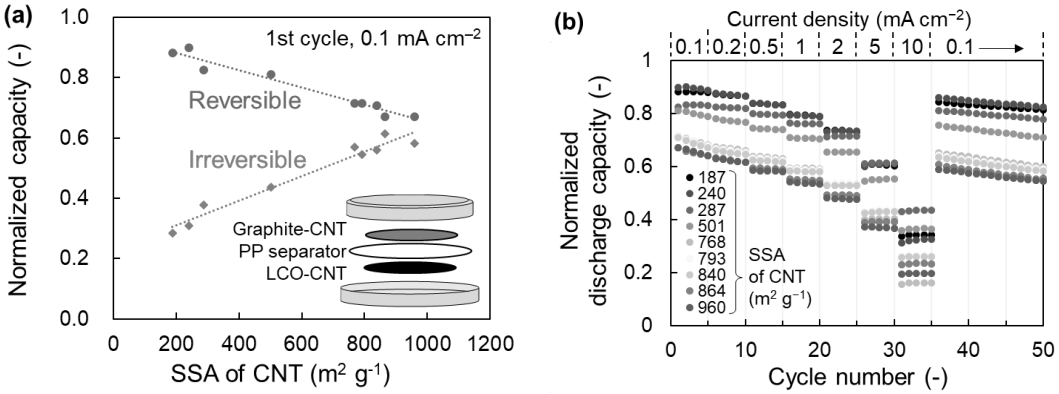

Fig. 1. (a) Reversible and irreversible capacities vs SSA of CNT. (b) Rate and cycle performance.

[1] K. Hasegawa, S. Noda, *J. Power Sources* **321** (2016) 155.
[2] M. Li, M. Risa, T. Osawa, H. Sugime, and S. Noda, *Carbon* **167** (2020) 256.

Corresponding Author: S. Noda, Tel: +81352862769, Fax: +81352862769 E-mail: noda@waseda.jp

Non-classical nucleation of monolayer WS_2 revealed by in-situ monitoring CVD

○ Y. Iwamoto, Q. Xiaoming, X. He, T. Kaneko, T. Kato

Graduate School of Engineering, Tohoku University, Sendai 980-8579, Japan

Transition metal dichalcogenide (TMD), two-dimensional material, is expected to be promising candidates for novel transparent flexible devices because of their excellent electrical and optical properties [1-3]. In terms of the industrial applications, there are still remained several issues to be solved in the growth stage of TMDs. Improving the quality of TMD is one of the most important issues, which can be overcome by clarifying the synthesis mechanism of monolayer TMD. We have recently succeeded in developing the in-situ monitoring CVD for the first time, which can contribute to uncovering the detailed growth mechanism of TMD [4].

In this study, we improved the in-situ monitoring CVD, where only the temperature of the synthetic substrate can be locally controlled by a spot heater. Auto-image analysis was also introduced to quantitatively analyze the initial growth stage. Systematic investigations reveal that the growth of monolayer tungsten disulfide (WS_2) is mainly dominated by not vapor-solid (VS) transition but liquid-solid (LS) transition. The incubation time (Δt_i), which is the time required for the nucleation of monolayer WS_2, was found to be strongly influenced by the substrate temperature. These results are in good agreement with the time-temperature-transformation (TTT) curve, which is known as a classical three-dimensional crystal growth model. It is found that WS_2 nucleation is determined by the balance between the diffusion of the liquid precursor and the driving force of lateral growth, which is decided by the chemical potential difference between liquid precursor and solid WS_2, respectively (Fig.) Furthermore, detailed image analysis suggested that the nucleation of WS_2 follows two-step nucleation, which is known as a non-classical nucleation [5]. These findings are important both for reaching deep understanding of 2D crystal growth as a fundamental study and improving the quality of TMD toward industrial applications.

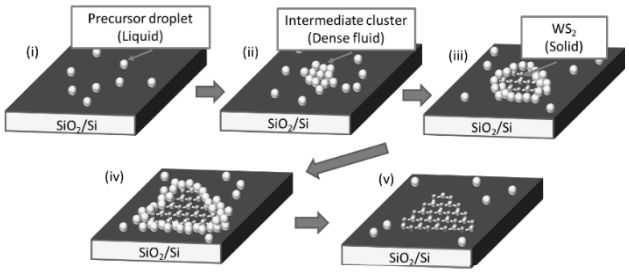

Fig. Schematic illustration of two-step nucleation of WS_2 revealed by in-situ monitoring CVD.

[1] T. Kato and T. Kaneko: ACS Nano, **8** (2014) 12777.
[2] T. Kato and T. Kaneko: ACS Nano, **10** (2016) 9687.
[3] T. Akama, W. Okita, R. Nagai, C. Li, T. Kaneko, and T. Kato, Sci. Rep., **7** (2017) 11967.
[4] C. Li, T. Kameyama, T. Takahashi, T. Kaneko, and T. Kato, Sci. Rep., **9** (2019) 12958.
[5] X. Qiang, Y. Iwamoto, A. Watanabe, T. Kameyama, X. He, T. Kaneko, Y. Shibuta, T. Kato, Sci. Rep. **11** (2021) 22285.

Corresponding Author: T. Kato
Tel: +81-22-795-7046, Fax: +81-22-263-9225,
E-mail: kato12@tohoku.ac.jp

Size enhancement of monolayer WS_2 with sandwiched growth substrates

○Ryoki Hashimoto[1], Yasuhiko Hayashi[1], Yasumitsu Miyata[2], Hiroo Suzuki[1]

[1]*Graduate School of Natural Science and Technology, Okayama University, Okayama 700-8530, Japan*
[2]*Department of Physics, Tokyo Metropolitan University, Hachioji 192-0397, Japan*

Transition metal dichalcogenides (TMDCs), one of the semiconducting two-dimensional materials, has been attracting attention for optoelectronic device applications such as solar cells, photodetectors, and light-emitting diodes due to their high flexibility, light absorption, and emission coefficient with direct band-gap. The most common issue on the crystal growth of TMDCs for practical applications is grain size control to achieve the smaller number of the grain boundaries in a continuous sheet of TMDCs, which can reduce the negative influence from defects and impurities at the grain boundaries. This research investigated the chemical vapor deposition (CVD) growth of monolayer WS_2 and their size control based on the vaper-liquid-solid (VLS) method with metal salt employing the modified configuration of growth substrates.

The cold-wall CVD system conducted the CVD growth with the infrared gold image furnace. Na_2WO_4 was employed as W sources, and its solution was spin-coated on a Si/SiO_2 substrate. The vapor of $(t\text{-}C_4H_9)_2S_2$ was introduced into a CVD chamber as an S source. We employed the modified configuration of the growth substrates; the spin-coated substrate (B) was covered by another clean substrate (A). The maximum crystal size obtained on the B side was more than 400 μm for WS_2 (Fig. 1(a)). These sizes were tens of times larger than the conventional case using a single substrate (~10 μm). We investigated the effect of growth temperature on the crystal size (Fig. 1(b)) and photoluminescence (PL) characteristics such as PL intensity distribution, PL peak energy, and full width at half maximum. These results suggested the increase in the growth temperature causes the size enhancement of WS_2 single crystal; however, it could decrease the crystallinity and its spatial uniformity.

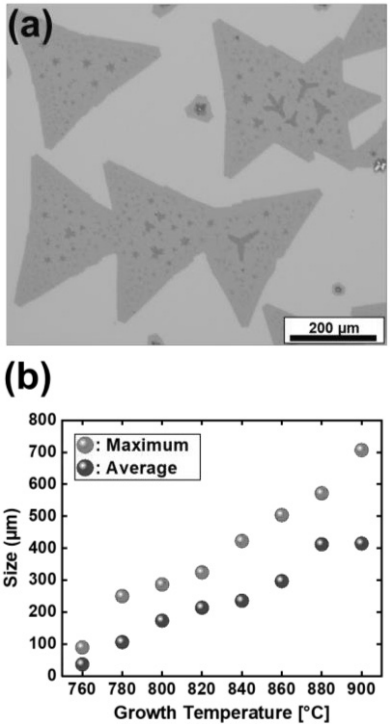

Fig.1: (a)Optical microscope image of the large-size monolayer WS_2. (b) Growth temperature dependence of the crystal size of monolayer WS_2.

Corresponding Author: H. Suzuki
Tel: +81-86-251-8133
E-mail: hiroo.suzuki@okayama-u.ac.jp

Optimization of plasma treatment conditions for Janus MoSeS synthesis

Yijun Liu, Ryoki Hashimoto, Kentarou Ishimura, Yasuhiko Hayashi, Hiroo Suzuki
Graduate School of Natural Science and Technology, Okayama University, Okayama 700-8530, Japan

Janus transition metal dichalcogenide (TMDC) is a TMDC with two different kinds of chalcogenide elements on the upper and lower surfaces. This configuration of the chalcogenide elements can break the out-of-plane asymmetry of monolayer TMDC, resulting in polarization in out-of-plane. Owing to this polarization, it shows new electronic properties such as piezoelectricity. For Janus TMDC synthesis, several methods have been reported. The combination of H_2 plasma treatment and thermal sulfurization[1], high-temperature sulfurization[2], and H_2 plasma treatment with a sulfur source at room temperature[3] have been studied for the Janus TMDC synthesis. In this research, we optimized the H_2 plasma treatment conditions to $MoSe_2$ with a sulfur source at room temperature for Janus MoSeS synthesis.

We prepared monolayer $MoSe_2$ by atmospheric chemical vapor deposition (ACVD) using a metal salt (Na_2MoO_4) solution spin-coated on SiO_2/Si growth substrates and Se vapor. For the H_2 plasma generation, an antenna coil was installed upstream of the vacuumed quartz tube with a 13.56 MHz radiofrequency (RF) power supply set to 20 W. The pressure in the tube was maintained at 35 Pa with 20 sccm H_2 gas flow. A CVD-grown $MoSe_2$ and sulfur powder (2 g) were set at x and 10+x cm from the tail of the H_2 plasma, respectively (Fig. 1(a)). The crystallinity of samples was characterized by Raman and PL spectra. The crystal's chalcogens were mixed in the H_2 treatment with x exceeding 2 cm. Through the tuning of x, we found that $MoSe_2$ can successfully convert to Janus MoSeS within at x of 2 cm without appearance damages in the sample. We carried out the optimization of H_2 plasma treatment time (t_p) by measuring Raman and PL spectra (Fig. 1(b,c)). After t_p = 1 min, the Raman and PL peaks of $MoSe_2$ drastically changed to be that of Janus MoSeS. We observed the A_{1g} and E_{2g} modes of Janus MoSeS at 285 and 352 cm^{-1}, respectively, and the PL peak energy was around 1.66 eV. By increasing t_p from 1 to 3 min, the peak width of A_{1g} mode decreased and the PL intensity increased, indicating the improvement of the crystallinity of Janus MoSeS. From t_p = 3 to 5 min, the PL intensity slightly decreased even though the Raman spectra did not change, suggesting the small number of defects were introduced in the Janus MoSeS crystal by the treatment for a long time.

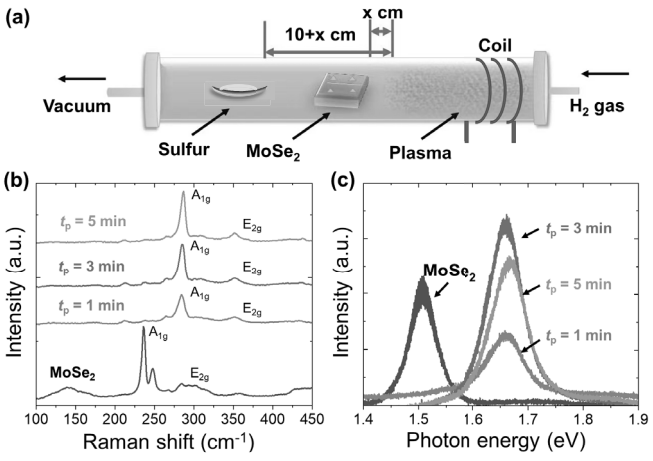

Fig. 1. (a)Schematic illustration of the sample and sulfur positions in the plasma device. (b)Raman and (c)PL spectra of H_2 plasma-treated $MoSe_2$ with different treatment times.

[1] A.-Y. Lu *et al*., *Nat. Nano technol.* **12**, 744 (2017).
[2] J. Zhang *et al*., *ACS Nano* **11**, 8192–8198 (2017).
[3] D. Trivedi. *et al*., Adv. Mater **32**, 2006320 (2020).

Corresponding Author: H. Suzuki
Tel: +81-86-251-8133
E-mail: hiroo.suzuki@okayama-u.ac.jp

One-dimensional spatially-separated excitons in an ultrathin one-dimensional lateral heterostructure

○Nanami Ichinose[1], Liu Zheng[2], Susumu Okada[3], Mina Maruyama[3], and Ryo Kitaura[1]

[1] *Department of Chemistry, Nagoya University, Nagoya 464-8602, Japan*
[2] *Innovative Functional Materials Research Institute, AIST Nagoya 463-8560, Japan*
[3] *Department of Physics, University of Tsukuba, Tsukuba 305-8571, Japan*

Two-dimensional (2D) heterostructers have attracted considerable attention. [1] [2] Although van-der-Waals-stackings-based heterostructers have been intensively studied so far [3] [4], the research on lateral heterostructers is still limited due to the difficulty in fabrication. In this work, we have focused on the growth and optical properties of lateral heterostructers with a periodicity of down to nanometer scale. These are atomically thin 2D layers with one-dimensional (1D) stripes, namely 1D quantum wells (QWs), that align periodically, providing a novel 1-2D mixed-dimensional platform for exploring properties arising from the one-dimensionality.

In this study, we fabricated 2D lateral heterostructers of WS_2/MoS_2 on hexagonal boron nitride by sequential growth of WS_2 and MoS_2 through rapid switching of supply of W and Mo source. Figure 1 shows high angle annular dark-field scanning transmission electron microscopy (HAADF-STEM) image of lateral heterostructers, WS_2/MoS_2. In the HAADF-STEM images, W atoms are imaged as bright spots, whereas Mo and S atoms are images as much darker spots. As seen in the image, the MOCVD-grown lateral structure possesses atomically steep interfaces with a width down to 0.8 nm; we have also confirmed that an one-atom-thick junction can also be grown by our MOCVD setup. Figure 2 shows a PL spectrum of hetero structer WS_2/MoS_2 with a periodicity of about 5 nm measured at 5 K. The PL spectrum shows PL peaks at 1.55 eV, which are absent in the PL spectra of WS_2 or MoS_2 monolayers alone. Judging from peak position, significant saturation, and long lifetime of 120 ps, we think this peak arises from 1D spatially-separated exciton at a 1D stripe. In the presentation, I will provide details of the growth process and detailed analyses of optical properties.

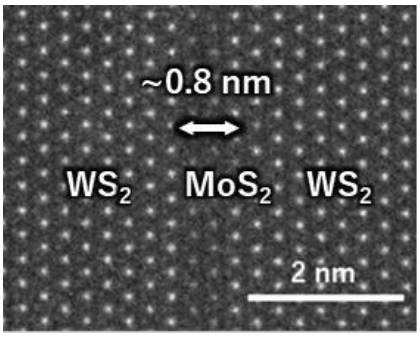

Fig. 1 A HAADF-STEM image of a WS_2/MoS_2 heterostructure.

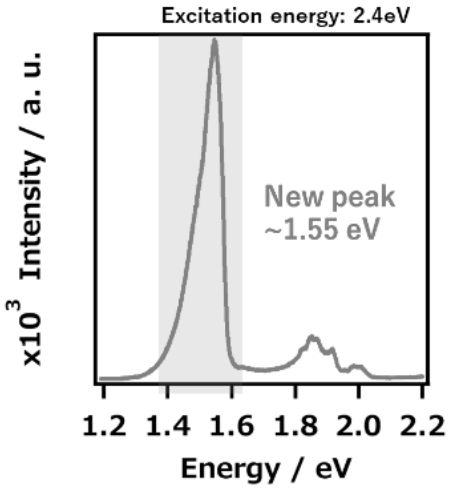

Fig. 2 A PL spectrum of a WS_2/MoS_2 heterostructure at 5K.

[1] A. K. Geim et al. Nature, 499, 419 (2013).
[2] Y. Kong et al. Nature materials, 13, 1135 (2014).
[3] C. Zhu et al. Nature communication, 11, 772 (2020).
[4] Y. Kobayashi et al. ACS Nano,13, 7527 (2019).

Corresponding Author: R. Kitaura
Tel: +81-52-789-2482, Fax: +81-52-747-6442
Web: http://nano.chem.nagoya-u.ac.jp/
E-mail: r.kitaura@nagoya-u.jp

Electronic transport properties of multilayer MoS_2-based PN diodes

○Seiya Kawasaki[1], Hiroto Ogura[1], Takahiko Endo[1], Yusuke Nakanishi[1], Hong En Lim[1], Kazuhiro Yanagi[1], Toshifumi Irisawa[2], Kosuke Nagashio[3], Yasumitsu Miyata[1]

[1] *Department of Physics, Tokyo Metropolitan University, Tokyo 192-0397, Japan*
[2] *Nanoelectronics Research Institute, AIST, Tsukuba, 305-8562, Japan*
[3] *Department of Materials Engineering, The University of Tokyo, Tokyo 113-8656, Japan*

The quantum tunneling effect in PN junctions, reported by Esaki et al. in 1958 [1], has attracted much attention in recent years for the realization of low power consumption devices. For example, the control of tunnel current has been demonstrated for the in-plane PN junctions based on two-dimensional semiconductors such as transition metal dichalcogenides (TMDCs)(Fig.1a) and black phosphorus [2,3]. In particular, multilayer TMDCs are promising for performance improvement because of their high air stability and highly-tunable carrier densities. In this study, we report the growth and characterization of in-plane heterojunctions based on multilayer MoS_2.

Nb-doped multilayer p^+-MoS_2 was exfoliated onto SiO_2/Si substrates. Multilayer n-MoS_2 was then grown from the edge of the p^+-MoS_2 flakes using chemical vapor deposition (CVD). Field-effect transistors (FETs) were fabricated by plasma etching and deposition of In/Au electrodes (Fig.1 b, c). As shown in Fig. 1d, the *I-V* curve shows the rectification characteristics at V_g = 0 V. In contrast, a negative differential resistance trend (NDR trend) was observed for V_g = 30~50 V. This suggests the band-to-band tunneling (BTBT) current flows for the forward bias due to the formation of broken gap semiconductor heterojunction as shown in Fig. 1e. The present results provide a basis to optimize the device structure and carrier control for the high performance of tunnel FETs.

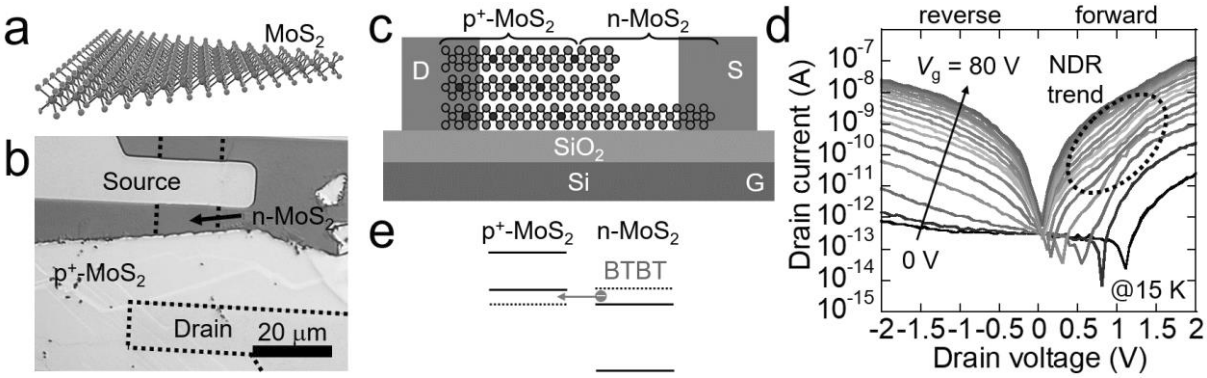

Fig.1: (a) Structure model of MoS_2. (b) Optical microscope image, (c) structure model, (d) *I-V* curves at different gate voltages, and (e) the expected band alignment of p^+-MoS_2/n-MoS_2 device at V_g = 30 V and V_d = 0.5 V.

[1] L. Esaki., *Phys. Rev.* **109**, 603 (1958). [2] S. Kim *et al*., *Nat. Nanotechnol.* **15**, 203-206 (2020). [3] T. Fukui *et al*., The 82nd JSAP Autumn Meeting, 13a-N307-11 (2021).

Corresponding Author: Y. Miyata, Tel: +81-042-677-2508, E-mail: miyata-yasumitsu@tmu.ac.jp

Electrically tunable moiré trions in twisted $WSe_2/MoSe_2$ heterobilayers

○Duanfei Dong[1], Wenjin Zhang[1], Kenji Watanabe[2], Takashi Taniguchi[2], Keisuke Shinokita[1], and Kazunari Matsuda[1]

[1]*Institute of Advanced Energy, Kyoto University, Uji, Kyoto 611-0011, Japan*
[2]*National Institute for Materials Science, Tsukuba, Ibaraki 305-0044, Japan*

The formation of moiré patterns provides a new platform for the exploration of optoelectronic properties of two-dimensional materials, which has attracted extensive attention in various research fields [1]. A moiré pattern can be formed by vertically stacking two monolayer semiconducting transition metal dichalcogenides with a twist angle or a mismatch in lattice constant. These periodic moiré patterns can generate spatially distributed potentials to trap the electron-hole pairs (excitons), which has been proved to have notable effects on optical emissions [2,3]. Besides excitons, their charging counterparts (charged excitons or trions) will add an aspect of moiré excitonic states, however, the impact of charging effects is still unclear.

In this study, we have studied the interlayer moiré excitonic states in superlattices, and explored the influences of electric doping. We fabricated the *R*-type heterostructure devices by stacking $MoSe_2$ to WSe_2 ($MoSe_2/WSe_2$ heterobilayer) with a very small twist angle of a few degrees, using mechanical exfoliation and dry-transfer techniques (inset of Fig. 1). The heterobilayer was encapsulated by hexagonal boron nitride (*h*-BN) with semi-transparent thin graphite gates. Figure 1 shows the counter map of gate-dependent photoluminescence (PL) spectra of heterostructure device at 5 K. The several discrete PL lines are clearly observed around 1.345 eV from gate-voltage of -10 to -20 V, which represents the PL peaks from moiré excitons in the neutral region. The new lines at the lower energy side around 1.335 eV appear from 0 to 20 V, which might come from the PL peaks of trions trapped in moiré potential due to the electron doping (moiré trion). The moiré trion peaks become weak and broaden above 20 V due to high carrier density. The binding energy of the moiré trion was evaluated as 10 meV. Moreover, we will discuss the detailed moiré trion structures from the temperature dependence of PL spectra of the device.

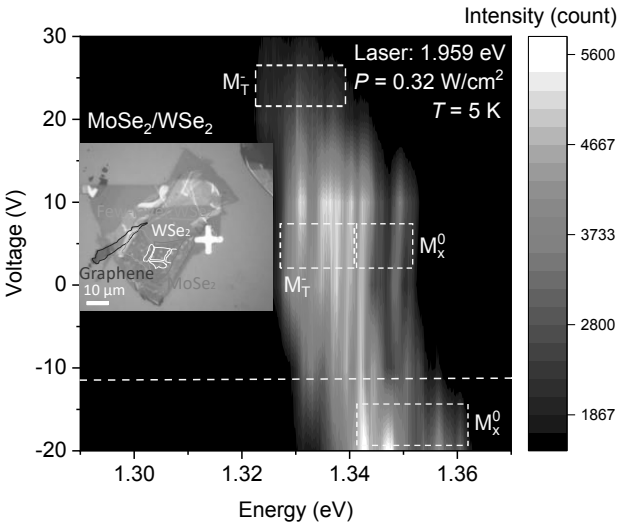

Figure 1. PL spectra of $MoSe_2/WSe_2$ heterobilayer at 5 K. M_T^- and M_X^0 are denoted as interlayer moiré trion and exciton PL signals, respectively.

[1] P. Rivera *et al.*, *Nat. Nano.* **13**, 1004 (2018).

[2] K. L. Seyler *et al.*, *Nature* **567**, 66 (2019).

[3] K. Shinokita *et al.*, *Nano Lett.* **21**, 5938 (2021).

Corresponding Author: Kazunari Matsuda
Tel: +81-774-38-3460, Fax: +81-774-38-3460
E-mail: matsuda@iae.kyoto-u.ac.jp

Nonlinear optical effect of few-layered NbSe2

○Ren Habara, Katsunori Wakabayashi

Department of Nanotechnology for Sustainable Energy, School of Science and Technology, Kwansei Gakuin University, Sanda Hyogo, Japan

Transition-metal dichalcogenide (TMDC) is a new class of two-dimensional (2D) electronic system and provides a platform to design functional opt-electronic devices. In TMDCs, electronic properties crucially depend on the combination of metal and chalcogen atoms. In particular, $NbSe_2$ is known as 2D materials to show metallic behaviors. Figure 1(a) shows the crystal structure of $NbSe_2$. Because of broken crystal inversion symmetry, large spin splitting is induced by Ising-type spin-orbit coupling in odd-number-layered $NbSe_2$, but absent for even-number-layered $NbSe_2$ with the inversion symmetry.[1]

In this paper, we numerically calculate nonlinear optical spin and charge Hall conductivities of few-layered $NbSe_2$ based on an effective tight-binding model which includes d_{z^2}, $d_{x^2-y^2}$ and d_{xy} orbitals of Nb atom. We show that the nonlinear optical Hall conductivity for second harmonic generation process has nonvanishing value in odd-number-layered $NbSe_2$ owing to the broken inversion symmetry [see Fig. 1(b)]. Also, we have found that the nonlinear optical Hall current strongly depend on layer numbers and polarization of incident light in visible range. Thus, we provide nonlinear optical selection rule in few-layered $NbSe_2$.[2]

In further, Figure 1(c) shows that for even-number-layered case, the nonlinear optical Hall currents can be generated by applying electric fields which breaks inversion symmetry.

Our results will serve to design potential opt-spintronics devices based on 2D materials.

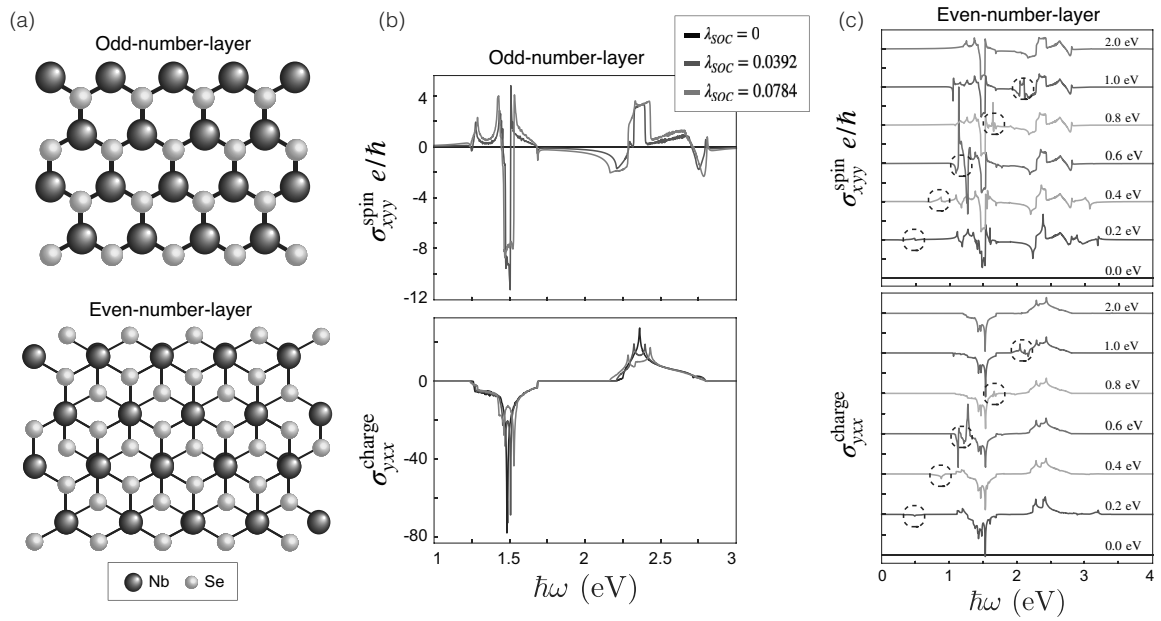

Fig. 1 (a) Crystal structure of $NbSe_2$. (b) Nonlinear optical spin and charge Hall conductivities. (c) Nonlinear optical Hall conductivities of even-number-layered $NbSe_2$ for several different applied electric fields.

[1] W.-Y. He, *et.al.*, Commun. Phys. **1**, 40 (2018). [2] R. Habara, *et.al.,* in preprint.

Corresponding Author: K. Wakabayashi, E-mail: waka@kwansei.ac.jp

Theoretical study of optical conductivity under circular polarized light irradiation in graphene on hBN

○Keisuke Nakagahara, Katsunori Wakabayashi

Department of Nanotechnology for Sustainable Energy, School of Science and Technology, Kwansei Gakuin University, Gakuen 2-1, Sanda 669-1337, Japan

Graphene on hexagonal boron nitride (G/hBN) has a long period moiré potential by the mismatch of lattice constant between the two layers, which also depends on twist angle. Figure 1(a) shows the crystal structure of G/hBN with twist angle $\theta = 0^{\circ}$, in which the rhombus is the moiré unit cell. The moiré potential of G/hBN makes a modulation of electronic states near the Fermi energy and breaks inversion symmetry of the system. In a system which has a valley structure such as graphene, broken inversion symmetry leads to valley selective optical transition rule under circular polarized light irradiation [1].

In this work, we numerically calculate the optical conductivity under circular polarized light irradiation in G/hBN. Figure 1(b) shows the energy band structure of G/hBN with $\theta = 0^{\circ}$ by using effective continuum model [2], where the red (blue) lines show the energy bands of the Hamiltonian for K (K') valley. Moiré potential opens band gaps at zone boundary of moiré Brillouin zone (mBZ) near Fermi energy. Figure 1(c) shows the photon energy dependence of valley polarization of G/hBN with Fermi energy $E_F = 0$ eV. Here, we define the valley polarization as $P(\omega) = \frac{\sigma_L - \sigma_R}{\sigma_L + \sigma_R}$, where σ_L (σ_R) is the optical conductivity calculated from continuum Hamiltonian for K valley under left-handed (right-handed) circular polarized light irradiation. Valley polarization has the largest peak around 2 meV for $\theta = 0$ and 1°, however the peak vanishes for $\theta = 2°$. Furthermore, we clarify the doping effect for several twist angle of valley polarization of G/hBN. We will discuss the details in the presentation.

In conclusion, we have found strong valley polarization for slight twist angle under circular polarized light irradiation in the infrared light region. Our results will serve to design valleytronics devices that enhance valley polarization with smaller twist angle below the visible light region.

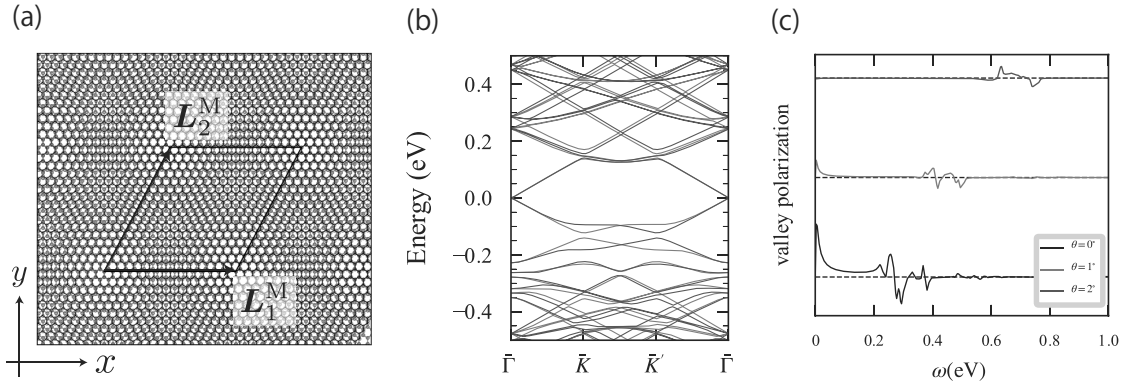

Fig. 1(a) The crystal structure of G/hBN with twist angle $\theta = 0^{\circ}$. (b) Energy band structure of G/hBN with $\theta = 0^{\circ}$. (c) Valley polarization of G/hBN with $E_F = 0$ eV for several twist angles.

[1] W. Yao, *et al*., Phys. Rev. B **77**, 235406 (2008). [2] P. Moon and M. Koshino, Phys. Rev. B **90**, 155406 (2014). Corresponding Author: K. Wakabayashi (E-mail: waka@kwansei.ac.jp)

Vapor-phase synthesis of single-walled MX_2 nanotubes templated on surfactant-dispersed boron-nitride nanotubes

○Shinpei Furusawa[1], Yohei Yomogida[1], Yuta Sato[2], Kazuhiro Yanagi[1], Kazu Suenaga[3], Yusuke Nakanishi[1*], and Yasumitsu Miyata[1*]

[1]*Department of Physics, Tokyo Metropolitan University, Hachioji, 192-0397, Japan*
[2] *National Institute of Advanced Industrial Science and Technology (AIST), Tsukuba 305-8565, Japan.*
[3] *The Institute of Scientific and Industrial Research, Osaka University, Osaka 567-0047, Japan.*

Transition metal dichalcogenide nanotubes (MX_2NTs) are one-dimensional (1D) materials that exhibit some intriguing phenomena such as exciton-polaritons and bulk photovoltaic effect [1]. Understanding the origin of these phenomena necessitates the characterization of single-walled (SW) MX_2NTs isolated from typical multi-walled ones. Recently, Xiang *et al* have realized SW-MoS_2NTs in 1D coaxial heterostructures based on carbon nanotubes [2, 3], yet detailed electronic properties of individual MoS_2NTs remains elusive. Electrically and optically inactive boron-nitride nanotubes (BNNTs) can serve as an ideal template for precisely studying the electronic properties of MX_2NTs; however, BNNT-templated syntheses of MX_2NTs is still limited due to the difficulties in the preparation of well-dispersed BNNT templates.

Here we present the facile synthesis of MX_2NTs using surfactant-dispersed BNNTs as templates. We have developed an efficient dispersion of as-purchased BNNTs by using Triton X-100, the surfactant that can be easily removed to provide clean BNNTs by simple thermal treatment. Comprehensive microscopic and spectroscopic analyses suggests that this approach can afford stable, clean, and well-dispersed BNNT networks. We demonstrated that the BNNT templates can be utilized to synthesize a variety of MX_2NTs including alloys (Fig. 1). The present methodology will accelerate the growing efforts to reveal the electronic properties and potential application of MX_2NTs.

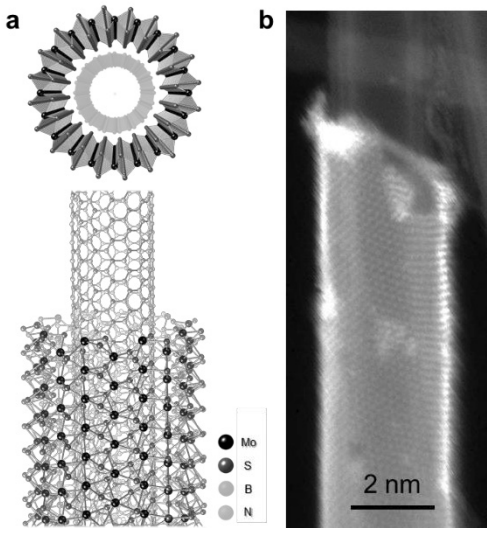

Figure 1 (a) Schematic and (b) HAADF-STEM images of a single-walled MoS_2NT coaxially grown on an individual BNNT.

[1] J. Musfeldt *et al*., *Phys. Today* **73**, 8 (2020) [2] R. Xiang *et al*., *Science* **367**, 537 (2020) [3] M. Liu *et al*., *ACS Nano* **15**, 8418 (2021)

Corresponding Author: Y. Nakanishi and Y. Miyata
Tel: +81-42-677-2498 E-mail: naka24ysk@tmu.ac.jp; miyata-yasumitsu@tmu.ac.jp

Intercalation of group-XIII metals in crystalline bundles of WTe atomic wires

○Ryusuke Natsui[1], Hiroshi Shimizu[1], Zheng Liu[2], Iori Kikuchi[3], Jiang Pu[3], Taishi Takenobu[3], Hong En Lim[1], Takahiko Endo[1], Yusuke Nakanishi[1*], and Yasumitsu Miyata[1*]

[1] *Department of Physics, Tokyo Metropolitan University, Hachioji 192-0397, Japan*
[2] *Innovative Functional Materials Research Institute, AIST, Nagoya 463-8560, Japan*
[3] *Department of Applied Physics, Nagoya University, Nagoya 464-8603, Japan*

Atomically thin wires of transition metal chalcogenides (TMCs) −labeled as MX with M: transition-metal and X: chalcogen− are quasi-one-dimensional (1D) conductive materials with the diameter of less than 1 nm (Fig. 1a), which can assemble into van der Waals 3D bundles as well [1]. Recently, we have developed the wafer-scale growth of 2D and 3D crystalline bundles of WTe atomic wires using chemical vapor deposition (CVD) [2]. In addition to the tunable dimensionality, assembled TMC wires possess inner hollow spaces to incorporate foreign atoms. Upon the intercalation of metal atoms, the electronic properties can be drastically changed, which allows for exploring emergent phenomena such as superconductivity [3].

Here we present the intercalation of group-XIII metals into crystalline bundles of WTe atomic wires. In and Tl-intercalated samples were first fabricated by vapor-phase intercalation into CVD-grown WTe bundles. The presence of intercalated In atoms was directly confirmed by cross-sectional HAADF-STEM observation (Fig. 1b, c). In addition, we successfully intercalated Tl atoms into the bundles. The present results show the possibilities that the electric properties of WTe bundles can be tuned by intercalating different atoms.

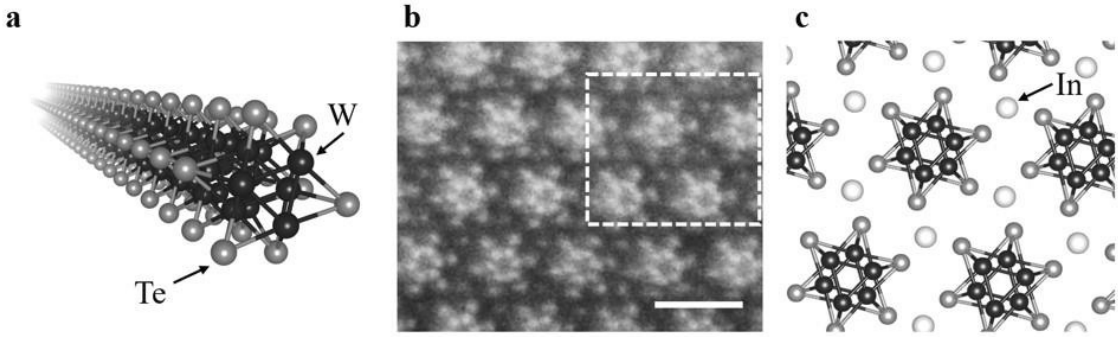

Figure. 1 **a** Schematic image of an individual WTe atomic wire. **b** Cross-sectional HAADF−STEM image of In-intercalated WTe bundles. Scale bar = 1 nm. **c** The structure model corresponding to the region marked by a square in **b**.

[1] H. Zhu *et. al., **Adv. Mater.*** **29,** 1606264 (2017). [2] H. E. Lim *et al.*, ***Nano Lett.*** **21**, 243 (2021). [3] A. P. Petrović *et al.*, ***Phys. Rev.*** *B* **82**, 235128 (2010).

Corresponding Author: Y. Nakanishi and Y. Miyata,
TEL: +81-42-677-2498, E-mail: naka24ysk@tmu.ac.jp;
Tel: +81-42-677-2508, E-mail: miyata-yasumitsu@tmu.ac.jp

Spontaneous photocurrent of $WSe_2/CrPS_4$ hetero-interface with in-plane polarization and highly air-stability.

○Shuichi Asada[1], Keisuke Shinokita[1], Kenji Watanabe[2], Takashi Taniguchi[2], and Kazunari Matsuda[1]

[1] *Institute of Advanced Energy, Kyoto University, Uji 611-0011, Japan*
[2] *National Institute for Materials Science, Tsukuba 305-0044, Japan*

Van der Waals (vdW) hetero-interfaces based on two-dimensional (2D) layered materials have recently attracted tremendous interest, because of the various material combinations and generation of new physical properties. By stacking properly selected 2D-layered materials with different rotational symmetries with a particular angle, the symmetry of vdW hetero-interface is reduced to only have a single mirror symmetry, which induces spontaneous in-plane polarization [1]. The in-plane polarization has been experimentally reported in WSe_2/black black-phosphorus (BP), both of which are non-polarizing materials. The WSe_2/BP vdW hetero-interface shows very promising results for spontaneous photovoltaic effect without *p-n* junction and bias voltage. However, the BP is very susceptible to degradation due to oxidization, and therefore the way for device applications of this hopeful photocurrent properties are strongly required.

Here, we designed a $WSe_2/CrPS_4$ vdW hetero-interface with uniaxial symmetry for in-plane polarization, where $CrPS_4$ is known to be much higher air-stability [2]. The crystal direction of each flake was confirmed by the edge of the flake [3]. The flakes were stacked at the proper angle, relying on the optical image (inset of Fig. 1(a)). The WSe_2 and $CrPS_4$ have threefold and twofold rotational symmetries, respectively, which can't be compatible, although only one mirror symmetry remains in the vdW hetero-interface. This symmetry causes polarization in the direction parallel to the mirror plane. As a consequence, we can expect the generation of anomalous photocurrent. Figure 1(a) shows the photocurrent measured in $WSe_2/CrPS_4$ vdW hetero-interface, where the electrodes were fabricated in the parallel direction to the mirror plane. We observed spontaneous photocurrent at 0 V depending on irradiation of laser light, which suggests that the in-plane polarization is also generated on this new combination hetero-interface. In the presentation, we will discuss more detailed photovoltaic properties and potential application of this hetero-interface.

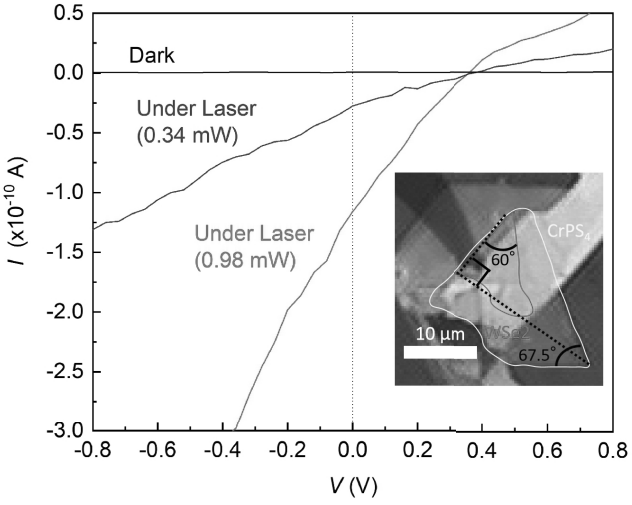

Fig. 1 Current-voltage (*I-V*) curve of $WSe_2/CrPS_4$ vdW hetero-interface under dark and light illumination of 532 nm. Inset shows optical image of $WSe_2/CrPS_4$.

[1] T. Akamatsu *et al., Science* **372**, 68 (2021).
[2] J. Son *et al., ACS Nano* **15**, 16904 (2021).
[3] J. Lee *et al., ACS Nano* **11**, 10935 (2017).

Corresponding Author: Kazunari Matsuda
Tel: +81-774-38-3460
E-mail: matsuda@iae.kyoto-u.ac.jp

Synthesis of [C_{60}] fullerene nanowhisker-glycine capped ZnS:Mn composites and their photocatalytic degradation of methylene blue

○ Seung Won Ko[1], Hoon Chung[1], Weon Bae Ko[1,2]

[1] *Department of Convergence Science, Graduate School, Sahmyook University, 815, Hwarang-ro, Nowon-gu, Seoul 01795, Republic of Korea*
[2] *Department of Chemistry, Sahmyook University, 815, Hwarang-ro, Nowon-gu, Seoul 01795, Republic of Korea*

ZnS:Mn-Gly nanocrystals were synthesized by capping the surface of ZnS:Mn with L-glycine and were characterized by UV-vis, Raman spectroscopy, XRD, SEM, and TEM [1]. The liquid–liquid interfacial precipitation (LLIP) method was used to create [C_{60}] fullerene nanowhisker-ZnS:Mn-Gly composites from C_{60}-saturated toluene, the ZnS:Mn-Gly solution, and isopropyl alcohol [2].The product of the hybrid nanocomposites was characterized by UV-vis, Raman spectroscopy, XRD, SEM, and TEM. The photocatalytic degradation of methylene blue was confirmed using [C_{60}] fullerene nanowhisker-ZnS:Mn-Gly composites by UV-vis spectroscopy. The kinetics study for the photocatalytic degradation of MB with the [C_{60}] fullerene nanowhisker-ZnS:Mn-Gly composites as photocatalyst under UV irradiation at 254 nm followed a pseudo first order reaction rate law.

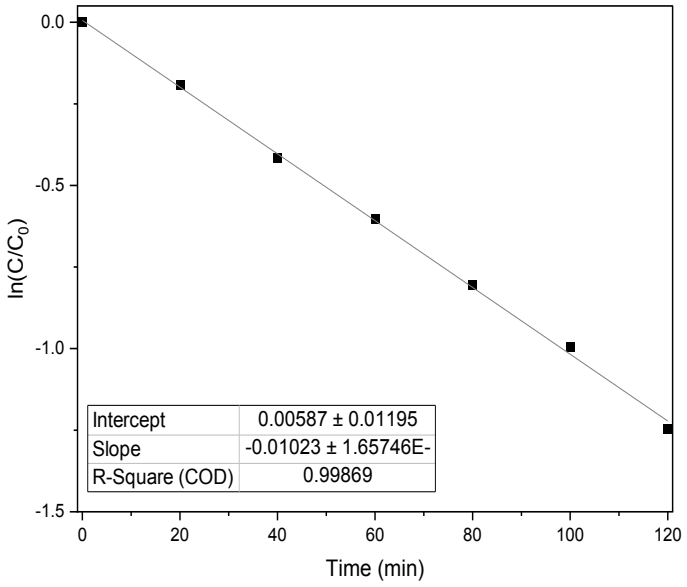

Fig. 1 Kinetics study for photocatalytic degradation of methylene blue with [C_{60}] fullerene nanowhisker-ZnS:Mn-Gly composites under UV irradiation at 254 nm.

[1] J.W. Lee, C.S. Hwang, Bulletin of the Korean Chemical Society, **35**, 189 (2014).
[2] K. Miyazawa, Journal of Nanoscience and Nanotechnology**, 9**, 41 (2009).
Corresponding Author: W. B. Ko
Tel: +82-2-3399-1700, Fax:, +82-2-979-5318,
E-mail: kowb@syu.ac.kr

Synthesis of Indano[60]fullerene Bromide for Oxidation to Evaporable Fullerene Derivatives

○Hirofumi Amada[1], Hao-Sheng Lin[1], Yutaka Matsuo[1]

[1] *Department of Material Science and Engineering, Nagoya University, Furo-cho, Chikusa-ku, Nagoya 464-8603, Japan*

Fullerene and its derivatives have been widely studied as an n-type organic semiconductor in solar cells owing to their excellent semiconducting properties. However, the poor thermal stability of fullerene derivatives limited their processibility to spin-coating, which commonly suffers the poor morphology, solvent residual issues. Recently, fullerene-fused ketone, a fullerene derivative with high thermal stability that can withstand thermal deposition has been achieved and attracted attentions.

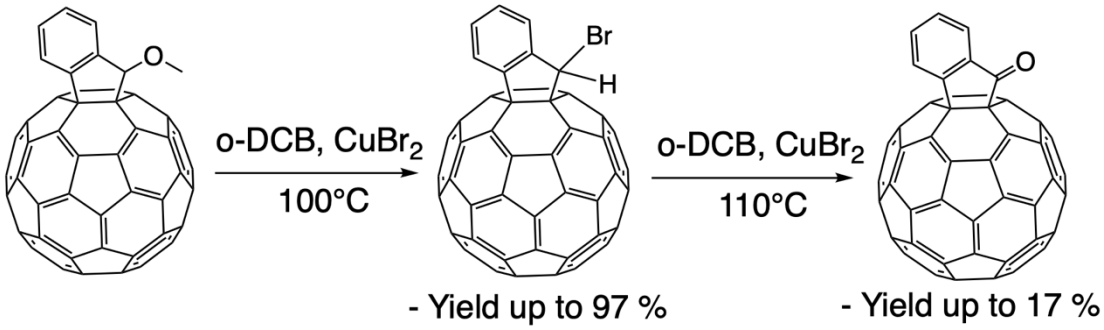

Fig.1 Synthesis process of fullerene-fused ketone

Although the fullerene-fused ketone has been successfully synthesized from fullerene-fused alkoxy ethers, the mechanism of generation of an intermediate namely Indano[60]fullerene Bromide is still unclear. Herein, we focused on the identification of Indano[60]fullerene Bromide using various measurement methods such as NMR shown in Fig.2 and synthesis process of the mechanistic study of the generation of Indano[60]fullerene Bromide in the process of $CuBr_2$ and its further conversation to fullerene-fused ketone.

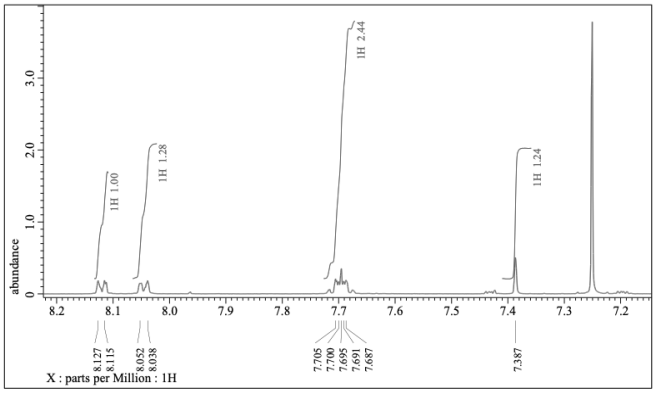

Fig.2 NMR spectrum of Indano[60]fullerene Bromide

Corresponding Author: Y. Matsuo

Tel:+81-52-788-6113

E-mail:yutaka.matsuo@chem.material.nagoya-u.ac.jp

Fabrication of nanocarbon hybrid structure composed of carbon nanotubes and carbon foams

○Shu Kondo[1], Moeri Sugiyama[1], Daiki Yamamoto[1], Shusaku Karasawa[1], Kamal P Sharma[1], Takahiro Saida[1,2], Shigeya Naritsuka[3], Takahiro Maruyama[1,2]

[1]*Department of Applied Chemistry, Meijo University, Japan*

[2] *Nanomaterials Research Center, Meijo University, Japan*

[3]*Department of Materials Science and Engineering, Meijo University, Japan*

1. Introduction

Because of their high specific surface areas, Carbon nanotubes (CNTs) are expected as support materials for catalyst particles in many fields such as batteries, chemical biosensors, and fuel cell. Previous study showed that, by depositing Pt catalysts on CNTs, their activity was enhanced. Furthermore, to increase the specific surface area, combining CNTs with other nanocarbon materials such as graphene has been attempted. In this study, we attempted to fabricate hybrid structure composed of CNTs and carbon foam to realize a support layer with high specific surface area.

2. Experimental procedure

After cleaning of a melamine foam (~1 cm^3), it was introduced into a furnace of a hot-wall chemical vapor deposition (CVD) system. After temperature rise to 300°C, ethanol vapor was introduced into the furnace, and the temperature was further raised to 600°C, and kept for 20 min to form a carbon foam. Then, it was treated by O_2 plasma, and immersed in aqueous solution of Co(II) acetate for 24 h. After it was dried in an oven, CNT growth was performed by CVD with ethanol as carbon source. The growth temperature and time were 750°C and 10 min, respectively. The samples were characterized by Raman spectroscopy and FESEM.

3. Result and Discussion

Fig. 1(a) and (b) show Raman spectra of samples grown using 0.01 M and 0.005M of aqueous solutions of Co(II) acetate, respectively. In both spectra, RBM peaks were observed, indicating single-walled CNTs (SWCNTs). As the concentration of Co(II) acetate increased, the SWCNT diameters were enlarged. Fig.1 (c) and (d) show FESEM images of the samples shown in Fig. 1(a) and (b), respectively. SWCNT growth were observed on carbon foams, formed by carbonization of melamine foams.

Part of this research was supported by the private university research branding project "Meijo University Brand Building Program by Creating New Nanomaterials" and JSPS Bilateral International Joint Research Projects.

[1] T. Onoe et al. Catalysis Commun. 8, 2007, 701.

Corresponding Author: T. Maruyama

Phone: +81-52-838-2386, Fax: +81-52-832-1172

E-mail: takamaru@meijo-u.ac.jp

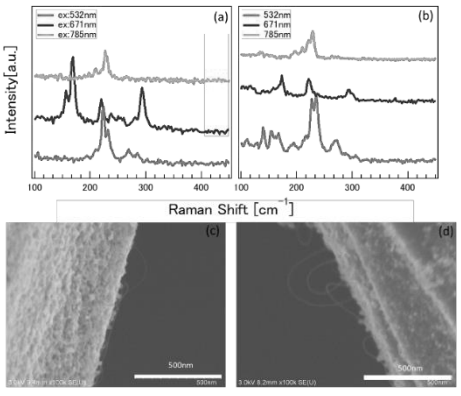

Fig. 1 Raman spectra of the sample using (a) 0.01 M and (b) 0.005M of aqueous solutions of Co(II) acetate. FESEM images of (c) the sample in (a), and (d) the sample in (b).

Synthesis of aligned carbon nanotubes from nanodiamond seeds by kite-growth mechanism

°Yuanjia Liu[1], Michiharu Arifuku[2], Noriko Kiyoyanagi[2], Masamitsu Satake[2], Taiki Inoue[1], Yoshihiro Kobayashi[1]

[1] *Department of Applied Physics, Osaka University, Osaka 565-0871, Japan*
[2] *Nippon Kayaku, Tokyo 115-8588, Japan*

Carbon nanotubes (CNTs) have received extensive attention due to their extraordinary thermal, electrical, and mechanical properties. Kite-growth [1] is a process to grow aligned CNTs by utilizing laminar gas flow and enables the formation of air-suspended CNTs, which are useful for physical property measurements. In the past research, metal particles are used as catalysts. However, they inevitably remain as impurities and often lead to defect formation, which deteriorates the performance of CNTs. In order to overcome these effects, this research performs metal-free kite-growth of CNTs. Nanodiamond (ND) is stable at high temperatures, easy to grow low-defect CNTs, and avoids remaining metal impurities. Another advantage of ND is that CNTs can be synthesized on any kind of substrate (including electrodes), which is convenient for device fabrication. [2] The results showed over 100 μm-long CNTs were grown by controlling growth conditions.

The kite-growth of aligned CNTs was performed by catalytic chemical vapor deposition (CVD) using ethanol as the carbon source. ND particles dispersed in ethanol were dropped onto half of the silicon substrates with a 300 nm thick SiO_2 layer. In a control experiment, Fe catalyst was prepared with $FeCl_3$ ethanol solution. The nanotube growth was initiated by introducing 35 sccm H_2/Ar bubbling through ethanol and 420 sccm H_2/Ar through another gas line at constant temperature (930ºC). After 30 min of growth, the sample was cooled down in Ar to room temperature. The whole CVD process was performed at atmospheric pressure. Scanning electron microscopy (SEM, Hitachi S-4800) was used for observing the morphologies of the synthesized CNTs. Raman spectra were measured for investigating the CNT structures with a laser excitation wavelength of 633 nm.

The SEM images (Fig. 1) compare the morphology at the tip of CNTs when CNTs are grown using metal catalysts and ND by kite-growth mechanism. When using Fe as the catalyst (a), it can be observed that there is a bright particle attached to the tip, which means that the CNT tip has a metal catalyst attached because Fe has more secondary electron (SE) yield than carbon [3]. The catalyst is always at the tip of the CNT during the growth process and moves as the CNT grows. That is, the kite-growth of Fe catalysts belongs to tip-growth mode, which is consistent with the previous experimental results. On the other hand, when using ND as the growth seeds (b), there is no bright particle attached to the tip. This means that the CNT is not grown from metal impurities. Although some examples of bright tip were also found in this sample, according to statistics, the proportion is less than 5%, which belongs to the influence of metal impurities. Thus, it can be concluded that the CNT in this sample is grown from ND. Although the growth efficiency of ND as growth seeds is significantly lower than metal catalysts, we demonstrate the feasibility of growing CNTs from ND using kite-mechanism.

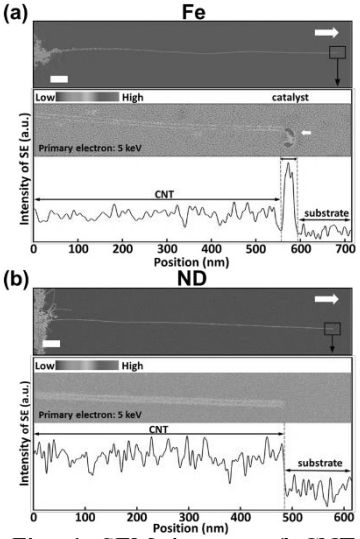

Fig. 1 SEM images of CNTs grown from (a) Fe catalyst and (b) ND seeds by kite-mechanism. The white arrow represents the direction of gas-flow. Scale bars are 2 μm. Primary electron energy is 5 keV.

[1] S. Huang *et al.* Nano Lett., **4**, 1025 (2004). [2] D. Takagi *et al.* J. Am. Chem. Soc., **131**, 6922 (2009). [3] H. Seiler, J. Appl. Phys., **54**, R1 (1983).

Corresponding Author: Y. Kobayashi, E-mail: kobayashi@ap.eng.osaka-u.ac.jp

Growth of single-walled carbon nanotubes from Ir catalysts on various buffer layers with stainless steel foil

○Shu Kondo[1], Daiki Yamamoto[1], Kamal P Sharma[2], Takahiro Saida[1,2], Shigeya Naritsuka[3], Takahiro Maruyama[1,2]

[1] *Department of Applied Chemistry, Meijo University, Nagoya 468-8502, Japan*

[2] *Meijo Nanomaterial Research Center, Nagoya 468-8502, Japan*

[3] *Department of Materials Science and Engineering, Meijo University, Nagoya 468-8502, Japan*

1.Introduction

Our group has succeeded in growing vertically aligned small-diameter single-walled carbon nanotubes (SWCNTs) on a SiO_2/Si substrate by alcohol catalytic CVD (ACCVD) method using an Ir catalyst [1]. However, Si wafers are not suitable for mass production due to their high cost. Here, we used a stainless steel foil as a substrate and have attempted to grow SWCNTs with an Ir catalysts using various buffer layers.

2.Experimental Procedure

As buffer layers, Al_2O_3 and SiO_2 were deposited on stainless steel (SUS304) foils by sputtering, dip-coating, and bar-coating, respectively. Then, Ir catalysts were deposited by pulsed arc plasma gun or immersing the stainless steel foil in 0.01 M iridium acetate ethanol solution. SWCNT growth was carried out in a hot-wall CVD apparatus. The substrate temperature was raised to 850°C in an Ar/H_2 atmosphere at a flow rate of 100 sccm, then, ethanol of 500 sccm was supplied for 10 min to grow SWCNTs. The samples were characterized by FE-SEM and Raman spectroscopy.

3.Results and discussion

Fig.1(a) and (b) shows FE-SEM images of SWCNTs grown from Ir catalysts on Al_2O_3 buffer layers deposited by sputtering and dip-coating, respectively. Fig. 1(a) showed that vertically aligned SWCNTs were grown on an Al_2O_3 buffer layer prepared by sputtering. In Fig. 1 (b), vertically aligned SWCNTs were not seen clearly, but growth of SWCNTs were confirmed. This shows that preparation method of Al_2O_3 buffer layers affect on SWCNT growth from Ir catalysts. We will also show the result of SWCNT growth from an Ir catalyst on SiO_2 buffer layer, and discuss the difference in the effect on SWCNT growth between the buffer layers.

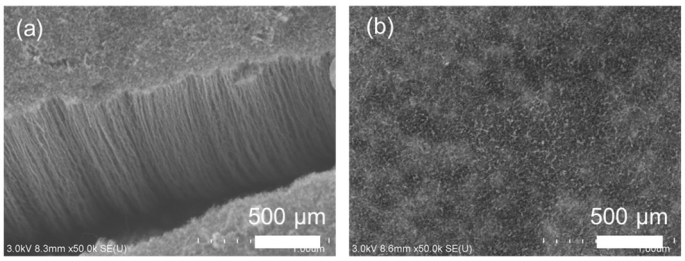

Fig. 1 FE-SEM images of SWCNTs grown from Ir catalysts on Al_2O_3 buffer layers deposited by (a) sputtering and (b) dip-coating.

Acknowledgments

This work was partly supported by Ministry of Economy, Trade and Industry (METI) Monozukuri R&D Support Grant Program for SMEs Grant Number JPJ005698 and the Meijo University Research Branding Project for Cultivation and Invention of New Nanomaterials under the Ministry of Education, Culture, Sports, Science, and Technology (MEXT) Private University Branding Project (Global Development Category), and also Nanotechnology Platform Program "Molecule and Material Synthesis" of the Ministry.

[1] T. Maruyama et al. Appl. Surf. Sci. **509** (2020) 145340.

Corresponding Author: T. Maruyama

Phone: +81-52-838-2386, Fax: +81-52-832-1172, E-mail: takamaru@meijo-u.ac.jp

Growth of single-walled carbon nanotubes by alcohol CVD using Ir catalyst with various buffer layers

○Daiki Yamamoto[1], Shu kondo[1], Kamal P Sharma[1], Takahiro Saida[1,2], Shigeya Naritsuka[3], Takahiro Maruyama[1,2]

[1]*Department of Applied Chemistry, Meijo University, Japan*
[2] *Nanomaterial Research Center, Meijo University, Japan*
[3]*Department of Materials Science and Engineering, Meijo University, Japan*

1. Introduction

Single-walled carbon nanotubes (SWCNTs) are one-dimensional materials, having various potential for future nanoelectronics. So far, we have succeeded in growing vertically aligned small-diameter SWCNTs by alcohol catalytic chemical vapor deposition (ACCVD) with an Ir catalyst on SiO_2/Si substrates [1]. However, there have been no researches on SWCNT growth using an Ir catalyst on other buffer layers, although catalyst activity can be enhanced by using appropriate buffer layers. In this study, we performed SWCNT growth with Ir catalysts on various buffer layers by ACCVD and investigated the effect of buffer layers.

2. Experimental procedure

SiO_2, Al_2O_3, and MgO buffer layers (20 nm) were deposited onto SiO_2/Si substrates by RF magnetron sputtering. Ir catalysts (nominal thickness: 0.2 nm) were deposited onto them, and an ultra-high vacuum (UHV) chemical vapor deposition (CVD) system was used for SWCNT growth. After the substrate was heated to a growth temperature of 800°C in H_2 atmosphere of ~1×10^{-3} Pa, ethanol gas was supplied onto the substrates through a thin nozzle to grow SWCNTs [1]. The growth time was 60 min. The grown SWCNTs were characterized by Raman spectroscopy and FESEM.

3. Result and Discussion

Fig. 1 (a-c) shows Raman spectra of SWCNTs grown just under the nozzle at 800°C with an ethanol pressure of 1×10^{-3} Pa. Considering the wavenumbers of RBM peaks, SWCNTs grown on MgO and Al_2O_3 had diameters larger than those on SiO_2. Fig. 1 (d-f) are cross-sectional FESEM images of the SWCNTs shown in (a), (b) and (c), respectively, where vertically aligned SWCNTs were observed on all buffer layers. We will discuss the effects of the buffer layer on the SWCNT yield and structure.

This work was supported in part by Private University Research Branding Project from the Ministry of Education, Culture, Sports, Science and Technology (MEXT), Japan.

[1] T. Maruyama et al. Appl. Surf. Sci. 509 (2020) 145340.

Corresponding Author: T. Maruyama
Phone: +81-52-838-2386, Fax: +81-52-832-1172
E-mail: takamaru@meijo-u.ac.jp

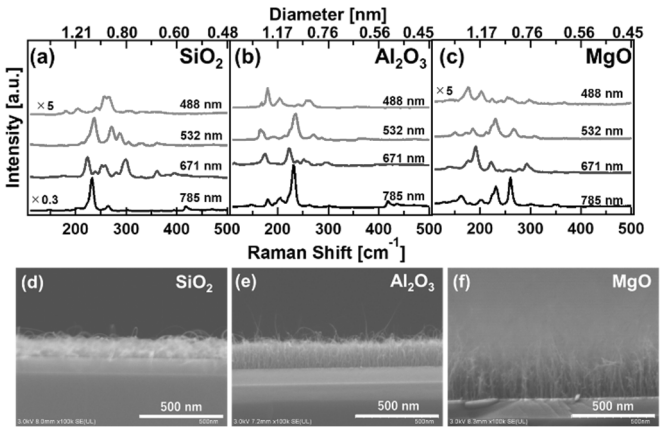

Figure 1 (a-c) shows Raman spectra in the RBM region of SWCNTs grown with Ir catalysts deposited on (a) SiO_2, (b) Al_2O_3, and (c) MgO layer. Figure 1 (d-f) shows the cross-sectional FESEM images of samples shown in (a), (b) and (c), respectively.

One-pot synthesis of Prussian Blue and nano-carbon composites

○Taisei Fujikawa, Yoshimitsu Taniguchi, Shinji Kawasaki, Yosuke Ishii

Department of Life science and Applied Chemistry, Nagoya Institute of Technology, Nagoya 466-8555, Japan

The recovery and utilization of low-grade heat is an urgent necessity to reduce its contribution to global warming, but there is the problem that the efficiency of conversion of low-grade heat to electricity is low. The Thermally Regenerative Electrochemical Cycle (TREC) is one technology that can solve this problem. Prussian blue (PB) analogs are some of use commonly for the positive electrode in the system, which offers efficient heat-to-electricity conversion but low power output, necessitating the use of a conductive supporting material. Therefore, we used Prussian blue nanocarbon composite as TREC electrode. Nano-carbon improves the ion transport in the composite due to its excellent electron conductivity and well-ordered porous structure, while maintaining the properties of PBA grown on their surface. We used two nano-carbon materials: single-walled carbon nanotubes (SWCNTs) and reduced graphite oxides (r-GOs).

The PB-SWCNT composite was obtained by adding a mixture of 1 mM $FeCl_3$ and 1 mM $K_3[Fe(CN)_6]$ to SWCNTs dispersion. XRD analysis, thermogravimetric analysis, SEM measurement, and TEM measurement were performed on the synthesized composite. Fig. 1 shows a tubular structure with bamboo segment-like deposits of PB on SWCNTs bundles. TEM measurement also showed PB particle layers on the surface of SWCNT bundles. These results indicate that the PB-SWCNTs composite has a core-shell structure in which PB crystals are deposited on the surface of SWCNTs. We'll discuss the TREC electrode properties of PB-SWCNT composite at the symposium.

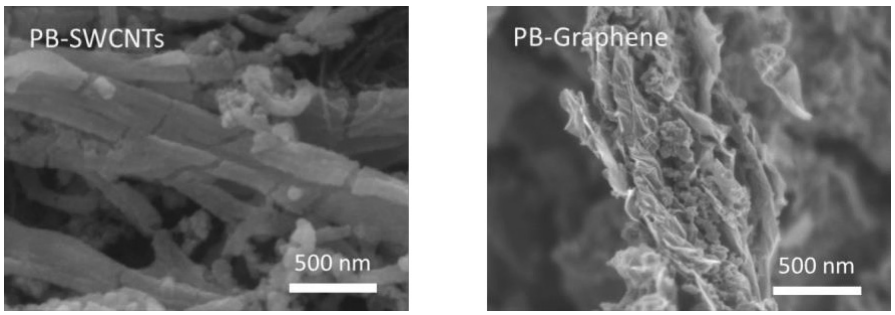

Fig. 1 SEM images of (right) PB-SWCNT and (left) PB-Graphene (r-GO) composites.

[1] Y. Ishii, A. Al-zubaidi, Y. Taniguchi, S. Jindo, S. Kawasaki, Single-walled carbon nanotubes as reducing agent for the synthesis of Prussian blue-based composite: a quartz crystal microbalance study, Nanoscale Adv., (2021). DOI: 10.1039/d1na00739d

Corresponding Author: S. Kawasaki
E-mail: kawasaki.shinji@nitech.ac.jp

A quartz crystal microbalance study of ion adsorption behavior of single-walled carbon nanotubes

○Serina Kanematsu, Shinya Jindo, Yu Takeuchi, Yosuke Ishii, Shinji Kawasaki

Department of Life science and Applied Chemistry, Nagoya Institute of Technology, Nagoya 466-8555, Japan

Single-walled carbon nanotubes (SWCNTs) have been actively investigated as a new electrode material for Electric Double Layer Capacitors (EDLCs), because of their high electrical conductivity, chemical stability, and high theoretical specific surface area. Unfortunately, many research results show that the current electrode performance of SWCNTs is not high enough to replace existing EDLC electrode materials. However, most of the previous studies evaluated the electrode performance of SWCNTs without distinguishing between SWCNTs of different diameters and electronic states, and the details of the ion adsorption mechanism of SWCNTs are not clear. If this aspect is clarified, it will be possible to propose new SWCNT electrodes to improve the performance of EDLCs. In this study, the ion adsorption behaviors of several kinds of SWCNT samples having different mean tube diameters during the formation of the electric double layer in various electrolytes were investigated by Quartz Crystal Microbalance (QCM) method.

SWCNTs were deposited as a thin layer on the QCM substrate, then the substrate was used as the working electrode in a three-electrode cell. Carbon fiber wrapped by Pt mesh and Ag/AgCl were used as the counter electrode and Ag/AgCl as the reference electrode, respectively. Simultaneous Cyclic Voltammetry (CV) and QCM measurements were performed in 1.0 mol/L *M*Cl / H_2O (*M* = Li, Na, K, Cs) electrolyte, in order to investigate how the adsorption behavior on SWCNTs changes depending on the electrolyte.

Fig. 1 shows changes in mass as a function of charge obtained by QCM measurements of SWCNTs having mean tube diameter of 1.5 nm for four different alkali metal chloride electrolytes. It was found that the minimum point of the mass change data shifts toward high charge value side with increasing atomic number of alkali metal of the electrolytes. This can be explained by the difference of ion adsorption-desorption behaviors depending on the ion species.

[1] A. Al-zubaidi, M. Takahashi, Y. Ishii, S. Kawasaki, Switching of alternative electrochemical charging mechanism inside single-walled carbon nanotubes: a quartz crystal microbalance study, RSC Advances, **11**, 30253-30258 (2021).

Corresponding Author: S. Kawasaki
E-mail: kawasaki.shinji@nitech.ac.jp

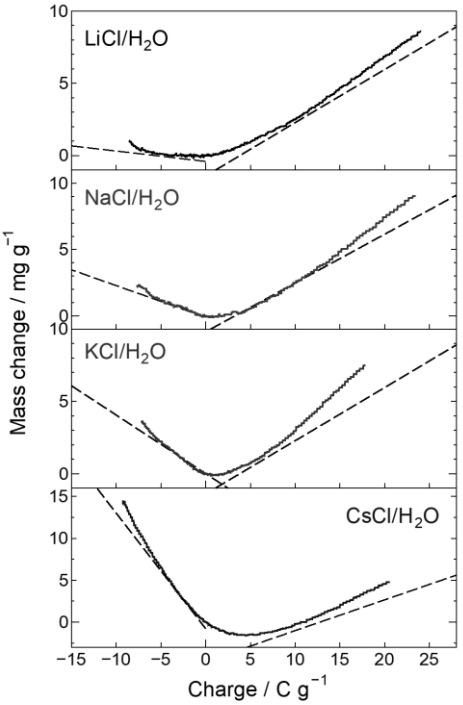

Fig.1 Change in mass as a function of charge obtained by QCM measurements of SWCNTs (*d* = 1.5 nm) electrode.

Solar CO_2 reduction properties of AgI/SWCNT/$AgIO_3$ and g-C_3N_4/SWCNT/Cu photocatalysts

○Jumpei Hayashi, Kenta Kobayashi, Sae Ishikawa, Shunsuke Sato, Yosuke Ishii, Shinji Kawasaki

Department of Life Science and Applied Chemistry, Nagoya Institute of Technology, Nagoya 466-8555, Japan

In recent years, there has been a lot of research on photocatalysts that can reduce CO_2 using solar energy. However, the conversion efficiency and selectivity of the reduction reaction are still low. In order to overcome this situation, several attempts have been done. One of the most promising way is to prepare photocatalysts consisting of two kinds of nanoparticles (NPs) having semiconductor/semiconductor or semiconductor/metal combinations, because these combinations enable to increase photo-absorption energy range and/or to depress the charge recombination between the excited electrons and holes. However, it is not easy to prepare such photocatalysts having good NP1-NP2 contacts. To help the charge transfer from NP1 to NP2, it is expected that single-walled carbon nanotubes (SWCNTs) can work as a bridge (i.e. NP1/SWCNT/NP2). We prepared two types of such composite materials: silver iodide (AgI)/SWCNT/silver iodate ($AgIO_3$) and graphitic carbon nitride (g-C_3N_4)/SWCNT/copper nanoparticles (Cu) by using the encapsulation properties of SWCNTs.

We prepared AgI/SWCNT/$AgIO_3$ by unique method using I@SWCNTs.[1] We found that AgI/SWCNT/$AgIO_3$ can work as a good photocatalyst for CO_2 reduction under visible light irradiation (Fig. 1).

On the other hand, g-C_3N_4/SWCNT/Cu was prepared by two steps. Firstly, we prepared SWCNTs including copper(II) acetylacetonate ($Cu(acac)_2$) ($Cu(acac)_2$@SWCNTs). Secondly, the prepared $Cu(acac)_2$@SWCNTs and melamine, which is the precursor of g-C_3N_4, were heat treated. We confirmed that g-C_3N_4/SWCNT/Cu works as a solar CO_2 reduction photocatalyst.

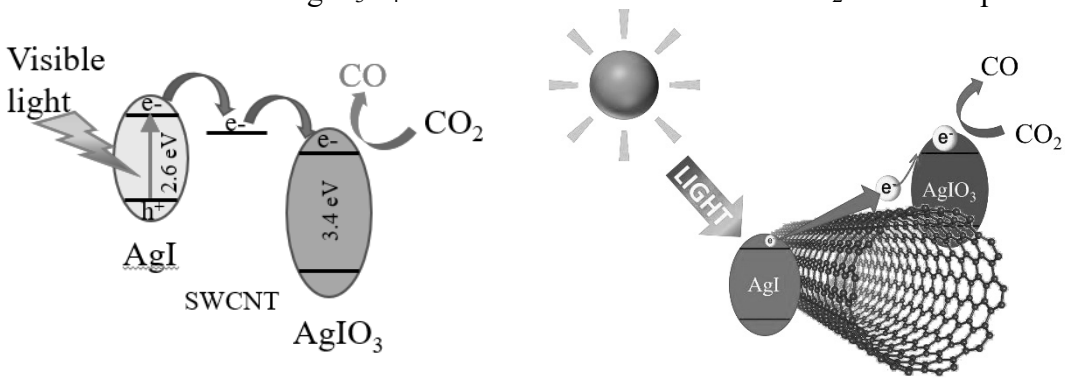

Fig. 1 AgI/SWCNT/$AgIO_3$ as a photocatalyst for CO_2 reduction.

[1] Al-zubaidi, et al., One-step synthesis of visible light CO_2 reduction photocatalyst from carbon nanotubes encapsulating iodine molecules, *Sci. Rep*., **11**, 10140 (2021).

[2] Y. Ishii, et al., Ultra-fine metal particles dispersed on single-walled carbon nanotubes for energy devices, *J. Mater. Sci*., in press.

Corresponding Author: S. Kawasaki
Tel: +81-52-735-5221,
E-mail: kawasaki.shinji@nitech.ac.jp

Performance and stability evaluation of transparent heater based on polymer-acid-doped carbon nanotube

○Emina Hara[1], Rongbin Xie [1], Suguru Noda[1,2,*]

[1] Department of Applied Chemistry and [2]Waseda Research Institute for Science and Engineering, Waseda University, Tokyo 169-8555, Japan

Today, transparent heaters (THs) have gained significant attention as deicers and defoggers of headlights on automobiles. Carbon nanotube transparent conductive film (CNT-TCF) is the one of the promising materials for THs because of its flexibility and transparency. However, its high sheet resistance required high input voltage (50 V) to obtain enough amount of Joule heat [1]. Recently, our lab developed a highly conductive CNT-TCF by using poly(p-styrene-sulfonic acid) (PSS) as a dispersant and dopant of CNT [2]. In this study, CNT-PSS THs was fabricated and its heating performance and stability to humidity and temperature were evaluated.

CNT-PSS-THs were fabricated as following. 1 mg of CNT were dispersed in PSS acid aqueous solution (2 wt%, 30 mL) by stirring and sonication. After sonication, the dispersion was centrifuged. The supernatant was diluted with pure water and filtrated to obtain CNT-PSS -TCF. CNT-PSS (T=85 %, R_s= 67 Ω/sq) achieved T_{max} =100 °C when 12 V was applied (Fig. 1). Next, the stability test was conducted. CNT-PSS-TCF and pure water were put in a sealed container and left in a constant temperature bath at 85 °C. As a comparison, the humidity test of CNT-HNO_3, CNT-SDBS, CNT-PSS-Na were also conducted. Humidity test was conducted for 5 times on each CNT-TCF. After the 1st humidity test, the resistance of CNT-PSS increased by 1.3-fold compared to its initial value (Fig. 2). After the 5th humidity test, the resistance of CNT-HNO_3 increased by 2.3-fold while the increase resistance ratio of CNT-PSS stabilized at 1.35 which was almost the same value as those of non-doped samples; CNT-SDBS (1.39) and CNT-PSS-Na (1.38). No correlation was observed between the changes in I_D/I_G and resistance increase. Changes in the CNT network structure was carefully examined and discussed.

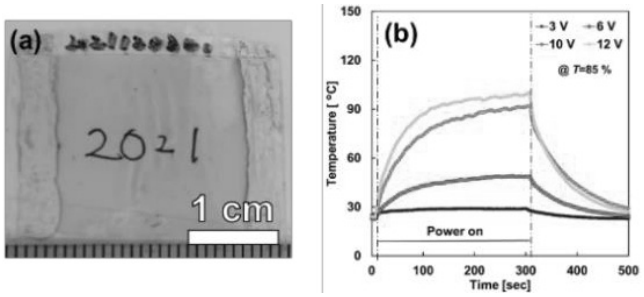

Fig.1 CNT-PSS transparent heater
(a) Image (b) Heat performance

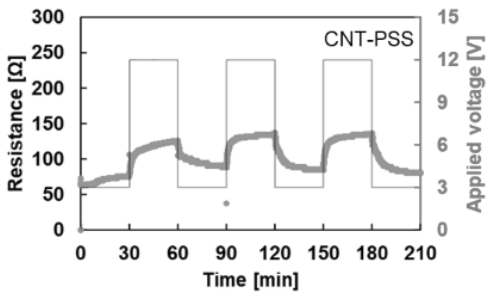

Fig.2 Resistance of CNT-PSS during the 1st humidity test

[1] D.T.Papanastasiou *et.al.*, *Adv. Funct. Mater*, **30**,1910225 (2020).
[2] R.Xie *et.al.*, *Carbon*, **164**, 150 (2020).

Corresponding Author: S.Noda Tel:, Fax:＋81-3-5286-2769, E-mail: noda@waseda.jp

Aqueous electrolyte batteries using the encapsulation properties of single-walled carbon nanotubes

○Yuna Yokoya, Yosuke Ishii, Shinji Kawasaki

Department of Life Science and Applied Chemistry, Nagoya Institute of Technology, Nagoya 466-8555, Japan

Lithium-ion batteries (LIBs) with high energy density are widely used. However, LIBs have the problems of (1) flammability and (2) high cost. Therefore, in recent years, aqueous secondary batteries have been attracting considerable attention because they are much safer than LIBs. Furthermore, if we can use organic compounds and iodine, which are abundant in nature, as electrode materials, we can reduce the cost. However, quinone organic compounds and iodine have the problems of poor electrical conductivity and insufficient charge-discharge cyclability. We anticipated that encapsulating these active materials in single-walled carbon nanotubes (SWCNTs) would offer an effective solution to the problems. Here, we propose two aqueous solution-based secondary batteries that utilize the encapsulation properties of SWCNTs. The first is a zinc-iodine battery and the second is a quinone-iodine battery (Fig. 1).

For zinc-iodine battery, zinc metal and porous carbon materials are usually used as the anode and the cathode, respectively. However, the cycling performance of the battery is usually not very good because the porous carbon materials cannot hold iodine electrode active species very firmly. We showed that SWCNT zinc-iodine battery shown in Fig.1 has good cyclability.[1]

We also confirmed that charge-discharge cycling performance of quinone-iodine battery is greatly improved by SWCNTs.[2] In the previous study, phenanthrene quinone (PhQ) and anthraquinone (AQ) were used as anode active materials. Here, we report that we can improve the electromotive force of the quinone-iodine battery by using 1,5-diaminoanthraquinone (1,5-DAAQ) and 2,6-diaminoanthraquinone (2,6-DAAQ), which have lower redox potential.

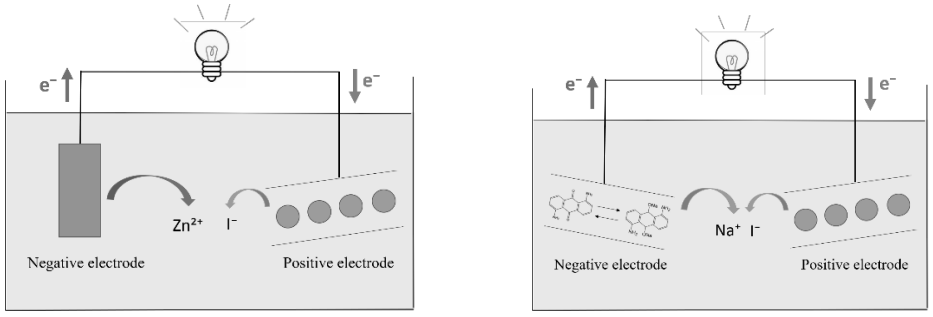

Fig. 1 Schematic pictures of (right) zinc-iodine battery and (left) quinone-iodine battery.

[1] Al-zubaidi, Y. Yokoya, *et al*., Iodine redox reactions in carbon nanotube hollow cores for rechargeable aqueous zinc-iodine batteries, to be submitted.

[2] C.Li, *et al*., Safe, economical and fast-charging secondary batteries using single-walled carbon nanotubes, J. Appl. Phys., **58**, SAA02 (2018).

Corresponding Author: S. Kawasaki
Tel: +81-52-735-5221,
E-mail: kawasaki.shinji@nitech.ac.jp

Selective monolayer growth of WS_2 nanoribbons on W_xO_y nanowires

○Hiroo Suzuki[1], Misaki Kishibuchi[1], Soya Ochiai[1], Zheng Liu[2], Yasumitsu Miyata[3] and Yasuhiko Hayashi[1]

[1]*Graduate School of Natural Science and Technology, Okayama University, Okayama 700-8530, Japan*

[2]*Innovative Functional Materials Research Institute, National Institute of Advanced Industrial Science and Technology (AIST), Tsukuba 305-8565, Japan*

[3]*Department of Physics, Tokyo Metropolitan University, Hachioji 192-0397, Japan*

Transition metal dichalcogenides (TMDCs) are promising two-dimensional (2D) materials for next-generation optoelectronic devices; they can also be a platform for further advances in physics. Structuring 2D TMDC sheets as nanoribbons has tremendous potential for electronic state modification. The two strategies for the synthesis of TMDC nanoribbons can be considered. One is top-down, and the other is a bottom-up process. The top-down approach by the conventional lithography technique is frequently used, however, there is a great advantage in the bottom-up process in terms of the cleanness of the surface and edge.

In this research, we have investigated the growth of WS_2 nanoribbons by chemical vapor deposition (CVD), which is a bottom-up process. The cold-wall CVD system with the infrared gold image furnace was established for TMDC growth. The aqueous solution of Na_2WO_4 was employed as a W source for WS_2 and deposited on SiO_2/Si substrates by spin-coating. The vapor of $(t\text{-}C_4H_9)_2S_2$ was introduced to a CVD chamber as an S source. From the systematic investigation of CVD growth, we found that the fiber-like materials can be grown with a relatively low $(t\text{-}C_4H_9)_2S_2$ supply. The atomic force microscopy (AFM) revealed that the fibers are around 3 nm in thickness, which is thicker than monolayer WS_2. The fibers showed both almost the same Raman and photoluminescence (PL) peaks as monolayer WS_2. The cross-sectional scanning transmission electron microscopy (STEM) observations revealed the presence of monolayer WS_2 nanoribbons grown on the W_xO_y nanowires. This method realized the high monolayer selection yield on a large scale and the growth of long (~100 μm) WS_2 nanoribbons. Regarding the growth mechanism, we supposed that the supply of source atoms from the vapor-solid bilayer and the chemical reaction at the atomic-scale interface might cause the self-limiting growth mechanism. Optical spectroscopy and electrical transport measurements characterized the electronic state of WS_2 nanoribbons.

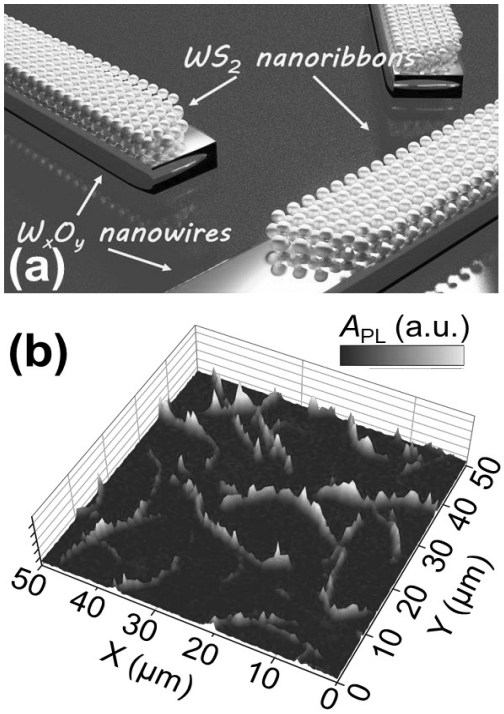

Fig. 1. (a)Illustration of WS_2 nanoribbons grown on W_xO_y nanowires. (b) PL mapping of WS_2 nanoribbons.

Corresponding Author: H. Suzuki
Tel: +81-86-251-8133
E-mail: hiroo.suzuki@okayama-u.ac.jp

Growth and anisotropic optical responses of MoS_2 nanoribbons

○Masahiko Kaneda[1], Hong En Lim[1], Kazuki Hashimoto[1], Yusuke Nakanishi[1], Takahiko Endo[1], Kenji Watanabe[2], Takashi Taniguchi[3], Yasumitsu Miyata[1]

[1]*Department of Physics, Tokyo Metropolitan University, Hachioji, 192-0397, Japan*
[2]*Research Center for Functional Materials, NIMS, Tsukuba 305-0044, Japan*
[3]*International Center for Materials Nanoarchitectonics, NIMS, Tsukuba 305-0044, Japan*

Recent advances in the growth technique of transition metal chalcogenides (TMDCs) enable the formation of structurally-controlled TMDC nanoribbons (NRs) and their superlattices [1,2]. The TMDC NRs are expected to provide a 1D-2D crossover system to study a wide variety of physical properties including electron transport, optical responses, and thermal properties. However, the study of such properties is still limited due to the short length of the NRs. Herein, we report the growth of long-length TMDC NRs and their anisotropic photoluminescence (PL) properties.

Long-length, NRs of monolayer MoS_2 were grown by metal-organic CVD [2]. First, a ribbon-shaped monolayer $MoSe_2$ core with dimensions of 2×20 μm was grown on a Si substrate. Next, the chalcogen source was switched from Se to S. This generates the MoS_2 NR growing around the $MoSe_2$ core, forming a MoS_2/$MoSe_2$ in-plane heterostructure (Fig. 1a). From Fig.1b-d, the MoS_2 NR shows the brightest PL intensity when the polarization direction of the linearly polarized laser was aligned in parallel to the ribbon axis at 0°. In contrast, such polarization dependence was not observed in that of $MoSe_2$ (Fig.1e). This implies a significantly reduced 1D geometry of the MoS_2 fabricated. From the similar trait reported in WSe_2 NRs [3], the anisotropic PL response observed can be explained by modulation of optical absorption coefficient due to the depolarization effect [4,5]. Our results present a useful way of studying the correlation between structure and physical properties of monolayer TMDCs.

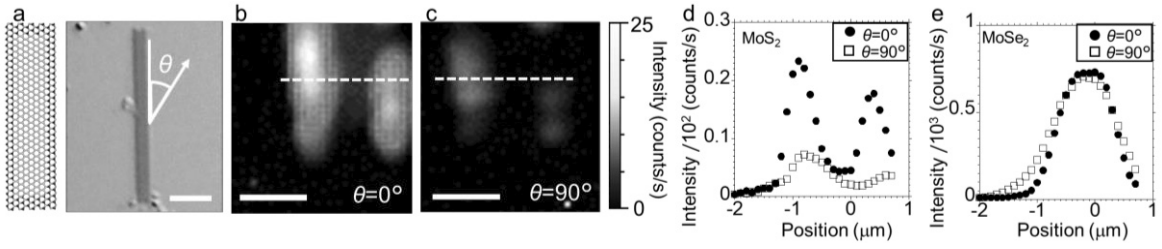

Fig. 1. (a) Structural model and optical image of the MoS_2 NR grown, surrounding the ribbon-like $MoSe_2$ core. θ refers to the angle between the polarization direction of the incident laser and the ribbon axis. Scale bar is 10 μm. (b, c) PL intensity maps of MoS_2 (1.8 eV) irradiated at the polarization angle of 0° and 90°. Scale bars are 1 μm. (d) PL spatial intensity profiles of MoS_2 (1.8 eV) and (e)PL spatial intensity profiles of $MoSe_2$ (1.56 eV) irradiated at the polarization angle of 0° and 90°

[1] S. Xie *et al.*, *Science* 359, 1131-1136 (2018), [2] Y. Kobayashi *et al.*, *ACS Nano* 13, 7, 7527−7535 (2019) [3] H. E. Lim *et al.*, *ACS Appl. Nano Mater.* (2021) DOI: 10.1021/acsanm.1c03160. [4] H. Ajiki and T. Ando, *Phys. Rev. B* 201, 349-352 (1994), [5] S. Uryu and T. Ando, *Phys. Rev. B* 74, 155411 (2006).
Corresponding Author: Y. Miyata, Tel: 042-677-2508, E-mail: ymiyata@tmu.ac.jp

A magnetic carbon sheet of hexagonally arranged fused pentagons

○Susumu Okada, Nguyen Thanh Cuong, Yanlin Gao, Mina Maruyama

Department of Physics, University of Tsukuba, Tsukuba 305-8571, Japan

Structural imperfections, such as point defects, pores, and edges, in graphene are the origin of the unusual physical properties of graphene derivatives. Topological defects, such as pentagon and heptagon, also play a crucial role in determining the physical properties of graphene derivatives containing such topological imperfections. Pentagons occasionally causes unusual electronic structures in graphene derivatives mainly comprising three-fold coordinated C atoms. Recently, covalent networks comprising fused pentagons, each containing four-fold coordinated C atoms, have been theoretically proposed (spiro-graphene) [1,2]. C atoms with four-fold coordination are situated at the vertex of four pentagons that share their edges with adjacent pentagons, so that the networks display a nanometer-scale rippling and large pores without dangling bonds. These structures also create unique electronic structures depending on the mutual arrangement of the C atoms with four-fold coordination and other topological imperfections.

Because of structural variations in these covalent networks comprising three- and four-fold coordinated C atoms, we explore the structure that leads to a unique electronic structure. Our first-principles total-energy calculations demonstrate that the two-dimensional hexagonal and pentagonal covalent network of four-fold and three-fold coordinated C atoms (called hexagonal spiro-graphene) is a potential representative of a ferromagnetic carbon allotrope with a Curie temperature of 422 K that results from the slow Dirac electrons at the Fermi level. In addition to the ferromagnetic phase, the hexagonal spiro-graphene can have antiferromagnetic phase as its metastable states which is almost degenerate in energy. The polarized electron spin is distributed throughout a hexagonal network of three-fold coordinated C atoms surrounded by four-fold coordinated C atoms. The hexagonal spiro-graphene possesses an electrostatic polarization normal to the atomic layer because the atomic arrangement along this direction is asymmetric.

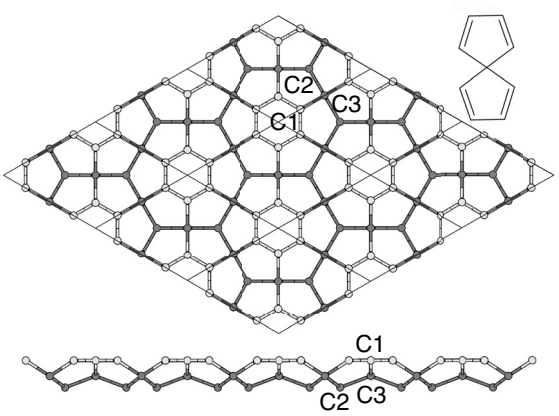

Fig. 1: A geometric structure of hexagonal-spirographene and that of its constituent unit ofspiro[4,4]nonatetraene.

[1] S. Okada, et al. Carbon 185, 404 (2021).
[2] S. Okada, et al. J. Phys. Soc. Jpn. in press (2022)

Corresponding Author: Susumu Okada
TEL: +81-29-853-5921, FAX: +81-29-853-5924
E-mail: sokada@comas-tsukuba.jp

MD evaluation of thermal conductivity of double layer hBN ribbon at different geometries using energy exchange eHEX algorithm.

○Wataru Yuhara[1], Tatiana Zolotoukhina[1]

[1] *Department of Mechanical Engineering, University of Toyama, Toyama 930-8555, Japan*

Materials with high thermal conductivities (κ) are valuable to solve the challenge of waste heat dissipation in highly integrated and miniaturized modern devices. Materials with high thermal conductivities (κ) are one of the key solutions to this challenge. All boron nitride (BN) materials, including single atomic layer (1L) BN, are electric insulators and considered as candidates for waste heat dissipation in power chips as both an insulating layer as well as a heat spreader for local hotspots with high heat flux. Bulk cubic (c) and hexagonal (h) BN crystals are good thermal conductors with κ of ~690 and 420 W/mK at room temperature [1]. It was reported that high-quality and surface-clean 1L hBN had a κ of 751±340 W/mK [2]. This κ increase with reduced thickness down to the atomic level is attributed to a decrease in the number of phonon branches and states. We investigate the thermal conductivity of 2L hBN samples as related to the in-plane & out-of-plane energy transfer channels, coupling to the sample size and layer interaction. The 1 and 2 layers hBN samples with AA stacking of single and double-width were used. The eHEX [3] energy exchange algorithm was utilized in molecular dynamics (MD) simulation to maintain stable heat flow.

The hBN layers were of the 1440 x 173.52 (347.04, double width in *y*) Å size with AA stacking and Δz=3.3 Å distance between layers. We utilized the eHEX energy exchange algorithm at periodic boundary condition in the *x*-direction with varying periodicity in *y*. Calculations were carried in LAMMPS. The conduction area was $L_x/2$ in the *x*-direction, heating and cooling areas were taken to be 8 Å wide. The thermal conductivity of the samples with *x*, *y* periodic BC was found to be low. Ribbon samples of 2 different widths gave values of κ varying between 100 and 800 W/mK with time. Increased width of nanoribbon was associated with a better balance between components of the in-plane values of κ.

(a) thermal conductivity, *x*-direction (b) thermal conductivity in *y* & *z* directions, 2L

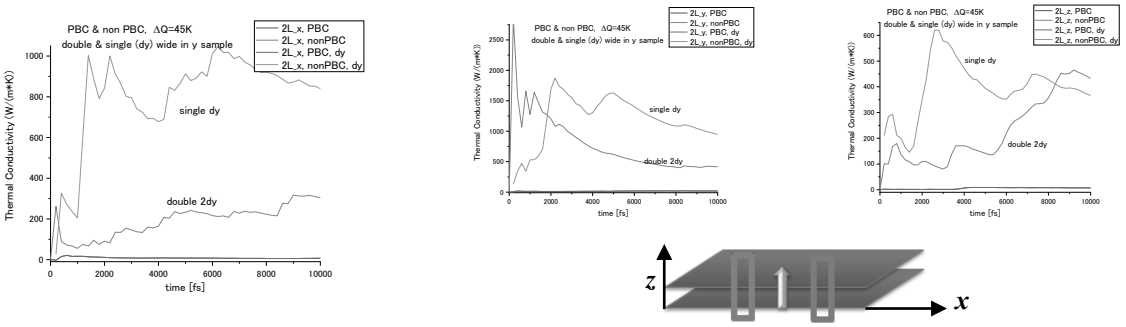

Fig1 Thermal conductivity in hBN 2 layer interacting system (T=300 K, conduction area in *x*)

[1] P. Q. Jiang, X. Qian, R. G. Yang, and L. Lindsay, *Phys. Rev. Mater.* 2, 064005 (2018).

[2] Q. Cai, D. Scullion, W. Gan, A. Falin, S. Zhang, K.Watanabe, T. Taniguchi, etc., *Sci. Adv.,* 5, eaav0129 (2019).

[3] P.Wirnsberger, D.Frenkel, C. Dellago, *J. Chem.Phys*., 143, 124104 (2015).

Corresponding Author: T. Zolotoukhina

Tel: +81-76-445-6739, Fax: +81-76-445-6739, E-mail: zolotu@eng.u-toyama.ac.jp

Temperature Dependency on the Layer Spacing of Graphene Oxide Polyethyleneimine Composite Membranes

○Norihiro Fukaya[1], K. Kanishka H. De Silva[2], Masamichi Yoshimura[2], Hiroya Tanaka[1]

[1] *Toyota Central R&D Labs., Inc., Nagakute 480-1192, Japan*
[2] *Graduate School of Engineering, Toyota Technological Institute, Nagoya 468-8511, Japan*

Two-dimensional membranes have attracted much interest in the filtering and transport of chemical and molecular species [1, 2]. Graphene oxide (GO) has huge potential because its permeability and selectivity can be controlled with its functional groups. In particular, the adaptation capability has been programmed in the membrane formed by GO and Polyethyleneimine (PEI). In this presentation, we study temperature dependency on the interlayer spacing of the GO-PEI membranes to prove its suitability of selective ion permeability and water permeability.

The membranes were prepared by vacuum filtration of suspension of GO (0.1 mg/mL) and PEI (2 mg/mL) on filters (Anodisc, pore size 100 nm). For reference, we also made GO membranes (w/o PEI) via the same process. Figures 1a and 1b show XRD spectra of GO and GO-PEI membranes heated at different temperatures in air, respectively. In Fig. 1a, peak position shifts to wide angle with the increase of temperature. This means that the interlayer spacing of GO decreases with the increasing temperature due to the removal of oxygen groups.

In Fig 1b, the peak of the curves is located at a lower angle (5~7°) due to the insertion of PEI between the GO layers. In addition, a new peak appears around 22° from 150℃ to 200℃. This angle coincides with reduced GOs. It can be understood that the PEI enhanced the reduction of GO, and reduced GOs were obtained at lower temperatures than those w/o PEI.

In conclusion, we explored the temperature dependency of interlayer spacing of the GO and GO-PEI membranes via variable temperature XRD analysis. Moreover, we reveal that PEI plays an important role in removing the oxygen groups in GO.

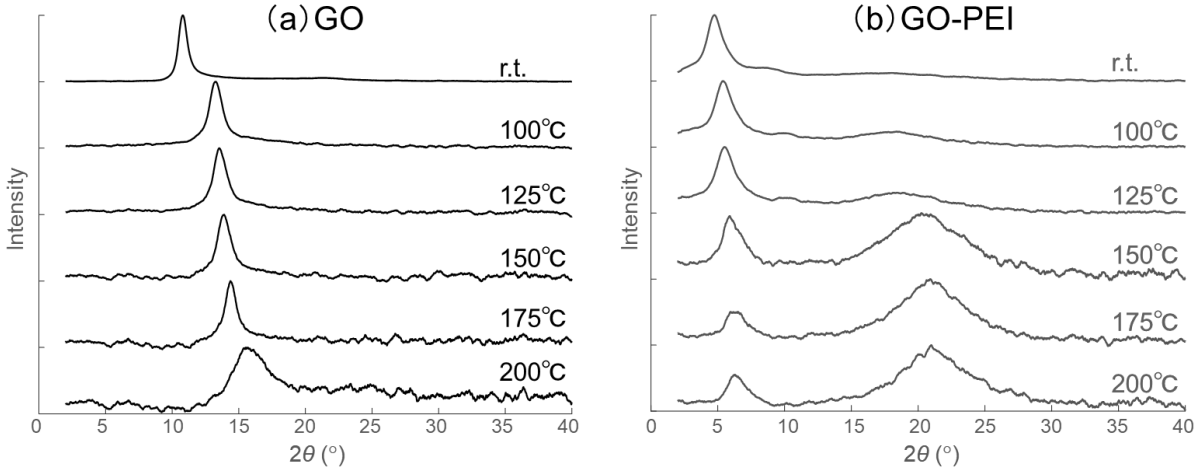

Fig. 1. XRD patterns of (a) GO and (b) GO-PEI heated at different temperatures (r.t.= room temperature).

[1] D. V. Andreeva *et al*., Nat. Nanotechnol. **16**, 174 (2021).
[2] H. Huang *et al*., J. Membr. Sci. **572**, 12 (2019).

Corresponding Author: N. Fukaya
Tel: +81-561-71-8137, E-mail: fukaya@mosk.tytlabs.co.jp

Effect of iron ion beam irradiation on MoS_2 fluorescence

○Takumi Hidaka[1,2], Kosuke Nakamura[1], Tomoaki Nishimura[2], Kazuyuki Takai[1,2]

[1]*Graduate School of Science and Engineering, Hosei University, Tokyo 184-8584. Japan*
[2]*Research Center of Ion Beam Technology, Hosei University, Tokyo 184-8584. Japan*

In 2D material, defects and impurities significantly affect the electronic properties compared to 3D materials due to its low-dimensional structure. Meanwhile, ion beam implantation is one of the methods that can quantitatively and reproducibly introduce defects and impurities into materials. We can achieve the maximum implanted ion distribution on 2D materials by using a sacrificial layer [1]. It is not well known yet how chemical properties of the implanted ion affects on 2D materials in spite of many reports on the ion-dose dependence on 2D materials. In this study, Fe^+ as a magnetic impurity that can cause spin scattering were introduced by ion beam irradiation into 1L-MoS_2 in which fluorescence strongly correlates with the degree of freedom of spin. The irradiation effects on structural and electronic properties were investigated using Photoluminescence (PL).

Cr / NaCl of 10 nm / 250 nm was deposited as a sacrificial layer on 1L-MoS_2 obtained by the cleavage method on a SiO_2 / Si substrate. The film thickness of the sacrificial layer was optimized using Monte Carlo simulation for Fe^+ distribution by SRIM2013. Fe^+ irradiation to the sample was performed at an acceleration voltage of 200 keV with a dose of 10^{12}, 10^{13} cm^{-2}. MoS_2 before and after Fe^+ irradiation was measured by low temperature PL at 77 K using a spectrometer (LabRAMHR, Horiba).

In addition to the characteristic peaks of MoS_2: A (1.89 -1.91 eV) and B (~2.06 eV), the D peaks (1.71 - 1.78 eV) which does not appear at room temperature also appeared at 77 K after the irradiation (**Fig. 1**). The D peaks are attributed to the physisorption of O_2 and N_2 in the air at the S defects introduced by Fe^+ irradiation, resulting in the formation of new defect levels [2]. The D / A ratio increased as the irradiation dose increased (**Fig. 2**). This is attributed to the increase in the amount of adsorbed molecules caused by the increase in defect sites due to Fe^+ irradiation. All the peaks slightly shifted to the higher energy side by Fe^+ irradiation (**Fig.2**). This suggests that the lattice constant changes due to the compressive strain caused by the introduced defects, resulting in the changes of the band gap.

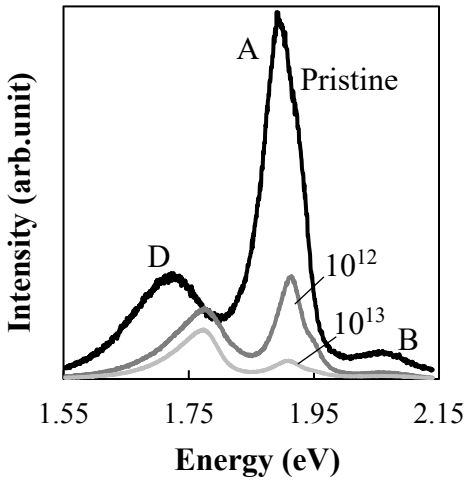

Fig. 1 PL spectra for MoS_2 before and after Fe^+ irradiation at 77 K

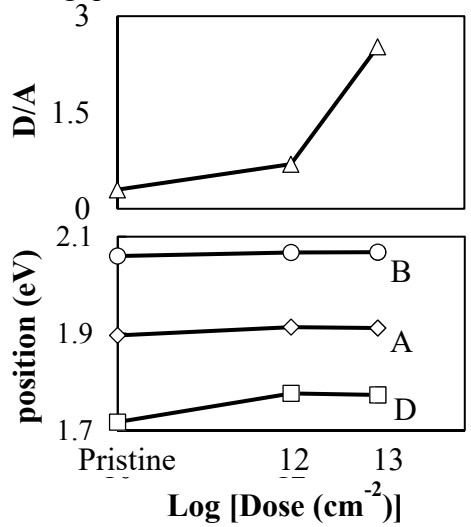

Fig. 2 (a) Change of D peak intensity (b) change of peak position of A(○), B(◇), D(□) upon Fe^+ irradiation at 77 K

[1] K. Nakamura *et al*, FNTG Symposium (2019)
[2] S. Tongay *et al*, *Sci. Rep.* (2013)

Invisible *N*-layer graphene on Si substrates

○Ken-ichi Sasaki[1], Masahiro Kamada[2], Takamoto Yokosawa[2], Taisuke Ochi[2], Tomohiro Matsui[2]

[1] *NTT Research Center for Theoretical Quantum Physics, NTT Basic Research Laboratories, NTT Corporation, 3-1 Morinosato Wakamiya, Atsugi, Kanagawa 243-0198, Japan*
[2] *Advanced Research Laboratory, Anritsu Corporation, 5-1-1 Onna, Atsugi, Kanagawa 243-8555, Japan*

The detection of graphene layers on Si substrates is a common task, but has the aspect of being a nontrivial scientific problem. In optical detection of graphene with the naked eye, the difference between the reflectance of visible light from the substrate and that from graphene on it must be sufficiently large for increasing their contrast. It is known that Si substrates with a SiO_2 surface layer of a certain thickness have an advantage [1]. Namely, when the optical thickness of SiO_2 is a quarter or three quarters of the light wavelength used, the reflectance from the substrates is minimized and the contrast takes a maximum. What happens to the contrast if the number of graphene layers on the substrates increases? [2]

We calculated the reflectance of an *N*-layer graphene on Si substrates using a transfer matrix method and found that the reflectance can vanish for a normal incident visible light with a specific *N* (~20) and wavelength (~560 nm) when SiO_2 thickness is 285 nm (See Fig.1). The zero-reflectance cannot occur without the surface layer [3], and it is inherent to a strange interference effect between the substrates and 20-layer graphene. On the other hand, 20-layer graphene is most easily detectable because the contrast becomes unity which is the maximum contrast. The result suggests that 20-layer graphene itself is invisible but easiest to be found by the contrast.

We will show experimental data that partly confirm the calculations, where the *N* value was measured by atomic force microscopy. Importantly, the reflectance is indeed suppressed for a normal incident visible light with the wavelength (~560 nm), however it does not vanish in contrast to the calculation. We discuss the reason of this discrepancy from the point of view of an enhanced Raman scattering light [4].

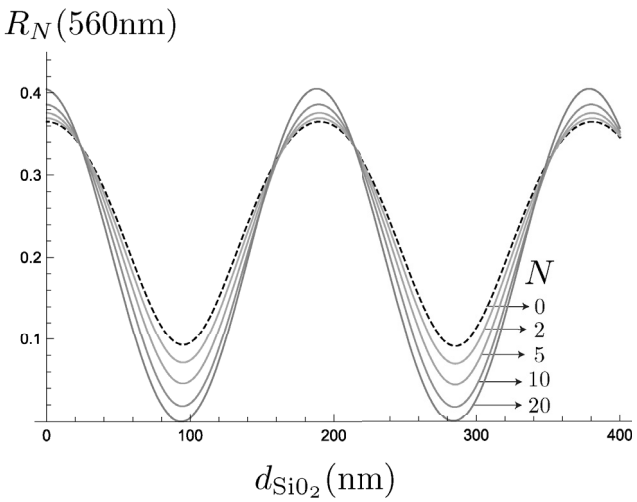

Fig. 1 The calculated reflectance of a normal incident visible light with the wavelength (560 nm) is plotted as a function of SiO_2 thickness. *N* denotes the number of graphene layers.

[1] Blake *et al*., APL **91**, 063124 (2007).
[2] Z.H. Ni *et al*., Nano Letters **7**, 2758 (2007).
[3] Kumar *et al*., Nanotechnology **24**, 165402 (2013).
[4] Y.Y. Wang *et al*., APL **92**, 043121 (2008).

Corresponding Author: K. Sasaki
Tel: +81-46-240-3033, Fax: +81-46-240-,
E-mail: kenichi.sasaki.af@hco.ntt.co.jp

Diffusion of Oxygen Atom on Graphene Sheet from One Side to the Other Through Atomic Vacancy

○Takazumi Kawai[1]

[1] *Graduate School of Integrative Science and Engineering, Tokyo City University, Tokyo 158-8557, Japan*

Graphene oxide is one of the most promising materials for the device application of 2D materials due to its easy fabrication, low cost, transparency and its interesting electronic properties. Recently, the application of graphene oxide as a non-volatile resistive switching random-access-memory (Re-RAM) attracts much attention with rather easy and practical fabrication methods[1-4]. For the mechanism of the resistive switching, diffusion of oxygen atoms are important process and it should affect the switching properties and endurance properties. Especially, the diffusion perpendicular to the graphene surface would be critical to gather the oxygen atoms in the vicinity of electrode.

In the last presentation, we investigated the diffusion of single oxygen atoms through the V_6 atomic defect, and found that the activation energy for the diffusion is fairly high and it would be difficult to diffuse from one side of graphene sheet to the other under room temperature, while it can diffuse on the clean surface.

In this presentation, we considered diffusion processes for an oxygen atom through the V_6 with the other oxygen at the edge via DFT calculations using quantum espresso code [5]. Using graphene 6x6 supercell with V_6 defect hole, the total energy variation along the diffusion path which go through the V_6 defect, where, another oxygen atom is adsorbed on the edge of V_6. Since the oxygen adatom at the V_6 edge takes some electrons away from the nearby carbon atoms, the adsorption potential for the diffusing oxygen atom becomes shallow compared to that without oxygen adatom at the edge, although the V_6 edge still attracts the oxygen atoms to its edge. We will further present the activation energy and effect of electric fields normal to the surface.

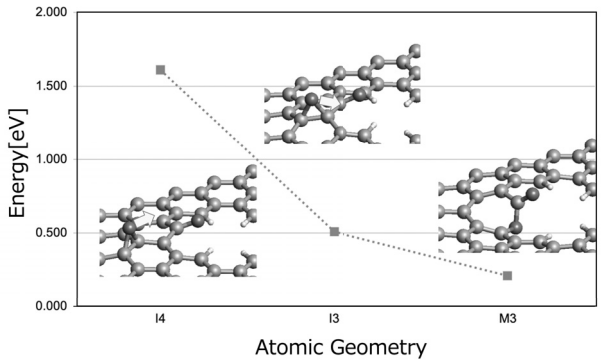

Fig.1 Total energy variation for each atomic geometry, where the diffusing oxygen atom approach to the edge of V6 defect and go through it by breaking C-C bond.

[1] H. Tian, *et al.*, Nano Letters, 14 (2014) 3214.
[2] A. Rani, *et al.*, small, 12 (2016) 6167.
[3] H. Liua, *et al.*, Mater. Today Commun. 25 (2020) 101537.
[4] M. Brzhezinskaya, *et al.*, J. Alloys Compd. 849 (2020) 156699.
[5] P. Giannozzi et al., J. Phys.:Condens. Matter 21 395502 (2009); P. Giannozzi et al., J. Phys.:Condens. Matter 29 465901 (2017); P. Giannozzi et al., J. Chem. Phys. 152 154105 (2020); URL http://www.quantum-espresso.org.

Corresponding Author: T. Kawai,
Tel: +81-3-5707-0104,
E-mail: tkawait@tcu.ac.jp

Electrical Conductivity of Nanodiamond Hydrogels #1: their measurements by using interdigitated electrodes.

○ Kazuya Yamaguchi[1], Masaya Yabuki[1], Toshihiko Tanaka[1], Tetsuya Aoyama[2], Yasuhiro F. Miura[3], Yoshiya Akagi[3], Eiji Osawa[4]

[1]Department of Chemistry and Biochemistry, National Institute of Technology, Fukushima College, 30 Aza-nagao, Tairakamiarakawa, Iwaki, Fukushima, 970-8034, Japan
[2]Ultrahigh Precision Optics Tech. Team, RIKEN RAP, 2-1 Hirosawa, Wako, Saitama, Japan
[3]Hamamatsu University School of Medicine, 1-20-1 Handayama, Higashi-ku, Hamamatsu City, Shizuoka, Japan
[4]Nano Carbon Research Institute Ltd., Asama Research Extension Center, Shinshu University, 3-15-1 Tokida, Ueda, Nagano, Japan

The solid surfaces of diamond often take mobile electrons due to its negative electron affinity and they have attracted much attention to apply them to device applications including sensors.[1] The interfacial water on the surfaces also have a high conductivity due to their protons.[2] We consider that electrons or protons in their interfacial water also account for the conductivity of the hydrogels.

Recently we have found the high electrical conductivity of nanodiamond (ND) hydrogels. To reduce the sampling amount of ND, we have developed a measurement method using a commercial interdigitated Au electrodes (Metrohm Drop Sens IDEAU200, Spain). They consist of two interdigitated Au electrodes with two connection tracks on a ceramic substrate. The substrate dimensions are small : L 22.8 mm x W 7.6 mm x H 1 mm and the interdigitated area is only 6.5 x 6.5 mm^2. Hence, we can measure the conductivity of a tiny liquid droplet down to ~0.03g, if their calibration are done with some standard KCl solutions; a cell constant and the resistance of Au electrode (nearly 15Ω) are obtained.（**Fig.1**）Impedance spectra were recorded with an LCR meter from 1 to 10^6 Hz and the resistance of Au electrode was subtracted, thus the DC conductivity of samples being calculated (up to at least 1.9 mS/cm as shown in #2 presentation.), which is significantly larger than those reported value for pellets of diamond particles with saturated water vapour.

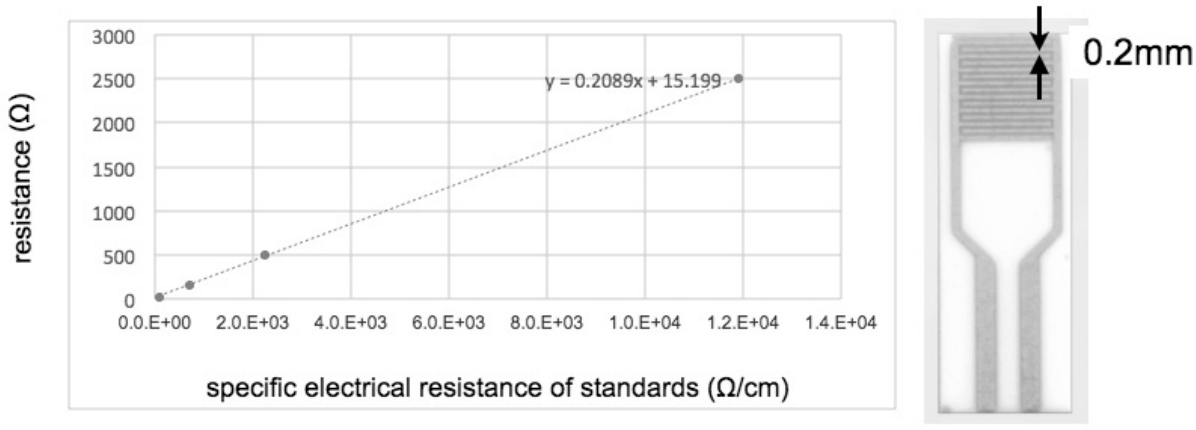

Figure. 1 Measured resistance vs. specific resistance of the standard KCL solutions.

[1] T.Kondo, I. Neitze, V. N. Mochalin, J. Urai,1 M. Yuasa, Y. Gogotsi, *J. Appl. Phys.* 113, 214307 (2013)
[2] V. G. Artemov,E. Uykur, P. O. Kapralov, A. Kiselev, K. Stevenson, H. Ouerdane, M. Dressel, *J. Phys. Chem.* Lett. 2020, 11, 3623−3628.
Corresponding Author:Toshihiko Tanaka / Tel: +81-246-46-0810 / E-mail: ttanaka@fukushima-nct.ac.jp

Electrical Conductivity of Nanodiamond Hydrogels #2: their temperature dependence

○ Masaya Yabuki[1], Kazuya Yamaguchi[1], Toshihiko Tanaka[1], Tetsuya Aoyama[2],
○ Yasuhiro F. Miura[3], Yoshiya Akagi[3], Eiji Osawa[4]

[1]*Department of Chemistry and Biochemistry, National Institute of Technology, Fukushima College, 30 Aza-nagao, Tairakamiarakawa, Iwaki, Fukushima, 970-8034, Japan*
[2]*Ultrahigh Precision Optics Tech. Team, RIKEN RAP, 2-1 Hirosawa, Wako, Saitama, Japan*
[3]*Hamamatsu University School of Medicine, 1-20-1 Handayama, Higashi-ku, Hamamatsu City, Shizuoka, Japan*
[4]*Nano Carbon Research Institute Ltd., Asama Research Extension Center, Shinshu University, 3-15-1 Tokida, Ueda, Nagano, Japan*

Here we have measured the high electrical conductivity of nanodiamond(ND) hydrogels[1] by using interdigitated electrodes explained in #1 presentation. The measured values have reached at least 1.9 mS/cm (presumably up to 7mS/cm) at room temperature, being significantly higher than those reported values for the interfacial water of pellets of diamond particles (5, 40, 80, 120,or 200 nm) with saturated water vapour.[2] What are the charge carriers for our cases? Are these similar to those for the pellets? Or are there any difference?

We concentrated an ND solution(NanoAmando@,*NanoCarbon Research Institute Ltd.*, containing EDIANs） from 2.5 to ~35wt% and cooled while its conductivity was being measured by an LCR meter. The conductivity decreased as shown in **Fig.1**, its slope indicating nearly 0.21 eV of activation energy. This value is slightly different from 0.17 eV that reported[2], where Artemov *et al.* suggested protons as carriers because of the value. Lower temperatures give a larger slope, indicating significant larger activation energy nearly 0.7 eV. Hence, we have to determine the carriers carefully. One possibility is proton conduction and we have to explain the larger slope in this case. Otherwise, we have to postulate another possibility. Petit, *et al.* demonstrated the solvated electrons in the interfacial water of hydrogenated ND and NanoAmando is similar to hydrogenated ND because of their rich CH terminations.[3] Hence, we also have to consider this possibility. We will discuss them here.

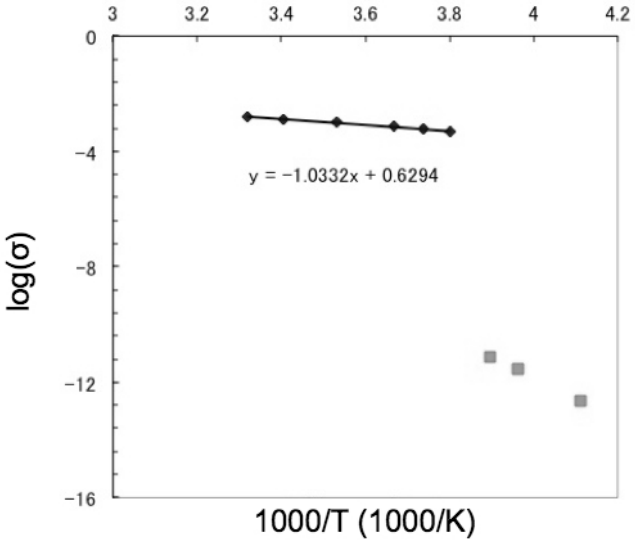

Figure 1. Temperature dependence of the electrical conductivity σ （S/cm） of the ND hydrogel (~ 35%) through cooling it.

[1]E. Ōsawa, D. Ho, H. Huang, M.V. Korobov, N.N. Rozhkova, Dia. Rel. Mat. **18** , 904(2009)
[2]V. G. Artemov, E. Uykur, P. O. Kapralov, A. Kiselev, K. Stevenson, H. Ouerdane, M. Dressel, *J. Phys. Chem. Lett.* 2020, **11**, 3623(2020),;
[3]T. Petit, et al., *J. Phys. Chem. C*, **121**, 5185(2017)
Corresponding Author:Toshihiko Tanaka / Tel: +81-246-46-0810 / E-mail: ttanaka@fukushima-nct.ac.jp

発表索引

Author Index

Author index

複写をご希望の方へ

フラーレン・ナノチューブ・グラフェン学会では、複写複製および転載複製に係る著作権を学術著作権協会に委託しています。当該利用をご希望の方は、学術著作権協会（https://www.Zaacc.org/）が提供している複製利用許諾システムもしくは転載許諾システムを通じて申請ください。

注意：著作物の引用、翻訳等に関しては、（社）学術著作権協会に委託致しておりません。直接、
フラーレン・ナノチューブ・グラフェン学会へお問い合わせください。

Reprographic Reproduction outside Japan

Fullerenes, Nanotubes and Graphene Research Society authorixed Japan Academic Association For Copyright Clearance (JAC) to license our reproduction rights and reuse rights of copyrighted wor8s. If you wish to obtain permissions of these rights in the countries or regions outside Japan, please refer to the homepage of JAC (http://www.Zaacc.org/) and confirm appropriate organixations to reQuest permission.

In order to obtain permission to Quote and/or translate, please contact the copyright holder directly.

2022 年 2 月 23 日 発行

第62回フラーレン・ナノチューブ・グラフェン総合シンポジウム
講演要旨集

≪フラーレン・ナノチューブ・グラフェン学会≫
〒464-8601 愛知県名古屋市千種区不老町
名古屋大学 未来材料･システム研究所
未来エレクトロニクス集積研究センター 大野研究室内
Phone/Fax：03-3830-4848
E-mail：secretariat@fntg.jp
URL：https://fntg.jp/jp_new/

印刷 / 製本　名古屋大学消費生活協同組合　印刷部

TELEDYNE
PRINCETON INSTRUMENTS
Everywhereyoulook™

高感度近赤外線
2次元 InGaAs ハイスピードカメラ
NIRvana® HS

- ハイスピード
  250 fps (full 640x512 pixels)
  1200 fps (200x200 pixels)
- 多彩な読み出しモード
  Integrate While Read (IWR) mode搭載
  マルチROI
- 低読み出しノイズ
- USB3.0接続

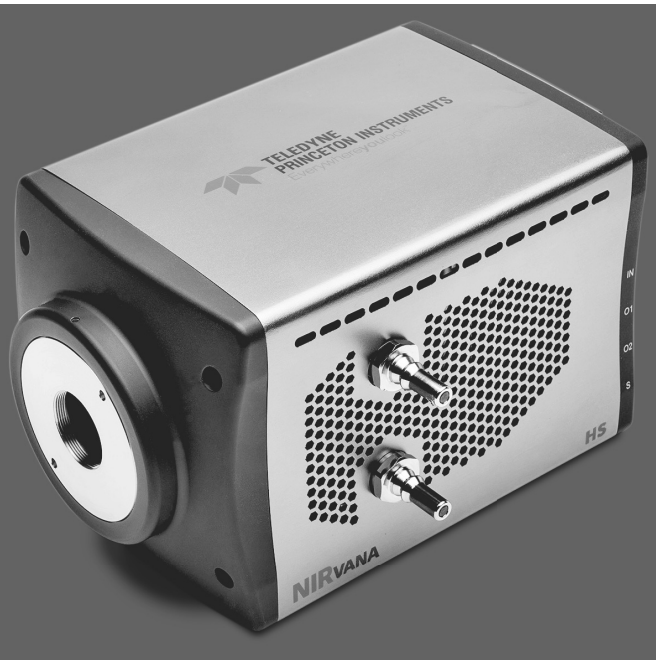

アプリケーション例

- フォトニック結晶PLイメージング及びスペクトル
- 一重項酸素イメージング及びスペクトル
- 太陽電池PLイメージング及びスペクトル
- 天体観測微弱光イメージング
- 食品断面イメージング
- In-Vivoイメージング　など

量子効率グラフ

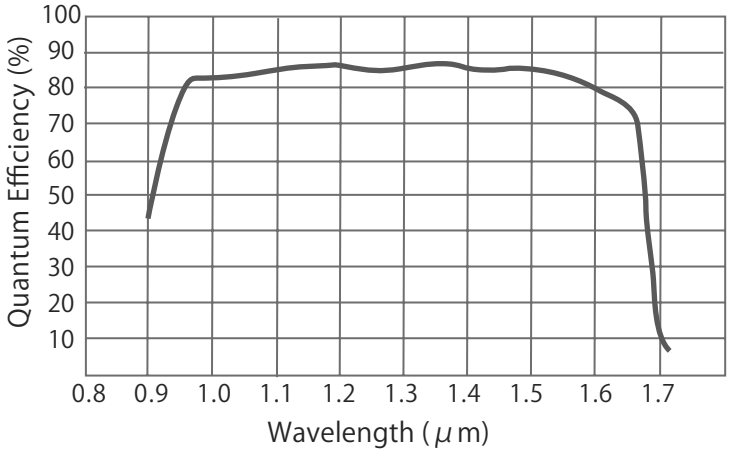

仕様

モデル	NIRvana HS	NIRvana:640	NIRvana:640LN
センサー	640 x 512 x InGaAs		
素子サイズ	20μm x 20μm		
波長範囲	0.9 ～ 1.7 μm		
冷却温度	-55℃(-50℃空冷)	-80℃	-190℃
ダークチャージ	700 e-/p/sec	300 e-/p/sec	<8 e-/p/sec
読み出しノイズ	<60 e-rms	<120 e-rms	15 e-rms
ダイナミックレンジ	16 Bit (>15Bit@1 素子)		
フレームレート	250 fps	110 fps	2.77 fps@250KHz
インターフェース	USB3.0	Gig E	

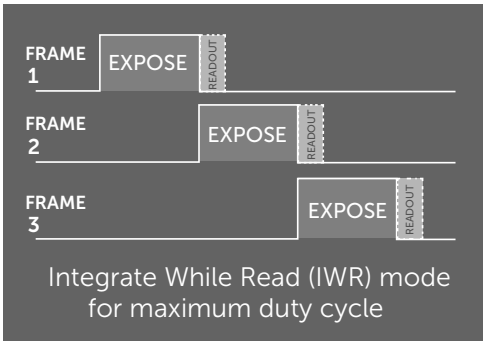

Integrate While Read (IWR) mode
for maximum duty cycle

www.pi-j.co.jp

テレダイン・ジャパン株式会社　プリンストンインスツルメンツ
〒170-0013　東京都豊島区東池袋 3-4-3 池袋イースト　　TEL 03-6709-0631　FAX 03-6709-0632

NKT Photonics

SuperK FIANIUM
スーパーコンティニューム光源

高性能・高信頼性・高操作性をさらに追求した汎用モデル

- 波長域 390-2400 nm, シングルモード出力
- ボタンを押すだけの簡単&フェイスセーフ操作
  堅牢&メンテナンスフリー（数千時間稼動）
- プラグ&プレイのフィルタアクセサリ、モジュール設計でアップグレードも柔軟に対応
- トリガ機能、パワーロック機能、NIM トリガ出力
- 繰返し周波数可変(オプション)：アクセサリ不要, レーザー稼動中も変更可

世界で高い実績

SuperKシリーズ スーパーコンティニューム光源

- 良質なビーム品質 M^2 <1.1
- 可変シングルラインフィルタオプションで波長可変レーザとしても使用可能
- 高輝度:照明用途、SLEDなどの置き換えに好適

モデル	光出力（VIS）	光出力（トータル）	繰返し周波数
SuperK FIANIUM	0.6-2 W	2.2-6.5 W	78 MHz（可変）
SuperK EVO	40 mW	1 W	20 MHz
SuperK EVO HP	400mW	2 W	20 MHz
SuperK COMPACT	20 mW	0.1 W	20kHz（可変）

※用途に応じてさらに最適化できる便利なオプション類も提供。

https://www.japanlaser.co.jp/ E-mail: nkt@japanlaser.co.jp

JLC JAPAN LASER 株式会社日本レーザー

本　　社 〒169-0051 東京都新宿区西早稲田2-14-1 TEL.03-5285-0861
大阪支店 〒533-0033 大阪市東淀川区東中島1-20-12 TEL.06-6323-7286
名古屋支店 〒460-0003 名古屋市中区錦3-1-30 TEL.052-205-9711

NIREOS

GEMINI *超高安定性 干渉計*

入力光から生成した2つのレプリカ間の時間遅延を制御。
比類のない安定性･精度･再現性を提供する究極の干渉計

主な特長

- 高感度、高スループット
- 高速スキャン(＜1秒)
- コンパクト、低コスト
- 約1アト秒の安定性(2つのレプリカ間の光)
- スキャン範囲選択可能
- 高い振動耐性

アプリケーション

- 干渉計
- パルス対生成

検出パス内での導入例

- 時間/周波数 分解蛍光寿命測定
- ポンププローブ分光
- コヒーレントラマン分光

励起パス内での導入例

- 蛍光励起/発光マッピング
- 単一分子分析

JLC JAPAN LASER 株式会社日本レーザー

https://www.japanlaser.co.jp/ E-mail: jlc@japanlaser.co.jp

東京本社 東京都新宿区西早稲田2-14-1 TEL 03-5285-0861
大阪支店 大阪市東淀川区東中島1-20-12 TEL 06-6323-7286
名古屋支店 名古屋市中区錦3-1-30 TEL 052-205-9711

モデルチェンジ　～スマートなデザインに簡単操作～

BRANSON 超音波ホモジナイザー

長くご愛顧いただいておりますBRANSON超音波ホモジナイザーで新たなモデルが誕生しました。

主な特長

1.電気エネルギーから超音波振動への変換効率が95%以上
→ 無駄なエネルギーロスが小さく、安定した振幅が得られる。

2.通常では、液体の種類によって振幅が安定し難い。
→ 条件を変えても一定の振幅を保つ機能がついている。

3.ジュール（watt×sec）による発振制御が可能
→ Total何ジュールでこの処理が完了するという情報が論文に掲載できる。

20kHz超音波ホモジナイザー
BRANSON SONIFIER SFX250,550

40kHz超音波ホモジナイザー
BRANSON SONIFIER SFX150HH

主なアプリケーション

分散

カーボンナノチューブ　有機顔料　無機顔料　セラミック　セメント　感光体　記録材料
磁性粉　粉末冶金　酸化鉄　金属酸化物　シリカ　アルミナ　カーボンブラック
ポリマー　ラテックス　製紙　ファンデーション
研磨剤　電池　フィラー　光触媒　触媒　ワクチン　体外診断薬　歯磨き粉　シャンプー
半導体　電子基盤　液晶　貴金属　金属　宝石　タイヤ　発酵菌類　その他

乳化

エマルジョン製剤　農薬　トナー　ラテックス　界面活性剤　クリーム　乳液　その他

日本国内販売総代理店　株式会社 セントラル科学貿易

東京本社:　〒136-0071 東京都江東区亀戸1-28-6 タニビル3F　TEL 03-5627-8150 FAX 03-5627-8151
技術物流センター:〒272-0146 千葉県市川市広尾2-1-9　TEL 047-701-6100 FAX 047-701-6116
大阪支店:　〒533-0031 大阪府大阪市東淀川区西淡路1-1-36 新大阪ビル　TEL 06-6325-3171 FAX 03-6325-5180
福岡営業所:　〒812-0016 福岡県福岡市博多区博多駅南1-2-15 事務機ビル　TEL 092-482-4000 FAX 092-482-3797
札幌出張所:　〒001-0911 北海道札幌市北区新琴似11条13-7-13-2　TEL 011-764-3611 FAX 011-764-3612
https://www.cscjp.co.jp

JEOL-IDES Products

Luminary Micro

レーザー照射による試料の局所加熱観察および光反応励起観察を実現

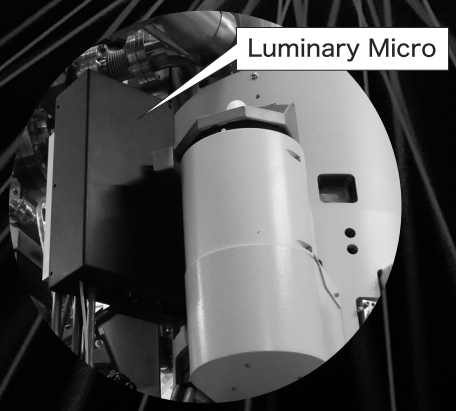

特 長

- 最大出力3 Wのレーザー
- 半値幅＜40 μmで集光したレーザーによる照射
- 変調パルスレーザー照射
  （μsからsまでのパルスコントロールが可能）
- 焦点位置、レーザー出力、パルス持続時間のリモートコントロール
- どの試料ホルダーでも観察が可能
- コンパクト設計のため、反射電子検出器（BEI）ポートからのレーザー導入を実現

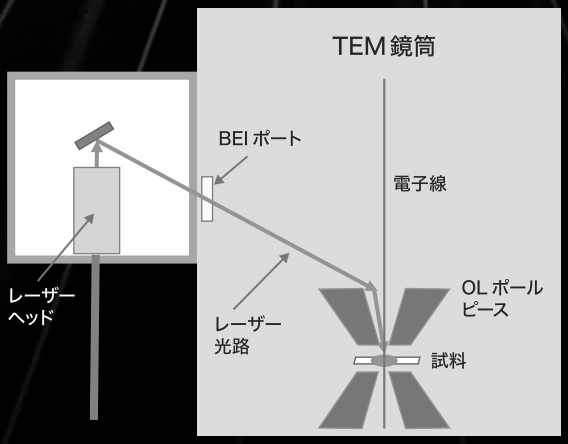

超硬合金のレーザー加熱実験のアプリケーション

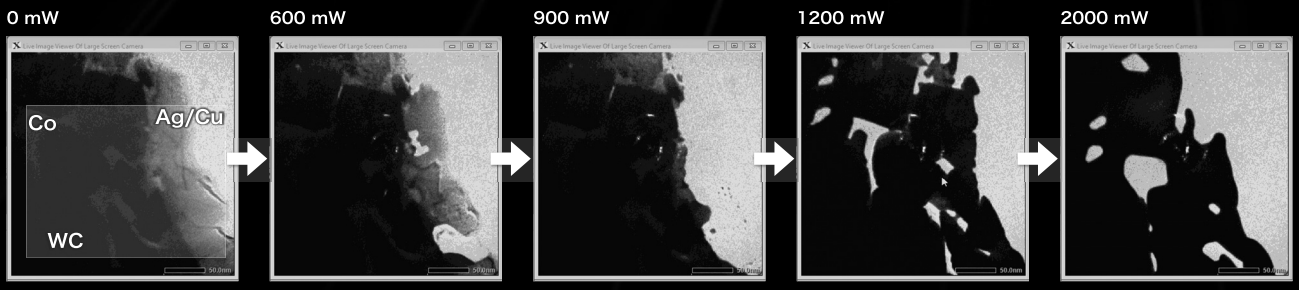

試料は主に炭化タングステン多結晶とコバルト・バインダーで構成されていて、微量の銅を含む銀ろうで覆われています。
レーザーの出力を上げながら照射していくと、600 mWで銀と銅が融け始め、1200 mWでコバルトが融け始めます。
さらに、2000 mWで炭化タングステンはアモルファスに変化します。

◀ 超硬合金のレーザー加熱実験（動画）

仕 様

パラメーター		備考
波長	577 nm（標準）	532, 642, 780 nm ご購入時にご選択ください。
ピーク出力	3 W @577 nm	2 W @532, 642, 780 nm
立ち上がり時定数	12.4 μs	
立ち下がり時定数	5.1 μs	
焦点距離	300 mm on 300 kV TEMs 250 mm on 200 kV TEMs	
集光サイズ（半値幅）	＜40 μm on 300 kV TEMs ＜33 μm on 200 kV TEMs	

対応機種：JEM-ARM300F2, NEOARM*1, JEM-2100F*2, JEM-2100Plus*2
*1 Luminary Microはプローブ Csコレクターが構成されている場合は対応可能。
*2 Luminary Microはゴニオカバーが構成されている場合は対応不可。

JEOL 日本電子株式会社

本社・昭島製作所　〒196-8558　東京都昭島市武蔵野3-1-2　TEL:(042)543-1111(大代表)　FAX:(042)546-3353
www.jeol.co.jp　ISO 9001・ISO 14001 認証取得

JEOLグループは、「理科学・計測機器」「産業機器」「医用機器」の3つの事業ドメインにより事業を行っております。
「理科学・計測機器事業」電子光学機器・分析機器・計測検査機器　**「産業機器事業」**半導体関連機器・産業機器　**「医用機器事業」**医用機器

書籍のご案内

カーボンナノチューブ・グラフェンハンドブック

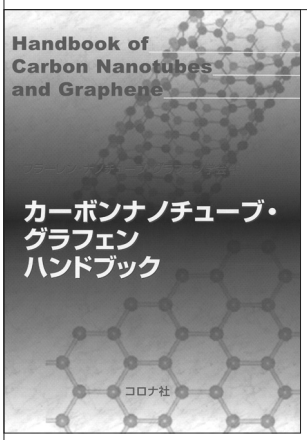

フラーレン・ナノチューブ・グラフェン学会 編
B5判／368頁
定価11,000円

本ハンドブックでは，カーボンナノチューブの基本的事項を解説しながら，エレクトロニクスへの応用，近赤外発光と吸収によるナノチューブの評価と光通信への応用の可能性を概観。最近嘱目のグラフェンやナノリスクについても触れた。

分子の薄膜化技術
ー有機EL，有機トランジスタ，有機太陽電池などの有機薄膜デバイス作製技術に向けてー

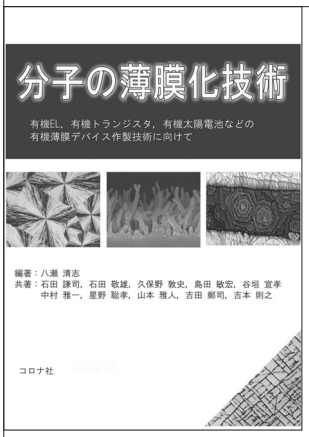

八瀬清志 編著
石田謙司・石田敬雄・久保野敦史・島田敏宏・谷垣宣孝・中村雅一・星野聡孝・山本雅人・吉田郵司・吉本則之 共著
A5判／288頁
定価4,620円

金属や無機物と多くの点で本質的に異なる有機分子の薄膜作製法，およびその素過程と成長機構の分子形状依存性について教育や研究に役立つよう記述した。また，有機EL，有機トランジスタなどのデバイス応用についても記述した。

カーボンナノチューブの基礎
齋藤弥八・坂東俊治 共著／A5判／220頁／定価3,080円

確率・統計から始める エンジニアのための信頼性工学
ー身近な故障から宇宙開発までー
山本久志 編著／A5判／222頁／定価3,300円

ドライプロセスによる表面処理・薄膜形成の基礎
表面技術協会 編／A5判／208頁／定価3,080円

ドライプロセスによる表面処理・薄膜形成の応用
表面技術協会 編／A5判／318頁／定価5,060円

物質科学を学ぶ人の 空間群練習帳
北條博彦 著／A5判／178頁／定価2,860円

化学系学生にわかりやすい 平衡論・速度論
酒井健一 他著／A5判／136頁／定価2,090円

カーボンナノチューブの材料科学入門
齋藤弥八 編著／A5判／250頁／定価3,740円

分子分光学のエッセンス
ー量子化学の基礎から機器分析の実際へー
植村一広 著／A5判／154頁／定価2,310円

相平衡の熱力学
ー熱力学体系の理解のためにー
梶原正憲 著／A5判／198頁／定価3,190円

真空科学ハンドブック
日本真空学会 編／B5判／590頁／定価22,000円

材料の熱力学 入門
正木匡彦 著／A5判／240頁／定価3,520円

基礎材料科学
伊藤公久 他著／A5判／200頁／定価2,860円

ゼロからの最速理解 プラスチック材料化学
佐々木健夫 著／A5判／256頁／定価3,740円

科学技術と共に歩む
株式会社 コロナ社
〒112-0011 東京都文京区千石4-46-10
TEL (03)3941-3131（代），-3132，-3133（営業部直通）
https://www.coronasha.co.jp FAX (03)3941-3137
E-mail eigyo@coronasha.co.jp

グラフェンの量産化に向けて…

Neutron

▼概要▼
Roll-to-Roll (R2R)
ロール状に巻いた金属ホイルを、巻き取りながら連続的にグラフェンを成長可能な量産用装置

◆特徴◆
- 連続成長
- 生産能力 20,000 m^2 / year
- Cuホイル及びSteelホイルの両方に対応
- 大気環境で成長可能で、真空チャンバ不要
- 生産コストの大幅削減

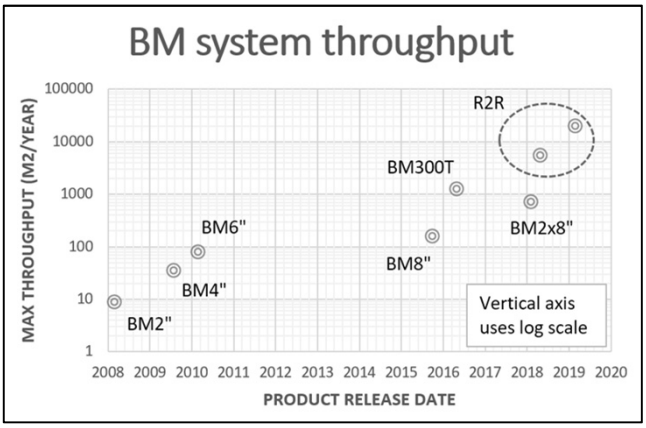

CCS 2D & NOVO

▼概要▼
2D材料及びグラフェンの成長装置

◆特徴◆
- Closed Coupled Showerhead(CCS) 技術を適用
- 成長温度は1400℃まで昇温可能
- 基板に直接2D材料またはグラフェンを成長可能
- プラズマ機能装備
- 多種原料を搭載可能(hBN, MoS2, WSe2)

BM300T

▼概要▼
ウェハ基板上CNT及びグラフェン成長装置

◆特徴◆
- 12”及び8” wafer 自動搬送対応
- プラズマ機能装備
- High 2D/G > 2.5の高品質を達成

アイクストロン株式会社 www.aixtron.com
〒140-0001 東京都品川区北品川1-8-11 Daiwa品川Northビル9F
E-mail: japaninfo@aixtron.com Phone: 03-5781-0931 Fax: 03-5781-0940

AIXTRON
Our technology. YOUR FUTURE